A CONTROLLABLE, VARIABLE WAVEFORM, HIGH VOLTAGE, SWITCHED MODE POWER SUPPLY FOR ELECTROSTATIC PRECIPITATORS.

Thesis submitted for the degree of Doctor of Philosophy at the University of Leicester

By

Phillip John Devine B.Eng (Hons)
Department of Engineering
University of Leicester

March 2000

UMI Number: U130145

All rights reserved

INFORMATION TO ALL USERS
The quality of this reproduction is dependent upon the quality of the copy submitted.

In the unlikely event that the author did not send a complete manuscript
and there are missing pages, these will be noted. Also, if material had to be removed,
a note will indicate the deletion.

UMI U130145
Published by ProQuest LLC 2013. Copyright in the Dissertation held by the Author.
Microform Edition © ProQuest LLC.
All rights reserved. This work is protected against
unauthorized copying under Title 17, United States Code.

ProQuest LLC
789 East Eisenhower Parkway
P.O. Box 1346
Ann Arbor, MI 48106-1346

CONTENTS

ACKNOWLEDGMENTS

This research was carried out with the financial support of EPSRC, DTI, Elequip Projects Limited and National Power PLC.

I sincerely thank Dr Paul Lefley, Dr John Fothergill, Mr Robert Deakin (Technical Director, Elequip Projects Ltd), Mr Ken Parker (Precipitator Technical Consultant), Mr Martin Selby (National Power PLC), Dr Gordon Smith (Loughborough University C.R.E.S.T) and Dr Kaori Fukunaga (Japanese Ministry of Energy) for their help, encouragement and guidance throughout the project.

I also thank Mr Tony Forrian (Leicester University) for his invaluable assistance in the practical construction of the power supply and Alex Smith (Didcot "A"Power Station) for his assistance during the prototype commissioning and testing period.

A CONTROLLABLE, VARIABLE WAVEFORM, HIGH VOLTAGE, SWITCHED MODE POWER SUPPLY FOR ELECTROSTATIC PRECIPITATORS

PHILLIP DEVINE

ABSTRACT

Increased awareness of the effects of atmospheric pollution has meant that electrostatic precipitators, which have been used since the early part of this century to separate particulate matter from process gas streams, are now required to achieve particulate collection efficiencies in excess of 99.7% for a number of processes. Increasingly stringent legislation concerning industrial particulate emissions has challenged the precipitation industry to consider how equipment can be improved to reduce, in particular, heavy metal and respirable size particulate discharges.

Electrostatic precipitators charge dust particles in a gas stream by corona-producing electrodes, and remove the charged particles by electrostatic attraction under high electric fields.

This thesis details the development of a prototype high frequency (20kHz), high voltage (50kV), high power (25 kW) switched mode precipitator power supply with technological advances over conventional units.

A high frequency, high voltage, high power precipitator supply using high frequency inverter technology coupled to a novel ferrite cored, high voltage transformer-rectifier unit has been designed and built. It is capable of delivering in a controlled and responsive way 25kW at 50kV into a load that may suffer from sparking and flashover.

The developmental stages of the prototype from initial concept through to field trials of the supply at a power station in the UK are detailed

DECLARATION

This thesis is submitted in fulfillment of the requirements of Doctor of philosophy in the Department of Engineering, University of Leicester, UK. All work recorded in the thesis is original unless otherwise acknowledged in the text or references. No part of it has been submitted for any other degree either to the University of Leicester or to any other University.

Signed

Phillip John Devine

1. INTRODUCTION

1.1 Atmospheric particulate matter

In recent years there has been a world-wide recognition of the problems associated with environmental pollution and how particulate matter suspended in the atmosphere as a result of industrial processes can significantly effect the health of the population [1-5]. Combustion of fossil fuels is the principal source of fine particulate emissions, including the burning of coal, oil, diesel fuel, coal-fired power stations and industrial boilers. High temperature industrial processes such as metal smelting and steel production are another significant source of particulate emissions.

1.2 The nature of particulate matter

There are a number of ways to classify atmospheric particulate matter; environmental regulators have chosen to divide particles up into various size fractions (as measured by diameter) and measure them in units of particle mass per volume of atmosphere. Suspended particles may be solid or liquid, organic or inorganic. They may be emitted directly as a result of an industrial process (primary particulates) or form later resulting from chemical and/or thermal reactions in the atmosphere (secondary particulates).

The entire domain of particulate matter in the atmosphere is known as the total suspended particulate (TSP). This includes all airborne solids and liquid particles, except pure water, ranging in size from approximately 0.005μm to 100μm in diameter.

1.3 Health effects of inhalable particles

If particles greater than 10μm are inhaled, they tend to collect in the throat or nose, and are eliminated from the body by sneezing, coughing, nose blowing (collectively known as the upper respiratory system), or through the digestive system.

Generally, these particles are not associated with human health problems since 10μm is the threshold for entering the human pulmonary system [5]. One obvious exception is pollen, which triggers allergic reactions among many people.

Of particular concern are particles that are less than 10μm in diameter. These are called 'PM10' particulates and are commonly referred to as inhalable or thoracic particles in that they can penetrate into the thoracic compartment (from the trachea down to and including the alveoli) of the human respiratory tract.

PM10 particulate matter has been shown to cause respiratory symptoms such as bronchitis, pulmonary inflammation and changes in lung function [1-5]. The five-fold increase in cases of asthma in the UK in the last 20 years has also been strongly linked to this and other forms of particulate pollution of the atmosphere [6].

Polynuclear Aromatic Hydrocarbons (PAH's) are another sub-group of PM10 particulates and are products of incomplete combustion in certain industrial processes such as coal/ wood burning. These have been shown to react with macromolecules such as human DNA and are considered toxic and "probably carcinogenic to humans" [7].

1.4 Legislation to minimise particulate air pollution

During the last decade, the link between air pollution and ill health has been at the centre of much political, public and media attention. This concern has been fuelled by evidence of increasing respiratory ill health, especially in children, and the search for an explanation has focused upon environmental pollution.

As concerns over health and the environment increase, the legislated limits concerning particulate emissions into the atmosphere have become increasingly stringent. Examples of this are the 1988 EC Directive, L336, 7.12.88 which specifies limits for emission of respirable size particulates as well as SO_2 and NO_x into the atmosphere [8] and The Canadian Environmental Protection Act of 1995 which specifies limits for respirable particulate emissions as well as SO_2, NO_x and PAH's [7].

As an example of the power of these and previous directives, the allowable particle emission rate from coal fired power stations in Great Britain has decreased ten fold over the last thirty years [9].

Increased modern day awareness of the effects that atmospheric pollution can have on the human body means that legislation will continue lowering the allowable emission limits in industrial processes.

Apparatus used to inhibit atmospheric particulate emissions in industrial processes such as coal fired power generation, cement production and heavy metal production are now required to capture in excess of 99.7% of all particulates produced as a result of the industrial process. [7-9]

These changes have challenged industry to consider how emission control equipment can be improved to meet ever tightening legislation concerning, in particular, respirable size particulate discharges.

There is an industrial requirement to further improve the equipment and processes used to reduce pollution if the trend of a steady reduction in air pollution is to be achieved.

1.5 Particulate collection apparatus

There are various apparatus available for the separation of particulates from industrial flows. They are each based upon a different physical operating principle and therefore the collection efficiency, cost and application suitability is distinct for each method.

The main methods are:

- Settling chambers
- Fabric filters
- Wet scrubbers
- Centrifugal collectors
- Electrostatic precipitators

1.5.1 Settling chambers

The gas stream containing the particulates is passed through a chamber of varying length depending on the application. The separation process of the particulates from the gas stream relies simply on gravitational forces.

Whilst this method is the cheapest to install and operate, its dust collection properties are only effective on particles of the size 100-1000 μm and therefore its range of applications is limited. A typical application of a settling chamber would be to separate grit, sand or heavy dusts from a gas stream [9].

1.5.2 Fabric filters

The gas stream containing the particulates is passed through a physical filter before being released into the atmosphere. The filter is constructed from porous man made fibres. As the entrapped particulates deposit and build up on the fabric filter, the particulate collection efficiency of the filter increases since particles of a diameter smaller than that of the fabric pore size will also be trapped. Fabric filters are capable of entrapping particles of a diameter less than 0.1 μm.

The disadvantage of this method is that the filters have to be regularly cleaned to avoid a large pressure build up between the industrial process equipment and the atmosphere. Maintenance costs are also a limiting factor since a large industrial process may use thousands of fabric filters, which have to be individually cleaned on a regular basis.

A typical application of a fabric filter may be in the separation of particulates such as fly ash, incinerator dust, bacteria and pollen [9].

1.5.3 Wet scrubbers

The gas stream containing the particulates is passed through a chamber where a liquid spray is introduced. The droplets of the spray (usually water) attach themselves to the particulates increasing their size and mass dramatically. The particulates are then removed from the gas stream through gravitational forces.

Wet scrubbers are effective at separating particulates of diameters as low as 0.1 μm.

A disadvantage of this method is the large power demands of the apparatus used to create the spray, the large water usage and the associated effluent problem due to the dilemma of being left with a large amount of contaminated (possibly acidic or toxic) water. A typical application of a wet scrubber would be in the separation of particulates such as fly ash, cement dust, incinerator dust and a limited range of bacteria [9].

1.5.4 Centrifugal collectors

The gas stream containing the particulates is made to spin rapidly within a cylindrical containment unit. This method is sometimes referred to as a cyclone chamber.

Because the mass ratio of particulate to gas molecule is high, the particulates are forced to migrate towards the outer area of the collector due to centrifugal forces. Here the turbulence / flow rate is low and the particulates are therefore separated from the high-speed gas.

Centrifugal collectors are effective at separating out particulates of a size as low as 50 μm. The main disadvantage of this method is the large amount of power required to maintain a cyclone.

A typical application of a centrifugal collector would be the separation of particulates such as grit, foundry sand and a limited range of cement dust and pollens [9].

1.5.5 Electrostatic Precipitators

In electrostatic precipitators, the gas stream containing the particulates is passed through an electric field. The charged particles then migrate through the electric field to a collection electrode where they are regularly removed into hoppers by mechanical rapping of the electrode. Electrostatic precipitator action is discussed in detail in chapter two of the thesis.

Electrostatic precipitators have collection efficiencies far higher than all other filtering apparatus [9]. They are capable of separating all of the previously mentioned particulate types as well as PM10 particulate matter. Electrostatic precipitators have several key advantages over other apparatus, which, for the majority of industrial applications, have made them the most attractive option:

- High particulate collection efficiency
- Low maintenance costs
- Low pressure loss
- The precipitator can operate over a wide range of pressures and temperatures
- Acceptable operational costs in comparison to other collection methods
- Long operational life
- High reliability

1.6 Summary

There is now worldwide recognition of the problems associated with environmental pollution. Research into atmospheric particulate pollution and its effect on human beings clearly show a correlation between ill health and atmospheric pollution.

This has lead to increasingly stringent legislation to minimise the levels of particulates in the atmosphere.

In many industrial processes, electrostatic precipitators are the only method that will maintain particulate emission levels within legislated limits.

For particulates in the PM10 size band, many of which are the most toxic and carcinogenic, the precipitator is the superior collection apparatus.

1.7 References

1. **Brook JR & Dann TF**, "The relationship among total suspended particulate, PM10 and inorganic constituents of atmospheric particulate matter at multiple Canadian locations", Journal of Air and Waste Management Association. 47: 2-19, 1997

2. **Acid News,** "Health effects of particles", 5: 16 December 1995
3. **Ministry of Heath,** "Air pollution: What you cant see may be very dangerous to your health!", British Columbia Ministry of Health, Health file #35 –Spring 1994
4. **Schwartz J**, "Is daily mortality associated specifically with fine particles?", Journal of Air and Waste Management Association. 46: 927-939, 1996
5. **Vedal** S, "Health effects of inhalable particles: Implications for British Columbia", Canadian Ministry of Environment, Lands and Parks, 1995
6. **Hare S** & McNairn J, "Air quality issues", ARIC, Manchester Metropolitan University, UK, May 1996
7. Canadian Environmental Protection Act, Germain, 1995
8. EC Directive on the limitation of emission pollutants into the air from large combustion plants. Official Journal of EC, legislation, L336, 7.12.88
9. **Parker KR**, "Applied Electrostatic Precipitation", 1997 Chapman and Hall, ISBN 0 7514 0266 4

2. ELECTROSTATIC PRECIPITATOR OPERATION

2.1 Electrostatic precipitation process

Electrostatic precipitators (ESPs) are used to collect solid or liquid particles (dust, mist or fumes) from large gas flows such as flue gas from coal-fired power stations. They do this by charging the particles and collecting them electrostatically.

Figure 2-1 shows two parallel electrodes connected to a high voltage source. Between the electrodes there is an assumed homogenous electric field.

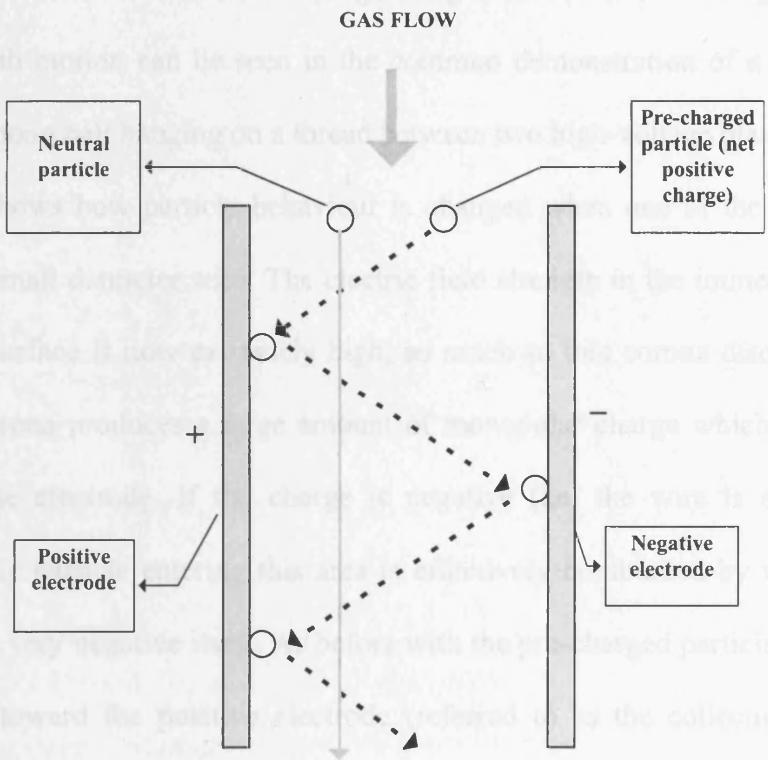

Figure 2-1 Parallel electrode model

Consider the cases of a neutral and a charged dust particle carried by the laminar gas flow in the electric field created by the electrodes. The neutral particle is influenced by the electric field, but the net electrostatic force acting on the particle is zero. Typically the particle will pass straight through the field since the dominant forces on it are only those due to the gas flow. The pre-charged particle in this example is assumed to have a net positive charge. It is therefore pulled towards the negative electrode under the influence of the electric field. Assuming the pre-charged positive particle is conductive, then, when it comes into contact with the negative electrode, the positive charges are transferred to the electrode and the particle gains a net negative charge. If the particle has negligible adhesion to the electrode, the net force on the particle is reversed and the particle is pushed toward the other (positive) electrode. Here the process is repeated and so in theory the particle will move back and forth between the two electrodes progressing in the direction of the gas flow. This back-and-forth motion can be seen in the common demonstration of a conductively coated ping-pong ball hanging on a thread between two high-voltage plates.

Figure 2-2 shows how particle behaviour is changed when one of the electrodes is altered to a small diameter wire. The electric field strength in the immediate vicinity of the wire surface is now extremely high, so much so that corona discharge occurs here. The corona produces a large amount of monopolar charge which drifts to the opposite plate electrode. If the charge is negative (i.e. the wire is at a negative potential), any particle entering this area is effectively bombarded by these charges and becomes very negative itself. As before with the pre-charged particle, the particle now moves toward the positive electrode (referred to as the collection electrode) under the influence of the electric field. There is now such an excess of negative charges within the flow area, however, that the particle charge does not change its sign through its contact with the positive electrode; it stays in place on the positive collecting electrode. The wire is referred to as the discharge electrode. This process illustrated through Figure 2-2 is the fundamental one underlying electrostatic precipitation [1,2,3]

As yet we have only discussed the behaviour of a single dust particle. A dust cloud contains a multitude of particles. The precipitation process operates on large numbers of particles in essentially the same way as it does on an individual particle; the sequence of charging, motion through the action of the electric field and adhesion on the plate electrode is still the same.

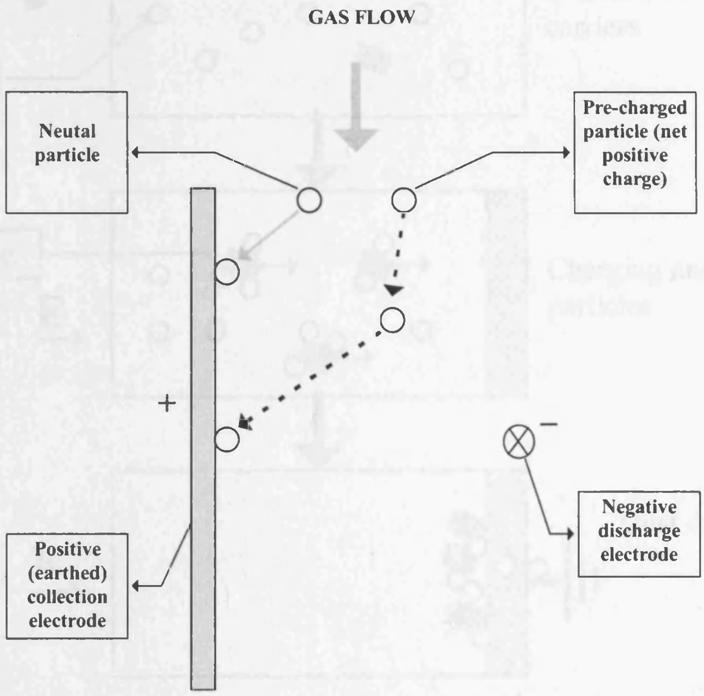

Figure 2-2 Precipitator model with a negative wire discharge electrode

2.2 Precipitator separation processes

In precipitators, the separation of particles from flue gases can be divided into three steps, which are illustrated in Figure 2-3:

1. Generation of charge carriers
2. Charging, deflection and separation of the particles
3. Dust deposition and dust removal

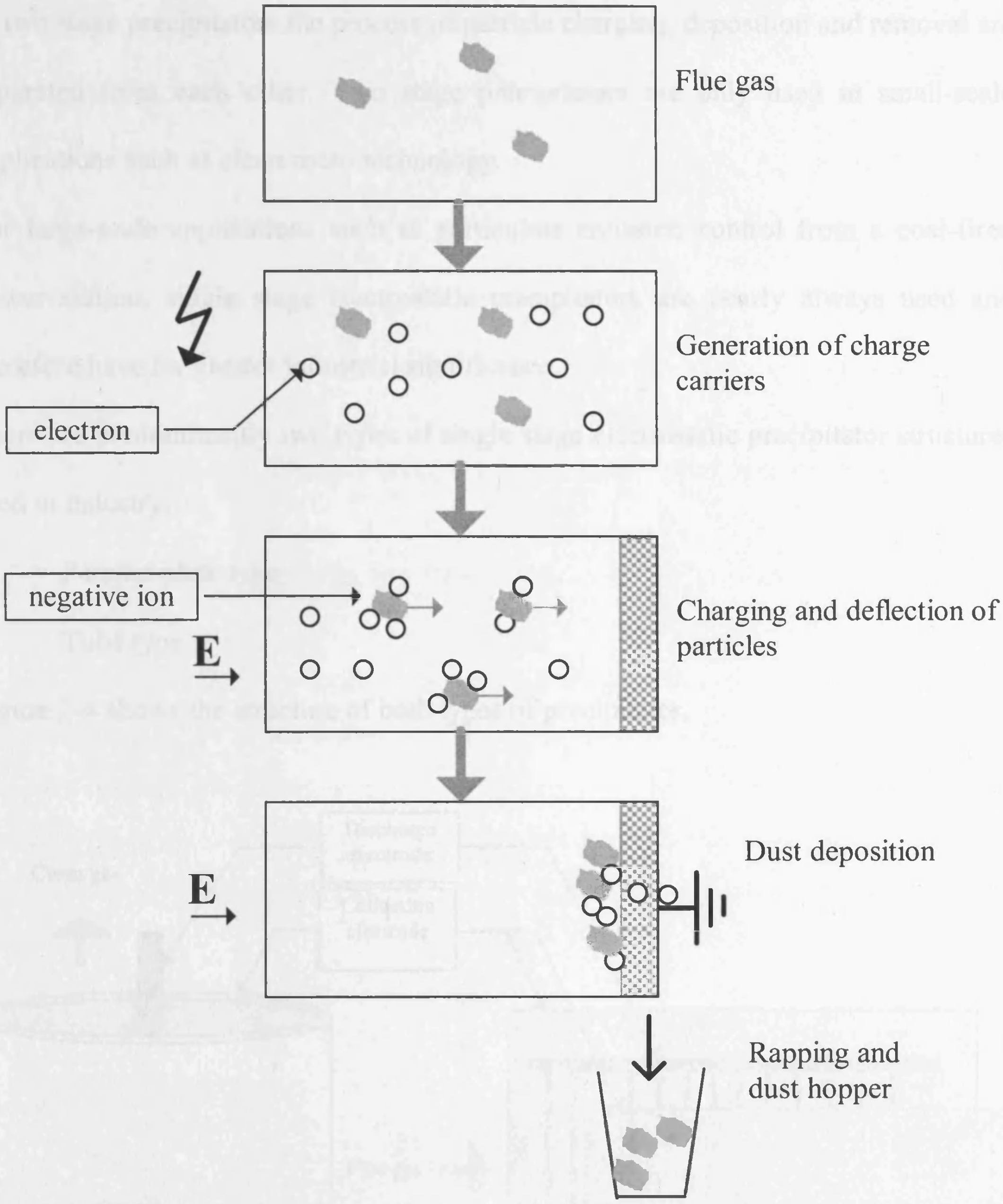

Figure 2-3 ESP separation process [1]

2.3 Physical structure of commercial precipitators

The physical structure of commercial electrostatic precipitators falls into two categories, single stage and two stage. In single stage precipitators the processes of particle charging, deposition and removal have no clearly defined physical boundaries within the precipitator structure.

In two stage precipitators the process of particle charging, deposition and removal are separated from each other. Two stage precipitators are only used in small-scale applications such as clean room technology.

For large-scale applications such as particulate emission control from a coal-fired power station, single stage electrostatic precipitators are nearly always used and therefore have far greater industrial significance.

There are predominantly two types of single stage electrostatic precipitator structures used in industry:

1. Parallel plate type
2. Tube type

Figure 2-4 shows the structure of both types of precipitator.

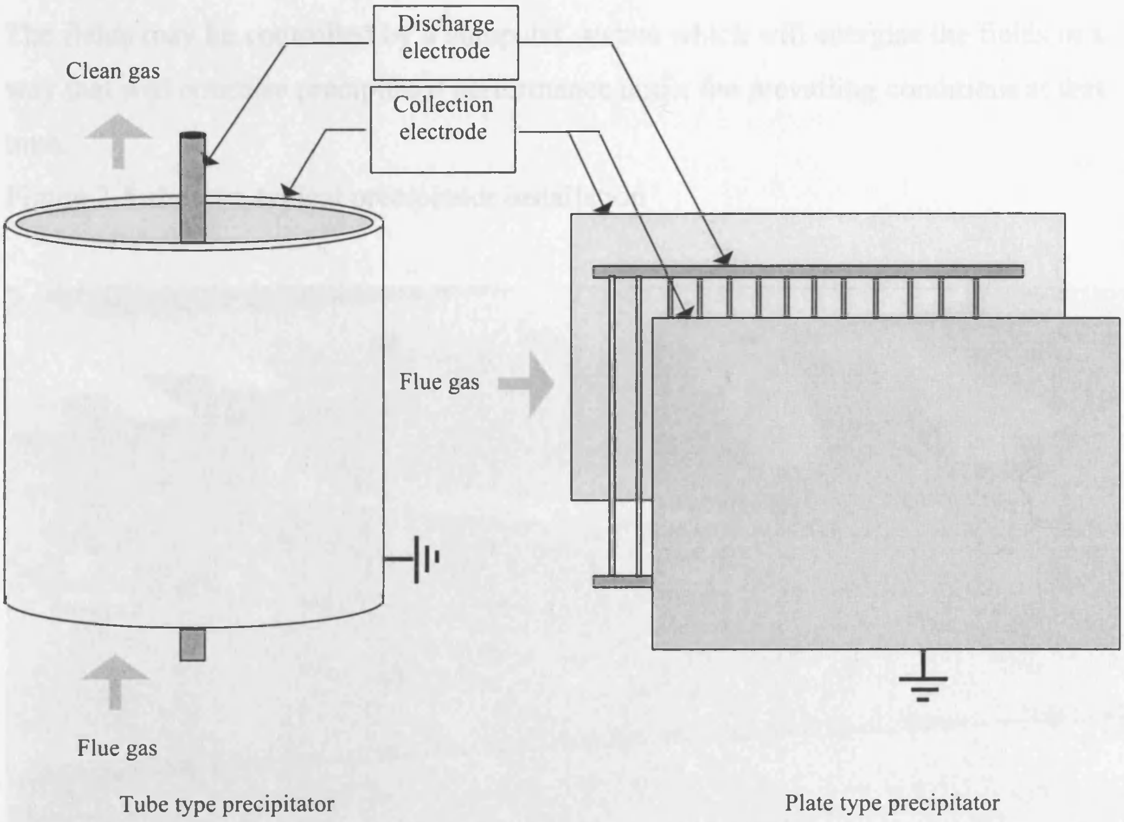

Figure 2-4 Commercial precipitator structures

In tube type precipitators the discharge electrode is positioned geometrically central to the cylindrical collection electrode. Tube type precipitators are often used in applications where the collected particles are a liquid form, e.g. acid mists. The collection plates are normally purged by flushing a liquid over the plates, which then runs down into a sump at the base of the precipitator.

In plate type precipitators, a row of discharge wires is positioned between parallel collection plates. The dust or large agglomerates collected on the plates are removed by mechanical rapping, falling into hoppers at the base of the precipitator.

2.3.1 Precipitator sectionalisation

In industrial applications, the precipitators are sectionalised into series and parallel fields, each field having its own power supply unit. The fields can therefore be energised differently to each other resulting in a unique electrical and dust collection situation for each individual field.

The fields may be controlled by a computer system which will energise the fields in a way that will optimise precipitator performance under the prevailing conditions at that time.

Figure 2-5 shows a typical precipitator installation

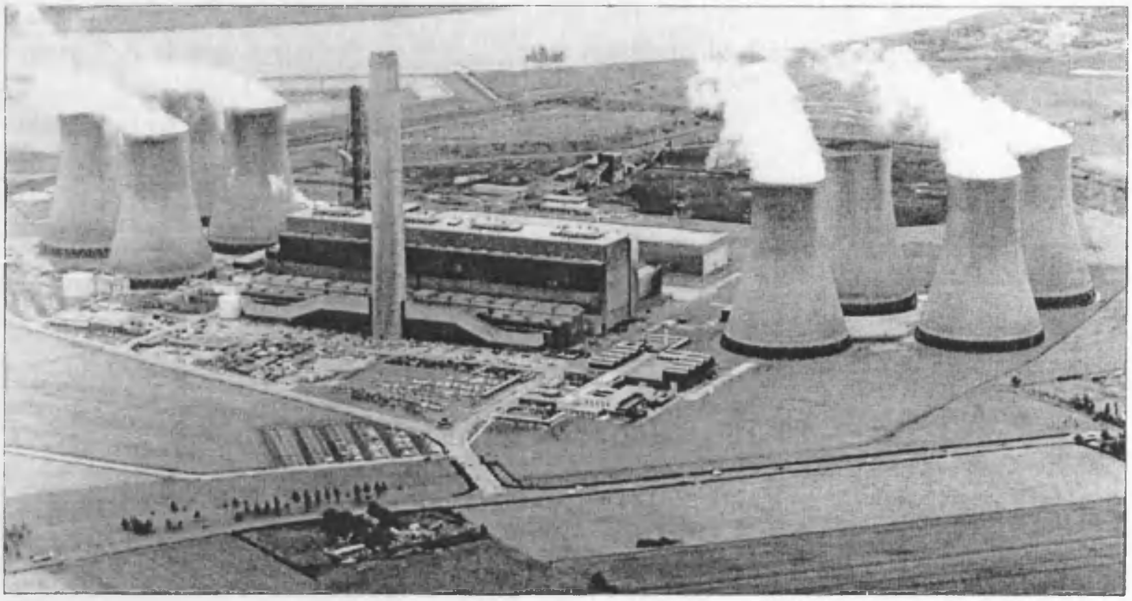

Figure 2-5 Precipitator installation

2.4 Electrical characteristics of a precipitator

2.4.1 Precipitator voltage - current relationship

To produce large numbers of charge carriers in the flue gas, a high voltage is applied to the discharge electrode. This creates a high electric field strength in the inter-electrode space. When the applied voltage reaches a distinct value, an electrical current between the discharge and collection electrodes can be measured indicating the onset of corona discharge within the precipitator. This is called the corona onset voltage. A further increase in discharge electrode voltage will lead to an increasing current until spark-over occurs which marks the electrical breakdown of the gas. The discharge electrode voltage can be either positive or negative. However, for a given geometry, the electrical breakdown of a gas occurs at higher voltages for negative than for positive energisation

Because of the higher electric field strengths, industrial applications prefer negative corona. Most precipitators work with the collection electrodes grounded and the discharge electrodes energised with a negative voltage [1,4]

Figure 2-6 shows a typical voltage-current relationship for a precipitator operating with a dust of moderate resistivity (10^{10} ohm-cm)

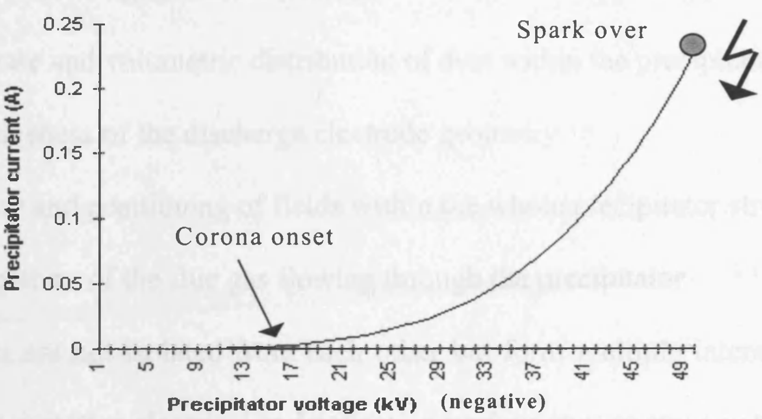

Figure 2-6 Typical ESP voltage-current relationship

2.4.2 Electrostatic precipitator equivalent circuit

Figure 2-7 shows the electrical equivalent circuit for a precipitator. It consists of an equivalent precipitator capacitance C_p and an equivalent voltage-dependent resistor R_p.

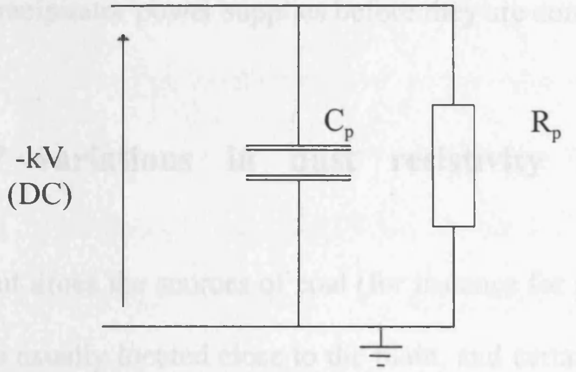

Figure 2-7 Precipitator equivalent circuit.

The precipitator capacitance C_p is a function of both the sizing and geometric layout of the precipitator discharge and collection electrodes. A typical value for an industrial size precipitator field may be in the order of 100-300nF [1].

The equivalent precipitator resistance R_p is a complex function of several factors;

1. The resistivity of the dust flowing through the precipitator at any time
2. The applied discharge electrode voltage
3. The flow rate and volumetric distribution of dust within the precipitator
4. The effectiveness of the discharge electrode geometry
5. The number and positioning of fields within the whole precipitator structure
6. The temperature of the flue gas flowing through the precipitator

These factors are not isolated from each other but form multiple interactions, which effect the precipitators electrical and collection performance at any one time [5]

However, to give the reader an idea of magnitudes, in a typical industrial precipitator installation, for instance, a coal fired power station, a field energised to -50kV DC may draw some 200-400mA of current. It must be stressed however that these values are completely dependent on the factors outlined above [1,6].

A parallel capacitor-resistor network as shown in figure 2-7 is often used as the in-house test load for precipitator power supplies before they are commissioned on site.

2.4.3 Effect of variations in dust resistivity on precipitator performance

Until relatively recent times the sources of coal (for instance for pulverised coal fired power stations) were usually located close to the plant, and certainly within the same country. Its properties were well known and the precipitator could be commissioned to deal solely with this form of dust. There would be little need to ever change the operating parameters of the precipitator to compensate for variations in coal type.

The availability of cheap coal from countries such as Australia, South America and South Africa means that power stations are now burning several different coals each with different electrical and physical characteristics [1,5,7]

This gives rise to differing electrical and collection processes within the precipitators, which will, in turn effect both the electrical and collection performance of the precipitator.

For particles with a resistivity in the range 10^{10} to 10^{11} Ohm-cm the charging of the particle within the inter-electrode space and consequent discharging of the particle when it reaches the collection electrode continues ordinarily.

As the particle resistivity increases, the charging process occurs normally, however, the particle on reaching the collection electrode only slowly loses its charge and a potential difference develops across the dust layer, the magnitude of which is dependent on the dust resistivity and layer thickness.

For dust particles with resistivities in the 10^{13} Ohm-cm range, the voltage developed across the dust layer can become so high as to cause sparking within the dust layer.

As a result of this, large quantities of positive charge are produced. These neutralize negative charges within the field which adversely effects the dust collection process.

This phenomenon is known as back-ionisation and results in a lower average precipitator voltage and an increase in current drawn by the precipitator.

Modern electrostatic precipitators, therefore, have to be designed such that the discharge electrode voltage can be altered to accommodate variations in dust resistivity and to maintain collection performance [5]

2.4.4 Factors effecting collection efficiency

For efficient operation of a precipitator field, several points may be established:

1. The magnitude of discharge electrode voltage should be set such that precipitator collection efficiency is maintained within legislative limits at all times. The discharge electrode voltage required to meet this criteria is dependent on the electrical and physical properties of the dust passing through the precipitator.

To maintain collection efficiency when the resistivity of the dust is moderate the discharge electrode voltage should be raised to a level whereby dust emission levels are within statutory levels. On the contrary when dust resistivity is very high the discharge electrode voltage may have to be lowered to avoid back ionisation occurring within the precipitator

2. Precipitator collection performance is not always improved with an increase in input power. An abnormal increase in power being drawn by the precipitator may

be an indication of back ionisation. The input power should be optimised for the prevailing operating conditions.

3. Apart from variations in dust resistivity there are additional factors which affect the performance of a precipitator:

- Excessive particle deposits on the collection plates

Efficient cleaning of the electrodes is a vital requirement to maintain precipitator operating efficiency. The collection plates are cleaned by subjecting them to a short mechanical impulse of set duration and period, a procedure known as rapping.

In a precipitator operating with an effective rapping schedule, the majority of the dust present on the collecting electrodes will fall into the hoppers situated below the precipitator after a rapping event. However, the dust, which does not reach the hoppers, will re-enter the gas stream. To minimise this loss of collection efficiency, a modern precipitator installation works in conjunction with the rapping system to ensure that the electrical conditions present immediately following rapping are ideal for rapid dust charging and collection.

- Uneven corona distribution on the discharge electrode wires

Figure 2-8 shows three scenarios (A, B & C) for corona discharge on the energised discharge electrode:

A. As the discharge electrode voltage is increased, a corona discharge spot develops at a certain point on the discharge electrode. The dust collection properties of the inter-electrode space are effective only at this point.

B. As the discharge electrode voltage is increased further, several more corona discharge points develop on the discharge electrode.

C. The discharge electrode voltage is increased further. Corona discharge points are evenly distributed across the surface of the discharge electrode leading to an even distribution of field strength within the inter electrode space and a subsequent high dust collection performance. This is the most favourable situation out of the three scenarios.

However, this is only possible with good discharge electrode design. Even then, dust collection efficiency may be affected by other factors such as turbulence within the dust flow.

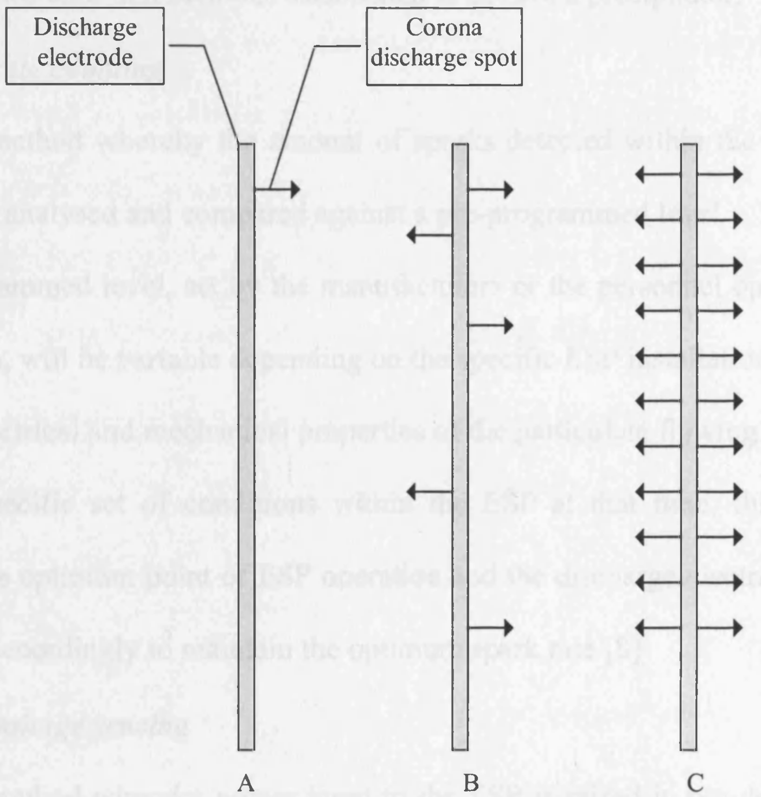

Figure 2-8 Corona discharge distribution on discharge electrodes

Modern coal fired power stations now produce much finer ash with far higher resistivity than several years ago. To retain an effective field strength in a precipitator dealing with high resistivity dust, the discharge voltage must be lowered. Consequently, the corona distribution shown on discharge electrode B in Figure 2-8 is often representative of precipitator operation [2]. This is a non- optimum operating situation and can lead to a loss of collection performance in the precipitator.

2.5 Precipitator performance optimisation

Methods by which precipitator performance may be improved are detailed.

2.5.1 Precipitator Control methodologies

There are two common methods established to control a precipitator:

- *Spark rate counting*

This is a method whereby the amount of sparks detected within the precipitator per minute are analysed and compared against a pre-programmed level.

This programmed level, set by the manufacturers or the personnel operating the ESP installation, will be variable depending on the specific ESP installation, its application and the electrical and mechanical properties of the particulate flowing through it.

For the specific set of conditions within the ESP at that time, this level will be deemed the optimum point of ESP operation and the discharge electrode voltage will be varied accordingly to maintain the optimum spark rate [8]

- *Mean voltage sensing*

This is a method whereby power input to the ESP is raised in pre-determined steps. The mean discharge electrode voltage is constantly monitored to find the point on the characteristic curve where the slope is neither positive nor negative. This is deemed the optimum working point.

Beyond this point, the mean discharge electrode voltage begins to reduce due to the increasingly high rate of sparks and flashovers. The disadvantage of this method is that the power levels have to be regularly reduced and then ramped back up to find the point of inflexion, which can temporarily affect the dust collection process [8].

2.5.2 Precipitator operational characteristics

With more stringent environmental controls being placed upon sources of dust emissions, an electrostatic precipitator may be required to operate with a collection efficiency as high as 99.7%. These stringent pollution control limits have resulted in a significant increase in electrostatic precipitator power consumption.

The assumption that precipitator collection performance is always improved by simply increasing the input power is incorrect. In fact, a point may be reached in the operating characteristic of a precipitator, depending on the dust type present, where an increase in input power above a certain level leads to excessive sparking and back ionisation which will limit the dust collection efficiency.

Figure 2-9 shows a typical operating characteristic for a precipitator operating with standard DC energisation and with a dust of moderate resistivity.

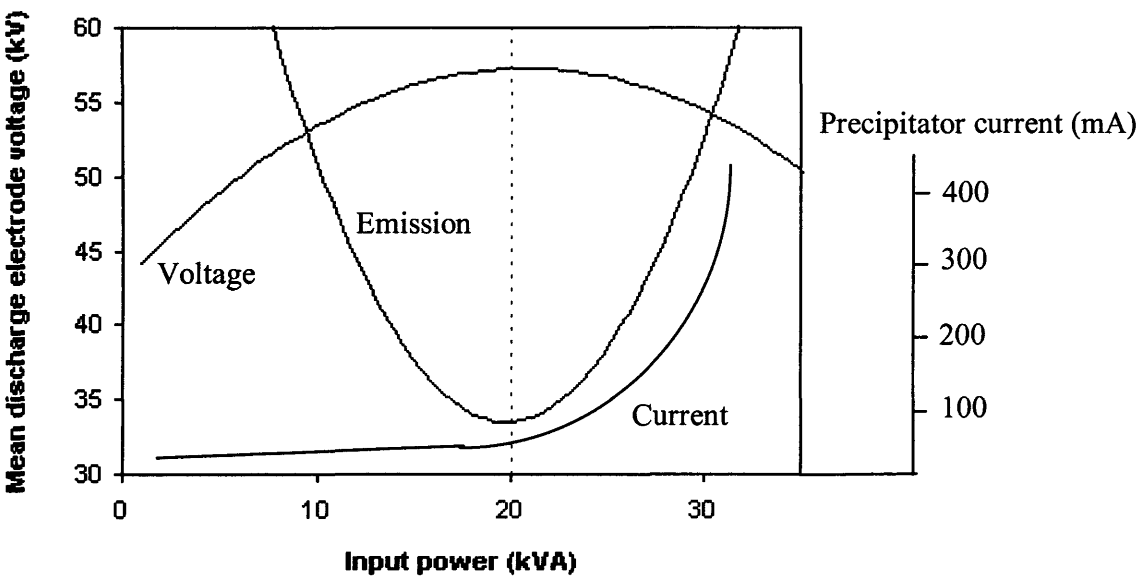

Figure 2-9 Typical operating curve for an electrostatic precipitator [2]

From Figure.2-9, Increasing the input power above 20 kVA results in a lower mean discharge electrode voltage, an increase in dust emission and a power wastage since the additional input power is simply dissipated in excessive sparking and eventually arcing within the precipitator. Sparking is a momentary short circuit between the discharge electrode and collection electrode and occurs randomly and frequently in any precipitator energised to operational levels. The sparking rate can increase to wasteful levels if the precipitator is operating at a point where there is excessive input power.

From Figure 2-9 it can be seen that a maximum of the mean discharge electrode voltage coincides with a minimum in dust emissions. This is the optimum operational point for the precipitator. This point will, however, vary depending on the electrical and physical characteristics of the particles passing through the precipitator.

2.6 Power saving and dust collection optimisation in a precipitator

There are four methods by which power consumption in a precipitator can be minimised. Under certain circumstances (depending on the electrical and physical properties of the dust), this reduction in power does not have an adverse effect on dust collection efficiency;

- Reduction of discharge electrode voltage
- Power control of individual units within the precipitator
- Intermittent energisation
- Pulse energisation

2.6.1 Reduction of discharge electrode voltage

This is a method whereby the discharge electrode voltage is minimised to a point where the precipitator is operating just within legislated limits. This method is an extremely effective way of saving power, especially when the precipitator has been designed for dust burdens which are higher than those typically encountered (or dusts more difficult to collect than those often encountered). In such cases, the operating point for maximum collection is often wasteful of power when weighed against returns in increased collection. This method is also particularly effective when the precipitator is dealing with highly resistive dusts, which are becoming more prevalent throughout the power industry.

2.6.2 Power control of individual fields within the precipitator

The normal practice in precipitator design is to sectionalise the precipitator into individual fields. The energisation levels of each field can then be set to optimise collection efficiency under the prevailing conditions at that time.

With certain dusts such as fly ash which are low in sodium it is possible to shut down the power to several of the precipitator fields without any noticeable variation in dust emission [1]. This clearly results in a significant power saving.

2.6.3 Intermittent / Semi - pulsed energisation

Intermittent or semi-pulsed energisation was introduced in the early 1980's as a way of saving energy and increasing collection efficiency (with certain types of dust).

Intermittent energisation systems operate by repetitively blocking the power supplied to the precipitator. The operator sets the time duration of this blockage.

Figure 2-10 shows a typical power flow waveform for intermittent energisation.

As a consequence of the suppression of power, the mean and rms values of precipitator voltage and current are lower than they would be with standard DC energisation.

The effect intermittent energisation has on precipitator collection efficiency is highly dependent on the resistivity of the dust. For dusts of low resistivity, the power reduction due to intermittent energisation can result in a lower collection efficiency compared to standard DC energisation. For dusts of high resistivity, however, the collection efficiency can be higher than that achieved with standard DC energisation. The reduced power consumption can lower the amount of back ionisation. Consequently, a saving in power consumption is made alongside an increase in dust collection efficiency [1,10]

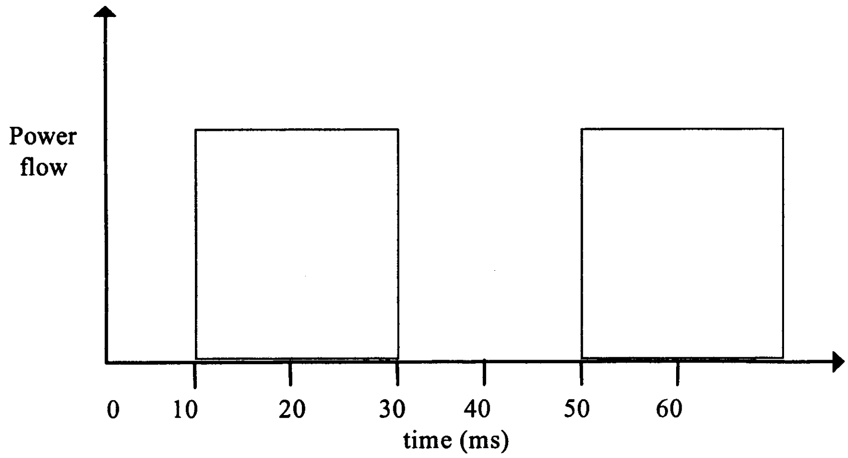

Figure 2-10 Intermittent energisation power flow time sample

2.6.4 Pulse energisation

Pulse energisation systems began entering the precipitator market in the early 1980's in an attempt to increase the collection efficiency of precipitator units dealing particularly with highly resistive dusts.

Figure 2-11 shows a typical voltage waveform from a pulse energisation unit.

Pulse energisation consists of a short duration, high voltage pulse superimposed on a base voltage, whose level is kept close to the corona onset voltage. A typical pulse may be 60kV above the base level. The pulse width may be 100uS with a repetition rate of 300 pulses per second. These three parameters are variable and are adjusted to suit the prevailing conditions in the precipitator.

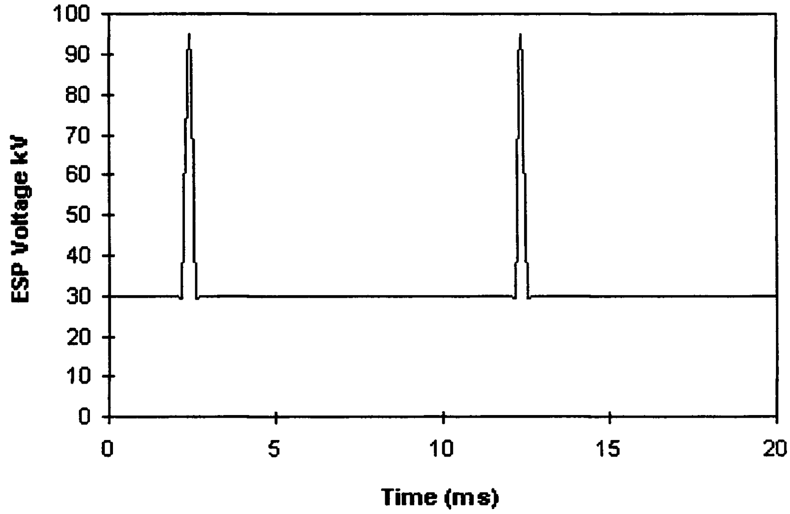

Figure 2-11 Pulse energisation waveform

A commercial pulse energisation unit is normally physically separate from the precipitator power supply. The high voltage pulses are introduced onto a common busbar, which is energised to the base level by a standard precipitator power supply [9,11]

Pulse energisation has several advantages over standard DC energisation:

- Corona discharge with standard DC energisation may not be evenly distributed across the discharge electrode surface. With pulse energisation, the peak voltage (pulse magnitude + base level) significantly exceeds the corona onset level, resulting in an intense corona discharge during a pulse. This has been shown to lead to a more uniform current density within the collection area and a consequent improvement in dust collection (particularly dusts of high resistivity) [9].

- By varying the pulse repetition rate, the precipitator current can be controlled independently of the constant precipitator voltage (Vdc + Vpulse). It is therefore capable of minimising the precipitator current to a level just before the onset of back corona without having to lower the precipitator voltage [11]
- Enhanced particle charging and collection due to the higher field strengths associated with pulse energisation.
- An enhancement in collection efficiency. For high resistivity dusts this enhancement factor has been shown to be around 2 compared to standard DC energisation and around 1.5 compared to intermittent energisation [1, 12]

2.7 Summary

The fundamental operational characteristics of an electrostatic precipitator have been detailed in this chapter. It is evident that a modern precipitator power supply must be designed with a high degree of operational flexibility incorporated into it. The power supply must be able to cope with the ever-increasing demands placed on precipitator operation due to tightening environmental legislation and the increasing variation of particulates entering the precipitator.

The trend, due to economic constraints, to source coal from various countries rather than utilising local, well defined varieties has lead to a general increase in the resistivities of particulates entering the precipitation process in coal fired power stations.

This can place significant demands on precipitator operation, namely, trying to achieve the correct balance between minimal power wastage and high particulate collection efficiencies. These factors will effect the choices made in reaching a specification for a modern power supply capable of effectively energising a precipitator under conditions detailed in this chapter.

2.8 References

1. **Parker KR**, "Applied Electrostatic Precipitation", 1997 Chapman and Hall, ISBN 0 7514 0266 4
2. **Jones AR**, "A total energy management system for electrostatic precipitators", Report, Lodge-Cottrell (Dresser UK Ltd) 1992
3. **Parker KR**, "Technological advances in high efficiency particulate collection", Proc Instn Mech Engrs Vol211 Part A, 1997
4. **Parker KR**, "Fundamentals and practice of Electrostatic Precipitation", Report, Lodge Sturtevant Ltd, UK, 1992
5. **Devine PJ**, "The requirements of an Electrostatic precipitator Power supply", Leicester university, Report 96-24, 1996
6. **White HJ**, "Industrial Electrostatic Precipitation", Addison-Wesley, 1963
7. Robinson M, "Electrostatic precipitation", Air pollution control, part1, John Wiley, New York 1971
8. **Reyes V**, "Comparison between traditional and modern automatic controllers on full scale precipitators", Proceedings of the EPRI/EPA symposium, 2A,March 1987, USA
9. **Peterson** HH, "New trends in Electrostatic precipitation: wide duct spacing, precharging and pulse energisation" IEEE trans. Ind. Appll., 1A-17, 496-501, 1981

10. **Tachibana N**, "Intermittent energization on electrostatic precipitators", Journal of Electrostatics, 25 (1990) 55-73

11. **Lausen P**, "Application of pulse energization on electrostatic precipitators for various processes", journal of Electrostatics, 25 (1990) 41-53

12. **Hall HK**, "History of pulse energization in electrostatic precipitation", journal of Electrostatics (1990) 1-22

13. **Dinelli G**, "pulse power electrostatic technologies for the control of flue gas emissions", Journal of electrostatics, 25 (1990) 23-40

3. THE CONVENTIONAL PRECIPITATOR ENERGISATION TOPOLOGY, ITS LIMITATIONS AND THE CONCEPT OF A NEW, STATE OF THE ART PROTOTYPE SWITCHED MODE BASED POWER SUPPLY AS A REPLACEMENT.

3.1 Conventional power supplies

The power supply topology shown in figure 3.1 has been the conventional circuit used to achieve high voltage energisation of a precipitator [1].

The single phase, line to line voltage (415V rms, UK) is regulated by a pair of anti-parallel thyristors before it is applied to the primary winding of a step-up, high voltage transformer. By variation of the firing angle of the thyristors, power flow to the precipitator can be controlled. The secondary voltage of the transformer is then rectified by a high voltage, full bridge rectifier and applied directly to a precipitator section. The full wave bridge rectifier is configured in such a way that the rectified output voltage feeding the precipitator section has a negative potential with respect to electrical earth.

Often, an inductor is placed in series with the primary winding of the transformer.

This has the effect of adding to the series impedance of the transformer, thereby limiting the input current to the power supply in the event of sparking or arcing within the precipitator section [2].

The topology shown in figure 3.1 is referred to commercially by precipitator manufacturers, as a 'thyristor- rectifier set" and has been the conventional precipitator power supply adopted by manufacturers for over 30 years.

The power electronics, current limiting inductor, switchgear and control electronics that constitute the supply are normally contained within the same cubicle. The high voltage transformer, however, is situated in its own containment storehouse to comply with health and safety legislation. This is detailed further in section 3.4.4.

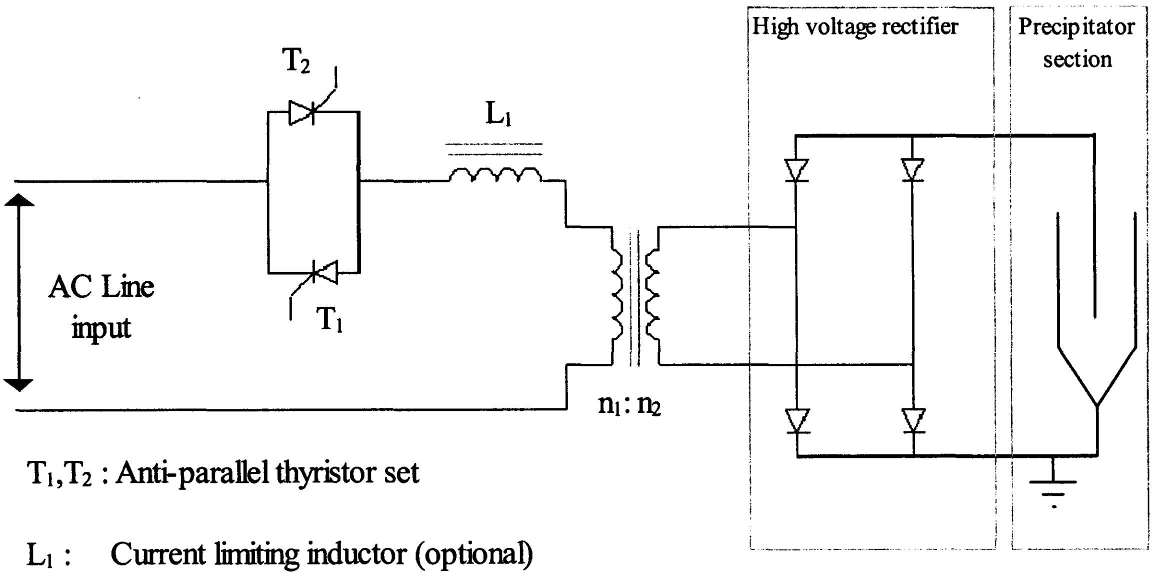

T_1, T_2 : Anti-parallel thyristor set

L_1 : Current limiting inductor (optional)

$n_1 : n_2$ High voltage step-up transformer

Figure 3.1 Conventional precipitator power supply

3.2 Operational principles of the thyristor regulated precipitator power supply.

The high (negative) DC output voltage of the power supply shown in figure 3.1 is controlled by the variation (advancing or delaying) of the thyristor firing angles with respect to the zero voltage crossover point of the AC input line voltage.

Figures 3.2 and 3.3 show typical line voltage, primary current, precipitator voltage and current waveforms for a thyristor-rectifier set supplying a precipitator section, illustrating how these parameters are influenced by a variation in thyristor firing angle.

From figure 3.2, in this particular example, with the thyristor firing angle set to 54^0, the precipitator voltage can be seen to have a peak value of 75kV and a minimum value of 45kV.

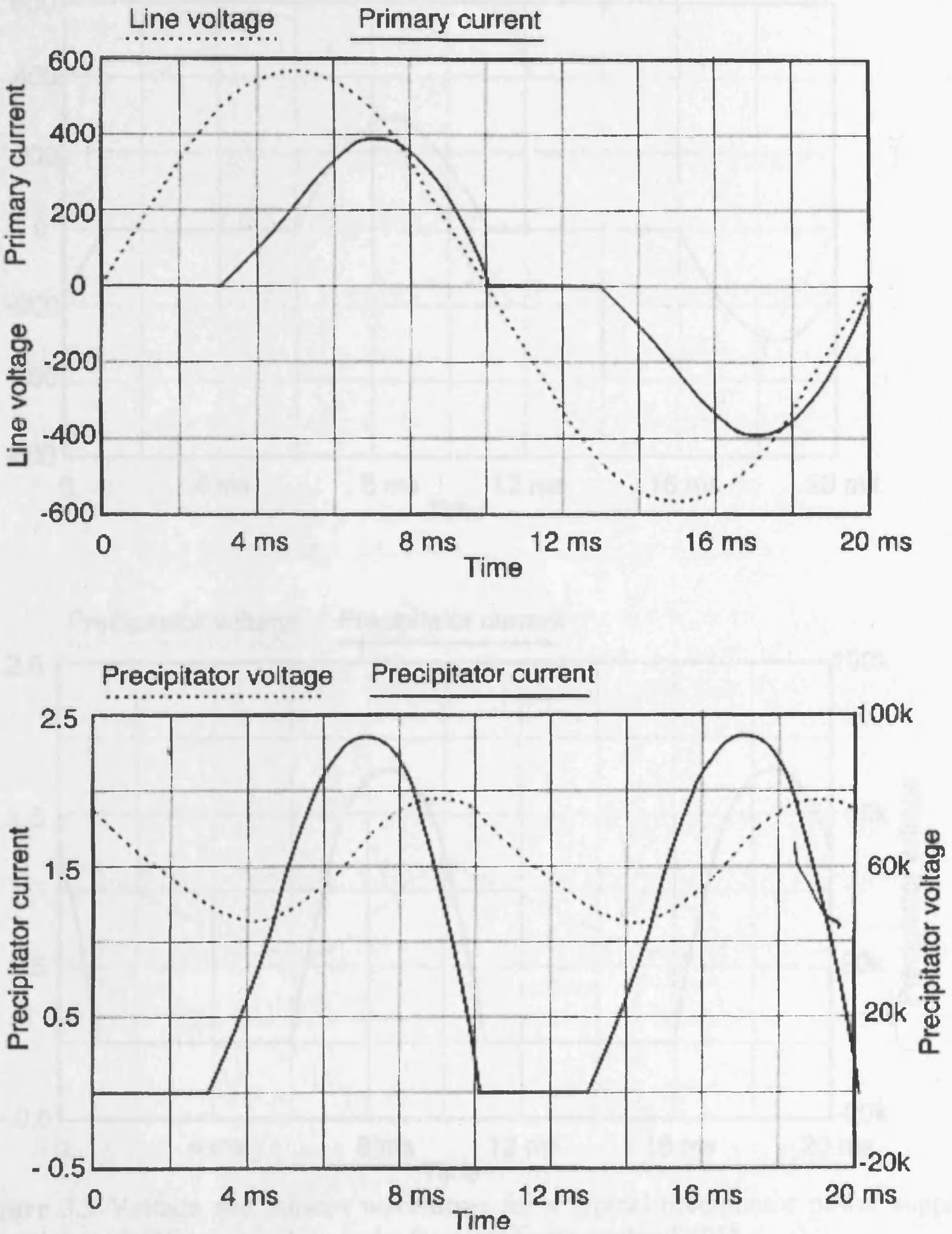

Figure 3.2 Voltage and current waveforms of a typical precipitator power supply operating with DC energisation and a thyristor firing angle of 54^0.
[Courtesy of K.Parker [2]]

In figure 3.3, the firing angle (delay time) is increased to 108^0, the precipitator voltage can be seen to have a peak value of 45kV and a minimum value of 23kV.

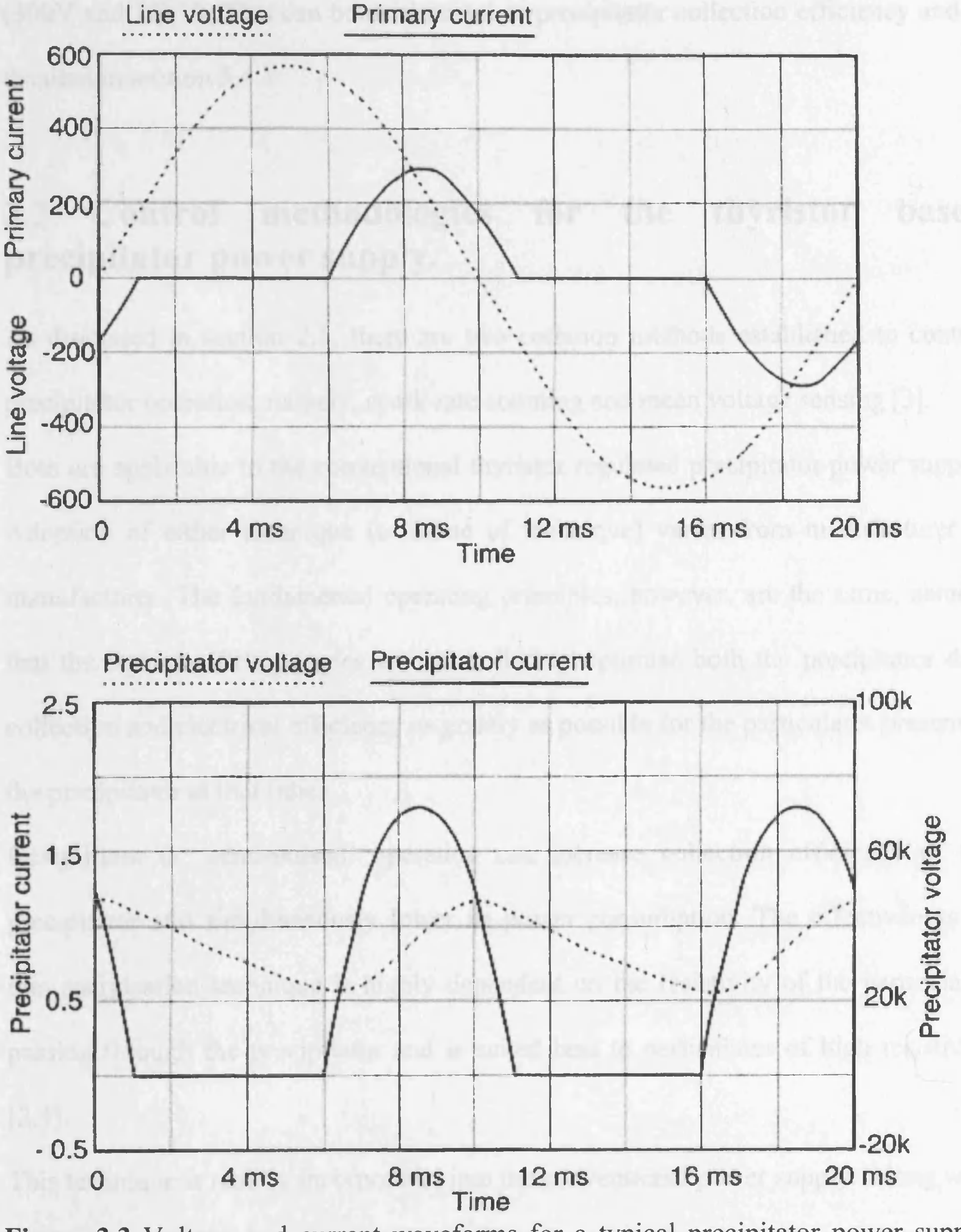

Figure 3.3 Voltage and current waveforms for a typical precipitator power supply operating with DC energisation and a thyristor firing angle of 108^0
[Courtesy of K.Parker [2]]

It is evident from the two examples shown in figures 3.2 and 3.3 that there is significant voltage ripple present on the DC output level supplying the precipitator (30kV and 22kV). This can be detrimental to precipitator collection efficiency and is detailed in section 3.4.1

3.3 Control methodologies for the thyristor based precipitator power supply.

As discussed in section 2.5, there are two common methods established to control precipitator operation, namely, spark rate counting and mean voltage sensing [3].

Both are applicable to the conventional thyristor regulated precipitator power supply. Adoption of either technique (or name of technique) varies from manufacturer to manufacturer. The fundamental operating principles, however, are the same, namely that the thyristor firing angles are controlled to optimise both the precipitator dust collection and electrical efficiency as greatly as possible for the particulates present in the precipitator at that time.

Intermittent or 'semi-pulsed' operation can increase collection efficiency of the precipitator and simultaneously lower its power consumption. The effectiveness of this energisation technique is highly dependent on the resistivity of the particulates passing through the precipitator and is suited best to particulates of high resistivity [2,4].

This technique is readily incorporated into the conventional power supply. Along with controlling the firing angle of the thyristors, the control electronics will allow suppression of a certain number of half cycles of the primary current delivered to the transformer by the single phase AC line input. This suppression is achieved by setting the thyristor firing angles to 180°.

The optimum suppression period, i.e. the period for which particulate collection and/or electrical efficiency is highest, is a complex function of many factors including precipitator particulate resistivity, discharge electrode geometry and flow rates within the precipitator as detailed in section 2.4.2.

In modern versions of the thyristor rectifier set, a range of suppression periods is stored within the control electronics of the power supply and the suppression period best suited to precipitator conditions at that time will be selected by operational staff [5].

3.4 Limiting factors of the thyristor regulated precipitator power supply.

3.4.1 Ripple magnitude

Conventional transformer–rectifier sets have output voltage ripples that are typically between 40% and 50% of the mean voltage. This can be seen in figures 3.2 and 3.3 where the ripple magnitudes are 30kV and 22kV respectively.

The secondary output of the high voltage transformer undergoes rectification by a full wave, single phase bridge rectifier. Hence, the fundamental frequency of the ripple voltage is twice that of the AC line supply. Arcing occurs if the peak of the voltage ripple exceeds a critical value and so for much of the cycle, when the voltage is much less than this critical value, little corona current is produced. Typically the mean current is much less than half that produced at the peak.

Figure 3.4 shows a typical precipitator V-I relationship for a dust burden of moderate resistivity. The ideal operational point would be with a ripple free DC voltage level, thereby maintaining a high average precipitator voltage and current. However, it is clear that the ripple magnitude lowers the minimum instantaneous voltage and current (point A). Consequently the average precipitator voltage deviates away from the optimum operational level. This can have an adverse effect on the collection efficiency of the precipitator, particularly when the precipitator is operating with a dust burden of low to moderate resistivity.

In this particular example, the optimum precipitator voltage for high collection efficiency is shown as point B. This point is highly dependent on several factors such as particulate resistivity, discharge electrode geometry and flow rates within the precipitator as detailed in section 2.4.2.

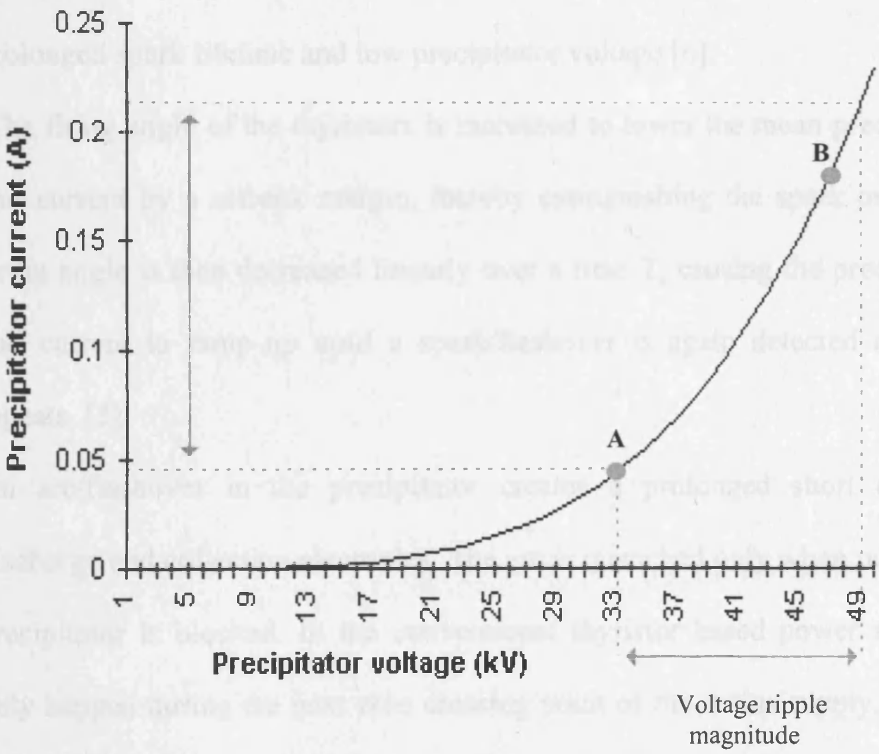

Figure 3.4 Typical Precipitator V-I relationship for a dust burden of Moderate resistivity

3.4.2 Power supply response to sparking and arcing within the precipitator

There are various control methodologies used by different manufacturers to energise a precipitator efficiently. Whilst the name, and operational claims of the control system varies from manufacturer to manufacturer, the fundamental principles of operation remain the same. Spark rate counting (section 2.5), as a control method, is still used widely throughout precipitator industry. Figure 3.5 illustrates the control strategy.

A spark is detected by monitoring of the precipitator voltage through a potential divider network. In the event of a spark a momentary dramatic decrease of precipitator voltage is experienced. An arc or flashover is characterised by a prolonged spark lifetime and low precipitator voltage [6].

The firing angle of the thyristors is increased to lower the mean precipitator voltage and current by a setback margin, thereby extinguishing the spark or flashover. The firing angle is then decreased linearly over a time T_s causing the precipitator voltage and current to ramp up until a spark/flashover is again detected and the process repeats [3].

An arc/flashover in the precipitator creates a prolonged short circuit between discharge and collection electrodes. The arc is quenched only when power flow to the precipitator is blocked. In the conventional thyristor based power supply, this can only happen during the next zero crossing point of the mains supply. It is, therefore, possible for an arc to last a duration of half a mains cycle (10ms on a 50Hz mains supply) and, to avoid multiple arcing, at least a further half cycle before recharging of the precipitator can take place [2].

On precipitators operating with multiple arcs, this 'down time' can become significant resulting in a lower average precipitator voltage, lower current and a consequent lowering of collection efficiency. Secondly, multiple arcing of long duration can be harmful to the precipitator installation and reduce its operational life expectancy.

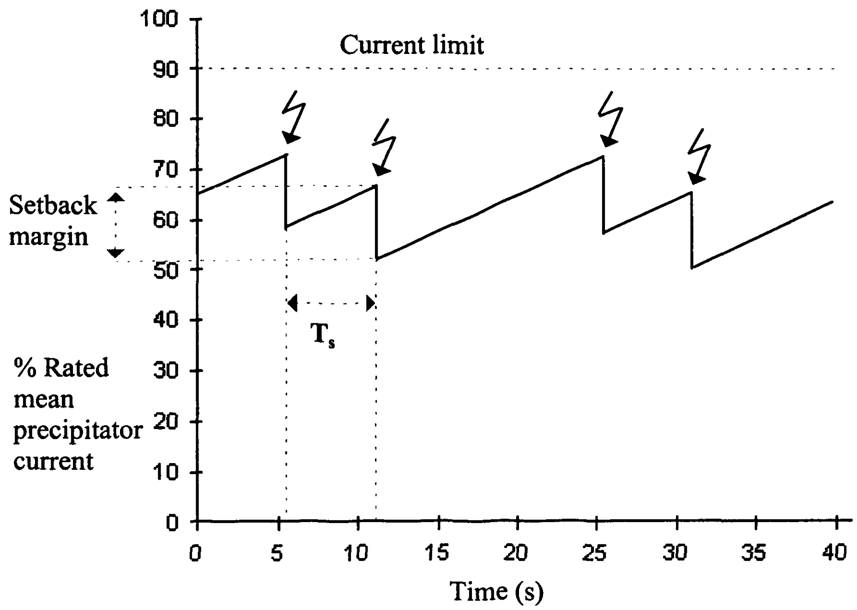

Figure 3.5 Spark rate counting control principle

3.4.3 Cabling and switchgear sizing to cope with single-phase operation.

The thyristor regulated power supply draws input power from a single-phase connection. Consequently the input line current is significantly higher than if the supply was based on a three phase input connection. This results in all mains voltage side components such as cabling and switchgear having to be dimensioned larger than if power was drawn from a 3-phase system. This problem was recognised some years ago and attempts were made to use three-phase energisation. However, this led to unresolvable problems with arc quenching within the precipitator and three phase investigations were halted [2].

3.4.4 Size, weight and cost considerations of the high voltage, oil insulated step up transformer.

The step up high voltage transformer used in the thyristor regulated power supply is based upon a mains frequency (50 Hz, UK), iron cored structure. To achieve the required insulation strengths within the transformer structure, oil is used as the insulating media. To avoid electrical breakdown of the oil due to a build up of impurities at areas of high electric stress, it must be continuously filtered and pumped around a sealed containment vessel [7].

Due to the iron core construction of the transformer, the low frequency mains operation and the use of insulating oil, the size and weight of the transformer is considerable.

Figure 3.6 shows such a transformer; taken out from a conventional thyristor based power supply at Didcot 'A' coal fired power station, UK

Because the transformer is oil insulated, a health and safety requirement is that it be housed in its own individual containment cell. In a typical precipitator installation there may be as many as 40 thyristor rectifier sets, each set energising a section within the whole precipitator. Therefore, the civil engineering costs of actually installing the power supplies, along with the required sealed transformer cells is significant.

A second consequence of this is that the 'primary' side of the supply (thyristors, switchgear, control electronics etc) is housed in a cubicle separate from, and possibly a considerable distance from the transformer rectifier units (figure 3.7). This again, increases the cost and complexity of installation .

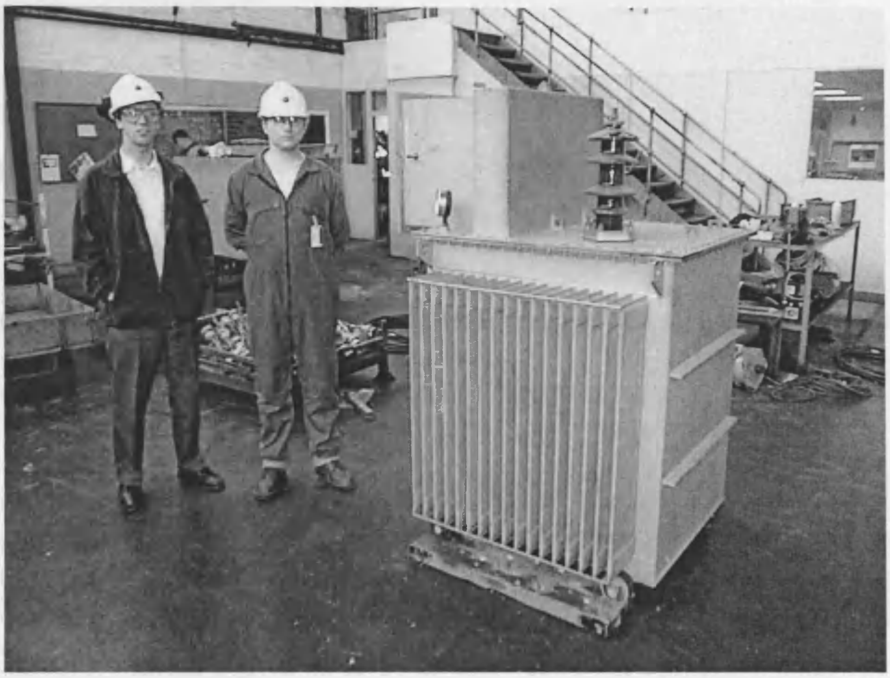

Figure 3.6 High voltage (54kV output) transformer-rectifier taken from a conventional precipitator power supply

Figure 3.7. Area containing all the precipitator power supplies cubicles at Didcot 'A' power station. The transformer- rectifier containment sheds are a considerable distance from this area

3.4.5 Summary of power supply characteristics

The following advantages and disadvantages of the thyristor regulated precipitator power supply can be summarised:

1. A robust, well known topology

2. Output voltage ripple is appreciable and can have a detrimental effect on the particulate collection efficiency of the precipitator

3. Power supply response time to sparks and flashover within the precipitator is poor due to the low frequency operation and switching characteristics of the thyristors

4. Since the power supply is itself powered from a single-phase supply, then input line current will be higher than that of a system powered by three-phase supply.

5. Consequently all switchgear and cabling will have to be rated for this higher current

6. The high voltage, oil insulated transformer is large, heavy and requires its own containment cell to comply with health and safety legislation

7. Because the transformer-rectifier and the rest of the power supply are separated from each other, power supply installation is made more complex and costly

3.5 Research Objectives

The specific objectives of the project was to produce a step change in precipitator power supply design, advancing it to encompass modern technology, and thereby making electrostatic precipitators more controllable and efficient. The EPSRC PEDDS LINK project entitled 'VARIWAVE' was funded to design, build and test a new high frequency, switched mode based precipitator power supply prototype.

3.6 Industrial motivation

Many plants in the UK need to reduce particulate emissions to meet new environmental legislation which requires that the amount of particulate exhausted to the atmosphere be strictly controlled. As concerns over health and the environment increase then the legislated requirements are becoming more stringent for example as stated in 1988 EC Directive which also specifies requirements for emission of SO_2 and NO_x [8].

Increased awareness of the effects of atmospheric pollution has meant that electrostatic precipitators, which have been used since the early part of this century to separate particulate matter from process gas streams, are now required to achieve efficiencies in excess of 99.7% for a number of application. These changes have challenged the precipitation industry to consider how the equipment can be improved to meet ever tightening legislation where control is now focusing on heavy metal and respirable size particulate discharges.

3.7 Market requirement

There is a market requirement for constructing a modern electronic power supply which would give the following advantages over the traditional supply:

- Higher efficiency
- Highly controllable and programmable
- No oil filled transformer
- Three phase supply

The estimated European market for power supplies for new precipitators is estimated at up to £10 million/year. If the new supply design is sufficiently advantageous to precipitator performance, this market may be expanded by the replacement of existing conventional supplies. During the lifetime of a precipitator, the total power and maintenance costs to the utility are normally reckoned at £2000 per kW rating of the precipitator (this is based on a typical penalty clause to a manufacturer by a utility). Typically a power station may use 300kW to supply its precipitators. If the efficiency of the supply is improved from 60% to 90% this would imply a 100kW saving or around £200,000 over the lifetime of the precipitator [9].

3.8 Design concept

There has been little change in the precipitator power supply market away from conventional thyristor regulator based power supplies.

This is in part due to the lack of availability of 'off the shelf' high voltage step-up transformers capable of operating efficiently at frequencies above that of the mains supply.

The transformer structures being used are still based around oil insulation, which bring with it the problems of regular oil cleansing [7], containment cells, and the distance between transformer/rectifier and the rest of the supply.

The aim of the research is to address the limitations of conventional precipitator power supplies by utilising modern power semiconductor device technology, modern magnetic material technology and novel methods of high voltage insulation.

These technological advances would be applied to produce a prototype precipitator power with significant operational improvements over the conventional supply.

3.8.1 Expected improvements of the prototype supply compared to conventional supplies

The improvements in power supply operation where expected to be:

- *Significant reduction of precipitator voltage ripple*

A significant reduction in precipitator voltage ripple due to the use of high frequency switching topologies. This results in a higher average precipitator mean discharge current and, as described in 3.4.1, an improved particulate collection efficiency.

- *A faster power supply response to precipitator sparking and flashover (arcing)*

A faster response to sparking/arcing in a precipitator implies less power wastage and less operational 'down time'. The conventional thyristor based power supply has severe drawbacks in its response to flashover within a precipitator as detailed in 3.4.2.

It was envisaged that if a topology was designed whereby switch off control was possible at any time, not being under the control of the mains cycle, then arc times would be minimised resulting in a higher precipitator electrical and particulate collection efficiency.

- *An increase in power supply efficiency*

High frequency switched mode operation would allow the adoption of low loss, ferrite technology in the design of the high voltage step up transformer core.

Consequently, transformer power losses would be reduced resulting in an increase in power supply efficiency.

- *Reduction in size and weight of the transformer-rectifier stage*

High frequency switched mode operation results in a higher transformer power density in comparison to mains frequency operation [10,11,12]. Consequently the required geometric size of the transformer will be reduced resulting in a more compact and lighter design.

The use of novel insulating techniques within the transformer rectifier unit would further minimise the sizing of the transformer- rectifier.

In fact, an aim of the research was to produce a transformer-rectifier unit compact enough to be housed in the same cubicle as the rest of the power supply. This would mean a complete power supply unit could be housed in a single containment cell.

This is unlike the conventional situation where the transformer-rectifier and rest of the power supply are separated and housed in different areas.

- *Reduced input line currents and consequent cabling/switchgear size reduction.*

The prototype supply would be developed with a three-phase diode bride rectification unit as the front end of the power supply instead of the conventional single-phase thyristor regulator. This will result in a reduction in sizing of required input cabling and switchgear.

- *Ability to improve the quality of power drawn from the utility*

As an optional feature of the proposed prototype power supply, investigating the use of a three phase diode rectifier with boost converter for active line current shaping and DC link voltage boost was carried out. The reasoning behind this decision was two fold:

1. To provide an input stage whereby high quality input line currents could be drawn from the utility resulting in low input current distortion and high input power factor.
2. A consequence of the active line current shaping is a boosting of the rectified DC output voltage of the topology above that which would normally be achieved with a standard three phase bridge rectifier. This feature could be utilised to provide a means of either minimising the necessary turns ratio of the high voltage step up transformer for a given precipitator output voltage or to increase the magnitude of the precipitator output voltage for an 'already built' transformer. Naturally, this increase would be limited by the electrical insulating strength of the transformer-rectifier unit in question.

3.9 The Prototype precipitator power supply system

Figure 3-8 (overpage) details a system diagram of the proposed prototype precipitator power supply.

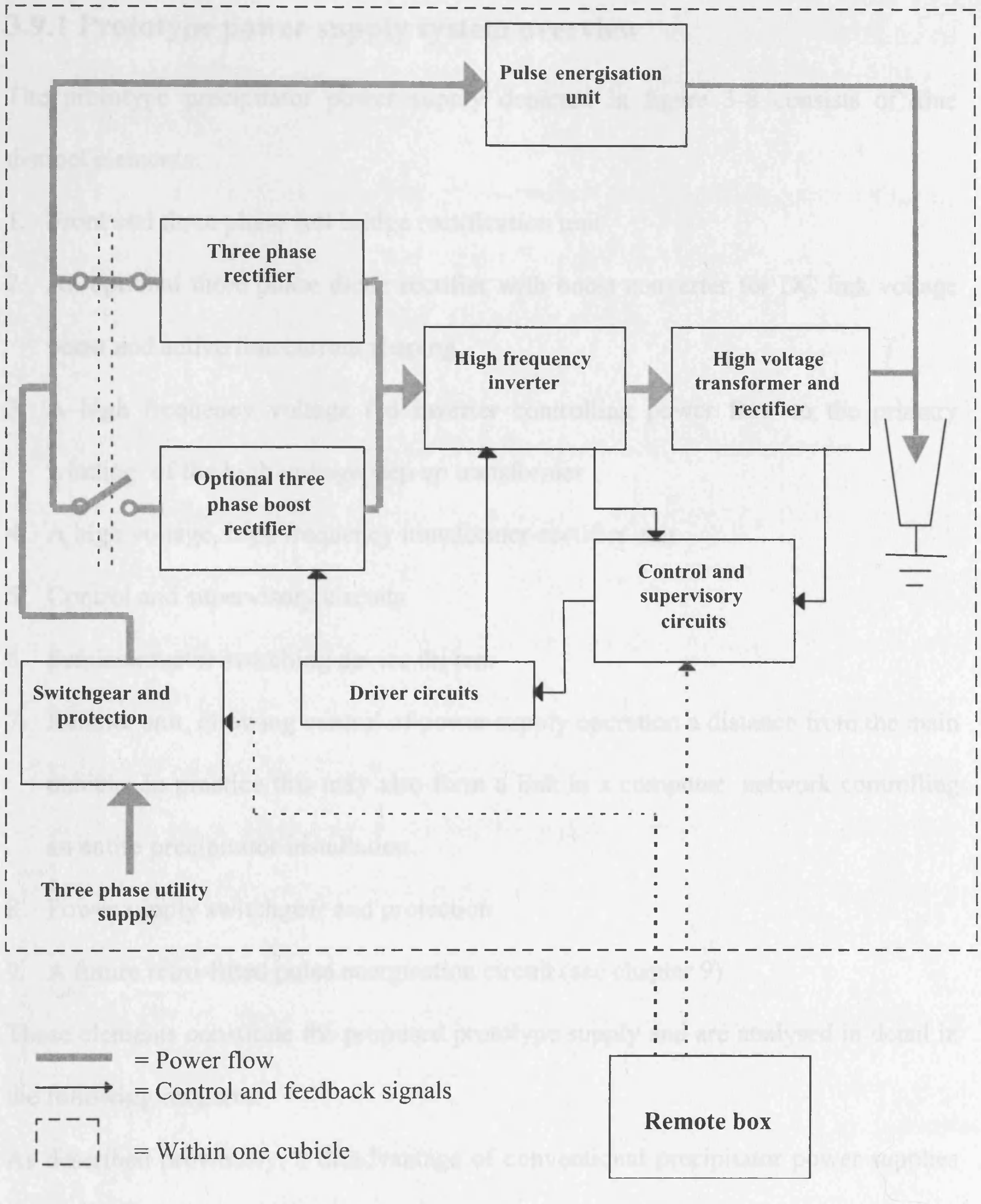

Figure 3-8 System diagram of proposed high voltage power supply

3.9.1 Prototype power supply system overview

The prototype precipitator power supply depicted in figure 3-8 consists of nine distinct elements:

1. Front end three phase full bridge rectification unit
2. An optional three phase diode rectifier with boost converter for DC link voltage boost and active line current shaping
3. A high frequency voltage fed inverter controlling power flow to the primary winding of the high voltage step up transformer
4. A high voltage, high frequency transformer-rectifier unit
5. Control and supervisory circuits
6. Semiconductor switching device drivers
7. Remote unit, allowing control of power supply operation a distance from the main cubicle. In practice this may also form a link in a computer network controlling an entire precipitator installation.
8. Power supply switchgear and protection
9. A future retro-fitted pulse energisation circuit (see chapter 9)

These elements constitute the proposed prototype supply and are analysed in detail in the following chapters.

As described previously, a disadvantage of conventional precipitator power supplies are that the main elements of the supply and the transformer-rectifier unit are separated from each other, often by a considerable distance. This increases installation costs due to extra wiring and civil engineering demands. All elements of the proposed prototype (including transformer-rectifier) are to be housed in one cubicle, apart from the remote access unit.

3.10 Review of current power semiconductor switching devices and recommendations of usage within the prototype power supply

This is a review of current switching techniques and power semiconductor switching devices available on the market. A comparison of devices is made to ascertain which is the most suitable for use in the prototype power supply.

3.10.1 PWM (Pulsed Width Modulation) switching technique.

The PWM Technique controls power throughput of a topology by varying the duty ratio (on: off) time of the semiconductor switching device.

Switching devices acting under PWM control can operate under hard turn on and turn off conditions. The main loses in such a topology (e.g. boost converter, buck converter, full bridge inverter) are the switching losses [13,14]. These tend to limit the maximum operating frequency at which the topology can successfully and reliably operate without excessive power loss in the device and consequent lowering of power supply efficiency.

The suitability of semiconductor devices operating under hard switched PWM conditions is dependent on the characteristics of the switching device.

3.10.2 Resonant switching techniques

A resonant switching concept was proposed to improve switching losses for semiconductor switching devices in a power topology [15,16]. The resonant method of operation processes power in a sinusoidal form. The power switches are turned on or off at either zero current and/or zero voltage. This technique minimises the power dissipated in the device during transition times. Consequently, devices operating under resonant conditions generally have the ability to operate at frequencies higher than if they were operated in hard switched mode.

A disadvantage of the resonant technique is that voltage and current stresses within the device can be increased to several times that of the supply voltage and average current value [17,18,19]. This has to be carefully considered when performing a suitability investigation of a semiconductor switching device for a resonant topology.

3.10.3 Demands placed upon switching devices

Since the introduction of semiconductor switching devices, the levels of operational stress and technical demands placed upon the devices has increased considerably:

- *Higher current handling capability*

There is an ever increasing need by industry to maximise the power throughput of a single device, thus limiting the need for paralleling up devices or substituting a different switching device altogether. The current handling capabilities of a device are limited by the on state resistance or voltage drop, the turn on/turn off time and the physical heat transfer characteristics of the device.

- *Higher blocking voltages*

This is a measure of the maximum reverse blocking voltage the semiconductor switching device can operate effectively at without overvoltage failure.

- *Resistance to a high di/dt and dv/dt*

High operational frequencies brings with it higher rates of change of voltage / current and can be a limiting factor in switching device operation.

The level of di/dt and dv/dt a switching device can handle is determined by the physical structure of the device, the breakdown strength of the materials used to fabricate the device and parasitic elements existing within the structure.

- *Lower on state losses*

This is linked to the current handling capabilities of the device and the maximum temperatures allowed within the switching device structure.

Any on state voltage drop across the device will lead to power dissipation within it. This is converted into thermal energy, causing the internal temperature to rise.

The maximum power dissipation is limited by several parameters. These parameters are the maximum junction temperature, ambient temperature and case temperature and are correlated by the thermal resistance of the device.

- *lower switching losses (i.e. shorter turn on & turn off times)*

This varies considerably from one device to another. Since these losses are proportional to the switching frequency of the device, a major motivation in power semiconductor technology is to minimise these switching times as much as possible. The 'ideal' switching device would, naturally, have zero turn on/turn off time. In practice however, these times do exist and place a limitation on maximum operational frequency and/ or power handling capability.

- *Higher operational frequencies.*

High frequency switched mode power topologies have several key advantages over low frequency power supplies operating in a 'linear' or regulatory mode:

- The minimisation of voltage and current ripple magnitudes within the switching topology
- High frequency operation allows the use of low loss ferrites as the core material in transformers and inductors. This results in a higher operational power density, a reduction in physical size and weight and lower core losses. The maximum switching frequency at which a device can operate is a function of not only the characteristics detailed previously (switching loss, turn on/ turn off times, heat

transfer characteristics) but also the manner in which the device is being switched. For example, an IGBT operating in a hard switched topology may be limited to an operational frequency of 20-30 kHz. The same IGBT in a resonant mode of operation may operate at frequencies upto 100kHz provided the IGBT rating is such that it can deal with possible elevated levels of voltage and current.

- *Simplified drive requirements.*

The methods required to successfully drive switching devices is naturally dependent on the semiconductor structure of the switching device and varies considerably from one device to another. Clearly, the simpler the device is to drive then the more attractive it is to the customer as it minimises complexity of the system, minimises component count and associated costs.

3.10.4 Power semiconductor devices

3.10.4.1 Power bipolar transistor

The power bipolar junction transistor is a two junction self-controlled device where the collector current is under the control of the base drive current. It is a linear device that is operated in switching mode. The bipolar power transistor has existed for many decades and in that time constant improvements have been made. Devices are now available with breakdown voltages above 1400V and average current ratings upto 1000A.

The current gain of a bipolar transistor is low, typically between three and seven and this value varies widely with collector current and temperature.

This indicates that considerable drive power is required to maintain a saturated switch under high load current conditions. The use of a Darlington BJT does increase the current gain, however, considerable base drive power is still required [20,21].

Although devices are manufactured at high current ratings it is not possible to operate the device at the maximum current rating since the gain would become impracticably low. Devices tend to be over-dimensioned in terms of their power handling capability. A further limitation of the power transistor is their susceptibility to 2nd breakdown effects, which occur when the collector current is switched on. An effect known as emitter crowding can develop whereby the collector current is constricted into a narrow area. This tends to create a hot spot and the device fails due to thermal runaway.

Typical applications of a power transistor would be motor drives and switch mode power supplies operating at several kHz.

3.10.4.2 Thyristor

A thyristor is a three-junction pnpn device where pnp and npn components are connected in a regenerative feedback mode. The thyristor is triggered into forward conduction by a short current pulse applied to the gate. Once the device is in a conduction state the gate loses control to turn off the device. Thyristors are available with blocking voltages upto 6500V and current ratings of 3500A.

Switching times of a power thyristor are slow in comparison with other switching devices and this normally limits thyristor operation to frequencies of a few kilohertz. They are, therefore not suitable in high frequency switched mode power supplies.

Typical applications of a thyristor would be DC motor drives, large power supplies (MVA) and electronic circuit breakers due to the large current surge capability of the thyristor [22].

3.10.4.3 Gate Turn Off Thyristor (GTO)

The gate turn off thyristor has a structure which is similar to that of a conventional thyristor. The difference between them is that a GTO can, not only be turned on by a positive gate current but also turned off by a negative gate current pulse.

GTOs are manufactured covering a wide range of power and voltage levels. Ratings of 4.5kV and 3000A have been achieved. The Turnoff current gain is poor (4 to 5) and because of high switching losses, GTO operational frequencies are normally limited to below 1kHz [22].

Currently, GTOs are mainly used in variable speed motor drives, and medium frequency inverter topologies with operating frequencies below 2kHz.

3.10.4.4 Static Induction Thyristor (SITH)

The Static Induction Thyristor (SITH) is a self controlled GTO like device that was commercially introduced in 1988. It is a 'normally on' device which ceases conduction when a negative current pulse is applied to the gate.

The turn off current gain of a SITH is low (< 3) and the device displays a large tail current. Unlike conventional thyristors the current surge capabilities of a SITH are usually limited to 3 to 4 times their average current rating. Typical operational switching frequencies are of the order of several kHz and modern devices have ratings as high as 1200V, 300A [23]

3.10.4.5 MOS Controlled Thyristor (MCT)

The MCT is a thyristor like device that can be turned on or off by application of a short voltage pulse to the MOS gate of the device. A negative pulse turns the device on; a positive pulse turns it off. Typical operational frequencies are in the order of tens of kHz and the on state conduction drop is low (typically 1.1V).

Developmental samples where released by Harris semiconductor in 1988. Commercial MCTs are now available with ratings of 600V, 60A. Typical applications are AC motor drives, high frequency switched mode power supplies and induction heating systems [24].

3.10.4.6 Power MOSFET

The Power MOSFET is a voltage controlled, insulated gate device developed in the late 1970's. If the gate voltage is positive and beyond a threshold value, a conducting channel is induced within the device permitting current to flow between drain and source. Because a power MOSFET is a majority carrier device, the turn on and turn off times are extremely short compared to thyristor technology. A disadvantage of the power MOSFET is its relatively large conduction drop (3.2V) [25].

Power MOSFETS have been applied widely in medium power, low voltage, high frequency switching applications where the operational frequency has been tens of kHz [26,27].

At medium to high power applications, especially when high blocking voltages are required (>500V) then the MOSFET suffers from high on state losses. At present, MOSFETS are available with ratings of 800V, 200A.

3.10.4.7 Insulated Gate Bipolar transistor (IGBT)

IGBTs combine the high input impedance and high speed characteristics of MOSFETS with the high conduction (low saturation voltage) of bipolar transistors.

The device is normally turned on by applying a positive voltage to the gate (8-15V) and turned off by applying a zero or negative voltage (0 to -15V).

The IGBT has a higher current density compared to a BJT and MOSFET, its input capacitance is significantly less than that of a MOSFET and its operational frequency range is higher than that of a BJT. An IGBT is a faster device than a BJT and can operate at high power levels upto 30kHz switching frequency. Modern commercial IGBTs are available with ratings of 1700V, 800A. The device has found popularity in applications such as AC motor drives, high frequency (>20kHz), high power switched mode power supplies and U.P.S applications. Due to these favourable characteristics IGBTs have replaced BJTs in the majority of applications and are now the 'switching device of choice' in the majority of high frequency, medium to high power applications [22,28,29]

Table 3-1 shows a detailed comparison of the power semiconductor devices covered in this review displaying key criteria, which determine suitability for a particular operation.

3.10.5 Choice of semiconductor device

The most popular power semiconductor devices in the industrial marketplace have been reviewed in this chapter to determine their technical advantages and limitations when used in a switched mode, high frequency power supply. The device which shows the most favourable properties for a medium power, high frequency switched mode supply is the IGBT which has the following desirable characteristics.

- Simple drive requirements
- Operation at realistic switched mode frequencies (20kHZ)
- Relatively low losses at switched mode frequency

- Device availability at high voltage and current ratings
- Reasonable cost and availability

	BJT	*thyristor*	*GTO*	*SIT*	*MCT*	*MOSFET*	*IGBT*
Present power capability	1400V 1000A	6500V 3500A	4500V 3000A	1200V 300A	600V 60A	800V 200A	1700V 800A
Gating	current	current	current	current	voltage	voltage	voltage
T j range	-40 to 150	-40 to 125	-40 to 125	-50 to 150	-55 to 150	-55 to 150	-20 to 150
Conduction drop at rated current	1.9V	1.9V	4V	4V	1.1V	3.2V	2.5V
Turn on time	1.7μs	1.1μs	4μs	2μs	1μs	0.9μs	0.5μs
Turn off time	5μs	220μs	10μs	9μs	2.1μs	1.4μs	0.5μs
Protection	base control	gate inhibit or fast fuse	gate inhibit or fast fuse	gate inhibit or fast fuse	gate inhibit or fast fuse	gate control	gate control

Table 3-1 Comparison of power semiconductor switching devices [23]

3.11 Summary

The conventional thyristor based power supply still used widely in electrostatic precipitators has been analysed. Both operating principles and control methodologies have been examined and limiting factors of these supplies discussed.

With ever tightening legislation concerning particulate discharge to the atmosphere Electrostatic precipitators are now required to achieve collection efficiencies in excess of 99.7%. This has challenged the precipitator industry to examine all means by which this collection efficiency can be maintained at economic costs.

A modern switched mode power electronic supply is proposed which has key advantages over the conventional power supply in electrical efficiency, voltage ripple reduction, installation, operational and maintenance costs.

Power semiconductor switching devices have been evaluated to determine suitability for use in the proposed power supply and the IGBT is found to be highly suitable to the required operating conditions.

3.12 References

1. **Hall** HJ, "Trends in electrical energisation of electrostatic precipitators", Proceedings of the Electrostatic Precipitator Symposium, pp.178-189, Birmingham, AL, USA, 1971.

2. **Parker** KR, "Applied Electrostatic Precipitation", 1997 Chapman and Hall, ISBN 0 7514 0266 4

3. **Reyes** V, "Comparison between traditional and modern automatic controllers on full scale precipitators", Proceedings of the EPRI/EPA symposium, 2A,March 1987, USA

4. **Tachibana** N, "Intermittent energization on electrostatic precipitators", Journal of Electrostatics, 25 (1990) 55-73

5. **Reyes** V, and Lausen P, "Utilization of computer systems for control and operation of electrostatic precipitators", 5Th International Conference on Electrostatic Precipitation, session C4, EPRITR 103048 Vol. 2, Cal, USA, 1993

6. **Reyes** V, "Determination of corona power in a precipitator section", FLS Miljo, 1991

7. **Pohl** HA. Dielectrophoresis, Cambridge University Press, Cambridge, 1978

8. EC Directive on the limitation of emission pollutants into the air from large combustion plants. Official Journal of EC, legislation, L336, 7.12.88

9. **Lefley** PW and Fothergill JC, "A high voltage power supply for electrostatic precipitators", LINK PEDDS grant application, 1995

10. **McLyman**,Wm.T, Transformer and inductor design handbook, New York, Dekker, 1978

11. **Pressman** AI, "Switching power supply design", McGraw-Hill, 1991, ISBN 0-07 050806-2

12. **Mohan** N, Underland, M and Robbins, P, "Power Electronics", John Wiley, 1989

13. **Kazimierczuk** MK, "A complete characterisation of boost zero-current-switching resonant DC/DC converter for steady state operation," Proc. Powercon. Intern. Conf, Sept. 1987

14. **Kazimierczuk** MK, and Jozwik J, "DC/DC converter with class E inverter and rectifier", High Frequency power Conversion, pp.383-394, 1989

15. **Buchanan** E and Miller, EJ, "Resonant switching power technique", IEEE Proc. Power Electronics Specialist Conference, pp. 188-193, 1975
16. **Miller** EJ, "Resonant Switching power Conversion", IEEE Power Electronics Specialist Conference, USA, pp. 206-222, 1976
17. **Schlect** MF and Casey, LF, "Comparison of the Square –wave and Quasi-resonant Topologies", IEEE Proc. APEC'87, pp.124-134, 1987
18. **Lotfi** AW, "Comparison of stresses in quasi-resonant and pulse width modulated converters", IEEE proc. Power Electronics Specialist Conference, Japan, pp.591-598, 1988
19. **Erickson** RW, Hermandez, AF and Witulski, AR, "A none linear resonant switch", IEEE Power Electronics Specialist Conference, USA, pp.43-50, 1989
20. **Sack** L, "Reduction of losses in drive circuits for bipolar power transistors", Proc. EPE, pp. 717-722, 1989
21. **Rozman** AF, "A new high speed, magnetically coupled base drive circuit for very wide duty application", Proc. High frequency power Conversion Conf. pp. 1999-127, 1988
22. **Bose** BK, "recent advances in power electronics", IEEE transactions on power Electronics, Vol7, No1, 1992
23. **Wouw** van de T, and Houldsworth, J, "Active switched for high frequency power conversion compared", Proc. PCIM, pp. 1-13, 1989
24. **MOS Controlled Thyristor** (MCT) Datasheet, Harris Semiconductor, 1996
25. **Lorenz** L, "Application guidelines for selecting power semiconductor switches", Proc. PCI, pp. 226-261, 1989
26. **Inniss** B, and Carli, G, " A novel 12kW switch mode power supply", IEEE CH2928-0/90/0000-0088$01.00, 1990

27. **Fujita** H, "An approach to a broad range of power control in voltage source series resonant inverters for corona discharge treatment", IEEE Trans. Power Electronics 0-7803-3840-5/97, 1997

28. **Heron** C, "Application advantages using IGBT technology", IXYS Corporation, San Jose, CA, USA, 1989

29. **Toshiba** IGBT Data Book, 1995

4. DESIGN AND CONSTRUCTION OF THE POWER SUPPLY TRANSFORMER AND RECTIFIER

4.1 Requirements of the high voltage transformer.

The high voltage DC requirement of an electrostatic precipitator has conventionally been achieved with a single phase thyristor based AC regulator. The regulator controls the power delivered to the low frequency, iron cored, oil insulated transformer. The secondary voltage of the transformer is subsequently rectified and transmitted to the precipitator installation through a high voltage cable.

There has been little progress from this system over the years due, in part to the lack of availability of high frequency, high voltage transformers commercially.

The topology, whilst robust and relatively simple has severe drawbacks:

- Low power supply efficiency due to the high leakage reactance of the transformer and the iron core losses of the transformer
- Sluggish operating characteristics
- Size, weight, civil engineering and maintenance costs associated with the oil insulated transformer- rectifier set.
- Significant ripple content in the output voltage resulting in a lower average voltage between the electrodes and a possible reduction in collection efficiency [1]

The improvements that may be expected from the adoption of high frequency switched mode operation are:

- High frequency operation will allow much more precise control over operational parameters such as precipitator voltage level, current level, and voltage rise times

- High frequency operation will result in a high power density within the transformer core and hence a significant reduction in the size and weight of the high voltage transformer and consequent installation and maintenance costs.
- The ability to modulate the output voltage (intermittent or semi-pulsed energisation) at much higher speed than can be achieved with the standard topology. In electrostatic precipitators this method may improve particle charging and collection depending on the characteristics of the dust or gas.
- In conventional 50Hz thyristor-rectifier based power supplies, the ripple magnitude can be in the order of 50% of the mean voltage. Figure 4-1 shows a typical voltage-current relationship for a precipitator installation. The significant ripple results in lower average voltage between the precipitator electrodes and a possible reduction in collection efficiency [1]. A reduction of ripple content in the output DC level, which is expected with high frequency operation will lead to a higher average precipitator current and a possible improvement in particulate collection. It is estimated that the ripple content may be reduced to as little as 1% (4.6.2)

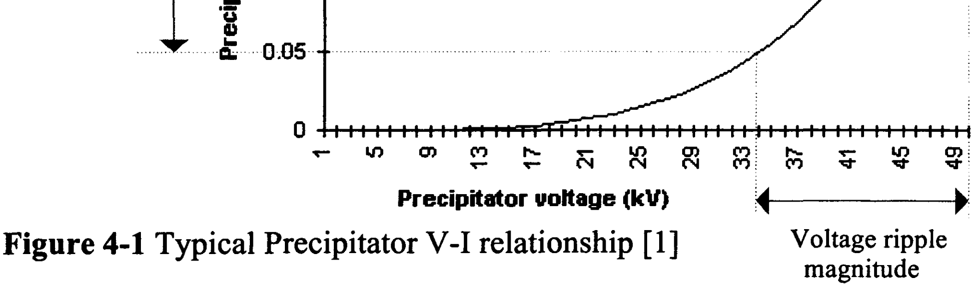

Figure 4-1 Typical Precipitator V-I relationship [1]

A thorough and careful design of a high voltage transformer is required to ensure that the electrical and magnetic loads are optimised, the electrostatic and thermal stresses are acceptable for the voltage and power requirements, and that parasitic parameters are minimised.

The design of a high voltage, high frequency transformer differs widely from the standard design methodology [2]. Several related issues must be analysed:

1. Insulation requirements
2. Corona effects
3. Core loss and heat dissipation
4. Parasitic elements
5. Rectification requirements

High voltage transformers generally have a large turns ratio, typically 600:1 to 900:1. Sufficient insulation thickness between the primary and secondary windings is required to avoid electrical breakdown. Therefore, the electromagnetic coupling of the primary and secondary winding will not be as tight as in conventional low voltage transformers. This results in a parasitic leakage inductance referred to the primary side, which can effect the maximum power throughput of the transformer and place overvoltage stress on power electronic switching devices. Hence, the design must be a judicious compromise between the two conflicting factors.

Furthermore, the high number of turns required for the secondary winding causes a high distributed capacitance. When referred to the primary this capacitance value is multiplied by the square of the turn's ratio and therefore is not negligible. This parasitic capacitance induces an ineffective current in the secondary winding which can result in a loss of power supply efficiency.

Corona discharge can seriously effect the operation and life expectancy of a high voltage transformer. Any sharp corner or protrusions may lead to an enhanced electric field and corona in this vicinity. A corona will create highly reactive molecules, which will, in time degrade the insulation leading to electrical breakdown.

Bearing these factors in mind a high voltage, high frequency transformer for an electrostatic precipitator power supply was designed with the following electrical specification:

- $Vprimary_{max}$ = 560V (quasi-square wave)
- $Vsecondary_{max}$ = 50kV
- Power rating = 25kVA
- Switching frequency = 20kHz
- Maximum operational flux density = 0.25T

4.1.1 Modular design of transformer and rectification unit.

The transformer is designed to drive a cascaded full wave rectification unit and to have a modular design so that different power supply voltage ratings may be specified. The transformer is therefore designed with two secondary bobbins each driving a diode bridge as shown in figure 4-2.

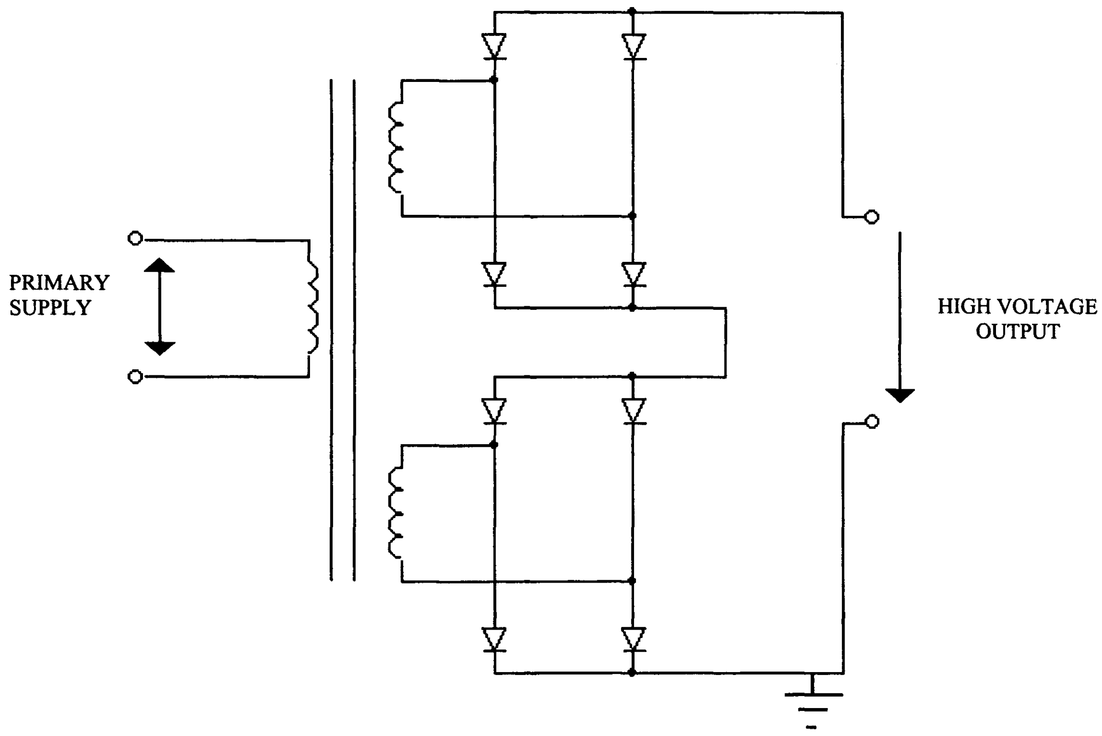

Figure 4-2 Transformer and rectification network.

4.2 Design of the high voltage transformer

The transformer design required consideration of the insulation materials, the magnetic materials and the management of electrical, magnetic and thermal stresses.

4.2.1 Magnetic Design

Because of the high frequency operation of the transformer, a low loss ferrite material is used for the core construction.

4.2.1.1 Ferrite characteristics

Ferrites are ceramic ferromagnetic materials having a crystalline structure consisting of mixtures of iron oxide with either manganese or zinc oxide. Their eddy current losses are negligible, as their electrical resistivity is very high, in the order of 10^5 to 10^6 ohm-m. Core losses are then due mainly to hysterisis losses which are so low as to permit use of some materials upto a frequency of 1Mhz [3, 4, 5]

4.2.2 Selection of ferrite material

The most common operational frequency range of a ferrite material in power electronics is 2-100 kHz. The cores used for frequencies in the 20 to 50 kHz range are generally operated at flux densities approaching 200 to 250 mT .[4]

In high power applications, losses within the core are specified as a power loss density (P_v) (the total power loss per unit volume or unit weight of the core) at a given frequency and flux density. Power losses are usually expressed in material data pages for power ferrites as the power loss density in mW/cm^3.

A high saturation manganese-zinc ferrite designed specifically for high power, high frequency applications was chosen as the core material to be used in the high voltage transformer (F44 - MMG Neosid Ltd). It is a low loss ferrite used at operational frequencies upto 300 kHz depending on flux density magnitude. Characteristics of the ferrite are shown in figures 4-3, 4-4 and table 4-1.

The power loss density of the ferrite at the working frequency of 20kHz and ambient temperature level can be seen from figure 4-3 to be approximately 170mW/cm^3.

Notably, figure 4-4 shows that the power loss density for this particular ferrite type can display an inverse relation to temperature over the range 0 to 100 °C.

At ambient temperature, the power loss density is 140 mW/cm^3 reducing to 85 mW/cm^3 at 100 °c.

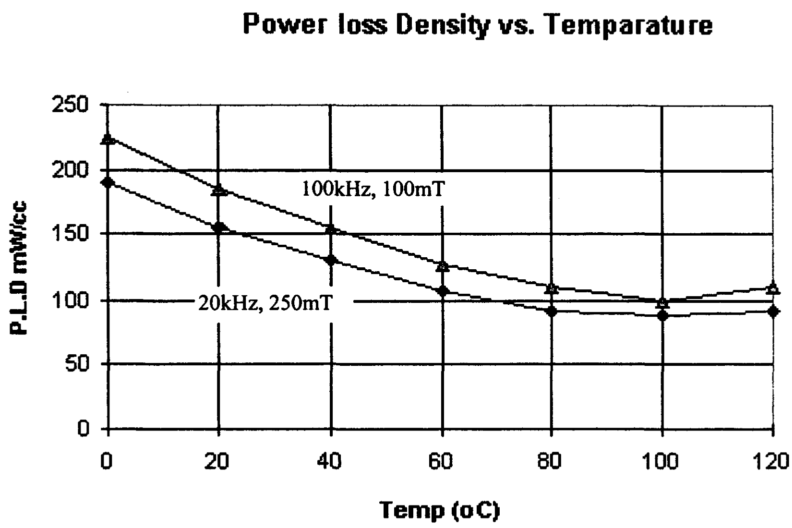

Figure 4-3 Power loss density vs. temperature

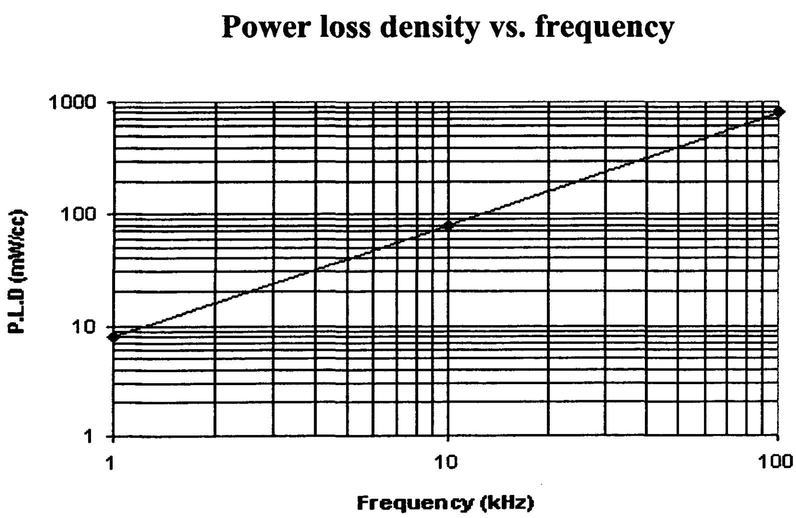

Figure 4-4 Power loss density vs. frequency

Parameter	Unit	F44 Ferrite
Initial permeability (nominal)	-	1900 (+/- 20%)
Saturation flux density (typical)	mT	500 @ 25^{0}C 400 @ 100^{0}C
Coercivity (typical)	A/m	27
Curie temperature (minimum)	^{0}C	230
Resistivity (typical)	ohm-m	10^6

Table 4-1 F44 Ferrite Characteristics taken from MMG Databook [4]

4.2.3 Mechanical properties of the chosen ferrite

A rectangular core of cross sectional area 2" x 2" was chosen, not only fulfilling the magnetic and thermal requirements but also providing enough mechanical strength to be able to withstand the weight of the bobbin structures and general high voltage framework surrounding the core.

The physical shrinkage during sintering of a ferrite core is a function of many manufacturing parameters and it is not possible to avoid its variations. Consequently the dimensional tolerances are large (+/- 0.06" is a typical value).

Despite an exhaustive supplier search worldwide it became clear that the required size and cross sectional area of ferrite core required could not be achieved with a single ferrite structure.

To achieve the required size of core it was necessary to purchase "I" shaped cores of dimensions 100 x 25 x 25mm, to machine and grind the ferrites to achieve acceptable tolerances (+/- 0.25mm) and bond these to the correct dimensions.

The bonding adhesive and clamping force used was after consultation with technical staff at the ferrite manufacturers.

4.2.4 Magnetic calculations

A method described by McLyman [6] was used for the magnetic calculations. This method has been implemented using MathCAD, the output of which is in Appendix A. This implementation is very useful as it facilitates an iterative design process in which the consequences of a parameter change are immediately reflected on the computer screen.

The key parameters are.

- Two primary windings in series, each containing 13 turns of AWG7 wire giving a primary copper loss of 4.6 W
- Two secondary windings in parallel, each containing 700 windings of AWG21 wire
- Total losses of 510W

4.2.5 Thermal analysis

The McLyman technique was also used for checking the thermal design of the transformer. The MathCAD output, shown in Appendix A, also shows such thermal calculations. A maximum temperature rise of 50°C is specified. The method indicates a minimum required area of 533 cm^2, which is considerably less than the area of approximately 1500 cm^2 that was actually used (although only about 50% of this is exposed) A temperature rise of less than 50°C was therefore to be expected.

4.3 Design of high voltage bobbins

4.3.1 Choice of insulating bobbin material

It is clear that the secondary bobbin needs to be large enough to prevent surface tracking from the high voltage winding to the transformer core or the primary winding. The thickness of the bobbin also has to be great enough to prevent breakdown through the insulation. Tracking always occurs when the surface electric field exceeds that of either the solid or the encapsulation surrounding it. It may occur at lower fields because of physical and chemical inhomogeneities on the surface and because of geometric field enhancements. Although reliable figures appear to be hard to find, a distance of at least 1 kV/mm is commonly allowed for well controlled surface conditions (for example Rowland and Nichols [7] found voltages of at least 15kV were required to sustain dry band arcing over a 10mm gap on an "arc resistant thermoplastic compound".)

The voltage waveform to be experienced by the high voltage bobbin is rather unusual in this application since it is of high frequency (20 kHz) and has a negative DC offset of half the supply output voltage. The negative DC offset may give rise to space charge injection [8] and consequent field distortion within the insulation. The maximum (Poissonian) field within the material may therefore be greater than the average (Laplacian) applied field. The high frequencies may also lead to accelerated ageing processes due, for example, to partial discharges. Because of the large bobbin size, it was decided not to use a very expensive material such as PTFE. Nylon 6,6 was chosen as a compromise between ease of manufacture, cost and insulation properties. The breakdown strength of such materials under these conditions is not readily available but work by Montanari, Dissado, Crine and others [9-11] suggests that they should be able to withstand such conditions at fields up to approximately 12 kV/mm. Because of the unknowns, especially to do with space charge effects, it was decided to limit the electric field in the bobbin to 5 kV/mm. Nevertheless, this is still high; typically 0.5 to 2.0 kV/mm are used in high voltage supplies for safety critical applications [12].

4.3.2 Primary and secondary bobbin structure

Two bobbins of the required thickness and geometric shape and size where machined from a solid block of nylon 6,6.

The primary and secondary bobbins where designed with several criteria in mind

- To provide a mechanically rigid structure for the primary and secondary windings
- To provide sufficient insulation to prevent electrical breakdown from the secondary to the primary windings
- To encase the ferrite core as tightly as possible providing mechanical rigidity
- To minimise both the leakage inductance and parasitic capacitance of the transformer as much as possible
- To provide an ease of assembly/ disassembly from a prototyping standpoint

Figure 4-5 shows the secondary bobbin structures. The secondary bobbins were designed to fit as firmly as possible over the primary bobbins providing sufficient insulation to prevent electrical breakdown and so producing a semi 'bifilar' winding topology. Figure 4-6 shows the primary bobbin structure. The bobbins where designed to fit the length of the core limb and to provide a firm 'slip' fit with respect to the core.

Both the primary and secondary bobbins where based on a machined cylindrical geometry.

Figure 4-8 shows a completed high voltage bobbin. The secondary bobbins contain two unusual features:

1: The use of electric stress relief rings

2: A slotted bobbin that allows layered secondary windings.

An analysis of these features is detailed in 4-5-3 and 4-5-4.

Figure 4-9 shows the high voltage transformer structure including secondary windings, ferrite core and insulating framework.

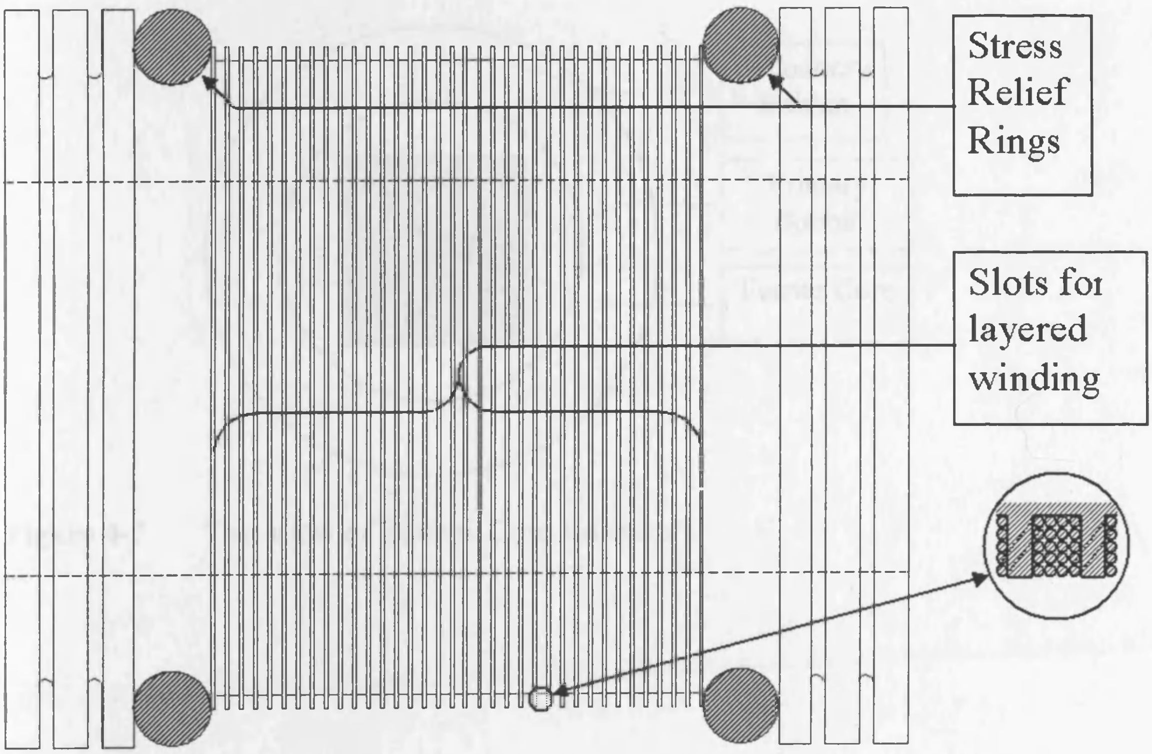

Figure 4-5 Secondary Bobbin

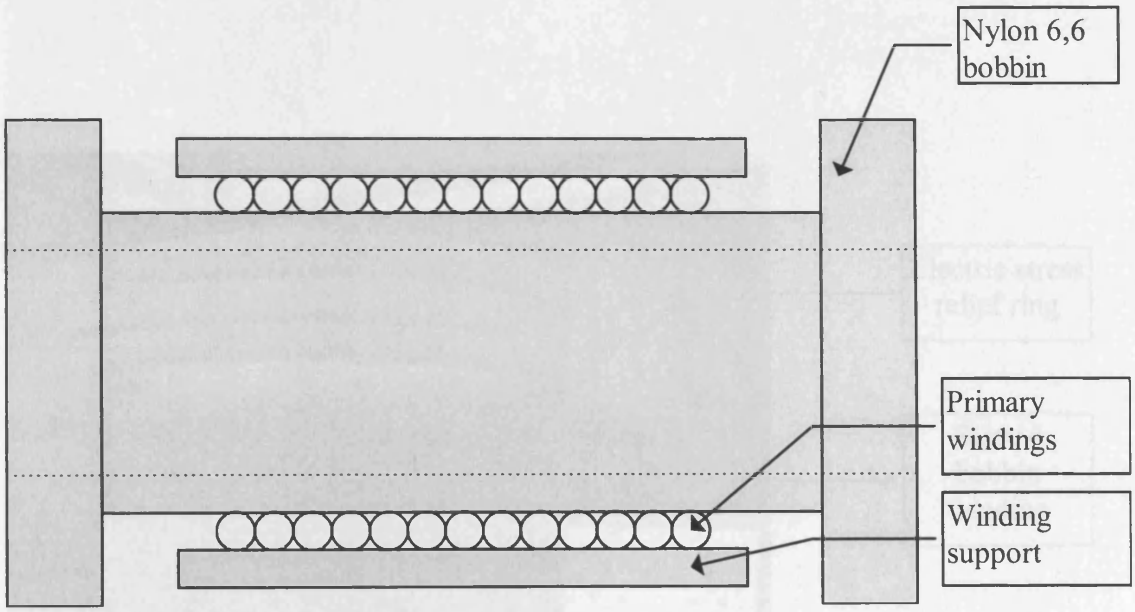

Figure 4-6 Primary bobbin

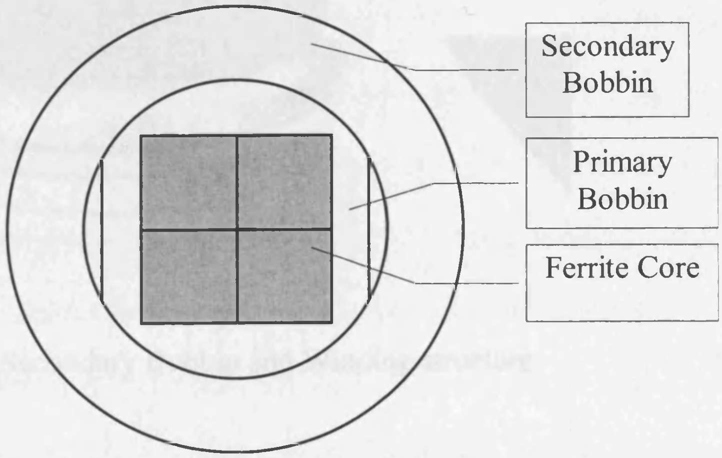

Figure 4-7 Top View of Bobbin/ Core structure

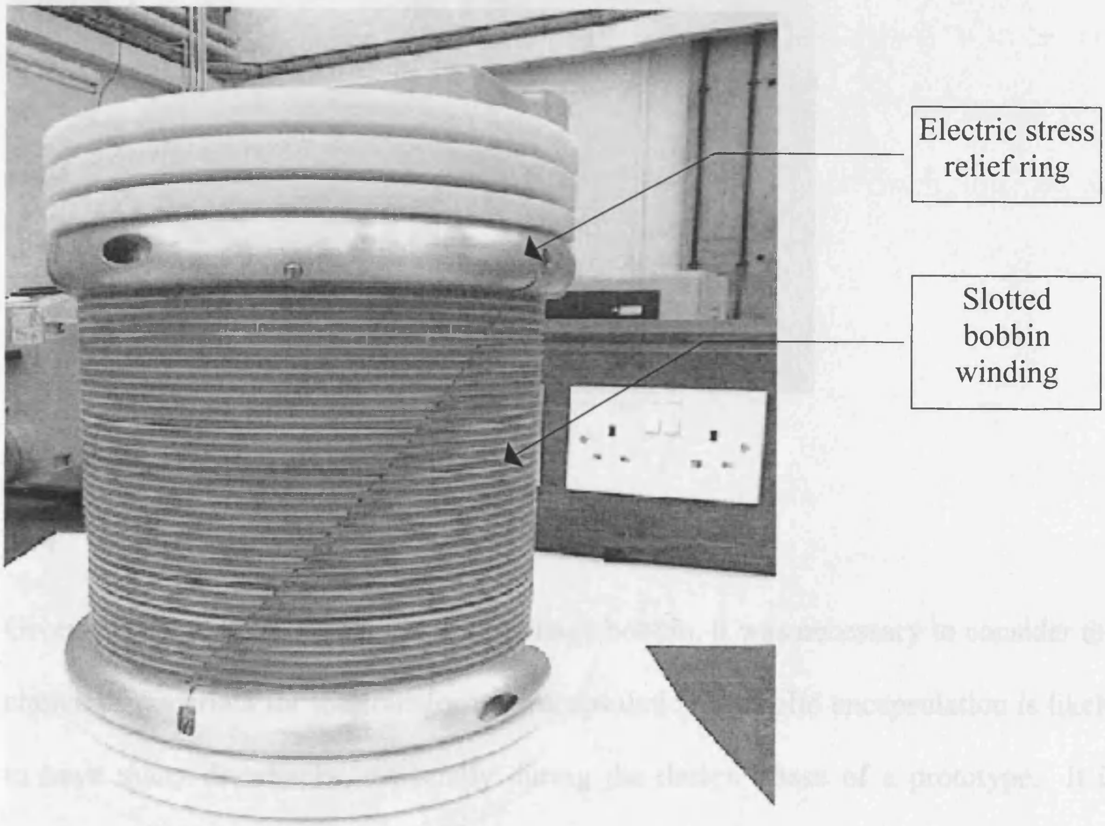

Figure 4-8 Secondary Bobbin and Winding structure

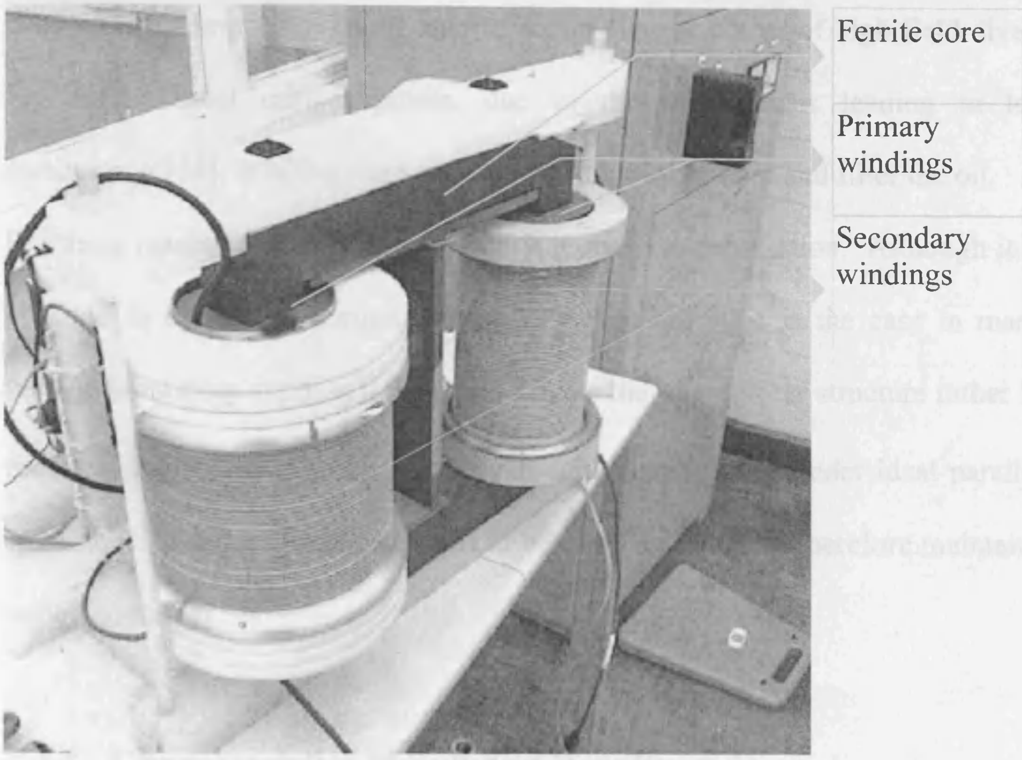

Figure 4-9 Transformer structure

4.4 Transformer encapsulation

Given the considerations for the high voltage bobbin, it was necessary to consider the choice of materials for the transformer encapsulation. A solid encapsulation is likely to have many drawbacks, especially during the design phase of a prototype. It is likely to be inferior in transporting heat from the transformer, it would be impossible to make modifications to the transformer once the encapsulation was in place and, if the encapsulation suffered electrical breakdown, it may be necessary to completely re-build the transformer. A fluid encapsulation such as transformer oil or an insulating gas was therefore considered. Transformer oil is a good medium for heat transport. Under ideal natural convection conditions it has a heat transfer coefficient of approximately 95 $W.m^{-2}K^{-1}$; this is equivalent to forced air cooling with a flow velocity of approximately 25 $m.s^{-1}$ [13]. In a prototype structure, however, oil causes severe disassembly problems, as the oil needs to be removed from the surfaces of all components. Impurities in oil tend to accumulate at points of high field divergence, i.e. at the most critical points, due to dielectrophoresis leading to localised discharging [14]. It is therefore usual to continuously pump and filter the oil.

For these reasons it was decided to use a gaseous encapsulation. Although it may be possible to use air at normal atmospheric pressure (this is the case in many high voltage laboratory supplies), this would make the transformer structure rather large as the breakdown strength of air is only 2 – 3 $kV.mm^{-1}$ even under ideal parallel plate conditions. The air would also need to be clean and dry and therefore maintained in a sealed container.

4.4.1 Characteristics of Sulphur Hexafluoride

Sulphur Hexafluoride (SF_6) is a non-toxic, inert, insulating gas of high dielectric strength and thermal stability. The strong interaction of high energy electrons with the polyatomic SF_6 molecule ensures that SF_6 breakdown is only possible at relatively high electric field strengths [13].

4.4.1.1 Electrical breakdown characteristics of SF_6

Figure 4-10 shows the breakdown strength of SF_6 as a function of gas pressure. [Figure 4-10: 50Hz breakdown strength in a homogeneous field for a 20 mm inter-electrode gap as a function of absolute gas pressure].

It can be seen that even at a pressure of 1 bar, the breakdown strength of SF_6 exceeds the maximum design strength for the bobbin (5 $kV.mm^{-1}$). At 2 bar, the breakdown strength is comparable with nylon 6,6 and so tracking resistance is unlikely to be improved above this pressure. It is noted that the breakdown strength of SF_6 is also independent of frequency.

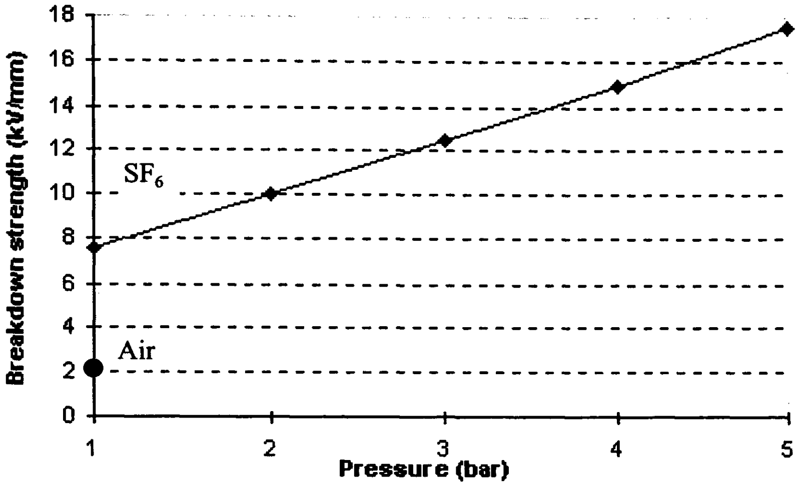

Figure 4-10 SF_6 breakdown strength vs. pressure [13]

4.4.1.2 Heat characteristics

Sulphur hexafluoride has a favourable heat transfer characteristic compared to air. Figure 4-11 shows the heat transfer coefficient of air and SF6. It can be seen that at a pressure of 2 bar and a gas flow velocity of $2 m.s^{-1}$ the heat transfer coefficient of SF_6 is approximately $66 W/m^2K$ compared to the transfer coefficient of air, which is 15 W/m^2K.

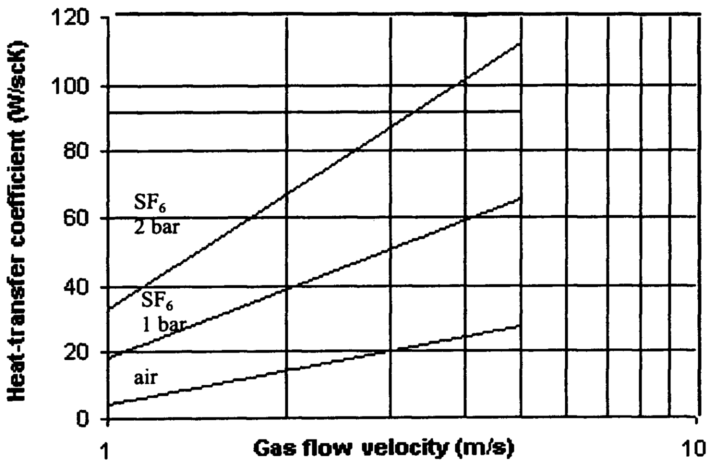

Figure 4-11 SF_6 Heat transfer coefficient vs. flow velocity [13]

It was for the reasons of dielectric strength and heat transfer capability that is was decided to use sulphur hexafluoride pressurised to a minimum of 2 bar as the encapsulation material for the transformer.

4.5 Requirements and design of the high voltage windings.

The transformer-rectification unit was required to provide a maximum DC output voltage of -50kV. The transformer topology was such that each of the two secondary windings would be energised to -25kV. These two secondary outputs would be subsequently rectified and the rectifier outputs connected serially to produce the 50kV requirement.

This meant that each secondary bobbin had to be able to accommodate 700 turns of secondary cable (Appendix A).

To achieve this it was necessary to find a cable which satisfied 3 criteria:

- Minimal cable diameter (< 1mm)
- Highest available voltage rating for a cable of this thickness
- A current rating of at least 1.6A (twice the design rating). The cable must also be able to withstand transient overcurrents of approximately 10A during precipitator arcing.

4.5.1 Selection of secondary winding cable.

A wire originally designed for aerospace and military high density wiring applications was found to be the most suited to the above criteria.

4.5.1.1 Cable specification.

The wire consists of 7 strands of 0.102 mm tinned annealed copper wire with a dual wall insulation of polyalkene and polyvinylidene fluoride, with the following specification.

1. Overall diameter = 0.68mm
2. Voltage rating = 600V
3. Current rating = 2A
4. Temperature range = -65°C to +150°C

The cable is highly flame resistant and displays a chemical inertness to most acids, alkalis, hydrocarbon solvents, fuels and lubricants. This is another favourable quality of the wire since SF_6 can produce corrosive by-products in the event of an electrical discharge (e.g. electric arcs due to a transformer fault).

4.5.2 Winding configuration

An obvious characteristic of a high voltage transformer is the high turns ratios involved requiring a large amount of secondary cable.

If we consider a secondary winding, wound in a conventional 'up-down-up' manner as shown in figure 4-12, the potential of any of the windings of the 1st layer is given by:

Eqn. 4-1 $\mathbf{V_{turn} = m \cdot b}$

m = secondary volts per turn

b = number of turns from start of layer 1

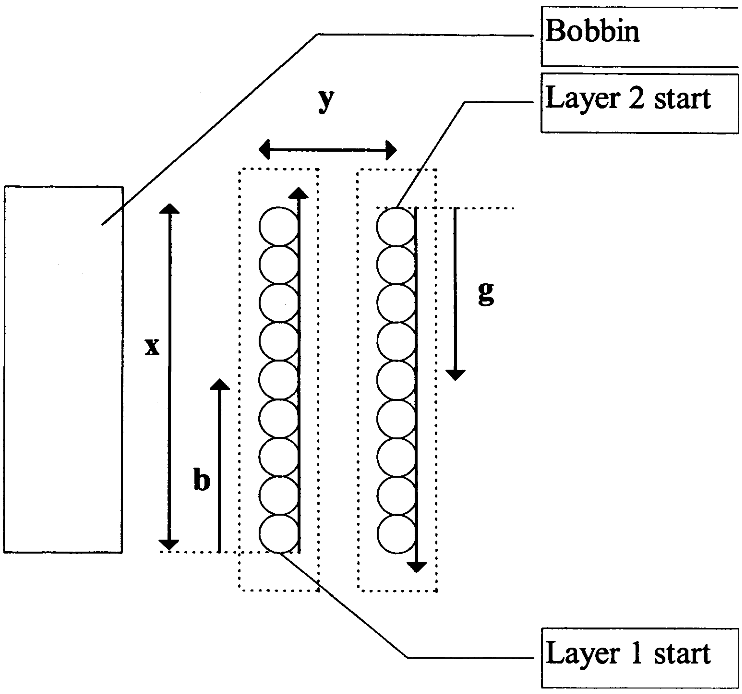

Figure 4-12 Standard bobbin winding

The potential V_{turn2} of any turn on the second layer is given by

Eqn. 4-2 $\quad \mathbf{V_{turn2} = (m.x + m.g)}$

where **x**= total number of turns in 1st layer

g= number of turns from layer 2 start point to the turn of interest

The potential difference between two adjacent windings on separate layers is

Eqn. 4-3 $\quad \mathbf{V_{adj} = m(x+g-b)}$

The maximum potential difference between two adjacent layers is

Eqn. 4-4 $\quad \mathbf{v_{max}= m(2x-1)}$

where $\quad x = \dfrac{r}{y}$ $\quad$ r = total number of secondary turns
y = total number of layers

(Equation 4-4 assumes the total number of turns per layer are equal)

Figures 4-13 and 4-14 show the normalised layer to layer voltage Vn As a function of secondary turns number and layer number . As an example, if the total number of turns was 700 distributed evenly over 5 layers the maximum normalised layers to layer voltage would be 279. In a 25kV transformer this would equate to a layer to layer electric stress of 9.96kV. As the number of layers increases the maximum electric stress between adjacent layers decreases.

This winding method requires an insulating media of suitable thickness to be placed between every winding layer to prevent electric breakdown. This results in a wound bobbin of increased size and complexity. An increase in the number of layers also results in a higher leakage inductance of the winding due to the insulating gap between layers and the consequent imperfect electromagnetic coupling coefficient [15]. This is detailed in 4.5.7.

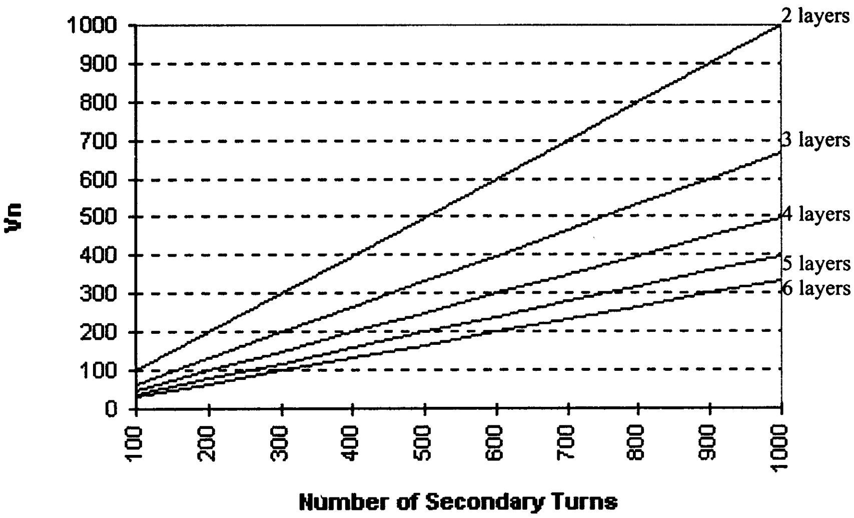

Figure 4-13 Normalised layer to layer voltage Vn vs. number of secondary turns.

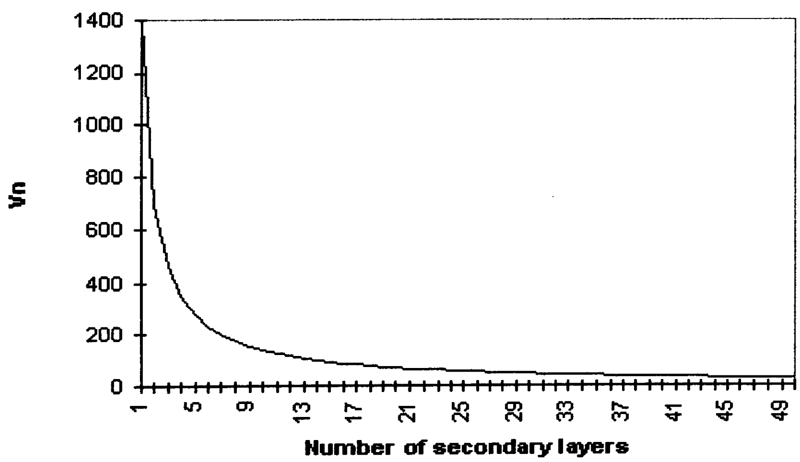

Figure 4-14 Normalised layer to layer voltage Vn vs. number of secondary layers. (Total number of secondary turns =700)

4.5.3 Slotted bobbin winding

To alleviate the problems highlighted in 4-5-2 it was necessary to think of a somewhat unusual method to wind the transformer which would minimise the electrical stresses placed on the winding layers and yet maintain a compact mechanically rigid one piece structure. Figure 4-15 shows the secondary bobbin, focusing on the slotted winding configuration adopted.

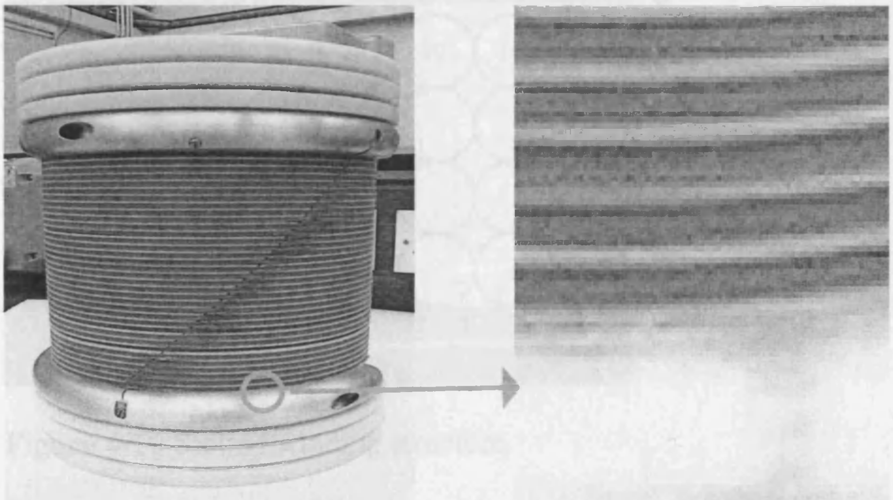

Figure 4-15 Secondary bobbin focusing on slotted winding structure

The bobbin is machined with 35 cells, each 3.75mm deep and 3mm wide. Each cell contains 20 turns wound over 5 layers in the direction indicated in figure 4-16 Each group of 20 turns is mechanically isolated from the adjacent cell by a separating wall of 1.5mm thickness. A 0.68mm channel is machined in each wall to allow continuity of the winding from cell to cell down the full length of the bobbin

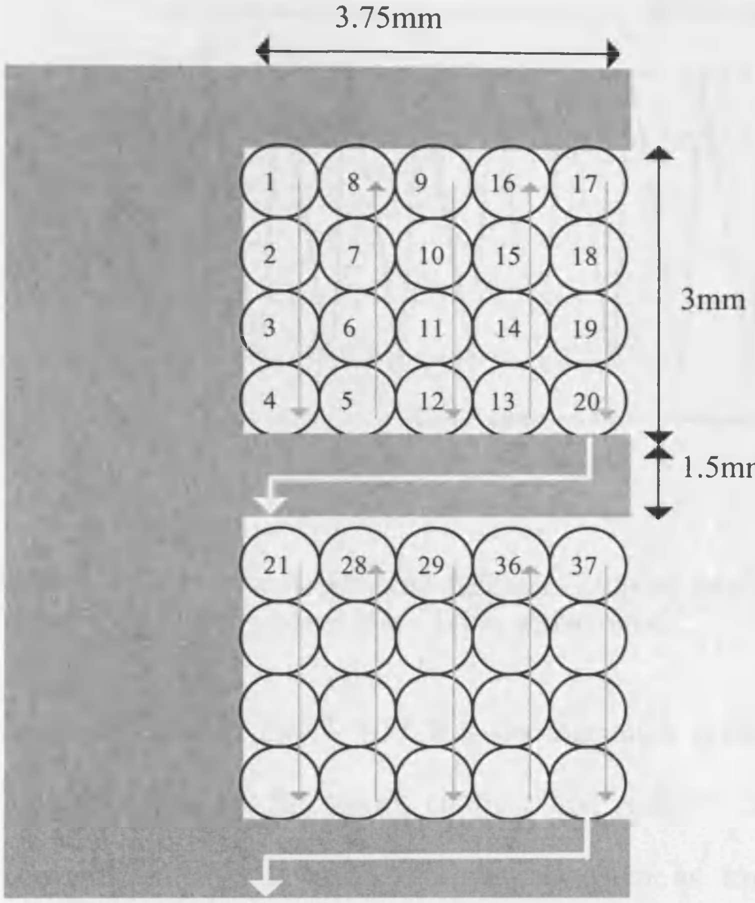

Figure 4-16 Slotted winding structure.

4.5.4 Voltage stress analysis of winding

A feature of this winding method is the significant reduction in demands placed upon the insulation of the winding wire.

Figure 4-17 shows a plot of the maximum potential difference between adjacent layers in the 2 cells shown in figure 4-16.

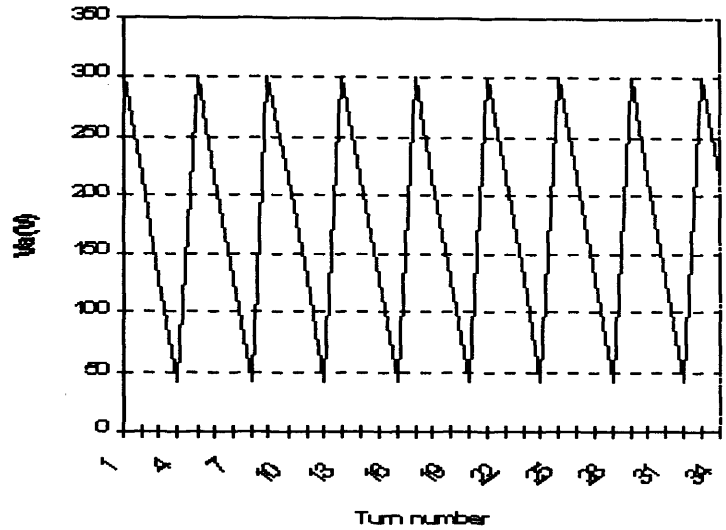

Figure 4-17 Maximum potential difference (Va) vs. turn number. Total number of turns =700; Vsecondary = 30kV (20% above rated)

It can be seen in figure 4-17 that the maximum potential difference Va between adjacent layers for the slotted configuration is 300V This can be compared to the conventional five layered configuration given as example in 4.5.2 where the maximum potential difference per layer is.9.96kV.

The voltage rating of the wire used to wind the secondary is 600V and so no extra layer to layer insulation is required.

The maximum potential difference across separating walls is 985V, which is well within the insulation strength of the material.

4.5.5 Electrostatic stress analysis of winding and bobbin

Such an arrangement does give rise to locally high divergent fields at the corners at the bottom of the slots and an electrostatic analysis was made to ensure that a field of 5 $kV.mm^{-1}$ was not exceeded. The results of this analysis are shown in figure 4-18.

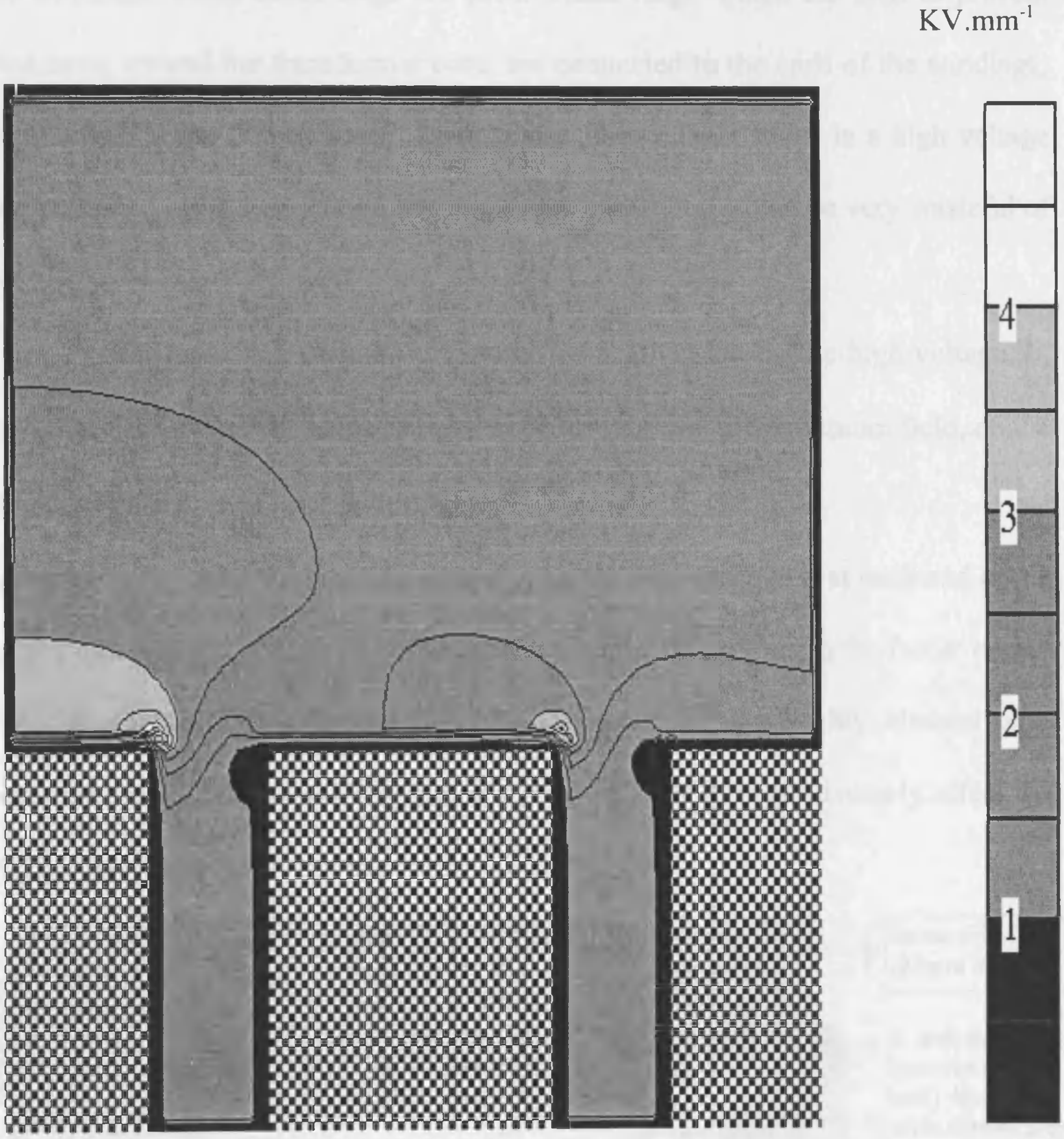

Figure 4-18 Electrostatic field analysis around slots in the high voltage bobbin. The hashed regions corresponding to the windings which are assumed to be equipotential regions. The highest fields of 5 kV.mm^{-1} can be seen to occur on the corners of the slots. (Courtesy of Dr JC Fothergill, Leicester University)

4.5.6 Electric stress relief rings and anti-tracking grooves

In order to obviate the divergent electric stress that would otherwise occur at the ends of the windings, stress relief rings are used. These rings, which are split to prevent shorted turns around the transformer core, are connected to the ends of the windings; indeed they form the connections. The usual way to relieve stress in a high voltage transformer is to alter the winding spacing at the ends but this can be very wasteful of space.

The stress relief rings decrease the divergent field ($\approx V/r$) due to the high voltage, V, by increasing the effective radius of the wire, r. In this way the maximum field, on the inside of the stress relief ring, is limited to 5 $kV.mm^{-1}$.

Two grooves of the dimensions shown in figure 4-19 are machined at each end of the bobbin to increase the effective path length from the winding ends to the ferrite core. Before the transformer is encapsulated, all surfaces are thoroughly cleaned with solvent to clear the surfaces of any inhomogeneities, which may adversely affect the breakdown strength.

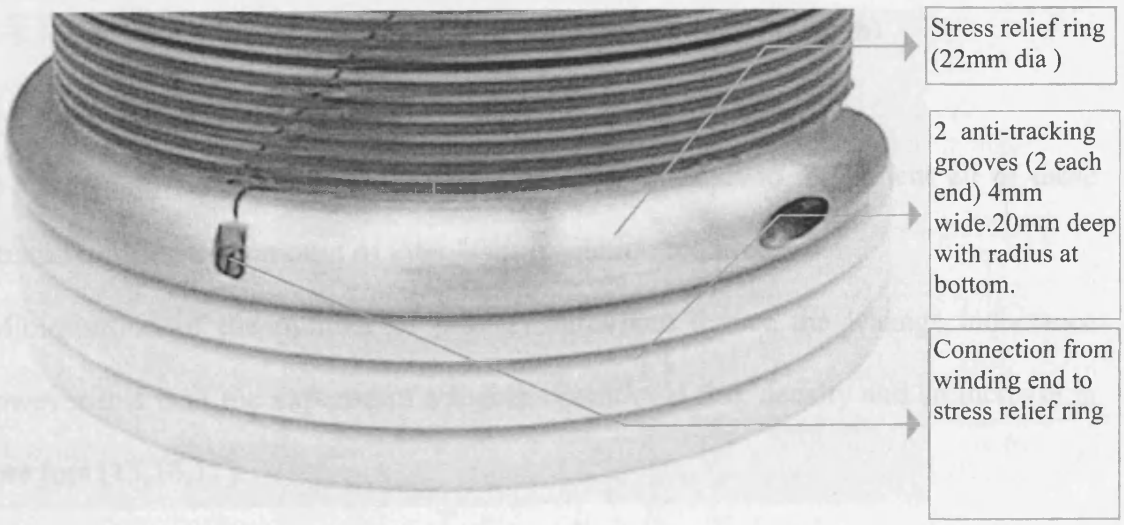

Figure 4-19 Electric stress relief rings and anti-tracking grooves

4.5.7 Minimisation of leakage inductance

When currents flow through windings of a transformer, they establish a resultant mutual flux that is confined essentially to the magnetic core. However, a small amount known as leakage flux links only one winding and does not link the other. The effects of this leakage flux can be accounted for by an effective leakage inductance L_p.

Energy that is stored in the leakage flux can be detrimental in a high frequency inverter because when it is released it can result in oscillatory overvoltages across the switch leading to device Failure [6]. Furthermore leakage inductance increases the impedance of the transformer which is unfavourable for high power applications.

Leakage inductance is dependent on the physical geometry of the transformer and the physical orientation and spacing of the windings. It is almost independent of core material [6].

The magnitude of leakage inductance can be minimised in several ways:

1. Minimise the number of primary turns
2. Reduce the build of the coil
3. Increase the winding width (ie. Fully cover the bobbin length)
4. Minimise insulation layer thickness between windings

In conventional high voltage transformers its is difficult to implement all of these because of the large amount of inter layer insulation required.

Minimisation of the number of primary turns can reduce the leakage inductance however this is at the expense of a higher operational flux density and an increase in core loss [15,16,17].

Figure 4-20 shows the model of a high voltage transformer including the lumped leakage inductance L_p, magnetising inductance Lm and lumped secondary parasitic capacitance C_p referred to the primary side ($C_p = C_s(n_2/n_1)^2$)

Core and copper losses are neglected in this model.

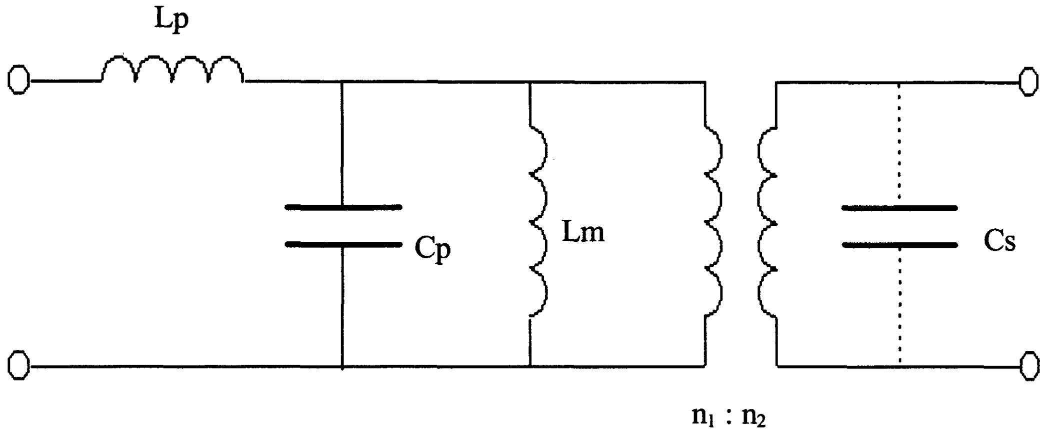

Figure 4-20 High voltage transformer equivalent circuit

The lumped leakage inductance L_p of a high voltage high frequency transformer is theoretically calculated from Equation 4-5 [15,17]. This expression assumes that both the primary and secondary windings cover the entire length of one limb of the core and that the bobbins are of a cylindrical geometry.

Eqn 4-5 $$L_p = \frac{\pi n_1^2}{h}(t_p + t_s)\left(\frac{w_1 + w_2}{3} + w_3\right) \times 10^{-7}\, H$$

Where n_1 is the primary turns number, t_p and t_s are the average one turn lengths of the primary and secondary windings respectively (m), h is the total winding length (m), w_1 is the winding width of the primary winding (m), w_2 is the winding width of the secondary winding (m) and w_3 is the insulation thickness between primary and secondary windings.

From Eqn.4-5 the estimated total leakage inductance referred to the primary winding is 16μH.

This leakage inductance value is greatly affected by the number of primary windings and the geometric size of a transformer structure. It is clear that a compact design with minimal distance between winding layers will minimise the leakage inductance of a high voltage transformer. The design of the primary and secondary winding structures attempts to follow this criteria as much as possible.

4.5.8 Winding capacitance

There are many stray capacitances that can exist in a transformer. The most important of these are listed below.

1. Winding to core
2. Winding to winding
3. Layer to layer
4. Turn to turn

In a conventional high voltage transformer, the stray capacitances exist mainly between each layer of the secondary winding [6]

When referred to the primary winding this secondary layer to layer capacitance is multiplied by the square of the turn's ratio and is often named the parasitic capacitance.

Due to the high turns ratio of a high voltage step-up transformer, this parasitic capacitance value may not be negligible and will induce an ineffective current through the secondary winding resulting in a overall loss of power conversion efficiency [15,17]

There are several known ways of minimising the parasitic capacitance of a transformer [6].

1. Increase layer to layer insulation thickness
2. Reduce the winding width
3. Increase the number of layers.

The lumped stray capacitance value is theoretically estimated in Equation 4-6 [15,17]. This expression assumes that the secondary bobbin is of a cylindrical geometry.

Eqn 4-6
$$C_p = \frac{8\pi\varepsilon_0\varepsilon_r r h_2 n^2}{3d(m_{layer}-1)m_{2nd}{}^2 m_{leg}}$$

Where ε_0 is the dielectric constant of a vacuum (8.85×10^{-12} F/m); ε_r is the dielectric constant of the inter layer insulation; r is the average radius of the secondary winding (m); n is the turns ratio of the transformer; d is the distance between 2 layers of the secondary winding (m); mlayer is the number of layers of secondary winding; m_{2nd} is the total number of secondary winding for each leg; m_{leg} is the number of legs.

The magnitude of parasitic capacitance is greatly influenced by the turn's ratio of the transformer and the total number of secondary windings

From Eqn.4-6 the estimated parasitic capacitance referred to the primary side is 130nF

4.5.9 Compromise between leakage inductance and parasitic capacitance

It is clear that compromises have to be made in the design of a high voltage transformer since corrective measures of minimising the leakage inductance and the parasitic capacitance work against each other. A tight, compact design lends well to the minimisation of leakage inductance; however, due to the insulation requirements of a high voltage transformer this is only possible to a certain extent.

A geometrically large transformer with a low turns ratio and a large number of secondary layers lends itself well to the minimisation of parasitic capacitance, but again, these factors would have an adverse effect on the leakage inductance, the high voltage requirement and the size cost and complexity of the transformer.

A judicious compromise was reached keeping both leakage inductance and parasitic capacitance minimal.

4.6 Design of the high voltage rectification stage

Figure 4-21 shows the high voltage rectification unit. The high voltage AC output voltages of both secondary windings are rectified by two full wave diode bridge rectifiers. The individual outputs of each rectifier are connected in series to generate the required negative DC Voltage level.

4.6.1 High voltage diode modules.

The full bridge rectification is achieved with eight separate high voltage diode modules.

These modules are designed specifically for high voltage, high power applications and consist of 30 diodes connected serially and capacitor compensated. These are then encased in an insulating material and machined to produce a module of required size.The specification for each diode module is shown in table 4-2.

Repetitive peak reverse voltage V_{rrm}	36kV
Average maximum forward current I_{favm} @55^{0}C	2.25A
Maximum forward voltage drop V_f	42V
Maximum surge current I_{fsm} (8.3ms)	150A
Maximum reverse recovery time t_{rr}	75ns

Table 4-2 High voltage diode module specification [18].

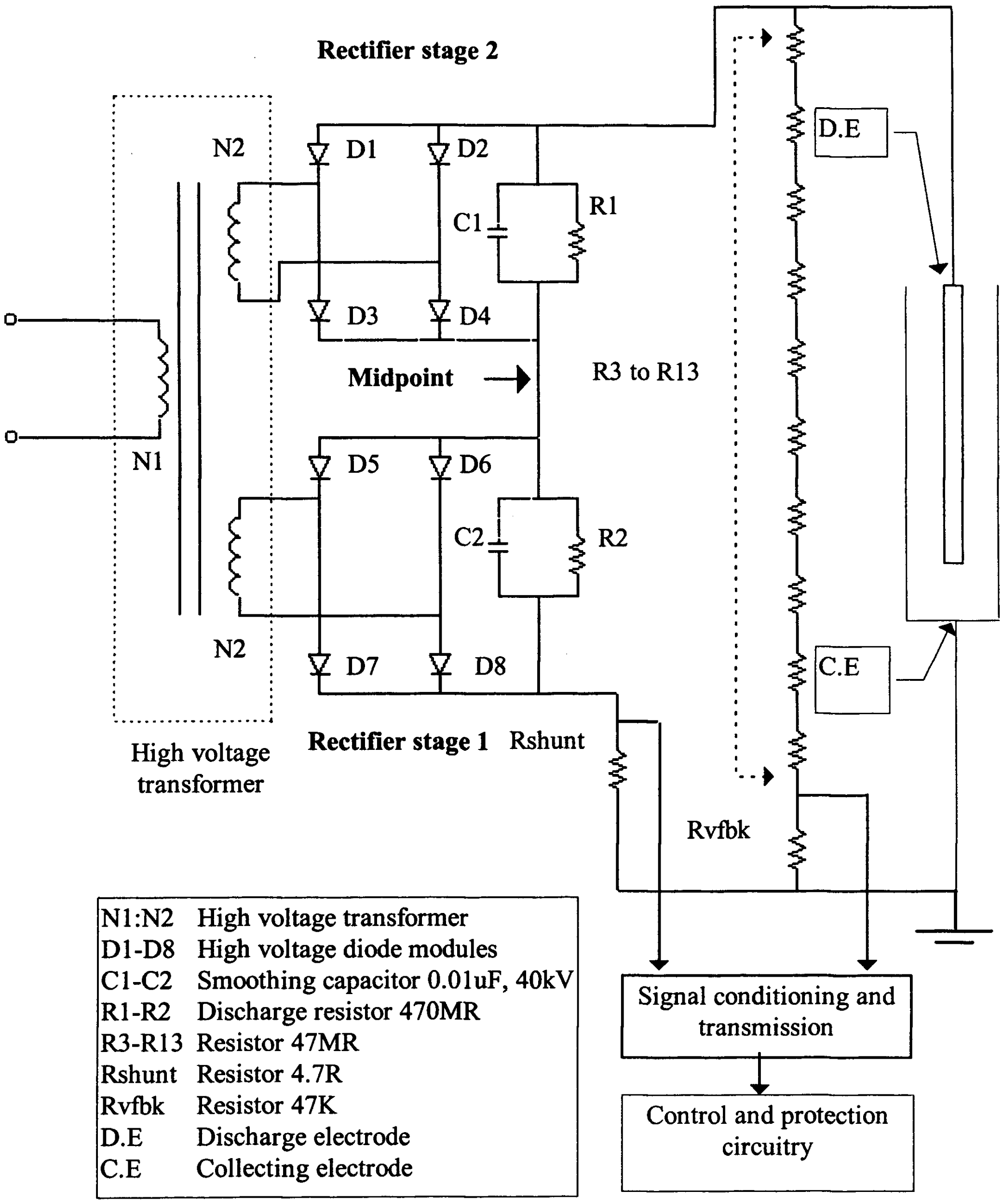

Figure 4-21 High voltage rectification unit

The cathode terminals of diodes D7 and D8 are connected to electrical earth through a 4.7R shunt resistor. This ensures that the output voltage of the power supply is of a negative potential with respect to the earthed precipitator collecting electrode.

Each of the two full wave bridge rectification stages consists of four diode modules. These four modules are grouped together and mounted on a common black anodised heatsink.

The thermal rating of the heatsinks is such that the diode module case temperature remains below the rated maximum of 75^0C under full load conditions.

The rectification structure is shown in figure 4-22.

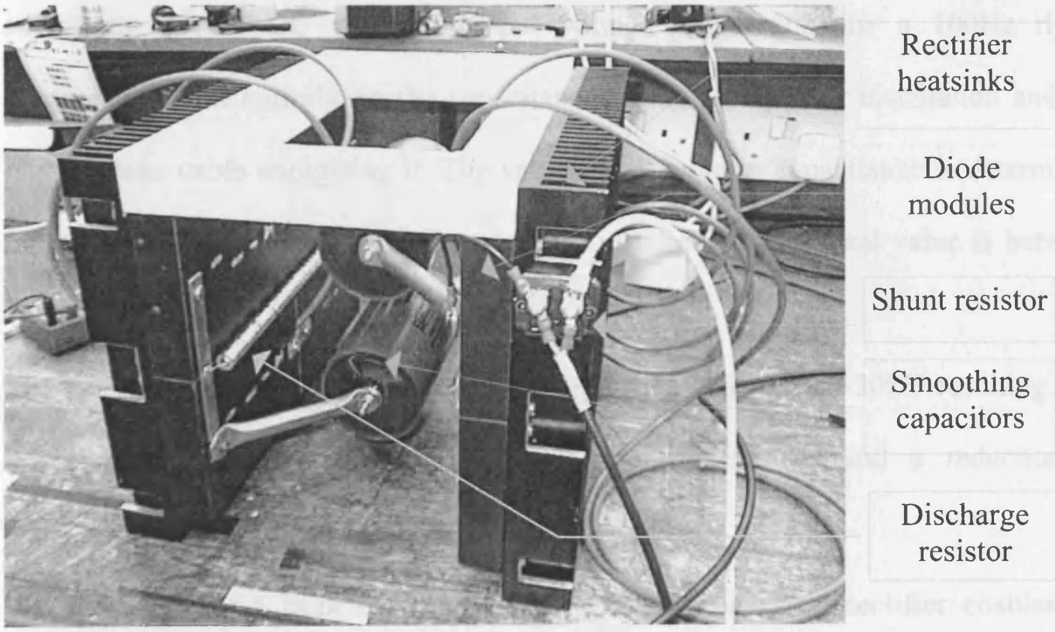

Figure 4-22 Rectification stage

The heatsink on which diode modules D5-D8 are mounted is connected to electrical earth. This is to prevent a "floating" potential occurring on the heatsink which could damage the diode modules. This method also limits the amount of damage sustained in the event of a rectifier failure.

The heatsink on which diode modules D1-D4 are mounted cannot be connected in the same manner. This is due to the fact that rectification stage 2 can exhibit, with respect to earth, the full working voltage of the power supply.

This potential difference would be beyond the breakdown strength of the diode module encapsulation. Nonetheless, it is still unfavourable to leave the heatsink electrically floating and so it is connected to the midpoint of the 2 rectification stages.

4.6.2 Smoothing capacitors

In conventional 50Hz thyrsitor-rectifier sets, capacitors are not normally used and the smoothing of the DC rectified output voltage which contains a 100Hz ripple component relies entirely on the capacitance of the precipitator installation and the high voltage cable energising it. The value of precipitator capacitance is determined by the size and geometry of the precipitator installation. A typical value is between 100-200nF [1].

The ripple magnitude (peak to peak) can be in the order of 20-30kV resulting in a lower average voltage between the precipitator electrodes and a reduction in collection efficiency.

The utilisation of a high frequency, high voltage transformer-rectifier enables the magnitude of this ripple to be considerably less than a conventional power supply.

Rather than relying simply on cable capacitance and the capacitance of the precipitator (which can vary from site to site), two high voltage capacitors of value 0.01uF are connected across each rectification output stage. These perform not only a smoothing role but also act as a potential divider network to ensure a voltage balance between rectification stages during a rapidly changing output voltage event (e.g. during sparking).

Figures 4-23 and 4-24 show Pspice simulations of the high voltage rectifier.

In the simulation the precipitator is modelled as a simple resistive load drawing maximum rated power from the rectifier. The transformer output voltage is modelled as a quasi-square wave of frequency 20kHz and duty 80%.

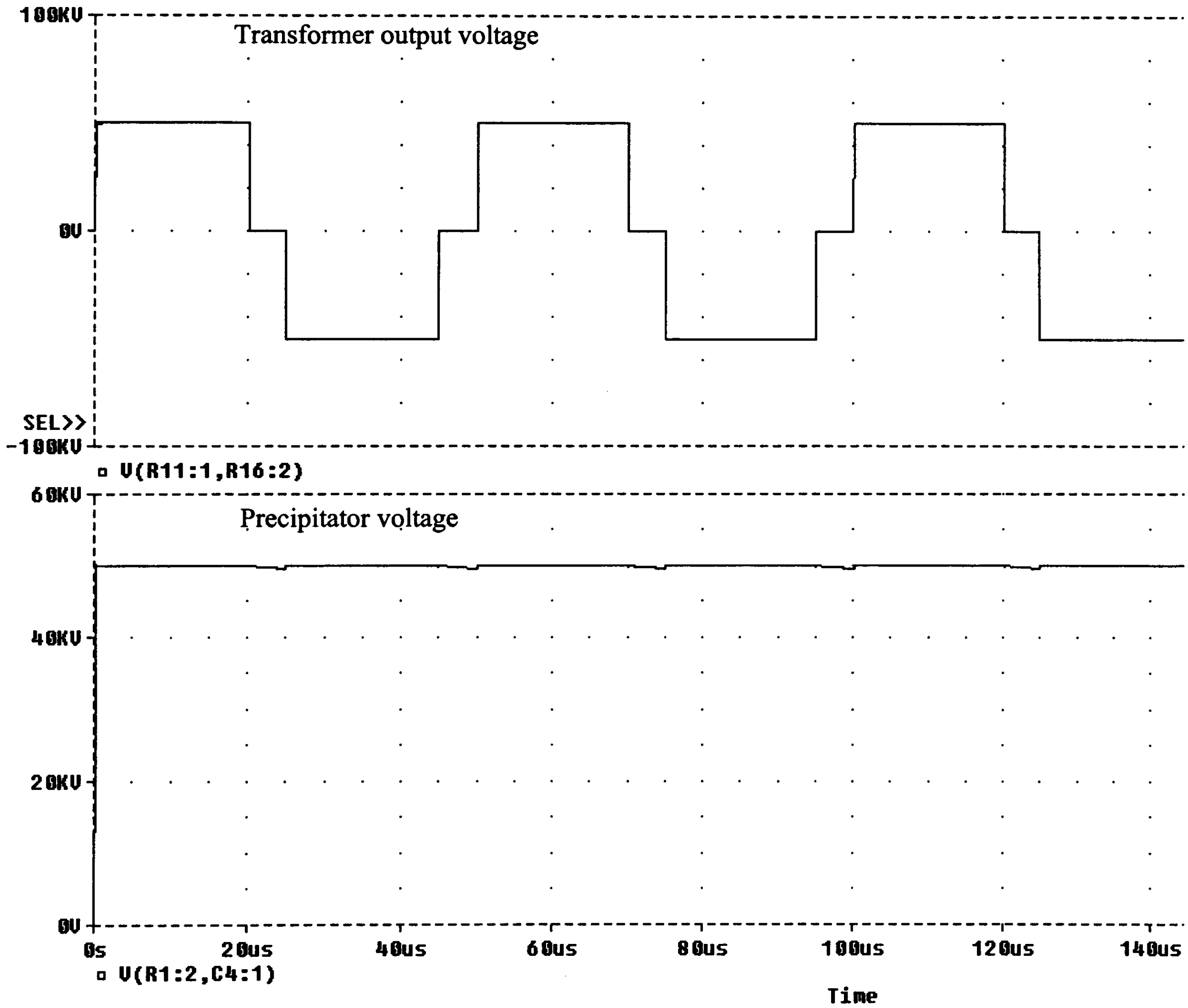

Figure 4-23 Transformer output voltage and precipitator voltage

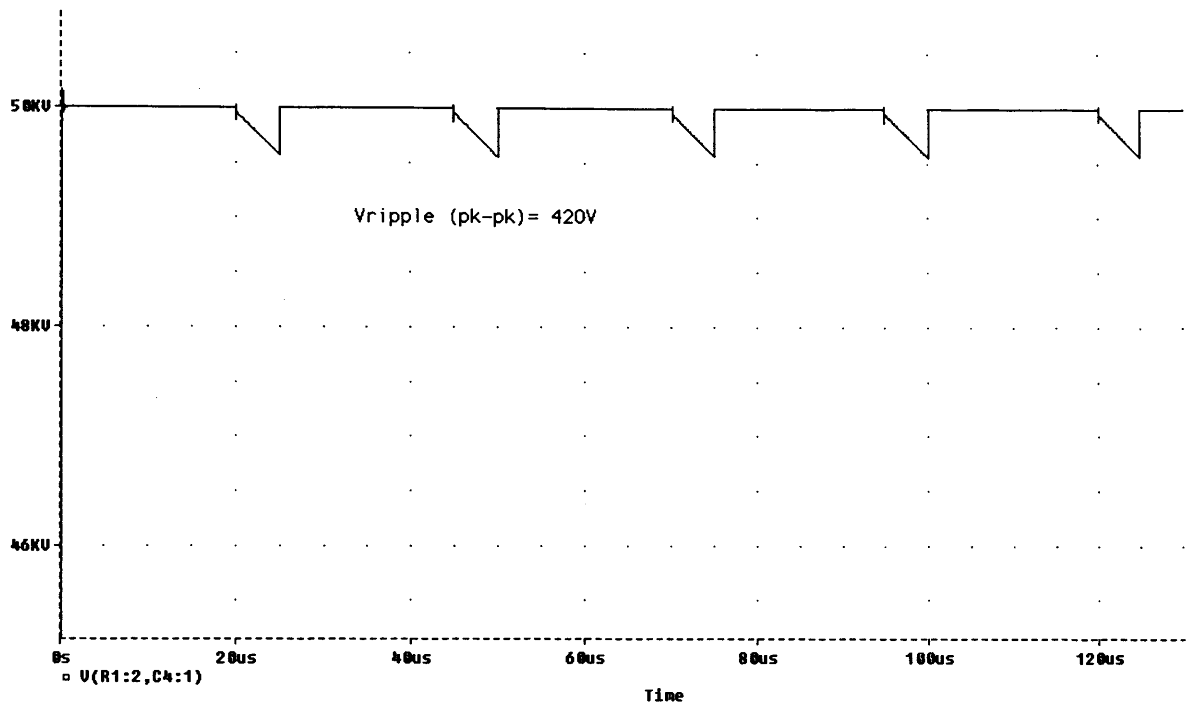

Figure 4-24 Voltage ripple magnitude

The maximum peak to peak ripple voltage is shown in fig 4-24 to be 420V (0.8% of The high voltage DC output).

In actual fact, the ripple magnitude may be considerably less since the simulation does not take into account the capacitance of the precipitator and the high voltage cable. This was omitted purposely to show the ripple reduction characteristic of the rectification stage regardless of precipitator and capacitance value.

The connection of the capacitors to the diode modules are made with hollow, rounded edged tube busbars as seen in figure 4-22. This is to obviate any enhanced electric field and corona, which could occur with a sharp corned connector. The busbar also provides rigidity to the rectification structure.

4.7 Instrumentation and measurement systems within the transformer-rectifier unit.

It is necessary at all times to be able to monitor the output voltage and current of the power supply. These parameters are used by control circuitry to detect sparking and flashover within the precipitator and to provide signalling to the analogue meters mounted on the remote control unit (chapter 7).

In addition, by analysis of the voltage/current data it is possible to characterise the precipitator installation performance under varying operating conditions (e.g. varying coal dust types, flow rate, temperature etc).

There are three sensors attached to the transformer-rectifier structure:

1. High voltage sensor
2. Current sensor
3. Temperature sensor

4.7.1 High voltage sensor

This comprises of a series resistor network consisting of ten precision (+/- 1%) ceramic resistors of rating 47MΩ, 10kV, 2W. The eleventh resistor is rated 47KΩ (+/- 1%), 600V, 1W.

This network is connected between earth and the high negative DC level of the power supply output. The potential difference across the 47K resistor is thus a 1:10000 representation of the power supply output voltage.

Figure 4-25 shows the circuit for transmission of the signal to the main control and protection circuits.

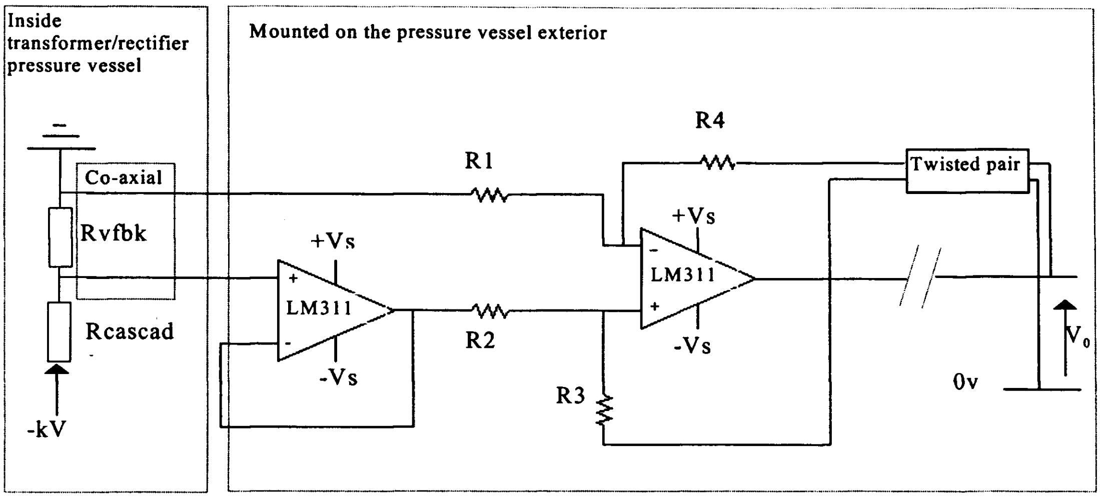

R1,R2,R3,R4 = 47KΩ
Rvfbk = 47KΩ
Rcascade = 470MΩ
+Vs = +15V
-Vs = -15V
Vo = Output voltage

Figure 4-25 High voltage power supply voltage sense and transmission circuit.

4.7.2 Current sense resistor

The current sense resistor is a 4.7Ω 10W isotop package connected between earth and the cathode side of diode modules D7 and D8 as shown in figure 6-19.

It is mounted on the side of the earthed heatsink and provides an effective method of power supply output current sensing.

Figure 4-26 shows the circuit used for transmission of the signal to the control circuits.

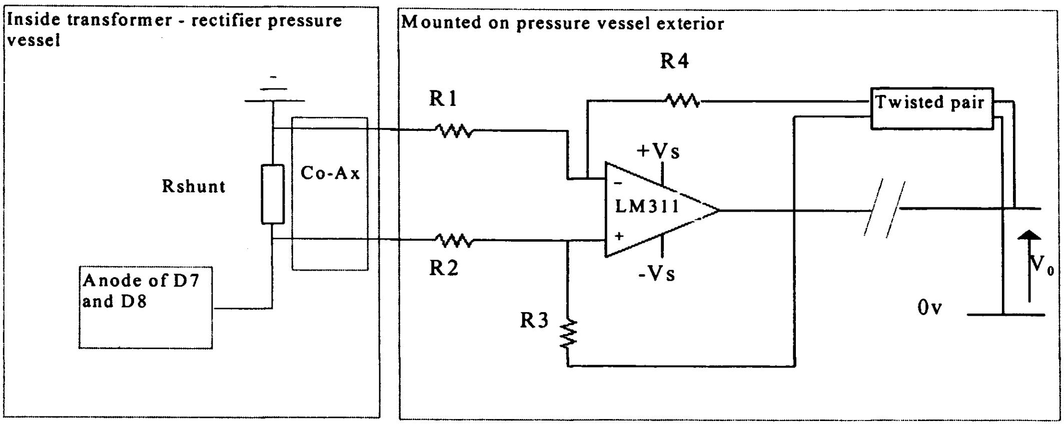

R1,R2,R3,R4 = 47KΩ
Rshunt = 4.7Ω
+Vs = +15V
-Vs = -15V
Vo = Output voltage

Figure 4-26 Current sense and transmission circuit.

4.7.3 Transformer temperature sensor

The temperature internal to the pressure vessel is measured with the use of two thermistor probes. One being clamped in contact with the earthed ferrite core of the transformer, the other mounted on the earthed diode module heatsink.

As a prototype power supply, these two measurements are not actioned upon by the control circuitry. They do, however provide useful data on the temperatures within the transformer-rectifier structure during operation.

4.7.4 Mechanical structure of transformer-rectifier and pressure vessel

A requirement was that the transformer-rectifier be held in a rigid framework that provided strength and rigidity to the structure without compromising the electrical insulation strength of the framework or encapsulation gas.

It was recognised that the unit would be installed within a sealed metallic container pressurised with SF_6 to at least 2 bar.

This placed several constraints upon the design of the structure:

1. The frame had to fit within a designated volume of container. There had to be sufficient spacing between high voltage elements and the electrically earthed container to prevent electric breakdown.
2. The layout of the transformer rectifier had to be such that connections to and from the unit could be routed in a sensible and minimal distance and could then be clamped to this route to prevent a high voltage element coming within close proximity of an earthed element.
3. Sharp corners / protrusions that could cause field enhancement and consequent insulation degradation must be avoided.
4. The insulating base of the unit had to fit tightly within the container walls to prevent any damage during transportation.
5. There had to be a means of routing a cable/busbar from the high voltage output of the rectifier to a suitable high voltage socket on the lid of the pressurised container. There had to be minimal play in this once it was in position and so a spring connection that would take up any cable slack as the lid was sealed into place was developed.

Figure 4-27 shows the final structure of the transformer, rectifier, sensors and cabling. The material used to manufacture the frame was nylon 6,6. This was used so as not to compromise the electrical insulation strength of the bobbins or the encapsulation media.

Rods of size 50mm by 50mm of nylon 6,6 where machined to the required size and fused together using a plastic welder to produce the required framework.

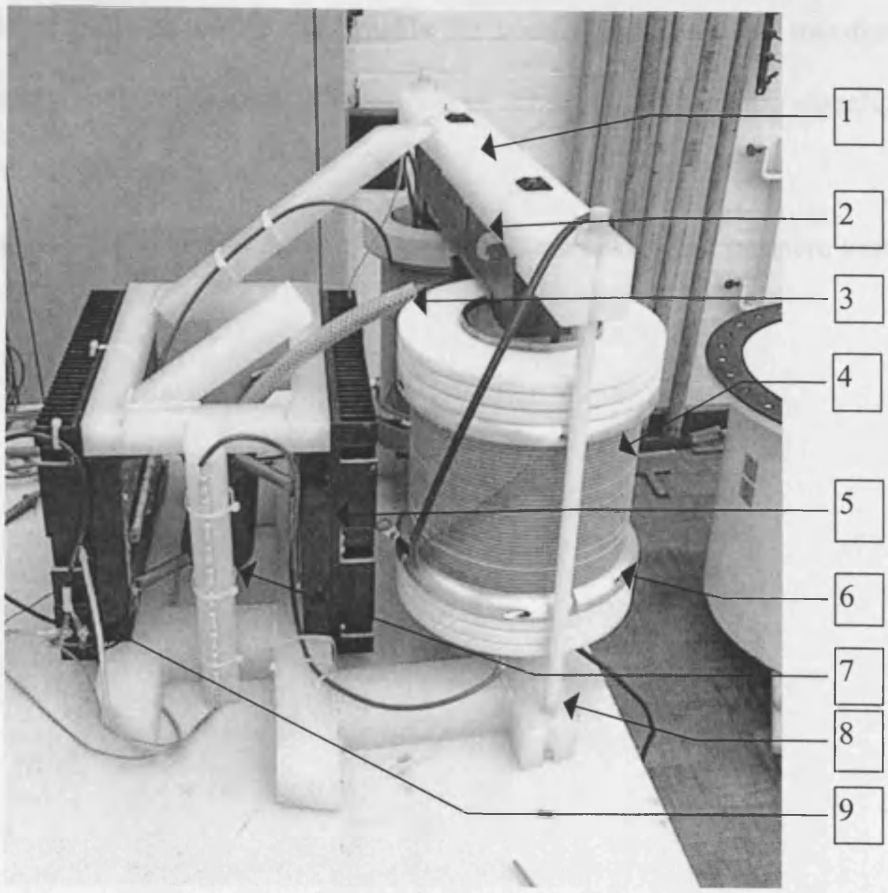

Figure 4-27 Structure of transformer rectifier framework

1: Nylon 6,6 frame; 2: ferrite core; 3: high voltage connector; 4: secondary winding; 5: rectifier and heatsink; 6: stress relief rings; 7: voltage sense network; 8: base; 9: shunt resistor.

4.7.5 Pressure vessel

It was recognised that in order not to compromise the insulating strength of the nylon bobbins and framework, the transformer- rectifier structure would have to be enclosed in a sealed unit and pressurised to at least 2 atmospheres with the gas SF_6.

This placed several requirements on the sealed container:

1. It must be able to withstand the force placed on its walls and lid due to the high internal pressure

2. There must be minimal gas leakage over time

3. The container must be easily machinable for connections from the transformer-rectifier (primary connection, high voltage output connector and sensing signals) and the inlet/outlet valves for the gas.

Figure 4-28 shows the technical drawing of the transformer-rectifier pressure vessel.

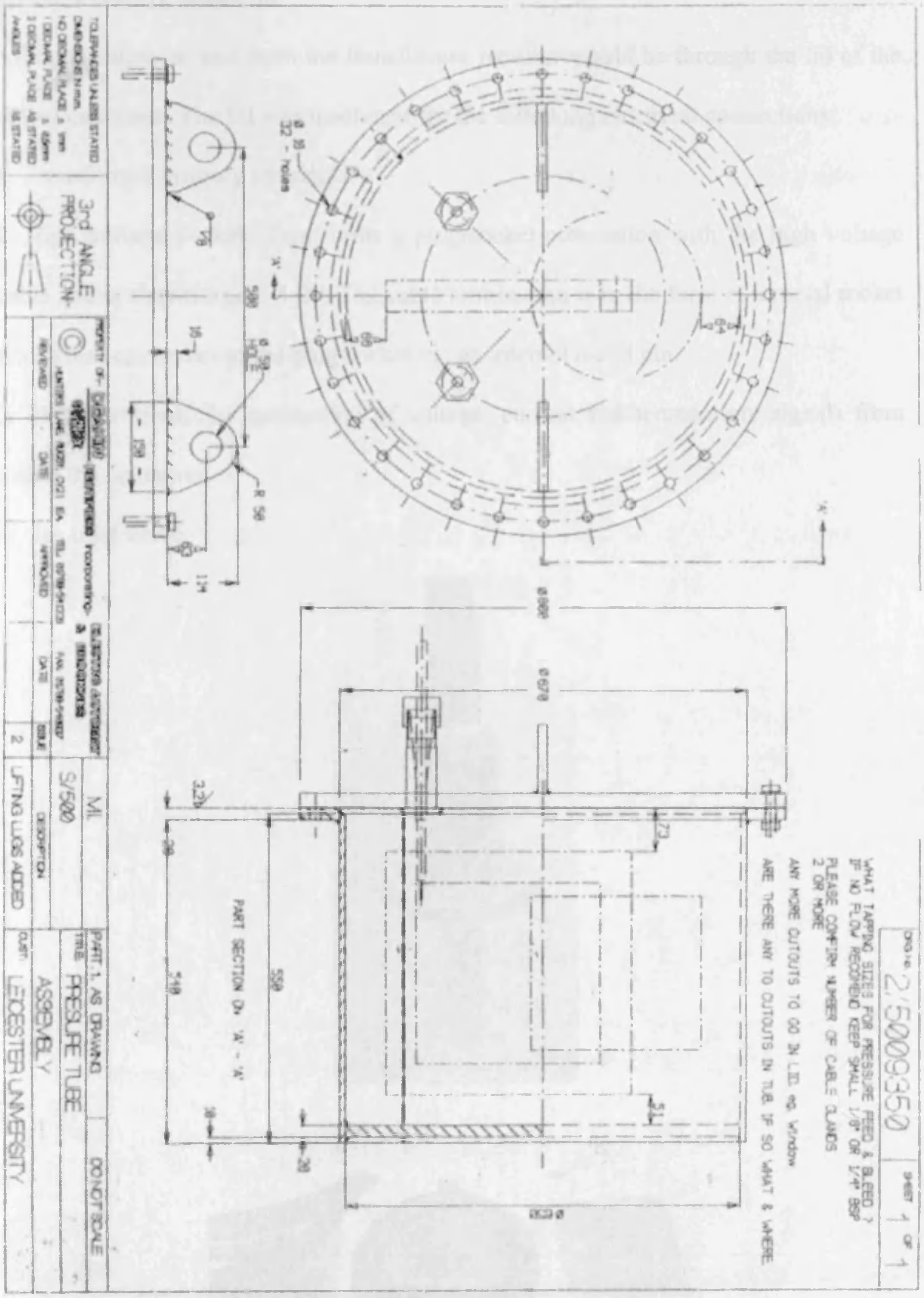

Figure 4-28 Technical drawing of the transformer-rectifier pressure vessel

4.7.5.1 Pressure vessel lid.

All connections to and from the transformer rectifier would be through the lid of the sealed container. The lid was machined for the following electrical connections:

1. Transformer primary terminals
2. High voltage socket: This forms a plug/socket connection with the high voltage cable and is shown figure 4-29. The cable termination is in the form of a metal socket which makes contact to the plug socket via an internal metal pin.
3. PET Terminals for connection of voltage, current and temperature signals from inside the container.
4. Gas inlet valve.

Figure 4-29 High voltage cable termination and socket

4.7.5.2 Gas pressure monitoring

An automatic system for evacuation of the gas in the event of an overpressure situation was designed. The lid of the pressure vessel was machined for the following:

1. A sealed pressure gauge measuring 0-10 bar
2. A 'normally closed' pressure switch, which open circuits in the event of an underpressure/ leakage situation (where the gas pressure drops below 2 bar).

 The switch forms part of the switchgear protection system detailed in chapter 7.

3. An overpressure blow-out valve.

In the event of an overpressure situation the unit had to be able to be evacuated to atmospheric pressure automatically and rapidly.

This was achieved by the installation of a one way, none resettable blow-out valve. If the pressure rises above 3.4 bar, the valve opens, rapidly evacuating the pressure vessel.

Figure 4-30 to 4-34 shows the transformer-rectifier/ pressure vessel under various stages of construction.

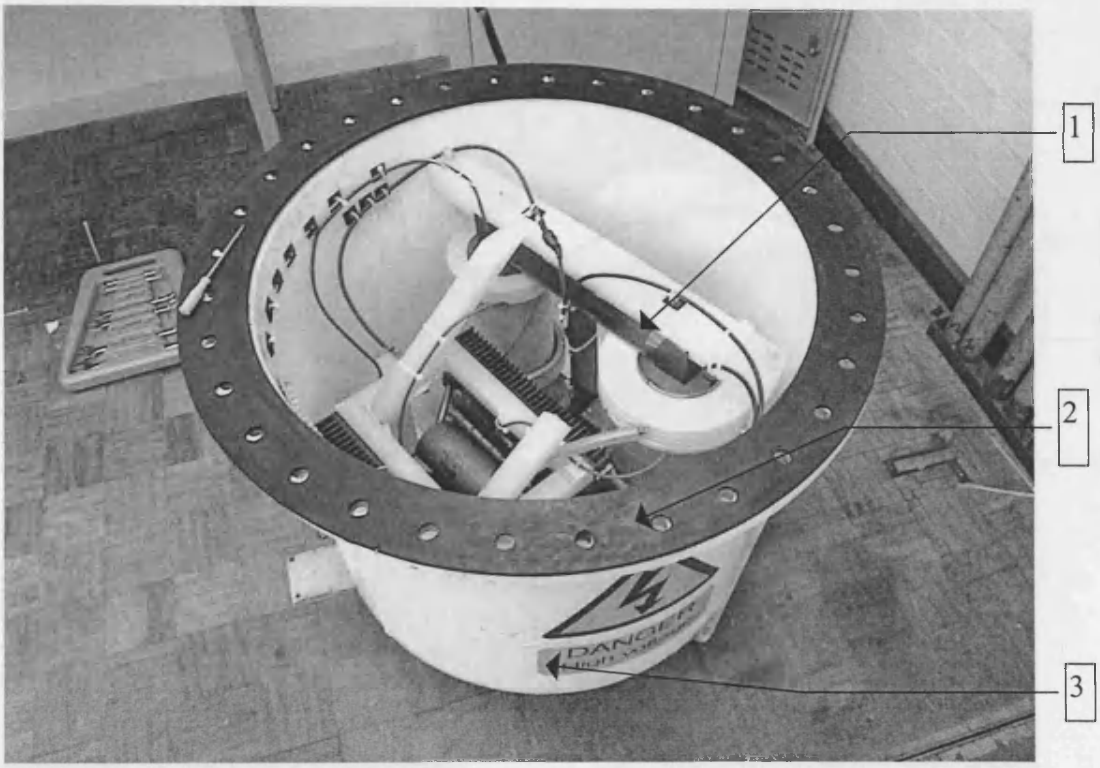

Figure 4-30 Pressurised transformer- rectifier vessel

1: Transfomer-rectifier; 2: rubber gland; 3: pressure vessel

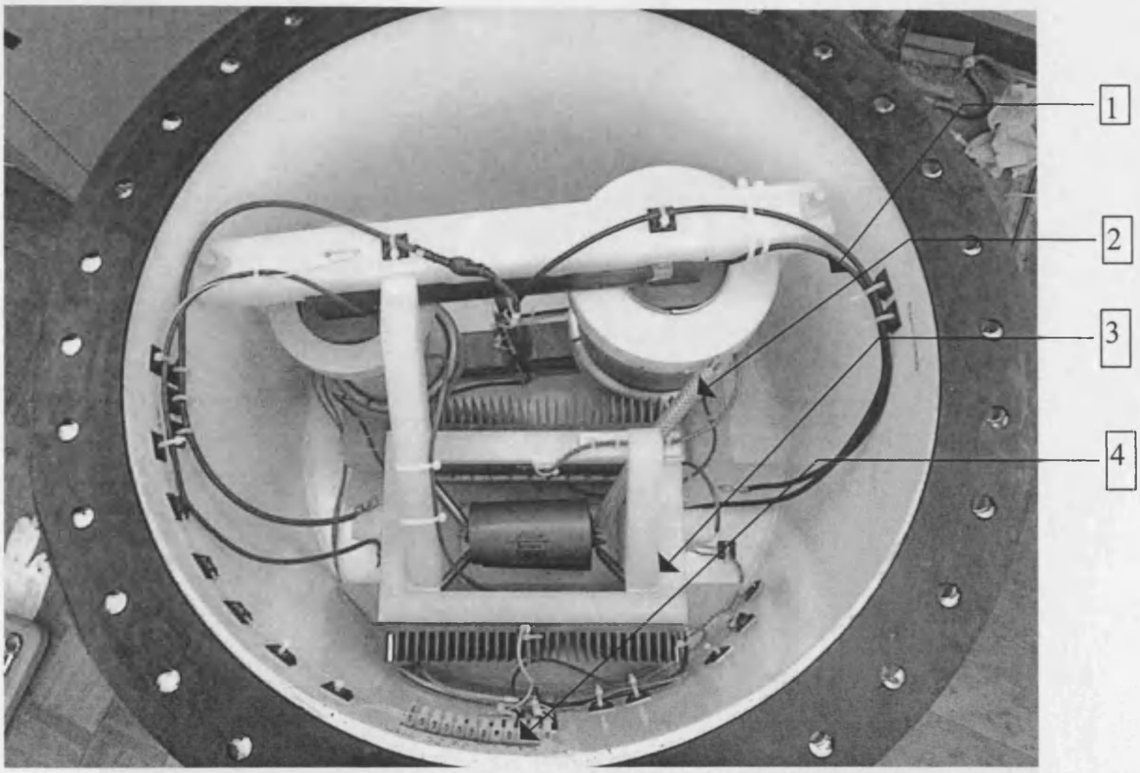

Figure 4-31 Internal pressure vessel structure

1: Primary cables; 2: high voltage spring connector; 3: rectification stage; 4: low voltage signal interface.

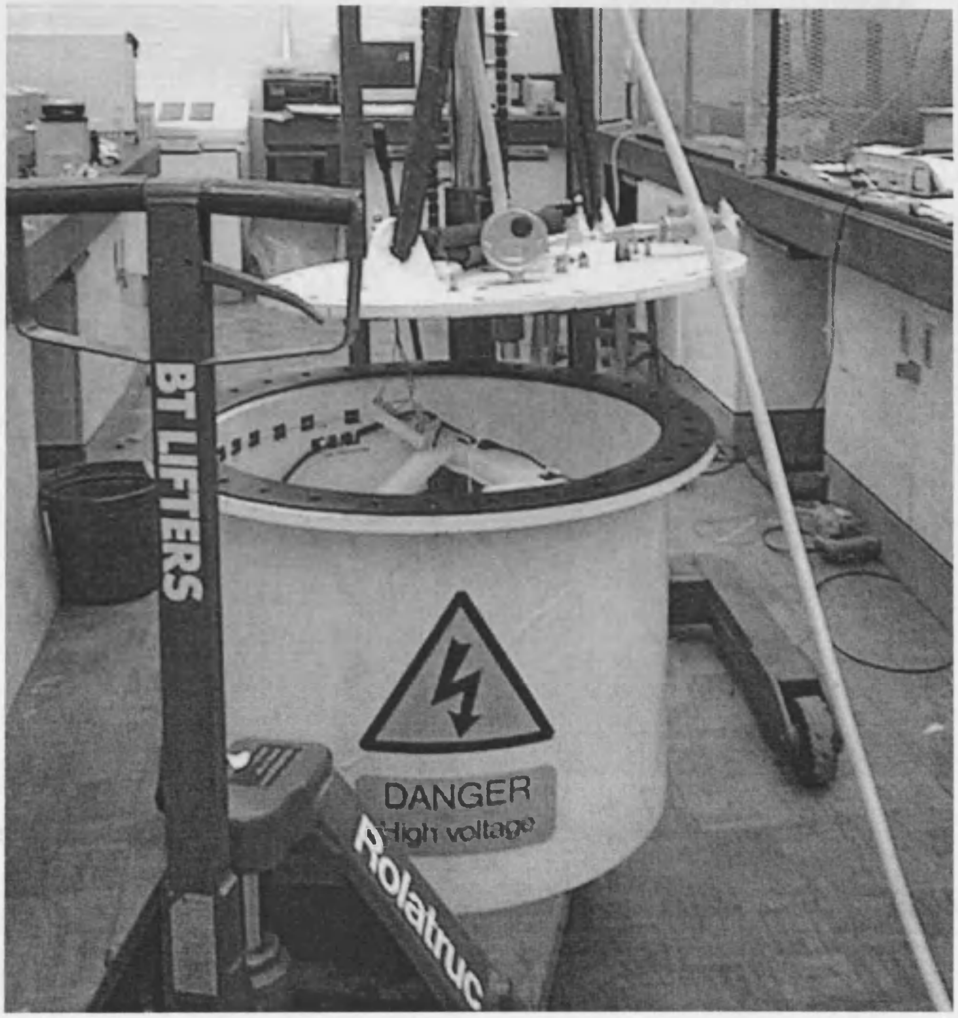

Figure 4-32 Installation of pressure vessel lid

Figure 4-33 Complete sealed transformer-rectifier pressure vessel.

1: Gas inlet valve; 2: pressure gauge; 3: overpressure blow-out valve; 4: high voltage cable; 5: gas cylinder pressure regulator; 6: gas cylinder

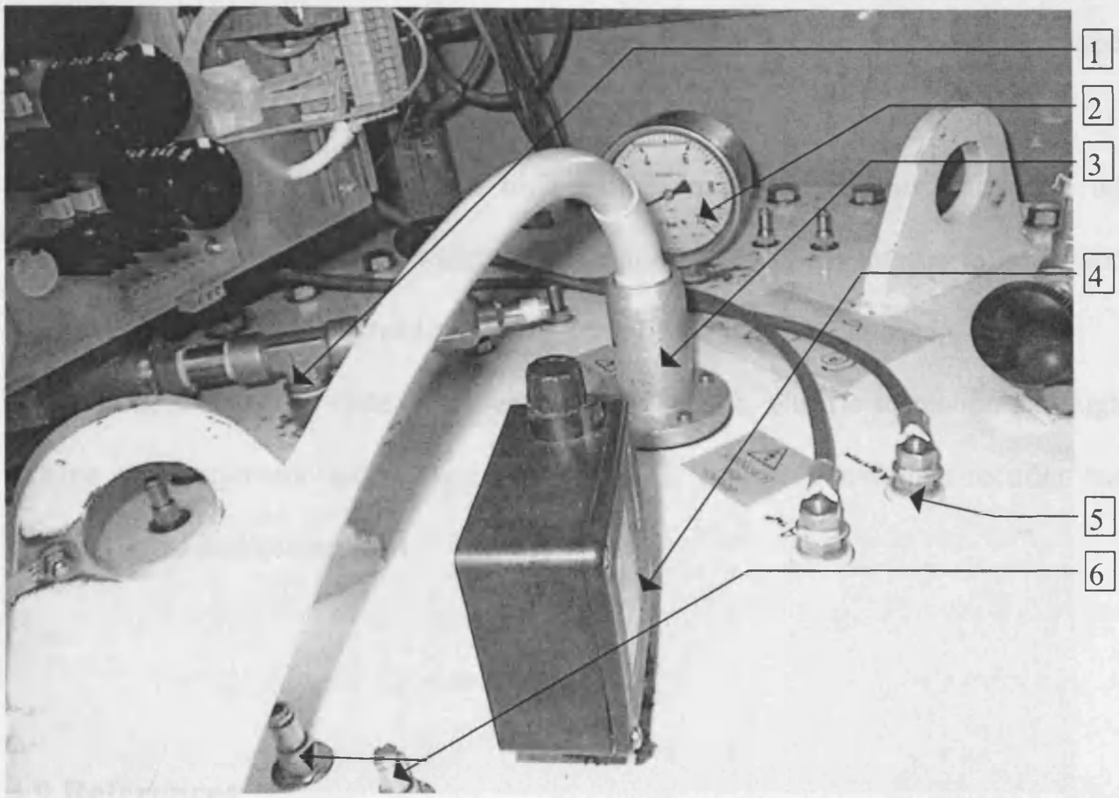

Figure 4-34 Pressure vessel lid

1: Overpressure blow-out valve; 2: pressure gauge; 3: high voltage terminal;

4: underpressure switch; 5: primary winding terminals; 6: voltage and current sense outputs

4.8 Summary

The requirements of a high voltage transformer suitable for use within the prototype precipitator power supply are investigated.

The disadvantages of conventional high voltage transformers (low efficiency, oil insulation problems, size and weight) are detailed and the advantages to be gained from a high frequency, oil free transformer-rectifier unit are established.

With the application of state of the art electromagnetic, electric insulation and high voltage semiconductor technology, a novel high voltage transformer-rectifier has been designed and constructed.

4.9 References

1. **Parker KR,** Applied Electrostatic Precipitation, 1st ed. Chapman & Hall, 1997
2. **Devine PJ,** The requirements of a high voltage DC power supply, Leicester University Engineering Department, Report 96-24, 1995
3. **Pressman AI,** Switching Power Supply design, 1st ed. McGraw-Hill, 1991
4. **MMG Neosid** Ltd, Product data book, 1993
5. **Sen PC,** Principles of Electric Machines and Power Electronics, Wiley and Sons, Inc, 1989
6. **McLyman Wm.T,** Transformer and inductor design handbook, New York, Dekker, 1978
7. **Rowland SM** and Nichols IV, "Effects of dry band arc current on ageing of self supporting dielectric cables in high fields" IEE Proc., Science, Measurement and Technology, vol. 143, no. 1, Jan 1996,

8. **Fothergill JC** and Dissado LA (eds), Space Charge in Solid Dielectrics, The Dielectrics Society, 1998, ISBN 0 9533538 0x,259-272

9. **Dissado LA**, Mazzanti G and Montanari GC, "The role of trapped space charges in the electrical ageing of insulating materials", IEEE Trans. DEIS, vol. 4,no. 5, Oct.1997, pp. 496-506

10. **Crine JP**, "A molecular model to evaluate the impact of ageing on Space Charges in Polymer Dielectrics", IEEE Trans. DEIS, vol. 4, no. 5, Oct 1997, pp. 487-495

11. **Connor P**, Jones JP, Llewellyn JP and Lewis TJ, "Mechanical origin for electrical ageing and breakdown in polymeric insulation", Proceedings of the 1998 IEEE 6th International Conference on Conduction and Breakdown in Solid Dielectrics, Conf code 49244, pp. 434-438

12. **Williams JW**, "Navy/Industry NAVMAT High Voltage Guidelines- An Overview", 1995 High Voltage Workshop, University of Utah, USA

13. **Conti-Elektro-Berichte**, July/September 1966, p.189

14. **Pohl, HA**, "Dielectrophoresis", Cambridge University Press, 1978

15. **Takano H** and Hatakeyama T, "Feasible characteristics of resonant PWM inverter linked DC-DC power converters using high voltage transformer parasitic circuit components" IEE Conf. Power Electronics and Variable Speed Drives, 23-25 Sept, 1996, Conf code. 429, pp. 525-533

16. Devine PJ, Lefley PW, Fothergill JC, "A high power high frequency transformer for high voltage applications", Proceedings of the Universities Power Engineering Conference, 1997, Vol.1, pp.511-515

17. Sun JM, Gamage L and Nakaoka M, "Comparative transient and steady state performances of three resonant PWM Inverter controlled DC-DC converters

using high voltage transformer and cable parasitic circuit components", IEEE Power Conv Conf, Conf code 47766, pp. 821-826, 1997

18. High Voltage Technology Ltd, High voltage diode data book, 1996

5. DESIGN OF THE HIGH FREQUENCY, HIGH POWER INVERTER TO CONTROL POWER TO THE PRIMARY WINDING OF THE HIGH VOLTAGE TRANSFORMER

5.1 Voltage fed, high frequency, high power inverter

The topology used to control power flow to the primary winding of the high voltage transformer is the voltage fed, full bridge inverter shown in figure 5-1. The power semiconductor switches used within the inverter are four individual IGBT power modules rated at 1200V, 200A.

5.1.1 Power control of the transformer primary winding

Control of power to the primary winding of the transformer is achieved with the application of fixed frequency variable phase modulation as shown in figure 5-2.

With this form of modulation the four IGBTs in the full bridge inverter are switched at a set frequency (20kHz) and fixed duty cycle (50/50). A switching frequency of 20kHz was chosen since the power supply transformer design detailed in chapter four is based upon this frequency of operation. Secondly, 20kHz is within the frequency limitations of the IGBT gate driver units used in the prototype (see 5.1.2).

Each device in a leg pair is fired on a complimentary basis (A-C, B-D). Control of power to the transformer is achieved by varying the relative phase angle of advancement between two leg pairs (B and D).

The disadvantage of conventional PWM switching techniques is that if the required duty ratio of the switches becomes very low under light load conditions (i.e., a very short on time) a situation may be reached where either the IGBT gate driver circuits or the IGBTs themselves experience difficulties in fully switching on and off in such a short time [1].

Phase modulation alleviates this problem since, although the effective duty ratio of the inverter under the same load conditions will still be low, the IGBTs are switched on a fixed 50/50 duty cycle [2,3].

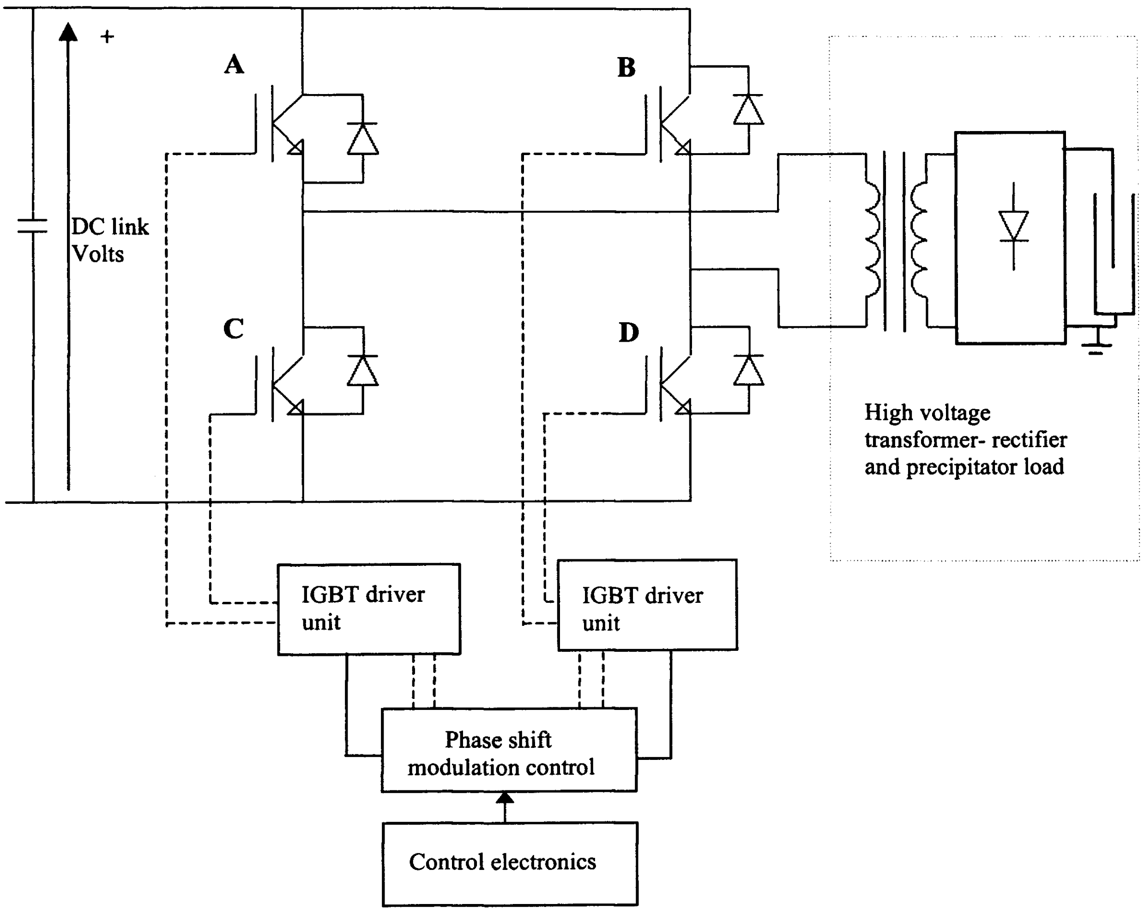

Figure 5-1 Voltage fed; full bridge inverter supplying power to the high voltage transformer-rectifier

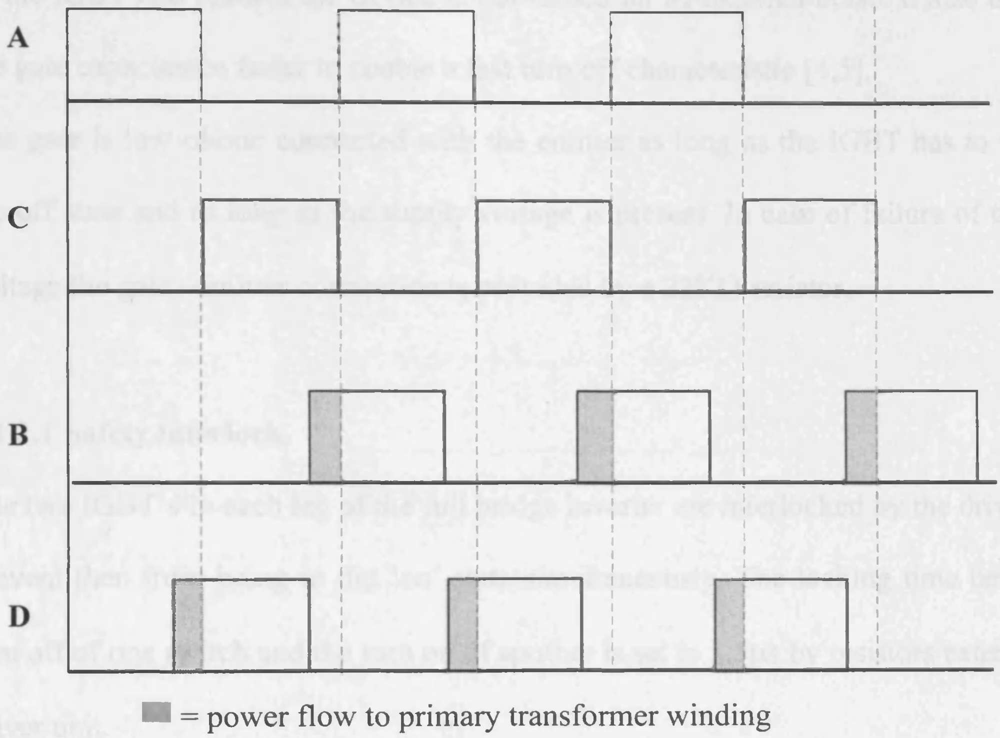

Figure 5-2 Typical gate firing patterns for the inverter operating in phase shift modulated mode.

5.1.2 Drive control and protection of the IGBT modules.

Two dedicated driver units control gate drive of the IGBTs. Each driver unit controls the two IGBTs in each leg of the inverter.

Internal magnetics within the units provide the necessary electrical isolation between the upper and lower IGBT gate signals and the low voltage power supply to the driver units.

The IGBTs are switched on by application of a +15VDC signal to the gate-emitter junction and switched off by a –15VDC signal. The +15VDC signal ensures that the device is fully saturated and that the collector-emitter voltage is at the specified minimum for the devices rated current. The –15VDC signal reverse biases the gate emitter junction of the IGBT and ensures the device is not turned on by external noise. It also discharges the gate capacitance faster to enable a fast turn off characteristic [4,5].

The gate is low ohmic connected with the emitter as long as the IGBT has to remain in the off state and as long as the supply voltage is present. In case of failure of the supply voltage the gate –emitter connection is provided by a 22KΩ resistor.

5.1.2.1 Safety interlock.

The two IGBT's in each leg of the full bridge inverter are interlocked by the driver unit to prevent then from being in the 'on' state simultaneously. The locking time between the turn off of one switch and the turn on of another is set to 1.5μs by resistors external to the driver unit.

5.2 Phase shift modulation circuit

The circuit controlling the signals to the IGBT driver modules and ultimately the precipitator power supply output voltage is detailed in figure 5-3.

The UC3879 is a dedicated phase shift modulator [6]. The internal transconductance amplifier of the i.c is bypassed and a DC voltage level of 0V to 3.8V applied directly to the compensation input will vary the phase shift angle between 0° and 180°.

This signal is provided by the power supply energisation circuitry detailed in chapter seven.

Soft start, in the event of a fault trip or power supply start/ re-start is provided by a 100nF capacitor connected between 0V and pin 6 (SS).

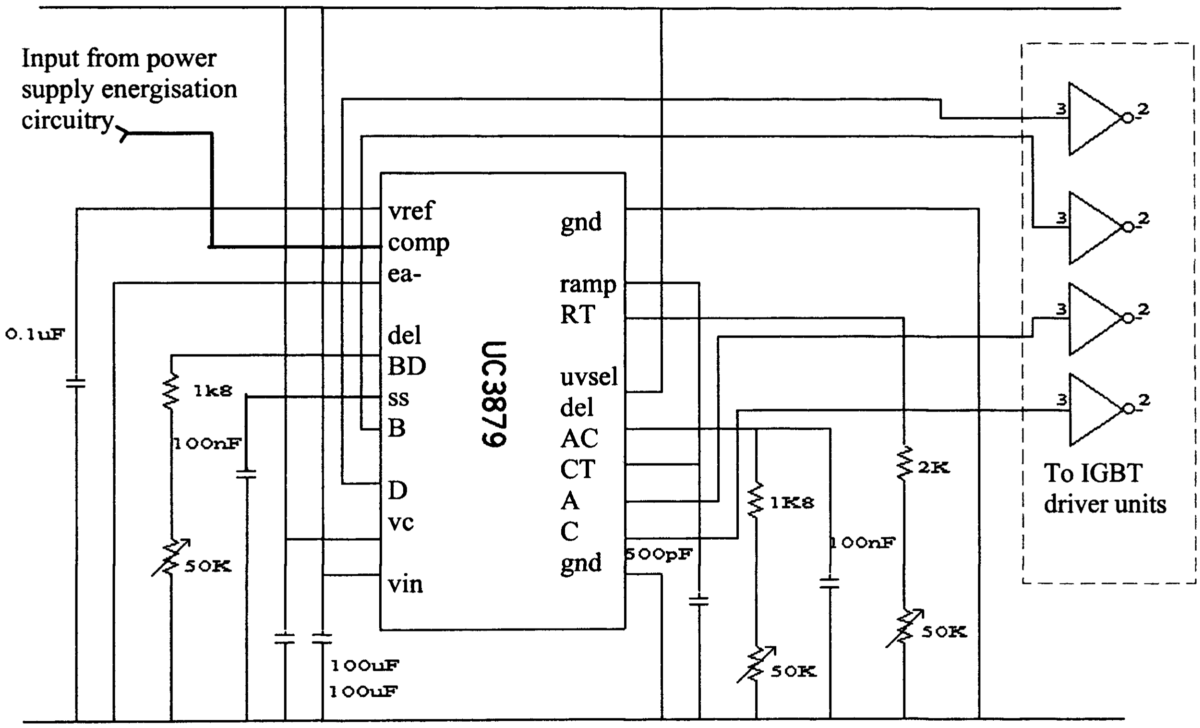

Figure 5-3 Phase shift modulation circuit

5.3 Overcurrent protection

V_{ce} monitoring of the four IGBT's provides overcurrent and switch fault detection within the inverter. The value of V_{ce} is compared with a pre-set value internal to the driver units [7]. If the value increases above the pre-set level at a time when the device should display the rated collector emitter saturation voltage, then the driver signals are disabled.

5.4 Over-temperature protection

Heatsink temperature of the inverter stage of the power supply is monitored by a bimetal thermal trip mounted on the heatsink surface and connected to the error input of the driver units. If heatsink temperature exceeds 70°C the gate driver signals to the IGBTs are disabled.

5.5 Summary

A high frequency (20kHz), high power (25kVA) full bridge inverter has been designed and constructed to control power to the high voltage transformer–rectifier of the precipitator power supply.

Phase shift modulation is implemented as the inverter switching method. This has key advantages over standard PWM methods in that the inverter devices are switched at a constant duty and frequency. This minimises control and drive complexity and can help minimise switching stresses on the IGBT devices under certain operating conditions.

Fault protection within the inverter topology is provided by monitoring of the collector-emitter voltages of the switching devices and the heatsink temperature.

5.6 References

1. **Barnes S.A** and Smith GA, "The use of a finite state machine to control a fixed frequency variable phase H bridge", Proceedings, UPEC 1994, pp. 720-722
2. **Unitrode**, "Power supply design seminar", Unitrode corporation, SEM-900, 1993
3. **Kazimierczuk M.K**, "Resonant power converters", 1995, John Wiley, TK7872.C8K39
4. **Toshiba** , "IGBT data book", 1995, Toshiba Electronics Europe
5. **Mitsubishi**, "Power module data book", 1990, Mitsubishi Electric
6. **Unitrode**, "Applications handbook 1995-1996", 1996, Unitrode corporation
7. **Semikron**, "Power semiconductor and drive data book", 1996, Semikron corporation

6. DESIGN AND ANALYSIS OF THE THREE PHASE DIODE BRIDGE WITH BOOST RECTIFIER FOR DC LINK VOLTAGE BOOST AND INPUT POWER FACTOR CORRECTION

6.1 Review of AC to DC conversion techniques

The prototype precipitator power supply shown in figure 3-8 is based upon a front end AC to DC converter, a capacitor based DC link and high frequency voltage fed inverter supplying the primary winding of a step-up high voltage transformer.

Front end conversion of AC mains supply voltages to a DC level suitable for energisation of a DC link has conventionally been dominated by diode bridge rectifiers. In low power applications this is generally achieved with a single-phase diode bridge rectifier. For medium to high power applications, AC to DC conversion is accomplished with a three-phase diode bridge rectifier. The non-ideal characteristics of the input line current drawn by these rectifiers are well known and create a number of problems for the utility supply and other electrical systems in the vicinity, namely:

- High input current harmonic content and low input power factor
- Large voltage ripple superimposed on the DC output causing voltage control problems, especially in inverter applications
- Input AC mains voltage distortion due to the associated higher peak input currents.

Based on the standards (IEC555-2) and recommendations (IEEE-519) aimed at maintaining power supply quality within acceptable levels [1], both passive and active current wave shaping techniques have been suggested in literature [2]-[19]

The technique of using passive filters is the most commonly used method which is easy to implement and operate but requires low frequency magnetic components that are bulky and expensive [6,7] The development of active current waveshaping techniques, namely unidirectional pulse rectifier systems operating at high frequency has been the object of increasing interest [3]-[19].

Three-phase rectification at close to unity power factor has, in the past, been realised using three single AC to DC converters (figure 6.1) with suitable input and output connections. This topology can yield close to unity input power factor but does exhibit several disadvantages:

- Requires complex input synchronisation logic
- Switching frequency is load dependent
- The number of components required to construct the topology is three times that of the single-phase converter making the topology complex and expensive.

In [3] which constituted a major advance in the development of three-phase rectification systems, a single switch discontinuous inductor current boost rectifier is introduced characterised by the following:

- Approximately sinusoidal input line currents
- The use of one single switching device
- Controllability of the output voltage to levels higher than the peak value of the mains line to line voltage.

The circuit diagram of this topology is shown in figure 6-2

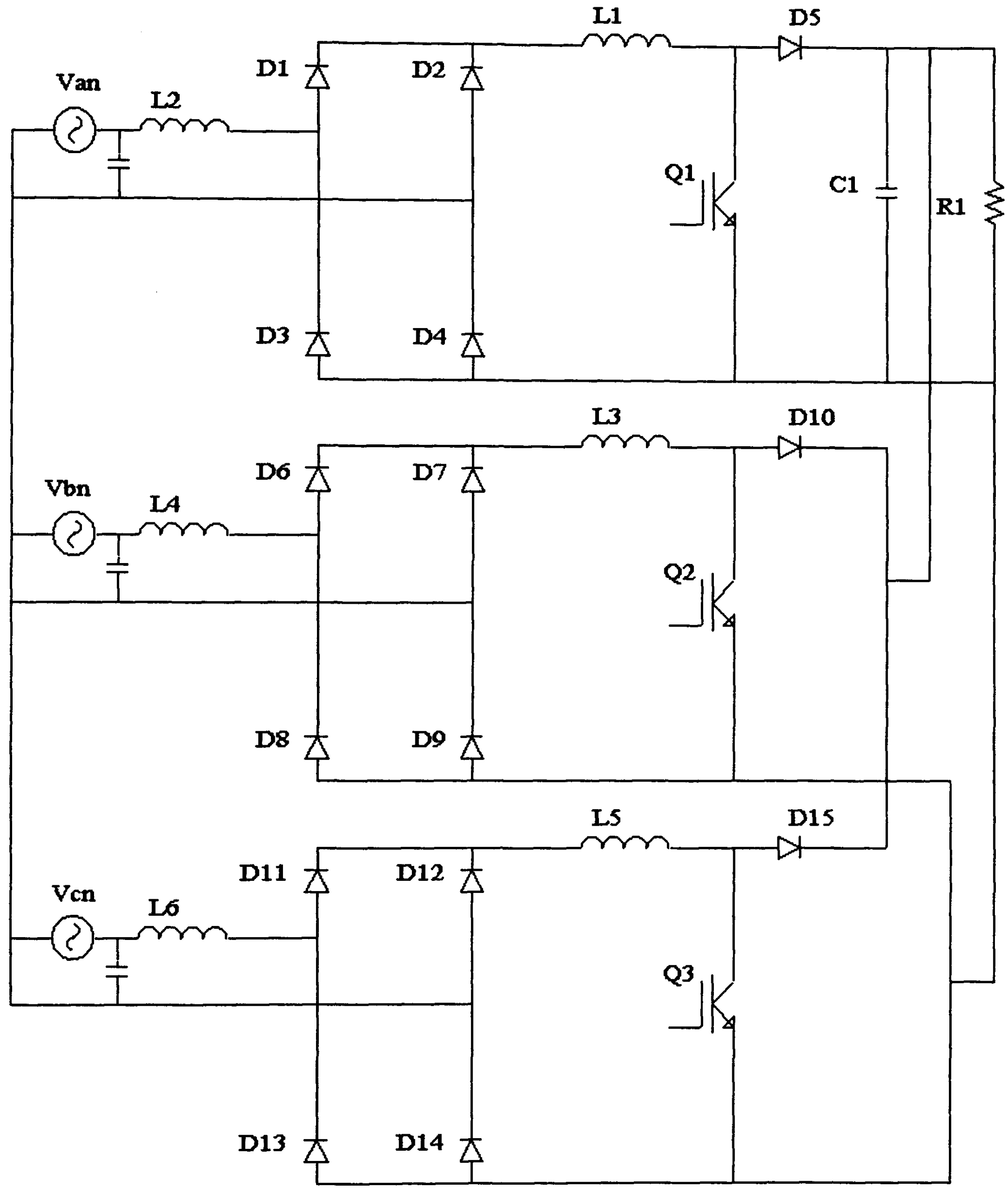

AC SOURCE AND INPUT FILTER	RECTIFIER	BOOST RECTIFIER & POWER FACTOR CORRECTION	DC LINK CAPACITOR AND LOAD

Figure 6-1 Conventional three phase AC to DC converter

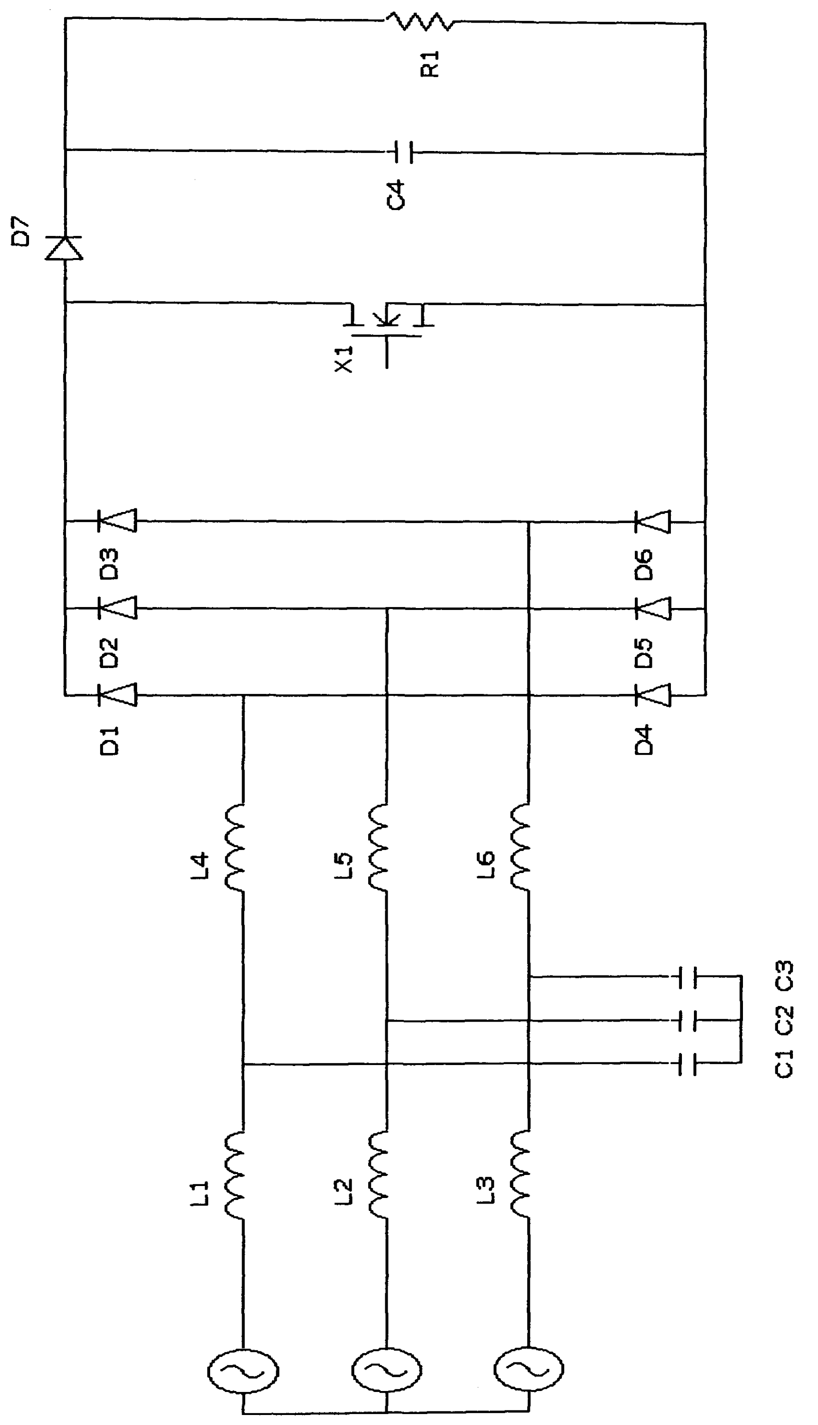

Figure 6-2 Circuit diagram of three phase, unity power factor, DICM single switch boost rectifier. L1, L2, L3: Filter inductor. L4, L5, L6: Boost inductor. C1, C2, C3: Filter capacitor. D1-6: Three-phase diode bridge. X1: IGBT. D7: Boost diode. C4: DC filter capacitor. R1: Load

6.2 Motivation behind usage of the three phase, unity power factor, DICM single switch boost rectifier as an element within the prototype precipitator power supply

The utilisation of the three phase boost rectifier as an alternative to a conventional three phase diode bridge rectifier for the prototype power supply has key advantages:

- The ability to increase the DC link voltage magnitude above that of a conventional three phase diode bridge has significant and favourable consequences in the design of a step up high voltage transformer. A higher applied primary winding voltage implies a lower required transformer turns ratio. This has the advantages of a consequent minimization of number of secondary turns which can help alleviate the problems associated with high voltage step-up transformers; namely transformer leakage reactance, significant stray capacitance referred to the primary winding and the required size of secondary bobbin to accommodate the windings [16]. These problems and measures taken to alleviate them are detailed in chapter 4.
- The ability to improve the quality of the input line currents drawn from the utility, thereby increasing the input power factor of the prototype supply.
- The minimisation of voltage ripple on the DC link due to high frequency switched mode operation.
- Minimisation of component count in comparison to the conventional three phase AC–DC switched mode converter shown in figure 6.1

6.3 Principle of operation of the three phase, unity power factor, DICM single switch boost rectifier

6.3.1 Circuit description

Figure 6-2 shows a circuit diagram of the rectifier. It consists of two main power conversion stages. The first stage is a three phase AC to DC rectifier consisting of three input low pass LC filters (L1-L3, C1-C3), three high frequency switched boost inductors (L4-L6) and a three phase diode bridge rectifier (D1-D6).

The second stage is a single switch boost rectifier consisting of a power semiconductor switch (IGBT X1), a high frequency, boost power diode (D7), a capacitor based DC link (C4) and a load (shown as purely resistive). In actual fact this can be analysed as any kind of load requiring a regulated or unregulated DC bus such as a single or three phase high frequency inverter, a DC-DC converter or a resistive load [3]

6.3.2 Principles of operation.

The active shaping of the three input current waveforms is obtained through the use of the five boost converter elements (inductors L4-L6, IGBT switch X1 and boost diode D4). The IGBT is switched on at a constant frequency. The on time with respect to cycle time (duty ratio) is altered to cope with load variations or to produce a desired change of output voltage (DC link voltage).

During the ON time of the boost switch, all three input phases are effectively short-circuited through L1-L6, the three-phase diode bridge and boost switch X1.

As a result of this the three input phase currents begin simultaneously to increase at a rate proportional to the instantaneous value of their respective phase voltages.

The specific peak current values during each ON interval are proportional to the average values of their input phase voltages during the same interval. Since each of these voltages average values varies sinusoidally, the input current peaks also vary sinusoidally as shown in figure 6-3. In discontinuous mode the current pulses always begin at zero, this means that their average values during the on time are also proportional to the phase voltage.

During the OFF time of the switch, the energy stored in the three boost inductors is discharged through the converter. The time required to discharge each inductor is dependent on its phase voltage, the DC output voltage and the inductance value.

The boost switch X1 is switched at a frequency considerably higher then the mains supply frequency. As a consequence of this all three input current consists of a fundamental mains frequency and a band of unwanted high frequency switching components.

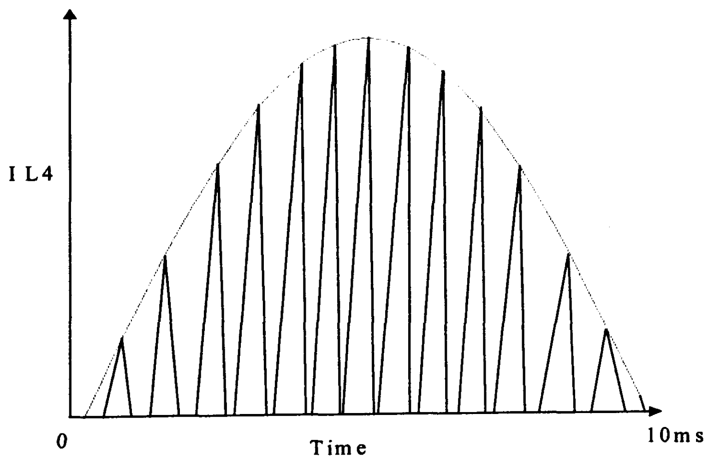

Figure 6-3 Single phase input line current before filtering (I L4)

Since the high frequency spectral component of the inductor currents IL4-IL6 are separated by an appreciable window from the fundamental utility frequency, it is a simple process to filter these with a relatively small LC filter at the input of the rectifier. (L1-L3, C1-C3).

The DC output voltage level of the rectifier is a function of the input supply voltage, the switch duty ratio, switching frequency and the load power [3,7].

Different strategies for control can be used. The simplest one is constant switching frequency and variable duty ratio. Other methods such as variable frequency and variable duty ratio can also be used however the advantage of the first method is its simplicity to implement [13].

To maintain discontinuous boost inductor current, the duty ratio of the boost switch is varied within a designed band dependent on the load considerations. For the rectifier operating in PWM discontinuous inductor current mode, both the output boosted voltage level and input power factor are a function of the duty ratio of the boost switch [3,19].

6.3.3 Output voltage control

Output voltage control is achieved with a suitable controller which senses variation in DC output voltage and varies the duty ratio of the power switch accordingly to maintain a constant output voltage. PWM based integrated circuits have, in the past few years come onto the market place designed specifically for this task. A specific IC (SG3526) was implemented within the control electronics of the prototype test rig and is detailed in 6.5.1.

6.3.4 Three phase boost rectifier specification.

A specification for a prototype rectifier was determined and component values were calculated using design procedures set down in [7].

The circuit was then modelled using the electrical simulation software package Pspice to verify correct choice of component values before a prototype rectifier was constructed.

<u>Converter specification:</u>

- Supply voltage = 415V 50Hz
- Converter output voltage = 800 VDC
- Output power rating = 15kW
- IGBT Switching frequency = 22 kHz
- L1, L2, L3 = 6.3mH
- L4, L5, L6 = 44μH
- C1-C3 = 6.8μF
- C4 = 4700μF

6.4 Pspice circuit Simulation results

Figures 6-5 to 6-8 show the simulation results of the converter depicted in figure 6-4. The converter delivers 15kW at 800VDC. The load on the converter is depicted as purely resistive (Rload =42R)

The switching device is modelled as a Toshiba IGBT (MG120V2YS40: 240A, 1700V) and is switched at a frequency of 22kHz. The duty ratio of the switch is controlled by a

Pspice voltage pulse source (V4) and is set to 40% to achieve the required boosted output voltage of 800Vdc.

Rectification and boost diodes within the spice circuit are modelled as the freewheeling diodes connected antiparallel across the collector emitter junction of a permanently off IGBT. This was done to overcome the lack of high power diodes present in the Pspice component library

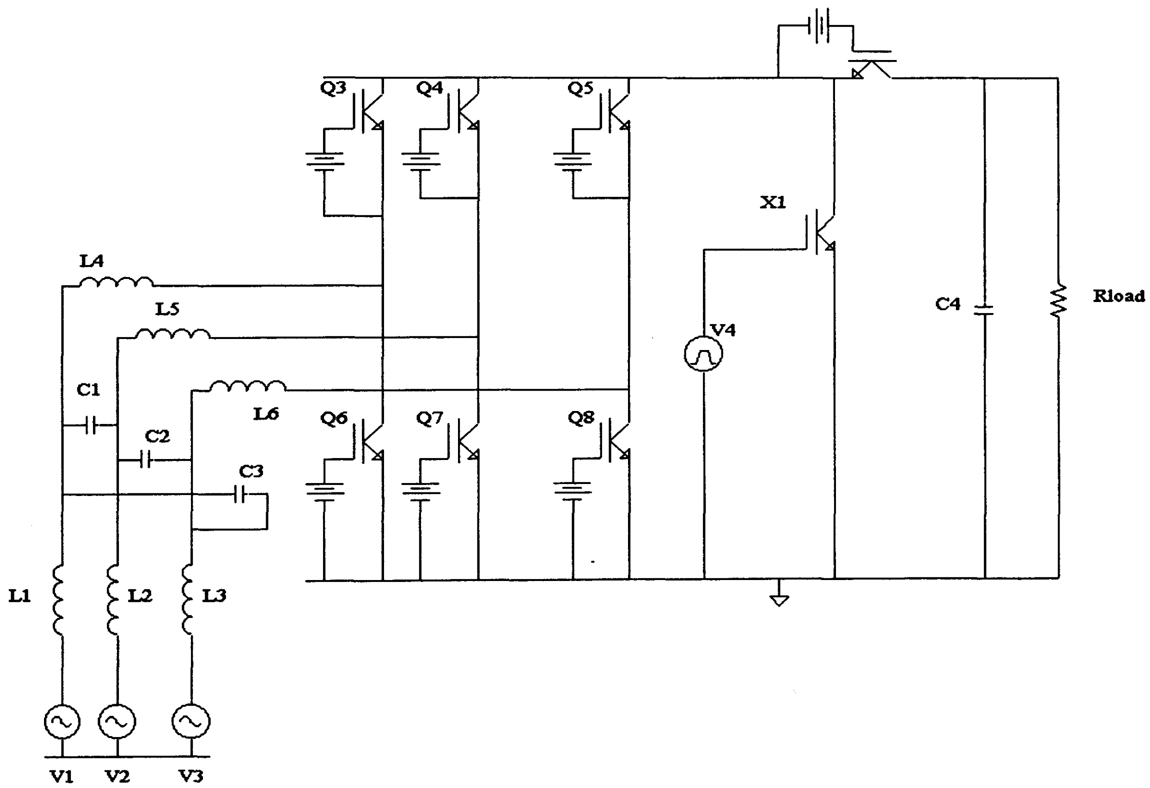

Figure 6-4 Circuit diagram of converter simulated in Pspice.

L1, L2, L3 = 6.3mH, L4, L5, L6 = 44uH, C1-C3 = 6.8uf, C4 = 4700uF, Rload= 42R
X1= IGBT (MG100V2YS40 TOSHIBA)

Transient analysis of the converter was performed over 20 cycles of the 50Hz mains supply to verify correct operation. A digital Fourier transform of the simulated input line currents was then performed in Pspice to verify elimination of the high frequency switching component.

Figure 6-5 (Top) shows the 3 input line currents after filtering by inductors L1-L3 and capacitors C1-C3. The pre-filtered line current with a high frequency 22kHz switching component is shown at the bottom.

Figure 6-6 shows a harmonic analysis of both the filtered (top graph) and pre-filtered input line currents (bottom).

Figure 6-7 shows the switching voltage waveform (Vce) of the IGBT switch, the collector current, the filtered input line currents and the pre-filtered input line current (boost inductor current)

Figure 6-8 shows a zoomed out waveform of the IGBT switch collector current displaying a six-pulse ripple due to the three-phase diode bridge rectification (bottom).

Figure 6-9 shows the boost diode current (ID4); 2nd IGBT collector-emitter voltage and Bottom: IGBT collector current over two switching cycles.

Figure 6-10 shows a zoomed in waveform of the three pre-filtered input line currents (boost inductor currents)

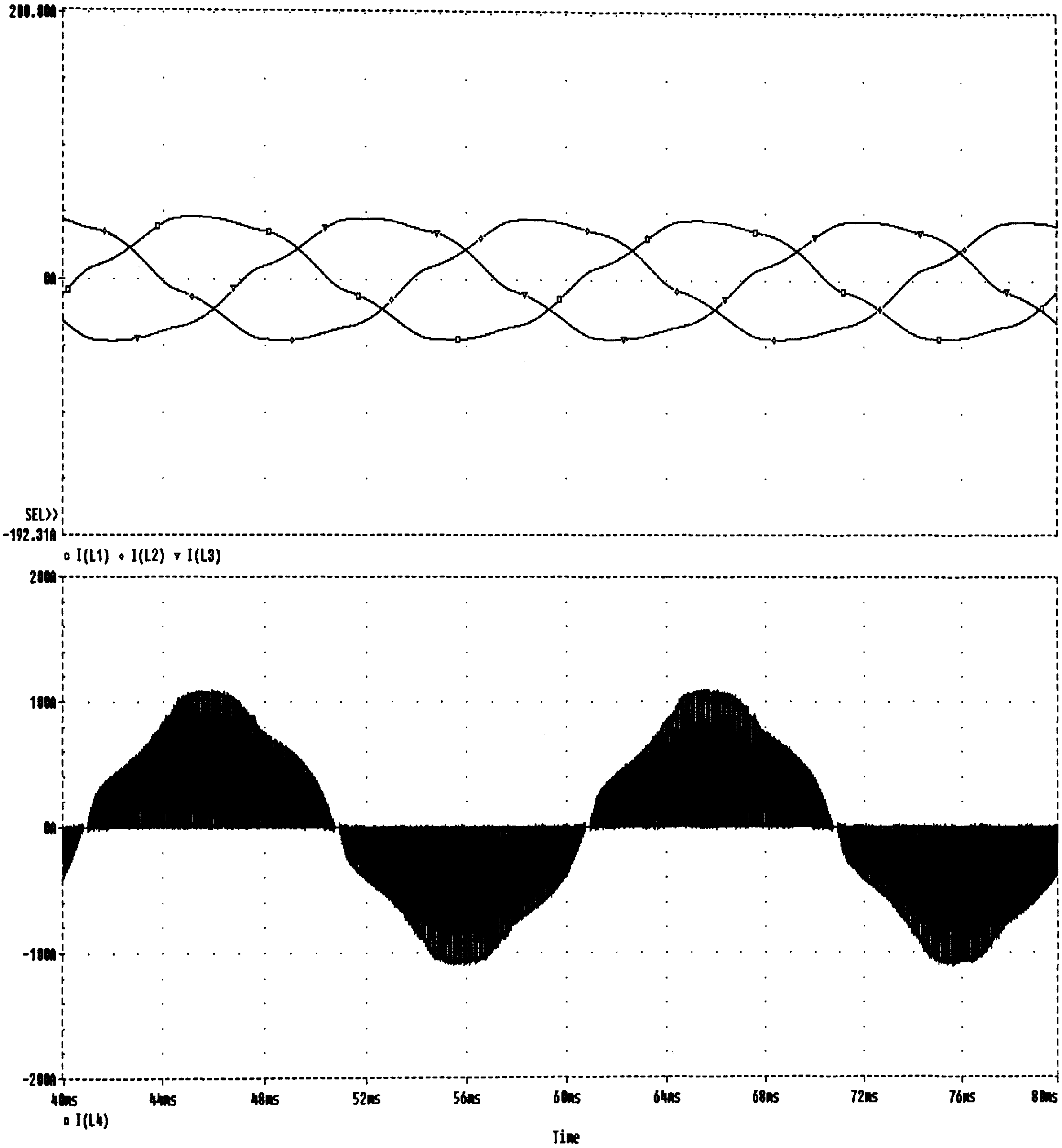

Figure 6-5 (Top) Three phase input line currents (IL1, IL2, IL3).

(Bottom) Boost inductor current (IL4)

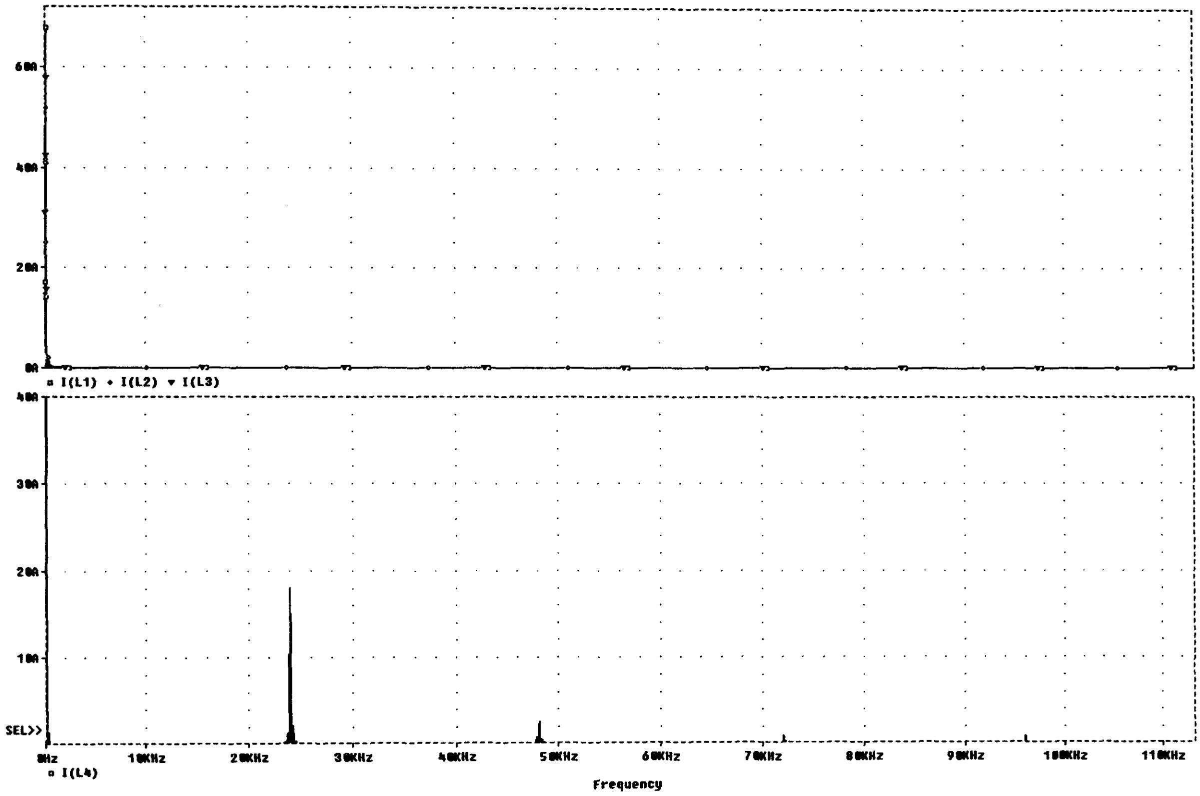

Figure 6-6 Harmonic analysis of input line currents: Top- IL1-IL3 (filtered input line current). Bottom- IL4 (high frequency switched inductor current)

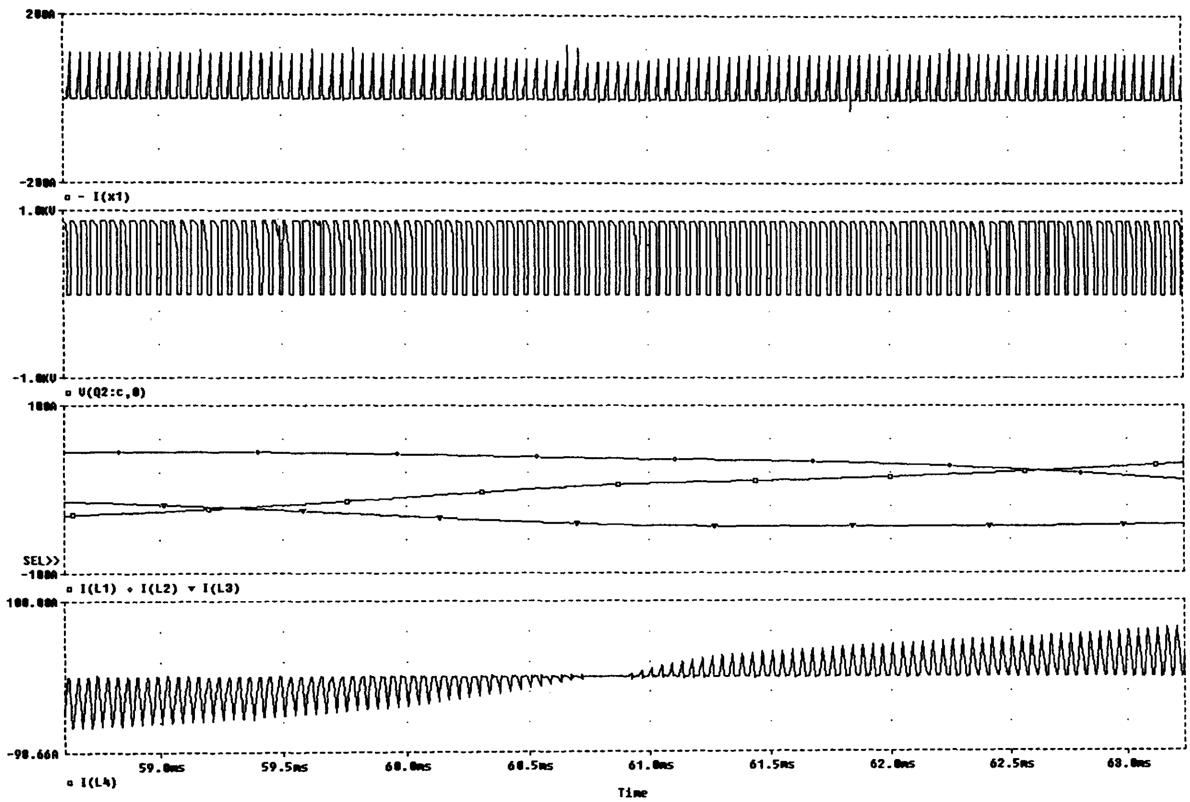

Figure 6-7 Top: IGBT collector current . 2nd: Vce of IGBT . 3rd: Input line currents IL1-IL3. Bottom: Boost inductor current (IL4).

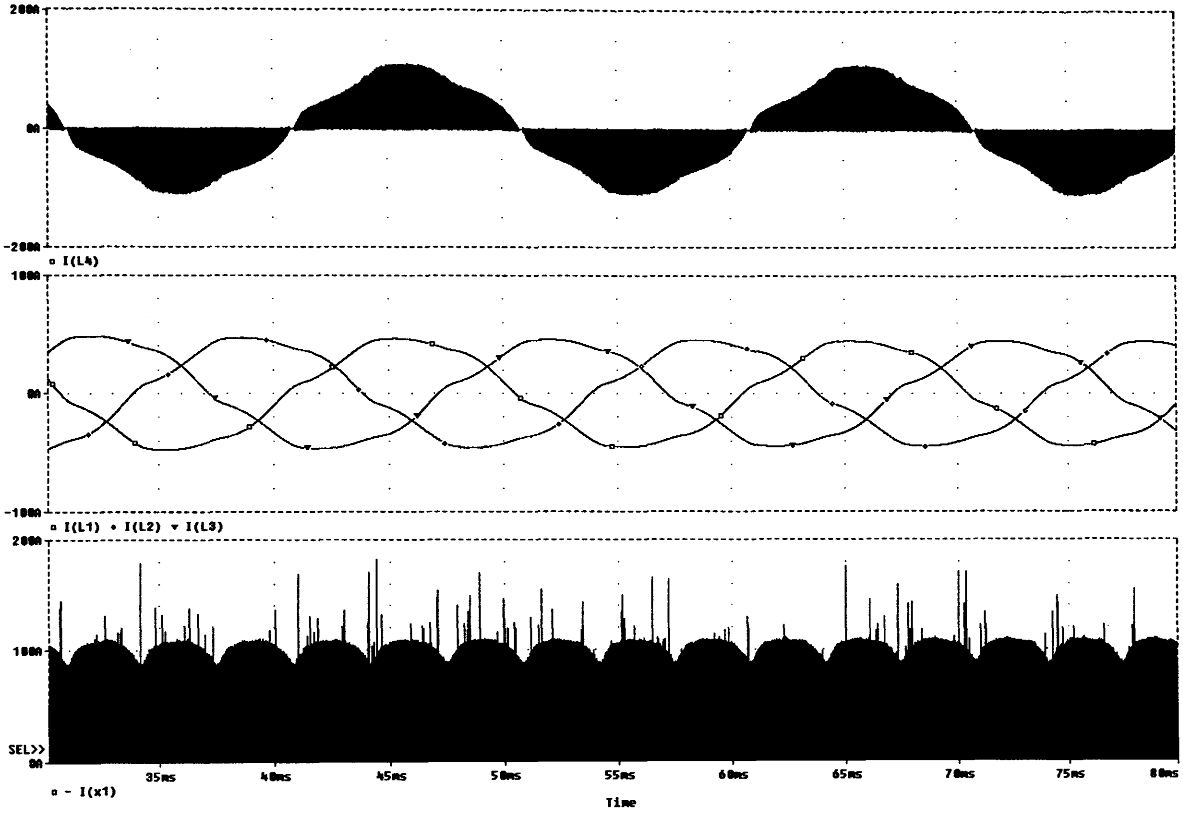

Figure 6-8 Top: Boost inductor current (IL4). 2nd: Input line currents (IL1, IL2, IL3). Bottom: IGBT collector current.

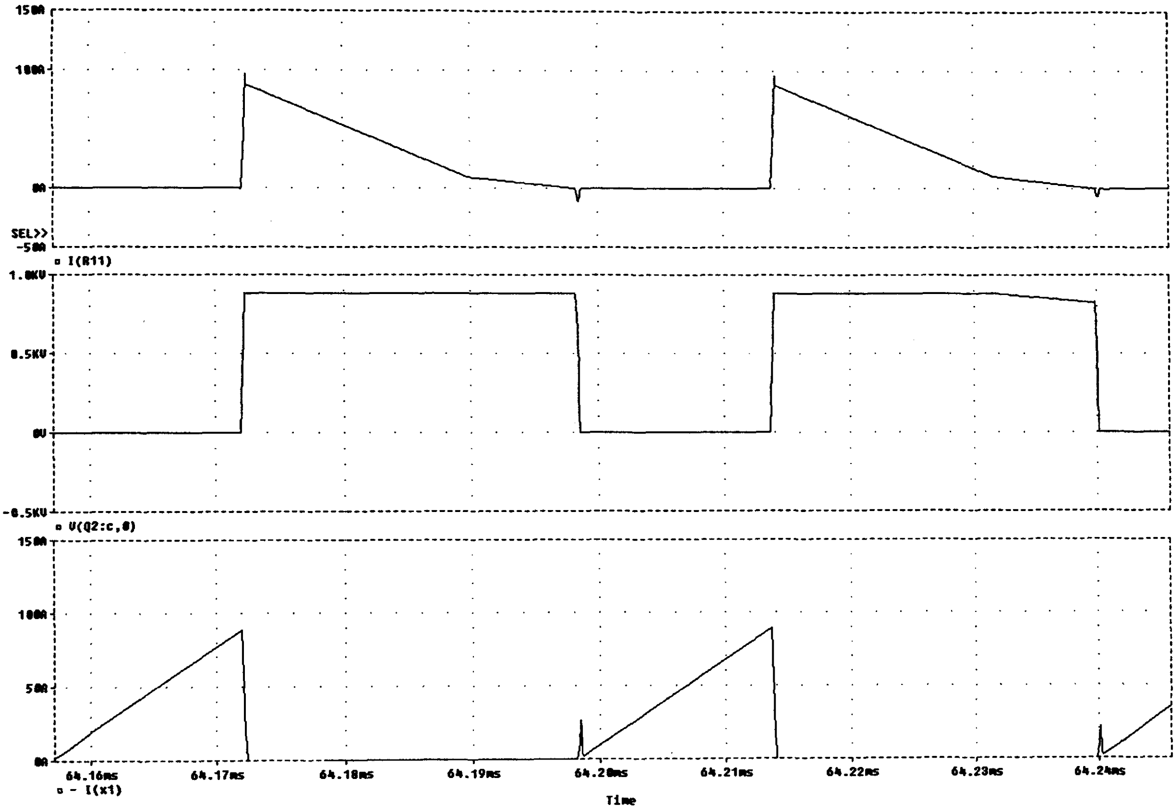

Figure 6-9 Top: boost diode current (ID4). 2[nd] :IGBT collector-emitter voltage
Bottom: IGBT collector current

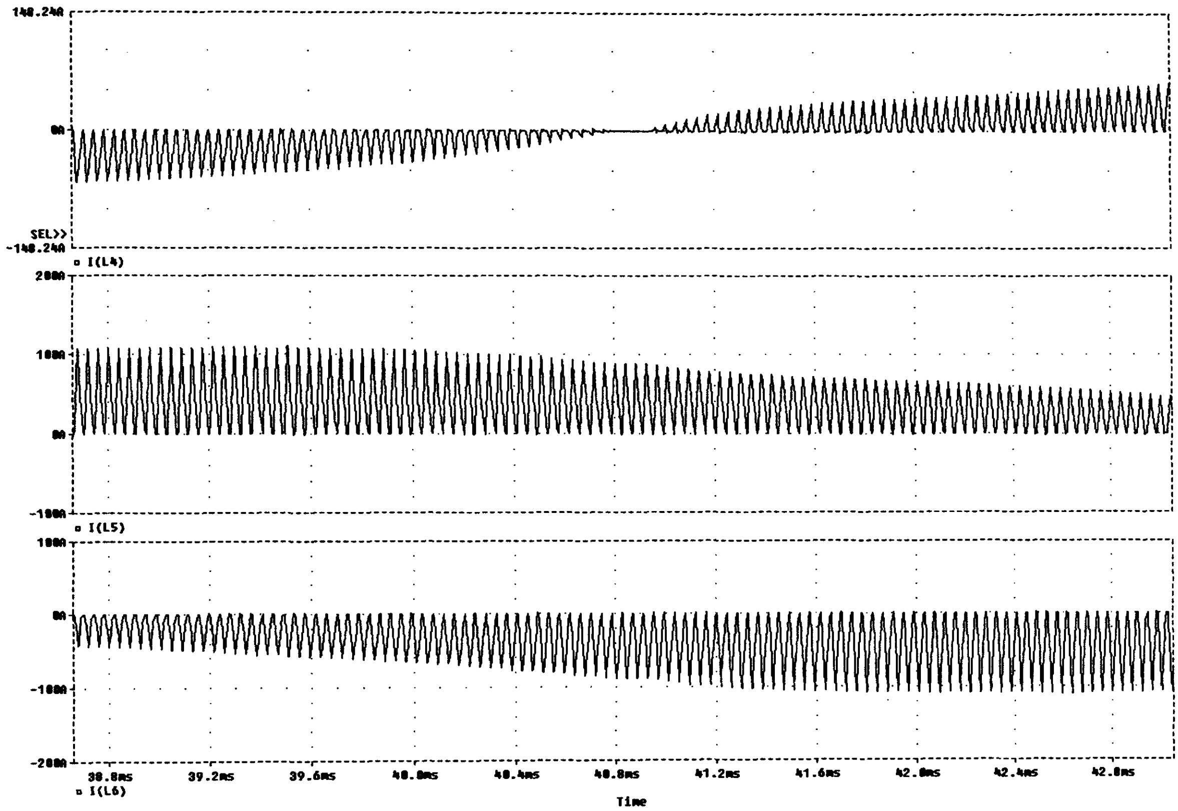

Figure 6-10 Zoomed in boost inductor currents IL4, IL5, IL6.

6.5 Construction and testing of the prototype rectifier

A three-phase, unity power factor, DICM single switch boost rectifier was constructed with the component values given in 6.3.4. Figure 6-11 shows the constructed rectifier.

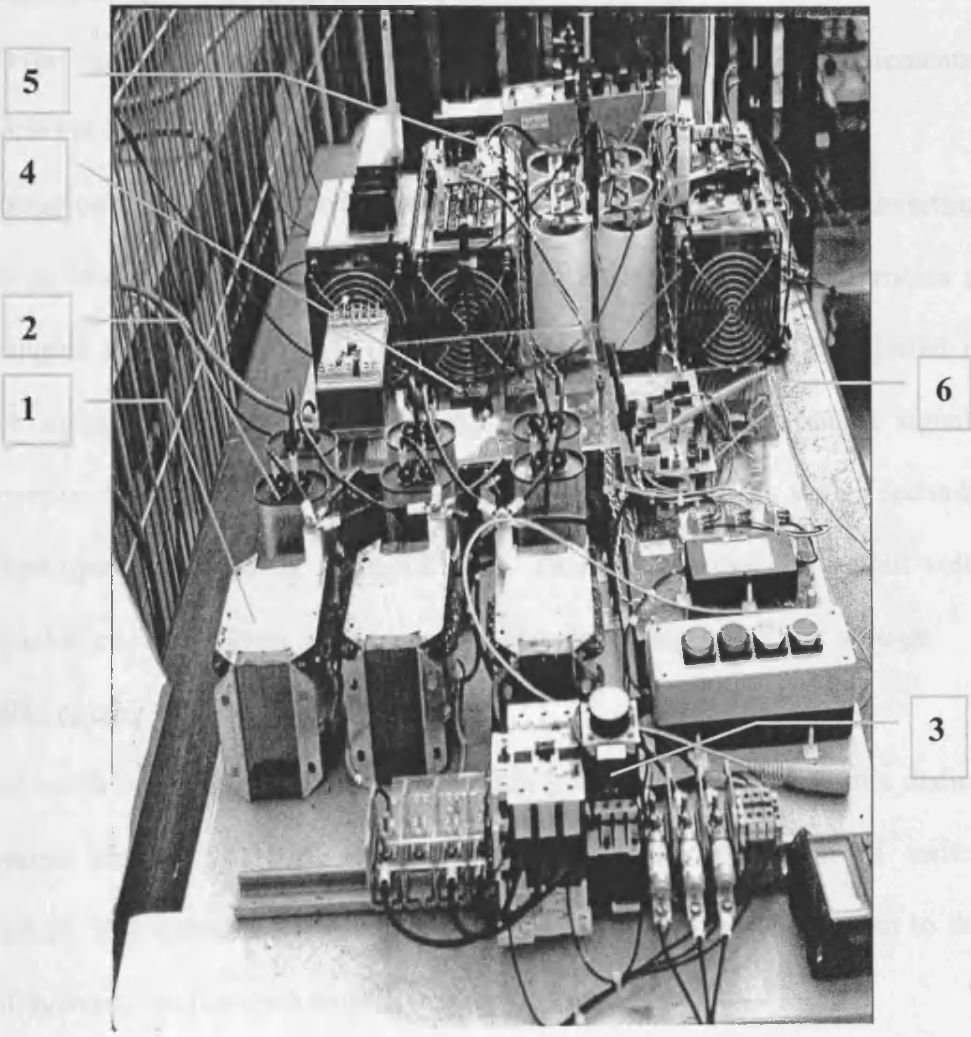

Figure 6-11 Prototype rectifier: 1: Input filter inductors. 2: Filter capacitors. 3: Switchgear and protection. 4: Boost inductors 5: IGBT/boost diode, heatsinking and DC link capacitors. 6: Control electronics

6.5.1 Control and drive electronics

A circuit diagram of the control electronics of the converter is shown in figure 6-12 and consists of four main stages

1: Converter output voltage sense, isolation and feedback

Converter output voltage sense and isolation is achieved by the implementation of an opto-tracker circuit.

A proportion of the converter DC output voltage is applied to a none inverting amplifier which is powered from a secondary source to the main control electronics supply. An optocoupler diode/transistor (ILD 74) in the feedback path of the amplifier isolates the output signal from the rest of the control electronics. The output signal from the optocoupler is then linearized by a second differential amplifier with a secondary closely matched optocoupler in its feedback path. This ensures that the output voltage of the optotracker circuit is linear with respect to changes in input DC link voltage

2: PWM circuit

Pulsed width modulation of the IGBT switch is achieved by the use of a dedicated PWM integrated circuit (SG3526) designed specifically for operation of switched mode converters. The output voltage of the opto-tracker circuit provides input to the inverting pin of the transconductance amplifier internal to the SG3526.

The Reference voltage to the none inverting pin is provided via a variable potential divider network. Gain and stability compensation is achieved through a parallel RC network applied to the COMP pin [20]

3: IGBT drivers.

The circuitry required to satisfactorily drive and provide protection for the IGBT switch is achieved by the use of a dedicated IGBT drive module (Semikron SKHI21)

This module provides an isolated positive (+15V) signal to switch the IGBT on and negative 15V to turn it off. The state of the driver is directly controlled by the SG3526 output.

4. Short circuit protection

In the event of a short circuit fault occurring at either the output of the converter or within the converter topology itself a supervisory current sense and protection circuit is implemented.

The input line current IL1 is monitored via a Hall effect current transducer. This is then compared against a pre-defined level by a single supply LM358 comparitor.

If the overcurrent threshold is reached then a 555 timer operating in monostable mode is triggered. This causes shutdown of the output of the SG3526 PWM IC for a set duration. Assuming that the fault has cleared (i.e. the output of the comparitor has returned to it high state, a soft start of the SG3526 is performed to regain circuit operation.

Conventional three-phase semiconductor fusing protects the converter. Timing switchgear is also used to ensure that control electronics supply is present before mains supply voltage is applied to the converter.

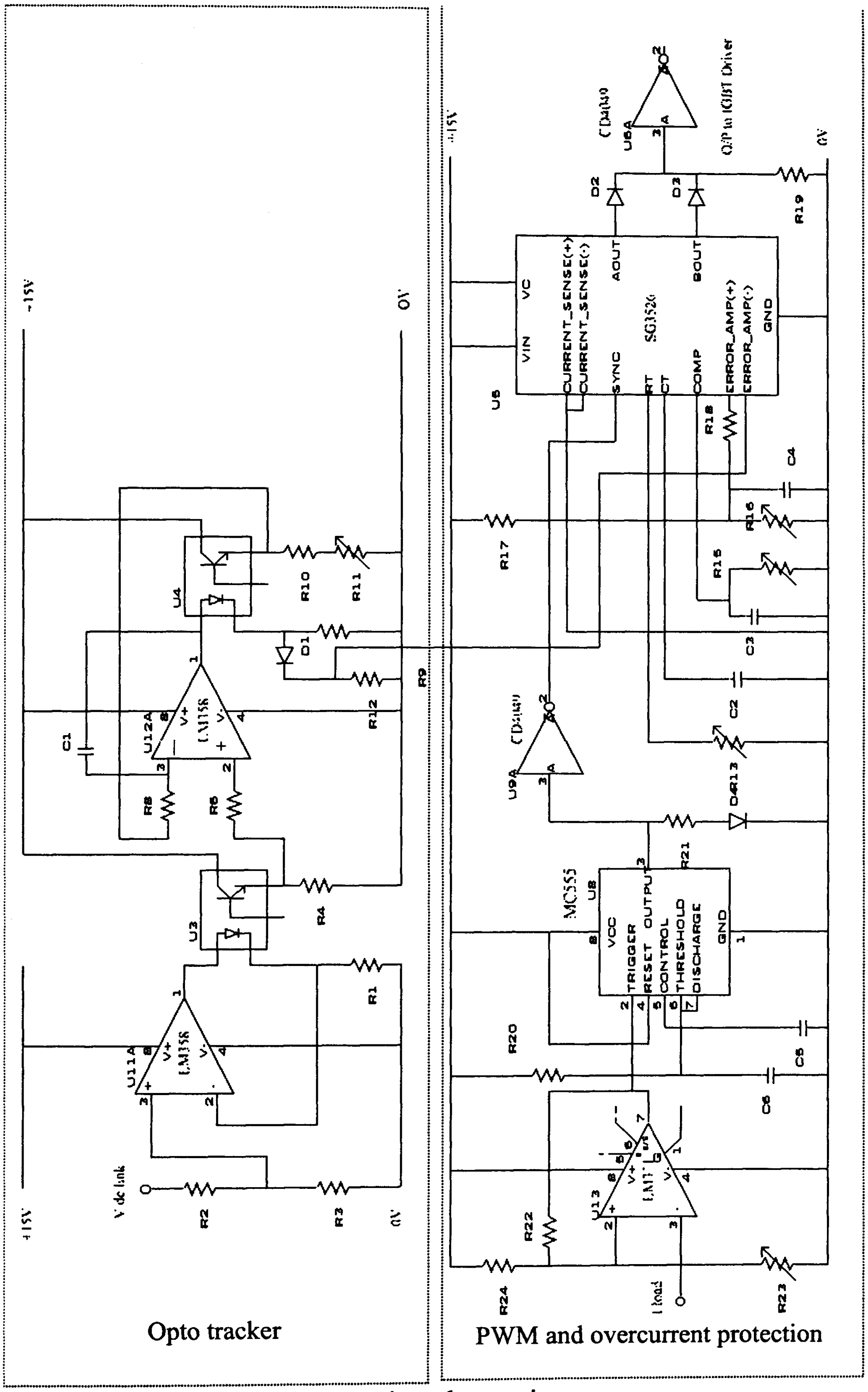

Figure 6.12 Control and protection electronics

Figures 6-13 to 6-16 shows the input line currents and the measured input power factor under increasing switch duty ratio. It can be seen that as the duty is increased, so too is the measured input power factor and the DC output voltage of the rectifier.

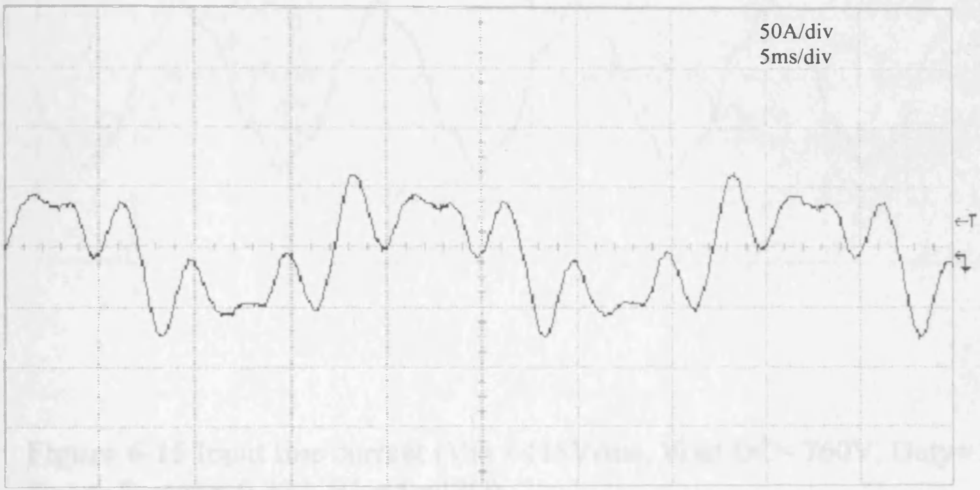

Figure 6-13. Input line current: (Vin=415Vrms, Vout DC=560V, Duty=0, Power factor =0.305, Rload=42Ω)

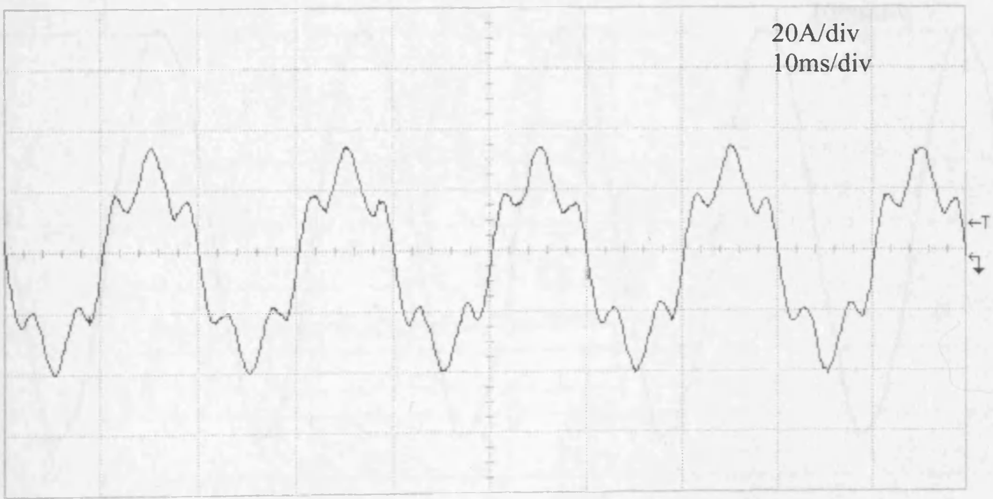

Figure 6-14 Input line current: (Vin=415Vrms, Vout DC=673V, Duty=10%, Power Factor 0.668, Rload=42Ω)

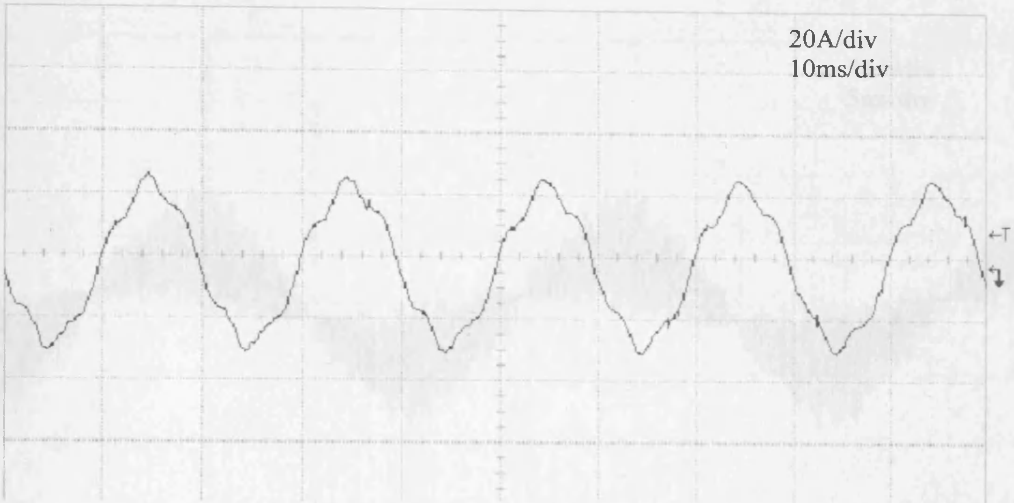

Figure 6-15 Input line current (Vin =415Vrms, Vout DC= 760V, Duty= 20%, Power Factor = 0.832, Rload =42Ω)

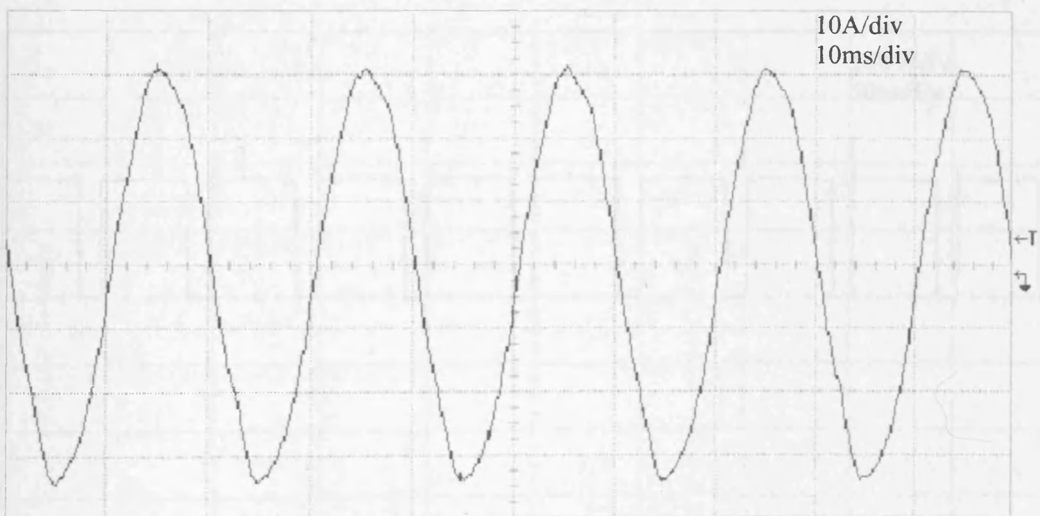

Figure 6-16 Input line current (Vin=415Vrms, Vout DC =806V, Duty = 40%, Power factor= 0.98, Rload=42Ω)

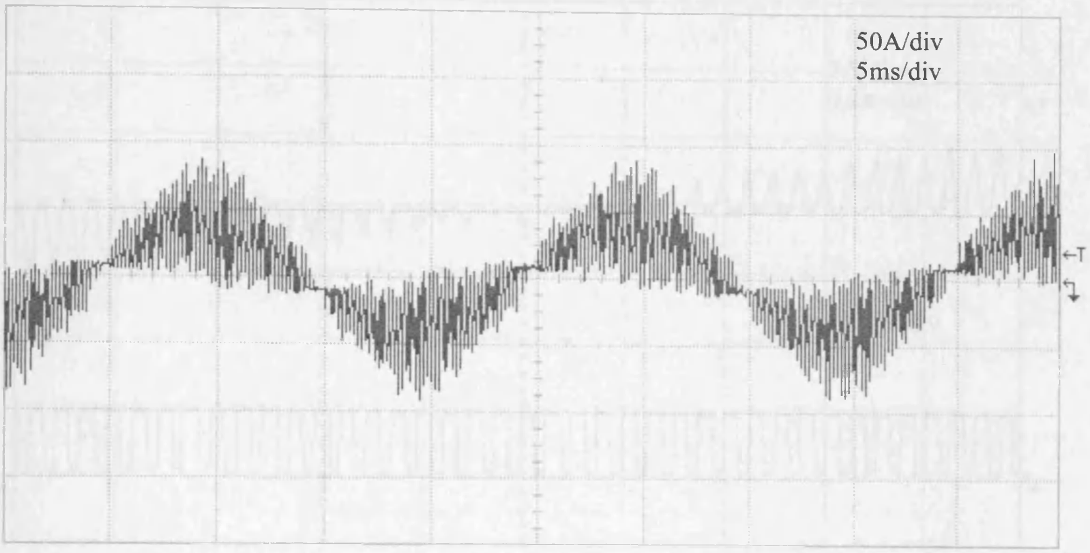

Figure 6-17. Boost inductor current (IL1)

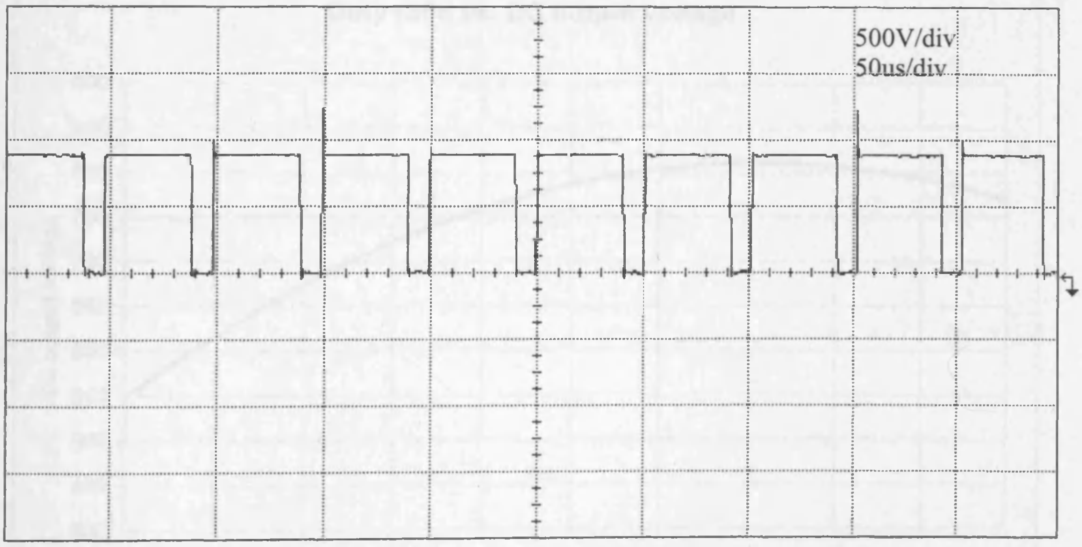

Figure 6-18 IGBT collector-emitter voltage

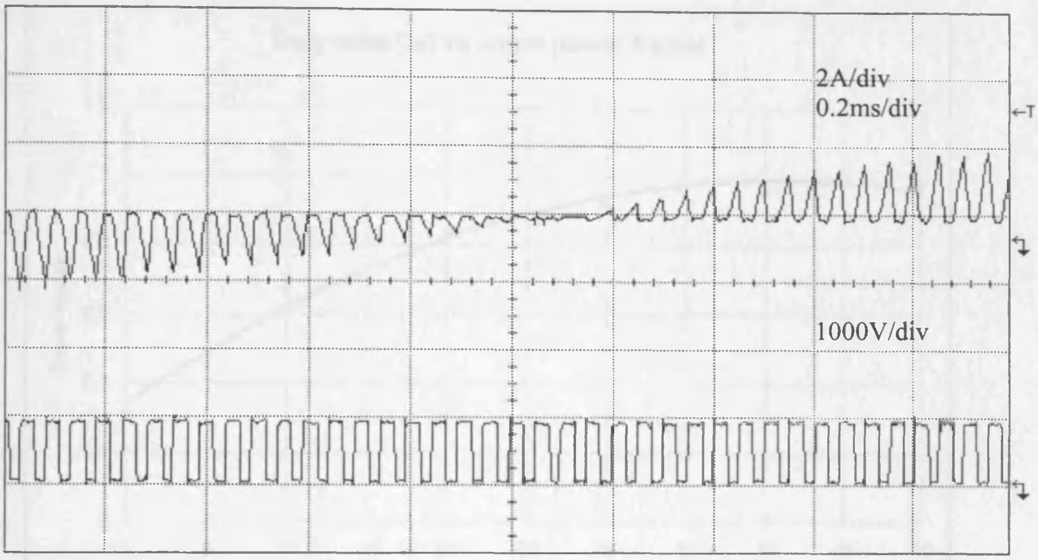

Figure 6-19 Boost inductor current (top). IGBT collector-emitter voltage (bottom)

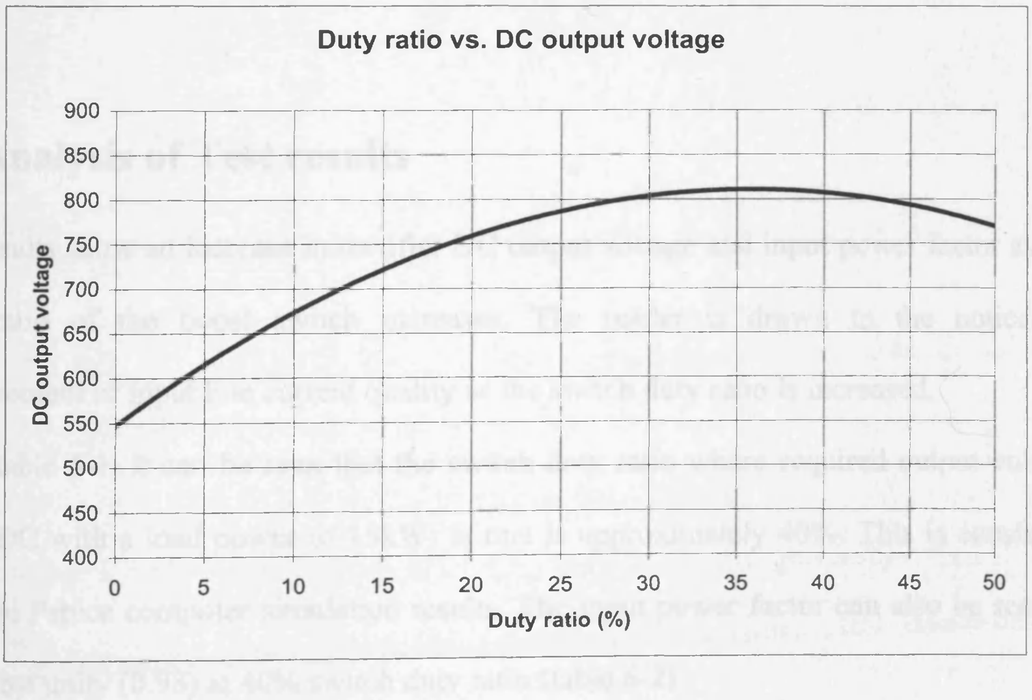

Table 6-1 Switch duty ratio vs. rectifier DC output voltage

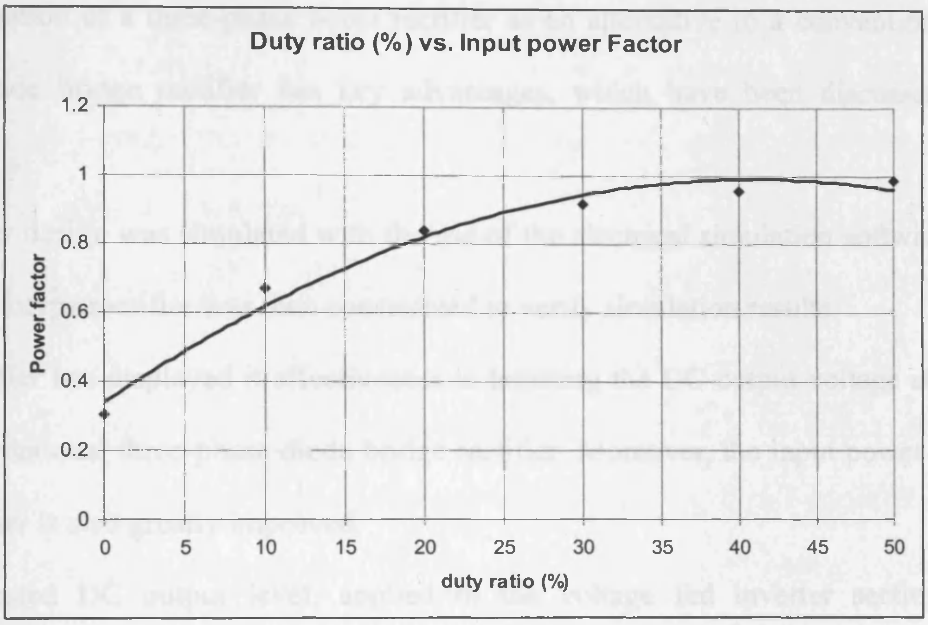

Table 6-2 Switch duty ratio vs. measured input power factor

6.6 Analysis of Test results

The results show an increase in rectifier DC output voltage and input power factor as the duty ratio of the boost switch increases. The reader is drawn to the noticeable improvement of input line current quality as the switch duty ratio is increased.

From table 6-1, it can be seen that the switch duty ratio where required output voltage (800VDC with a load power of 15kW) is met is approximately 40%. This is consistent with the Pspice computer simulation results. The input power factor can also be seen to be almost unity (0.98) at 40% switch duty ratio (table 6-2).

6.7 Summary

The utilisation of a three-phase boost rectifier as an alternative to a conventional three-phase diode bridge rectifier has key advantages, which have been discussed in this chapter.

A rectifier design was simulated with the use of the electrical simulation software Pspice and a prototype rectifier was then constructed to verify simulation results.

The rectifier has displayed it effectiveness in boosting the DC output voltage above that of a conventional three-phase diode bridge rectifier. Moreover, the input power factor of the rectifier is also greatly improved.

The boosted DC output level, applied to the voltage fed inverter section of the precipitator power supply, would enable a minimisation of the high voltage transformer windings or alternatively, a higher negative DC output level applied to the discharge electrode of a precipitator section.

6.8 References

1. **Duffey CK and Stratford RP**, "Update of harmonic standard IEEE-519. IEEE recommended practices and requirements for harmonic control in electric power systems", IEEE/IAS Petroleum and Chemical Industry Conf., TX, USA, 1988
2. **Ametani A**, "Generalised method of harmonic reduction in AC-DC converter by harmonic current injection", Proc, IEE vol.7, pp.523-529, 1972
3. **Prasad AR and Ziogas PD**, "An active power factor correction technique for three phase diode rectifiers.", IEEE Trans. Power Electronics, vol.6, pp. 83-92, 1991

4. **Prasad AR and Ziogas PD**, "A passive waveshaping method for single phase diode rectifiers,", IEEE PESC, pp.1042-1050, 1990
5. **Mohan N**, "Analysis of a new power electronics interface with approximately sinusoidal 3-phase utility currents and a regulated DC output", IEEE Trans. Power Delivery, April, 1993, pp.540-546
6. **Bose BK**, "Recent advances in power electronics.", IEEE trans. Power electronics, vol.7, pp.2-16, 1992
7. **Kolar JW and Ertl H**, "A comprehensive design approach for a three phase high frequency single switch discontinuous mode boost power factor corrector based on analytically derived normalised converter component ratings.", IEEE/IAS 93, pp.931-938, 1993
8. **Ismail E**, "A single transistor three phase resonant switch for high quality rectification.", IEEE Power Electronics Specialist Conference, 1992, pp. 1341-1351
9. **Koczara W**, "Controllability of the simple three phase rectifier operating with unity power factor", EPE 93, Poland, pp-183-187, 1993
10. **Kocher MJ**, "An AC to DC converter with high quality input waveforms", IEEE Trans. Industrial Appl. Vol. 1A-19, No. 4, pp. 586-599, 1983
11. **Marple WP**, "Low distortion three phase power regulator", IBM technical disclosure bulletin, Vol.22, No.3, pp.970-971, 1979
12. **Gauger D et al**, "A three phase off line switching power supply with unity power factor and low TIF.", IEEE INTELEC, pp.115-121, 1986

13. **Chen K**, "A soft switching active snubber optimised for IGBT's in single switch unity power factor three-phase diode rectifiers", IEEE Trans. Power Electronics, Vol10, No. 4, pp.446-452, 1995

14. **Kolar JW and Ertl H**, "Space vector based analytical analysis for the input current distortion of a three-phase discontinuous boost rectifier system", PESC Rec., pp.696-703, 1993

15. **Simonetti DSL**, "Single switch three-phase power factor pre-regulator under variable switching frequency and discontinuous input current", IEEE PESC Rec., pp. 657-662, 1993

16. **Devine PJ and Lefley PW**, "A high power three-phase unity power factor regulator for high voltage applications", UPEC Rec., 1996, pp. 417-420

17. **Tou M, and Al-Haddad K**, "Analysis and design of single controlled switch three-phase rectifiers with unity power factor and sinusoidal input current", IEEE Trans. Power Electronics, pp. 856-862, 1995

18. **Tou M, and Al-Haddad K**, "A new three phase unity power factor boost rectifier with capacitive type input", IEEE Trans. Power Electronics, pp.256-266, 1994

19. **Pforr J**, "Single ended resonant pre-converters for high frequency induction heaters", PhD Thesis, University of Teeside, 1992

20. **Unitrode** products and applications handbook, 1995-1996

7. POWER SUPPLY CONTROL ELECTRONICS, PERIPHERAL CONTROL AND INSTRUMENTATION

7.1. Control scheme

Figure 7-1 shows the flow diagram of the entire electronics and instrumentation scheme within the prototype precipitator power supply.

This may be divided into several sub-circuits such as boost rectifier and inverter control circuitry previously detailed in chapters 4 & 5, however, control, fault detection and instrumentation signals may be used by more than one of these sub-circuits.

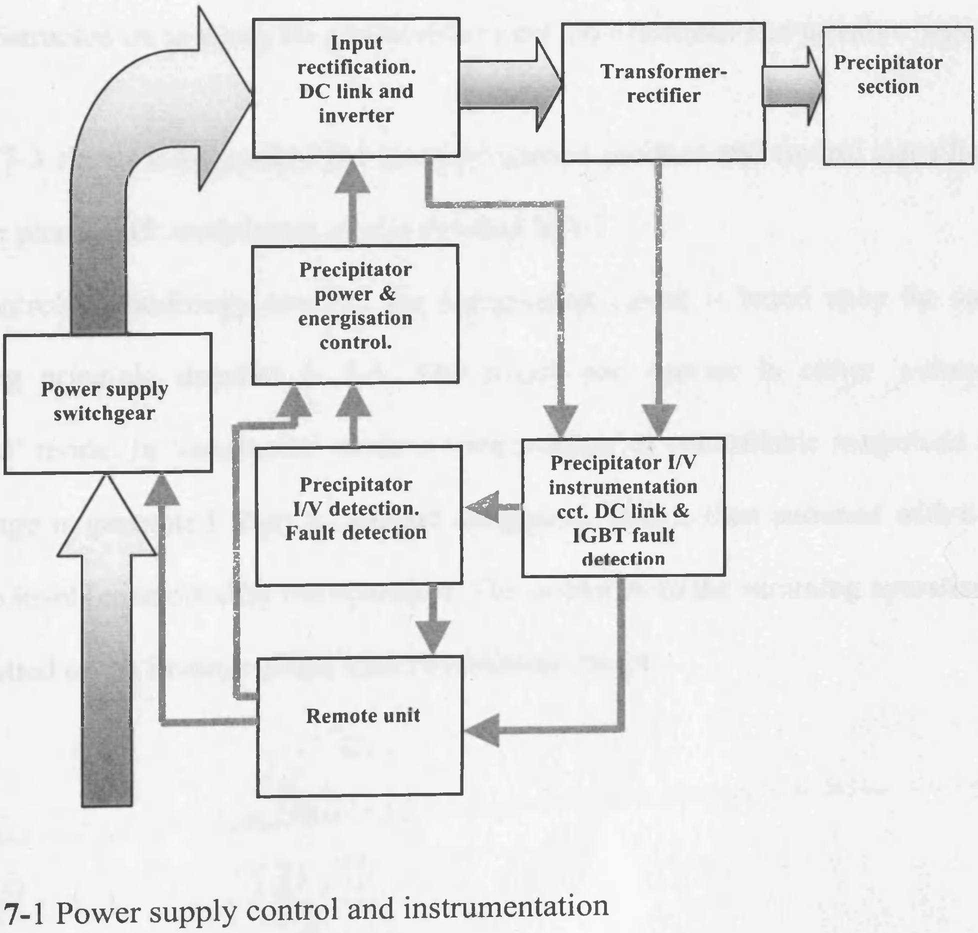

Figure 7-1 Power supply control and instrumentation

7.2 Precipitator energisation control

The control and instrumentation circuitry within the power supply was designed specifically for prototype commissioning and testing at National Power's Didcot "A" Power Station. The possibility of interfacing with existing precipitator hardware at the power station was investigated but since the existing power station control and instrumentation systems are based around conventional low frequency power supplies then interfacing was unsuitable.

The control and instrumentation circuits within the prototype had to be robust and of minimal complexity to allow rapid modifications to be made if required before undergoing testing at the power station. The circuits were based upon analogue designs and constructed on separate plug in boards to aid modifications and possible fault finding.

Figure 7-3 shows a diagram of the circuitry used to produce and control signalling to the inverter phase shift modulation circuit detailed in 5-2.

The control methodology used by the energisation circuit is based upon the spark rate counting principle detailed in 2-5. The circuit can operate in either 'automatic' or 'manual' mode. In 'automatic' mode a ramp voltage of controllable magnitude and rate of change is generated from a clamped integrator. This is then summed with a manual voltage level (controlled by the operator). The output from the summing operation is then transmitted to the inverter phase shift modulation circuit.

7.2.1 Spark/ flashover response

- Automatic mode

If a precipitator spark/ flashover is detected, then the detection circuit transmits a ramp 'shutdown ' signal to the energisation circuit. This forces the phase shift modulation circuit to lower the effective duty ratio of the H bridge inverter causing the transformer-rectifier output voltage to decrease to a manual base level.

This is in order to commence a further ramping sequence and to extinguish any possible prolonged flashover in the precipitator. This mode of operation is shown in figure 7-2.

- Manual mode

In 'manual' mode of operation, the ramping function is disabled and the transformer – rectifier output voltage is controlled by the operator via the remote control unit detailed in 7-6.

If, however, a precipitator spark/ flashover is detected, the monitoring circuit transmits a ramp 'shutdown' signal to the energisation circuitry forcing the inverter to temporarily switch off. Once the detected spark/ flashover clears then the effective duty ratio of the H bridge inverter is gradually increased over a pre-set time period causing an effective soft re-start of the power supply.

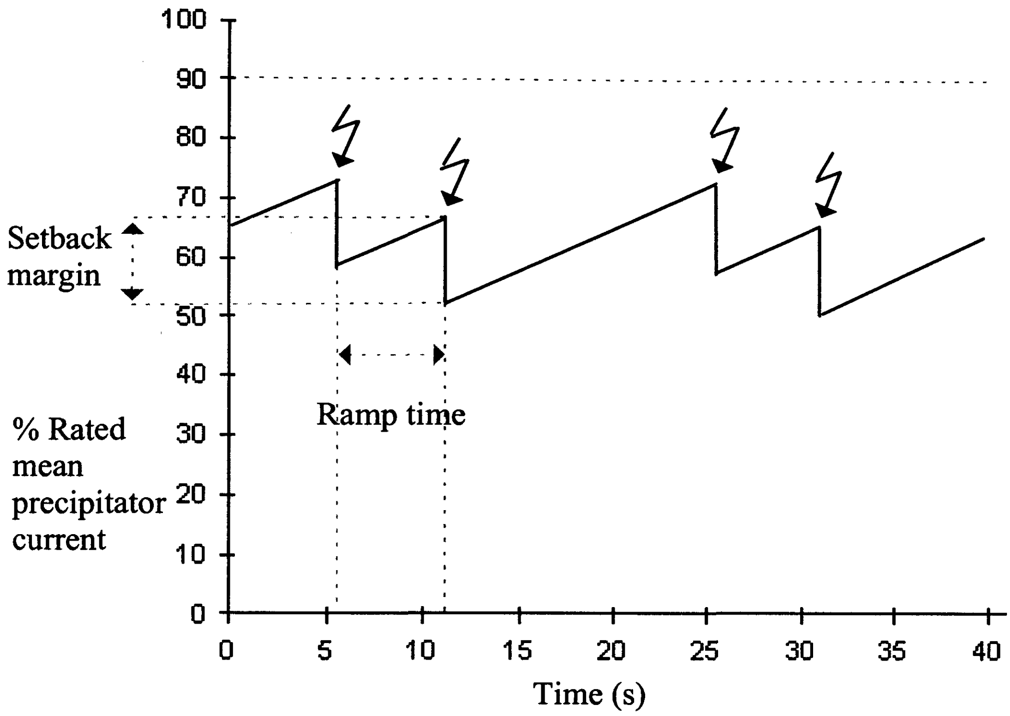

Figure 7-2 Precipitator energisation principle

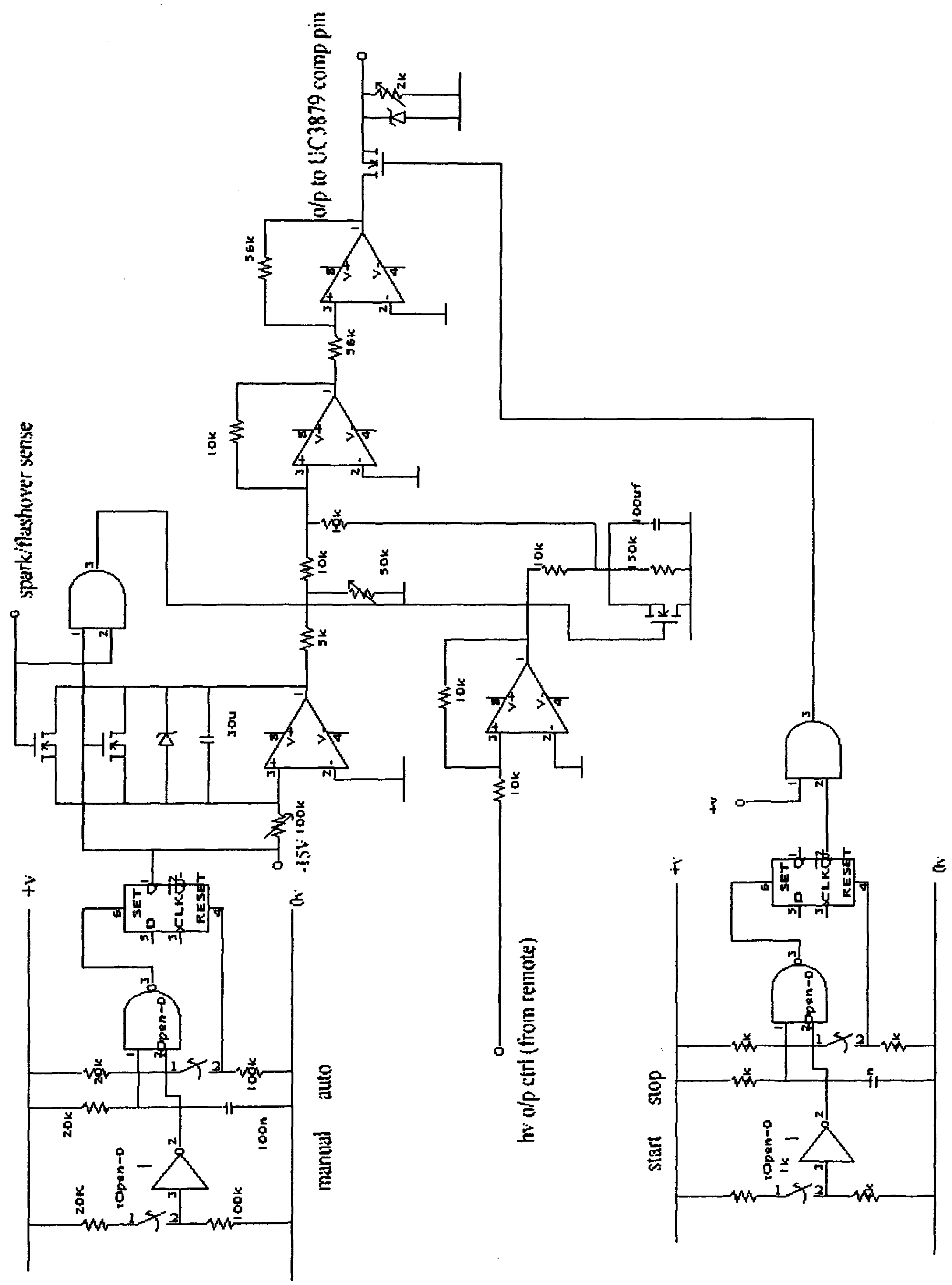

Figure 7-3 Precipitator energisation control

7.3 Transformer -rectifier voltage / current detection & signal processing

Effective monitoring of the transformer rectifier voltage and current is crucial in effective energisation of the precipitator. Both the transformer–rectifier's voltage and current signals are measured and transmitted as detailed in 4-7.

The detected current signal is used to identify sparks and flashover within the precipitator section. The signal is also used by the remote control unit to display the current being drawn by the precipitator section.

The detected rectifier output voltage is monitored for any possible over-voltage situation, which could take high voltage components and insulation within the transformer-rectifier above safe design limits. If an over-voltage situation is detected then a monitoring circuit rapidly trips the power supply by permanently shutting down gate drive signals to all power devices. The signal is also used by the remote control unit to display the precipitator voltage on an analogue meter.

A Hall effect sensor is also used to detect transformer primary current. If the current level rises above a pre-set maximum then the power supply is tripped in the same fashion as an over-voltage trip.

Figure 7-4 shows a diagram of the circuits used to monitor and process the transformer-rectifier input/output currents and output voltage signals.

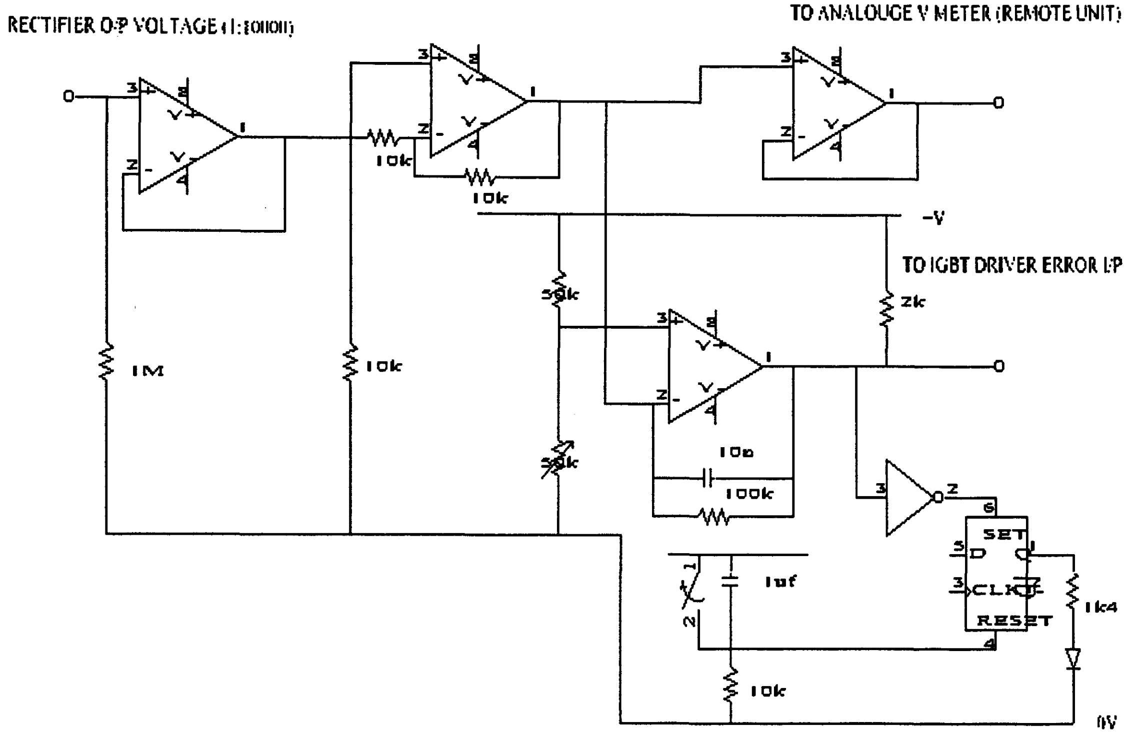
RECTIFIER O/P VOLTAGE
TO ANALOUGE V METER (REMOTE UNIT)
10k
10k
-V
TO IGBT DRIVER ERROR I/P
50k
2k
1M
10k
10n
100k
1uf
SET
CLK
RESET
1k4
10k
0V

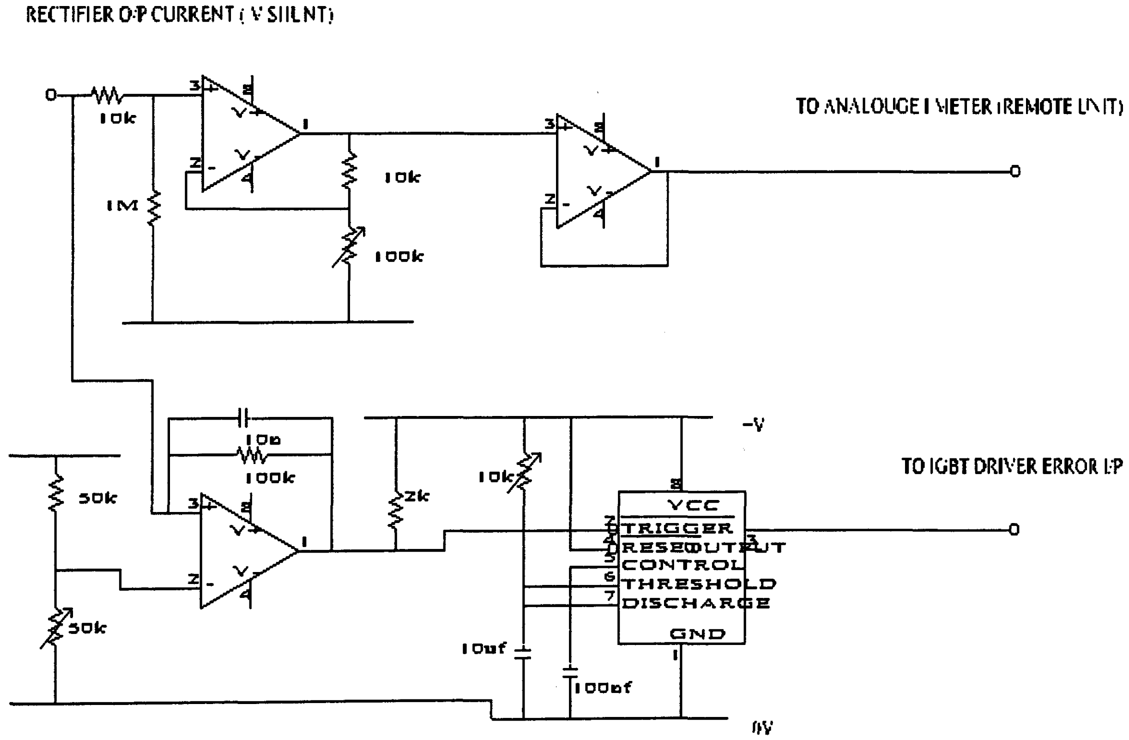
RECTIFIER O/P CURRENT (V SHUNT)
10k
TO ANALOUGE I METER (REMOTE UNIT)
1M
10k
100k
10n
100k
-V
50k
2k
10k
TO IGBT DRIVER ERROR I/P
VCC
TRIGGER
RESET
OUTPUT
CONTROL
THRESHOLD
DISCHARGE
GND
50k
10uf
100nf
0V

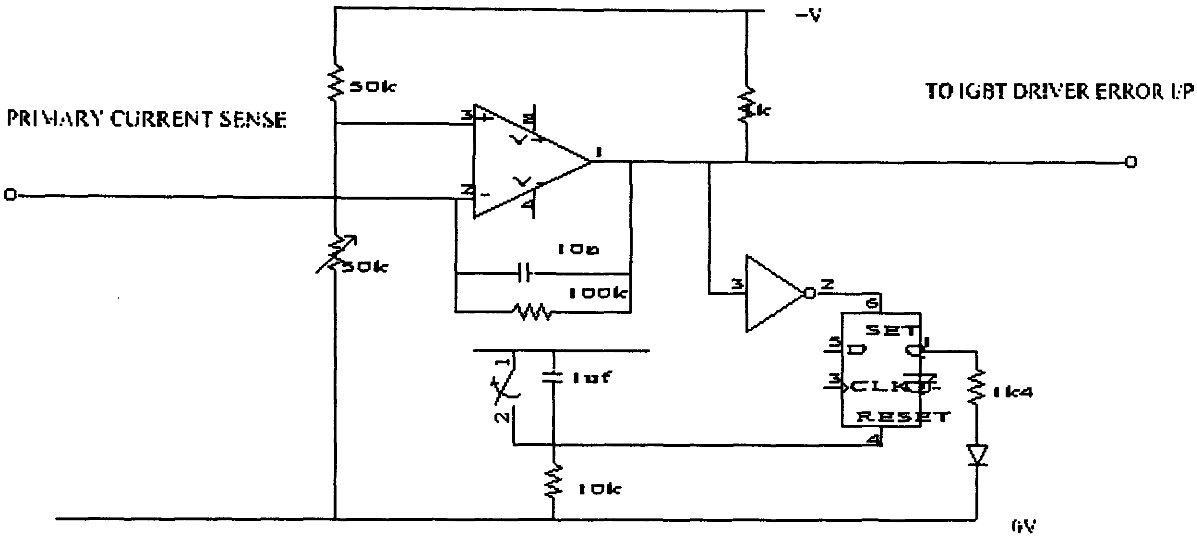

Figure 7-4 detection and processing circuits

7.4 Power supply switchgear and protection

Figure 7-5 shows the wiring diagram of the prototype power supply.

Energisation of the supply is initialized by closing of the master switch X1. A three-phase contactor K1 provides further protection. Closing of the start switch energises the contactor which then provides the unit with a connection to the mains supply.

Activation of the stop / emergency stop switch will open the main contactor.

The supply is further protected by an under-pressure switch mounted internal to the transformer pressure vessel. This opens if the pressurized sulphur hexafluoride within the transformer-rectifier vessel falls below 2 bar, causing the main contactor k1 to open.

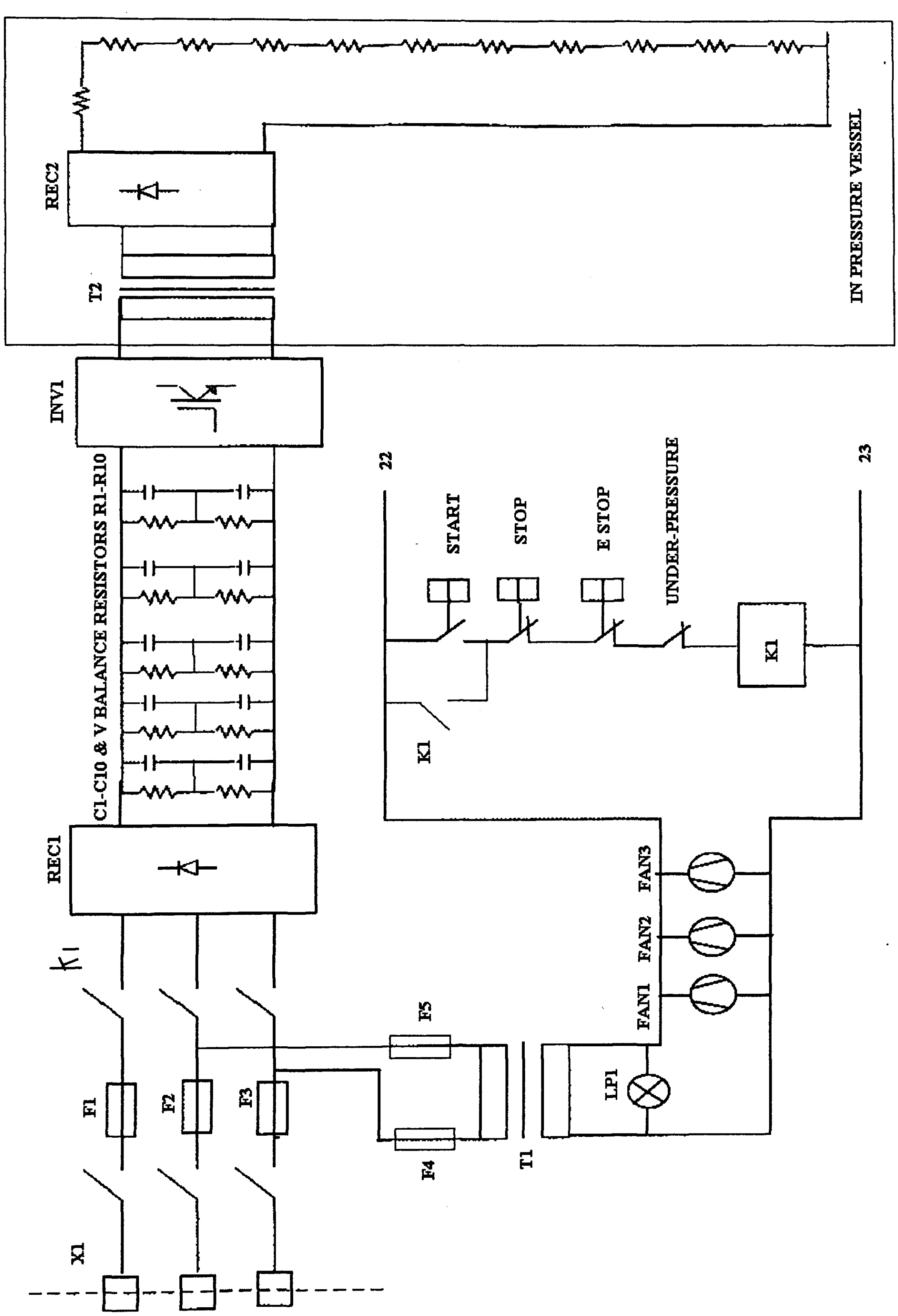

Figure 7.5 Power supply switchgear

7.5 Cubicle assembly

Figure 7-6 Precipitator power supply cubicle

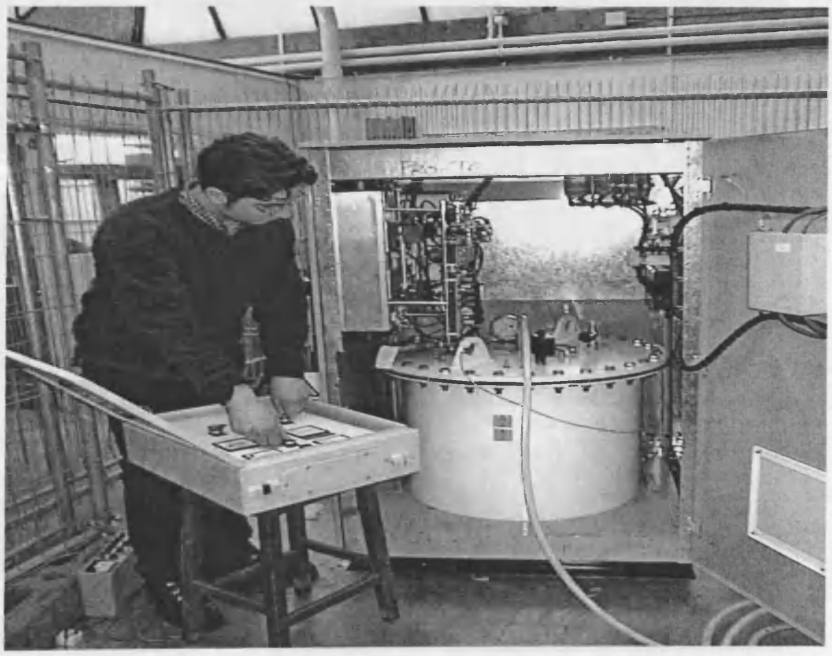

Figure 7-7 Precipitator power supply cubicle (ground view)

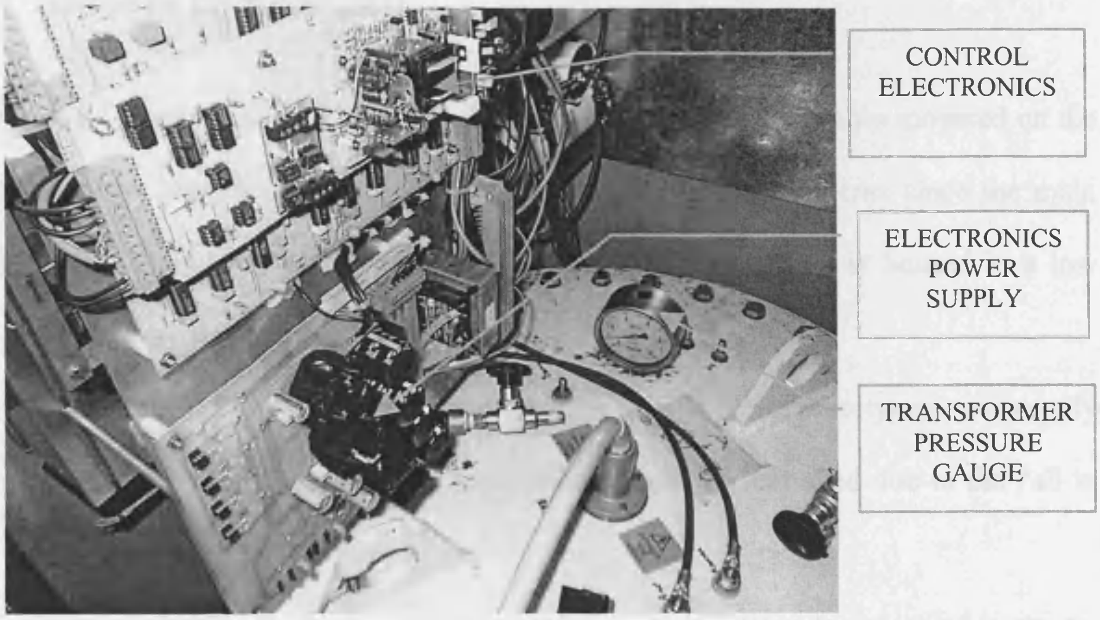

Figure 7-8 Power supply control electronics

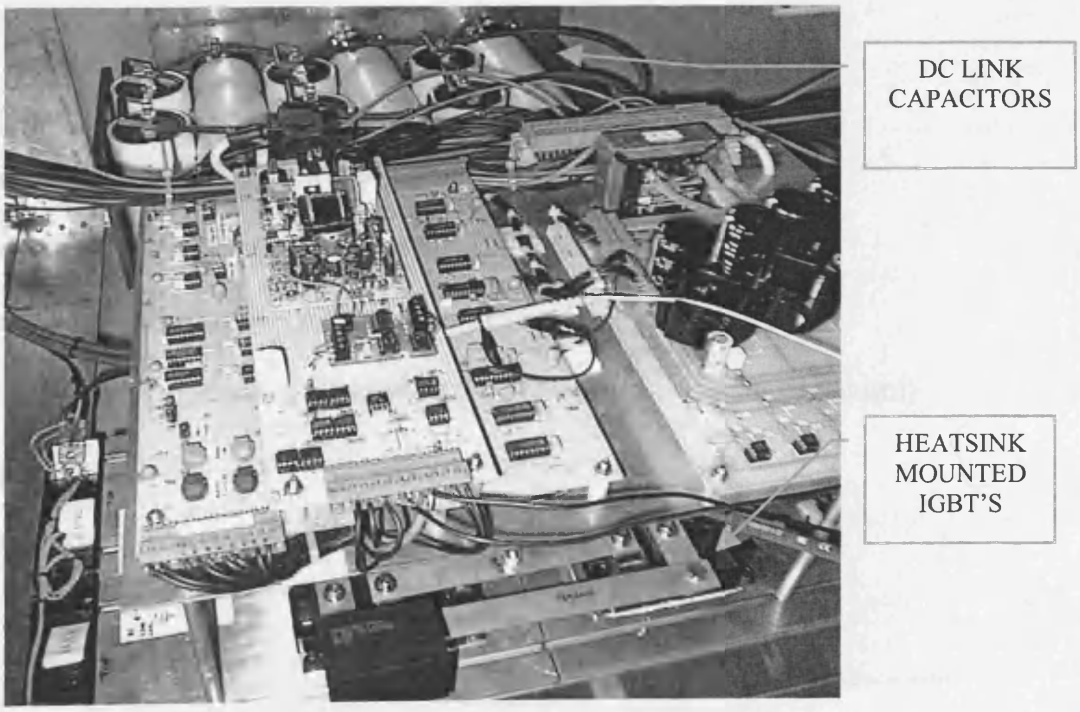

Figure 7-9 DC link and inverter stage

7.6 Remote control unit

Conventional transformer-rectifier power supplies have control switches mounted on the cubicle door as shown in figure 3-7. This causes no access problems since the main power supply cubicle of a conventional precipitator power supply is housed in a low voltage area, away from the transformer-rectifier.

During field trials at Didcot Power Station (chapter 8), The entire prototype power supply could be installed in a single vacated high voltage containment shed due to the "all in one" design philosophy of the supply.

Physical access inside the high voltage area during precipitator energisation is strictly forbidden. The remote unit was therefore constructed to enable manual control of the prototype power supply outside of the high voltage containment shed.

Figure 7-11 shows the remote control unit with the following features:

1. Analogue displays of power supply output voltage and current
2. Analogue display of input voltage and current
3. Start, stop, emergency stop and manual/automatic switches
4. Output voltage control potentiometer/ dial (active under manual control)
5. Power on, spark detect, start, stop and trip indicators
6. IGBT driver trip reset switch

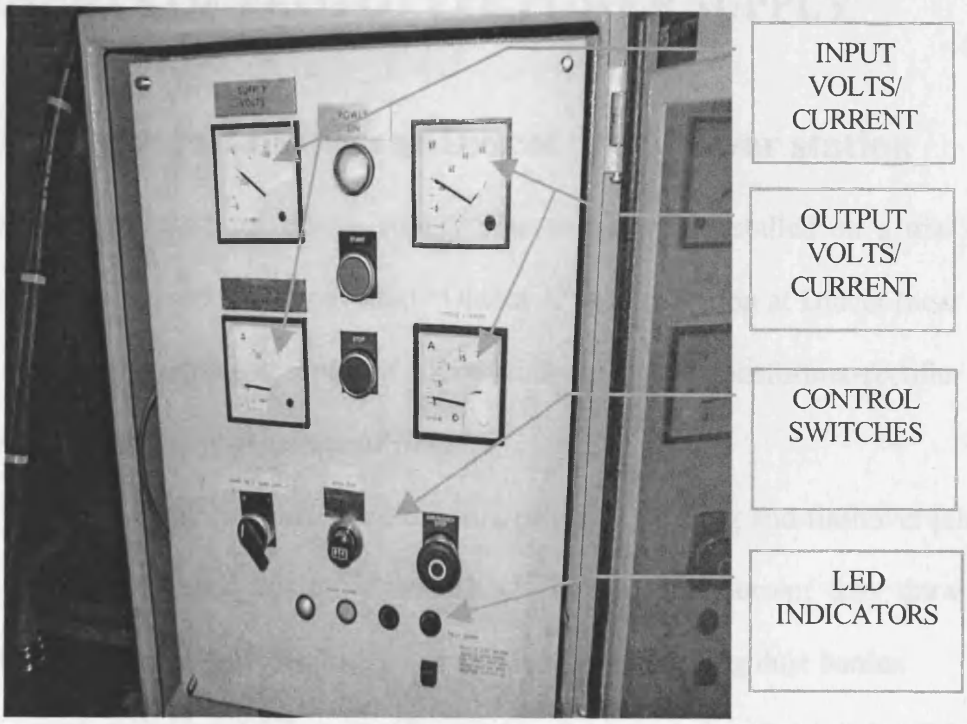

Figure 7-11 Power supply remote control unit

7.7 Summary

Control and instrumentation circuits within the power supply are detailed as well as the control system used for precipitator energisation and spark detection.

The assembly of the entire power supply into one single cubicle is discussed, as is the separate remote control unit.

8. RESULTS OF PROTOTYPE POWER SUPPLY

8.1 Prototype installation at Didcot "A" Power station

The prototype precipitator power supply was temporarily installed on a trial basis in National Power's 2035 MW coal fired "Didcot A" power station at Didcot (near Oxford) UK in July 1999 where it replaced a conventional 50Hz transformer-rectifier set and supplied an electrostatic precipitator field.

Precipitators are difficult loads since they are prone to sparking and flashover [chapter 2] during which time they act as virtual short circuits. The current they draw is very unsteady due to the corona discharge and continuously changing dust burden.

The power supply contained protection circuits to ensure that precipitator field supply voltage was rapidly reduced during arcing and sparking.

Until this point, high voltage testing had only been carried out on a specially designed high voltage, high power resistive load (50kV, 25kW) within the high voltage laboratory at Leicester University.

The field trial at Didcot was therefore a useful test to ensure that the prototype supply was sufficiently powerful and robust but it was difficult to obtain accurate results because of the unsteady current drawn.

Figures 8-1 to 8-3 show the installation of the precipitator at Didcot "A" Power station.

Figure 8-1 shows one of the 34 transformer rectifier containment sheds. The conventional transformer rectifier [figures 3 –6 and 3-7] was decommissioned and replaced with the prototype unit.

The power supply was controlled via the remote box detailed in chapter 7. This was installed on the safety interlock door of the containment shed (figure 8-2).

The output voltage of the power supply was applied to precipitator field by a direct mechanical connection of the high voltage cable termination to the high voltage discharge electrode busbar as shown in figure 8-3.

Due to the prototype nature of the experiment, in order to fulfil stringent safety criteria at the power station, it was required that utility power to the prototype supply and consequently to the transformer be manually controllable from outside the high voltage containment shed. Power was supplied to the prototype through a high power (25kVA) three-phase variac positioned outside the containment shed as seen in figure 8-1

Figure 8-1 Transformer-rectifier containment shed

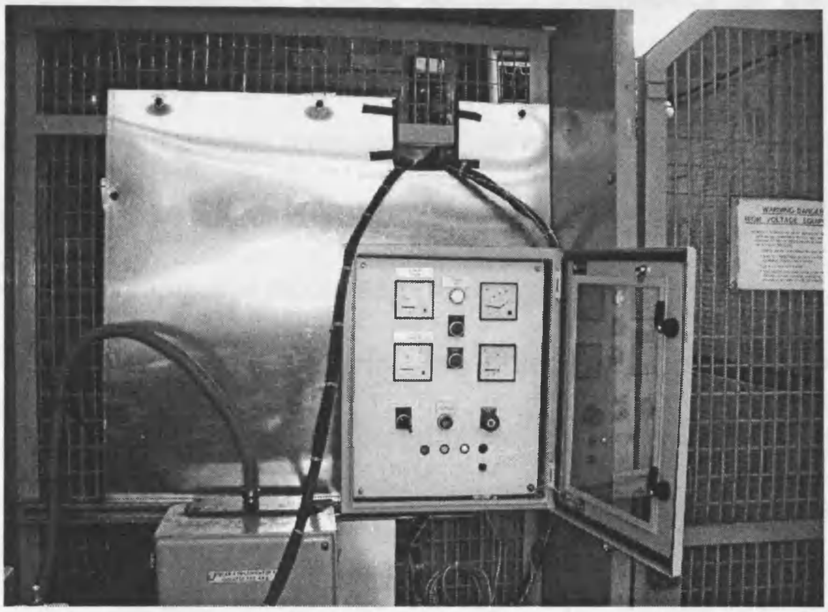

Figure 8-2 Remote Box

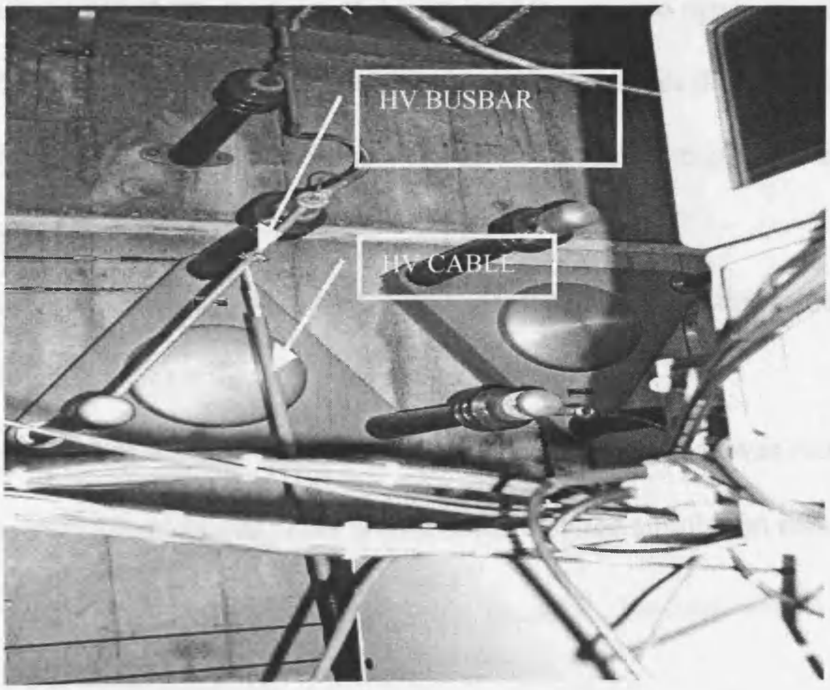

Figure 8-3 High voltage cable and busbar connection

8.2 Power supply results

Figure 8-4 shows the measured current voltage characteristics of the electrostatic precipitator load; the line is an exponential curve drawn to assist the eye. The current increased rapidly above a corona inception voltage of approximately 30kV. The circled groups of measurements at approximately 0.2A (~38 kV) and 0.4A (~43kV) were almost certainly made as the supply was recovering from a spark in the precipitator.

The voltage is increasing at this point but little corona is being produced. By extrapolation of the exponential, it may be estimated that the transient arcing current was several amps at the higher voltages. The dotted exponential curve shows the average "steady state" characteristics of the precipitator.

Conventional transformer–rectifier sets have output voltage ripples that are typically 50% of the mean voltage [1]. Arcing occurs if the peak of the voltage ripple exceeds a critical value and so for much of the cycle, when the voltage is much less than this critical value, little corona current is produced. Typically the mean current is much less than half that produced at the peak.

Figures 8-5 and 8-6 show the observed output voltage ripple of the prototype power supply. It can be seen that very little ripple was observed.

At 32kV the ripple was 85 ±10V, at 44kV it was 230 ±20V; i.e. it was much less than 1% under all operating conditions. This is consistent with the simulation results shown in 4.6.2.

It is therefore possible for the supply to produce more than twice as much current without arcing occurring than a conventional transformer-rectifier. This has considerable benefits to the particulate collection process and efficiency as detailed in chapter 3.

Figures 8-7 and 8-8 shows the primary current and voltage waveforms for an output of 38kV and 44kV. As the primary voltage is provided by a phase controlled H-bridge, there is a dead time between both positive and negative cycles when the duty is less than 100%. By considering the voltage waveforms in figures 8-7 and 8-8 it can be seen that the period is approximately 50μs corresponding to a switching frequency of 20kHz. The duty cycle was set to 60% with the dead times equal to 10μs and the positive and negative ON times being 15μs. the primary voltage was ±500V in figure 8-7 and ±560V in figure 8-8.

During the positive (negative) on times, the current increased (decreased) reasonably linearly to a value of approximately ±64A. Phase shift modulation ensures that during the dead time, either the two top or bottom IGBTs are 'on' and so there is always a current path through the IGBTs or flywheel diodes. The current during this period is otherwise uncontrolled and the small current oscillation during the dead time probably corresponds to a resonance of the magnetising and leakage inductance with the parasitic capacitance.

8.2.1 Estimation of power supply efficiency

It was difficult to estimate the efficiency of the transformer accurately because of the measurement uncertainty in the continuously fluctuating secondary current and unfortunately the experimental arrangement precluded measurement of the instantaneous secondary current.

All our estimates lead us to believe that the efficiency of the transformer with rectifier was better than 97%. The total rectifier voltage drop was 200V which, at 0.4A, would give an 80W power loss and contribute ~0.5% to the overall power lost. The best indication of power loss was the temperature rise of the transformer core, which was measured using the thermistor detailed in 4.7.3. The temperature rose from 16±2°C, to 33°C, a rise of 17±2°C, when the output voltage was 45kV, 0.4A, a power of 18kW.

The design calculations given in Appendix A suggest that with a loss of 510W, a temperature rise of 50°C would be found for a core surface area of 533cm^2.

The actual exposed surface area was 800 cm^2. An estimate of the actual power lost is therefore:

$$\frac{17^0 C}{50^0 C} \times \frac{800 cm^2}{533 cm^2} \times 510W = 260W$$

For an output power of 18kW this corresponds to an efficiency of 98.5%. The overall efficiency of the power supply was estimated to be > 95% which compares very favourably with conventional 50Hz transformer-rectifier sets with efficiencies of only ~60%.

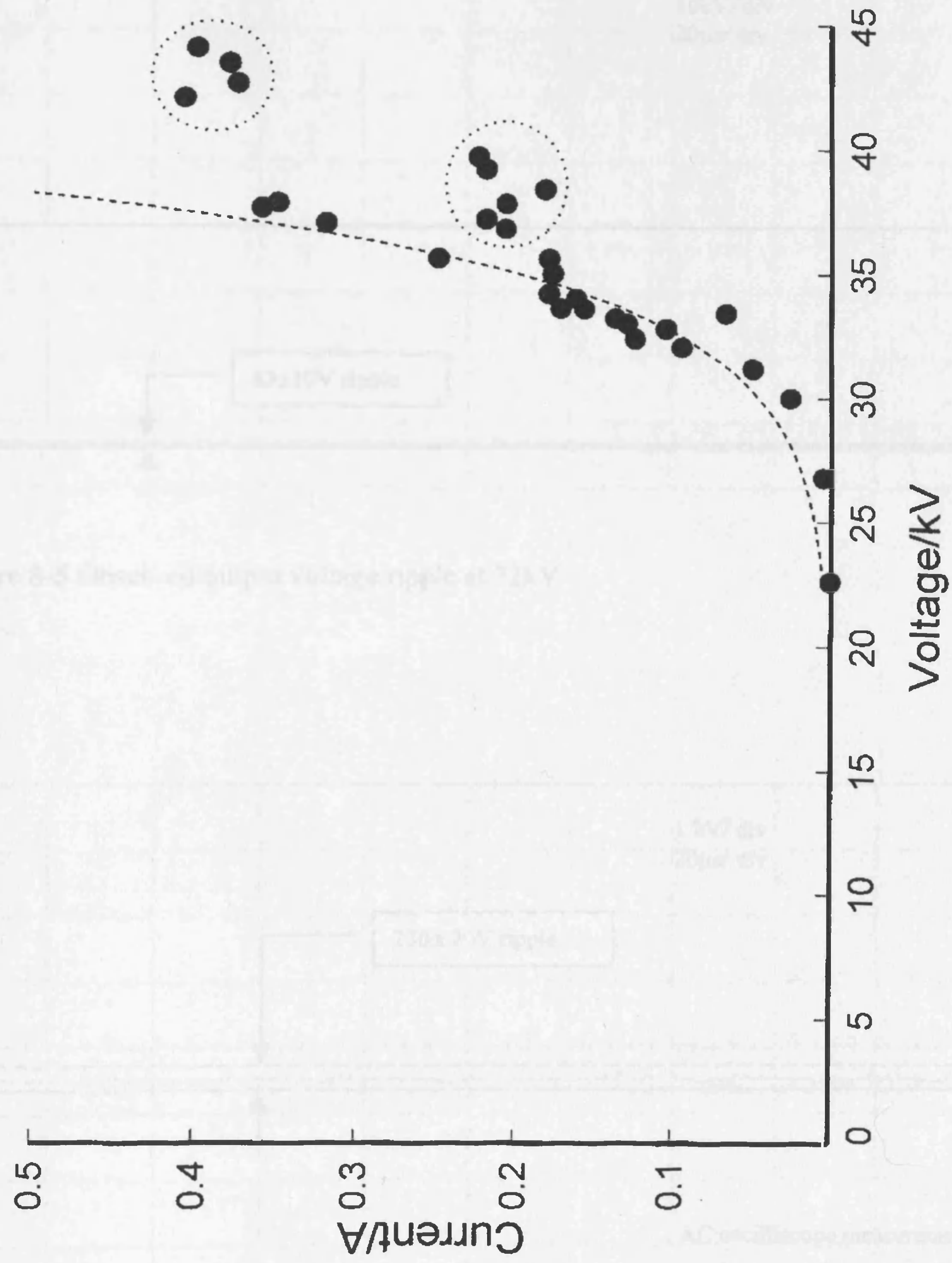

Figure 8-4 Measured precipitator voltage-current characteristic

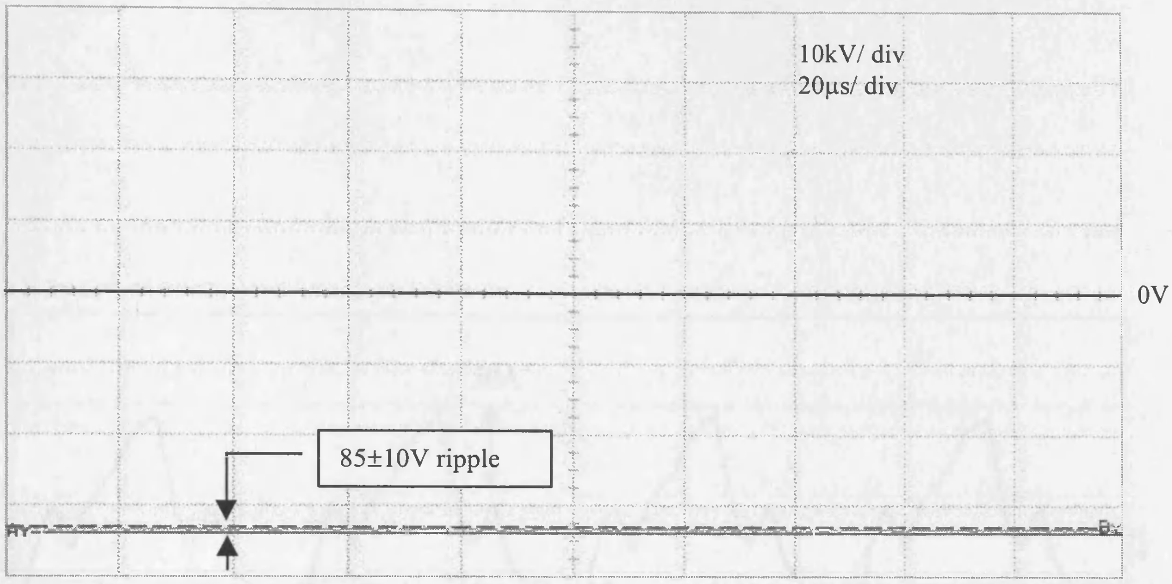

Figure 8-5 Observed output voltage ripple at 32kV

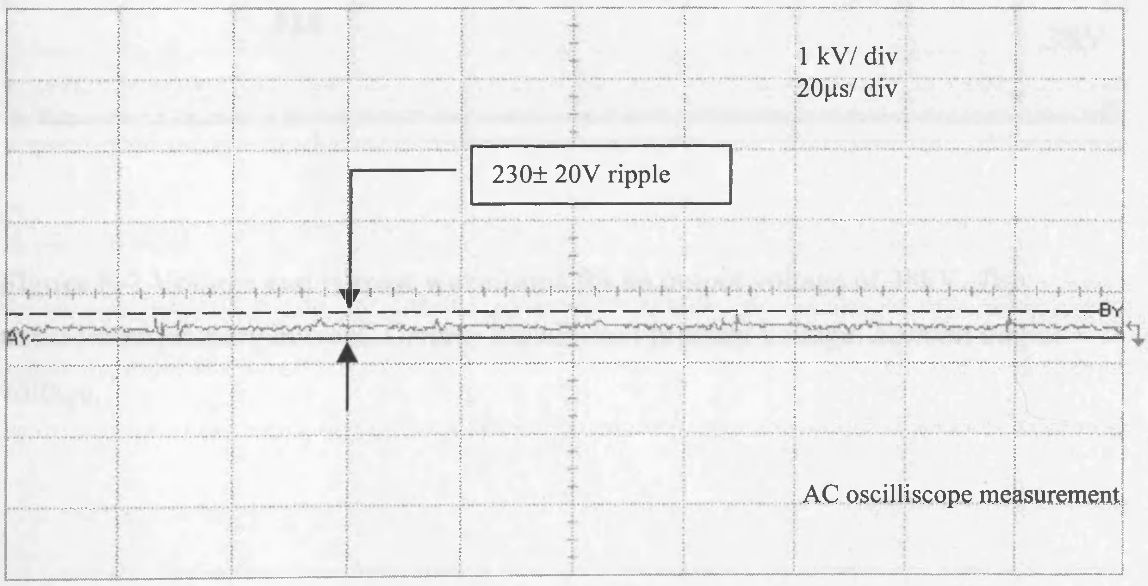

Figure 8-6 Observed output voltage ripple at 44kV

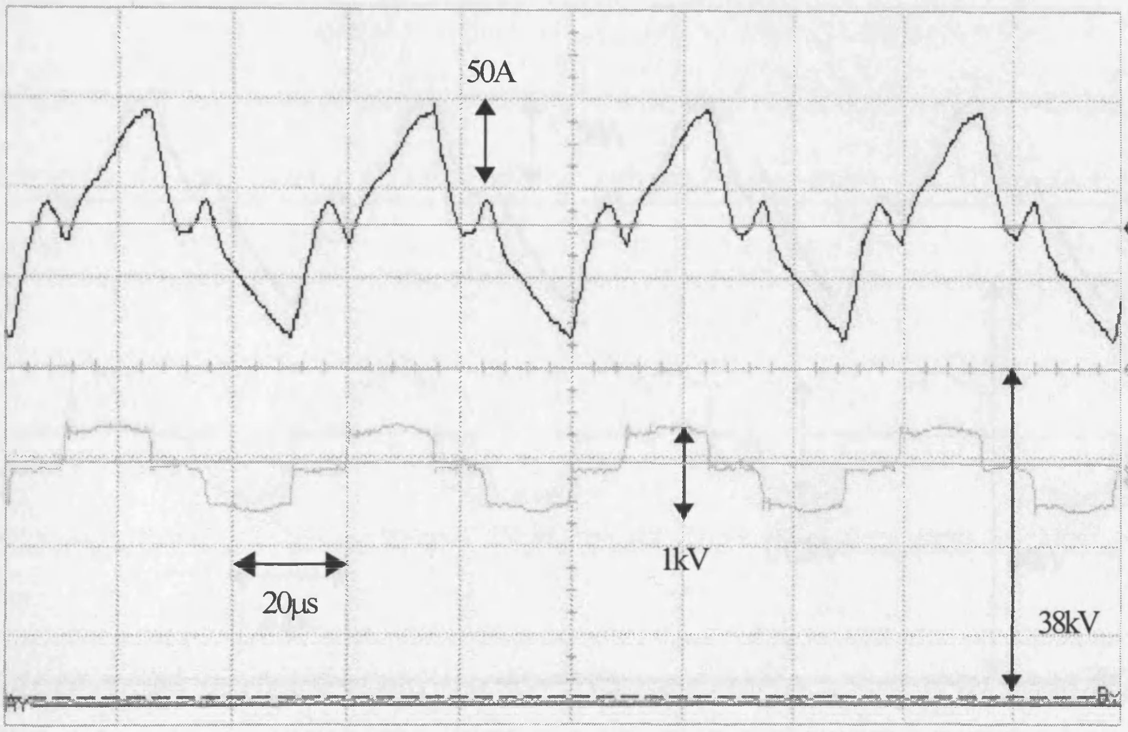

Figure 8-7 Voltage and current waveforms for an output voltage of 38kV. *Top*: transformer primary current. *Centre*: transformer primary voltage. *Bottom*: output voltage.

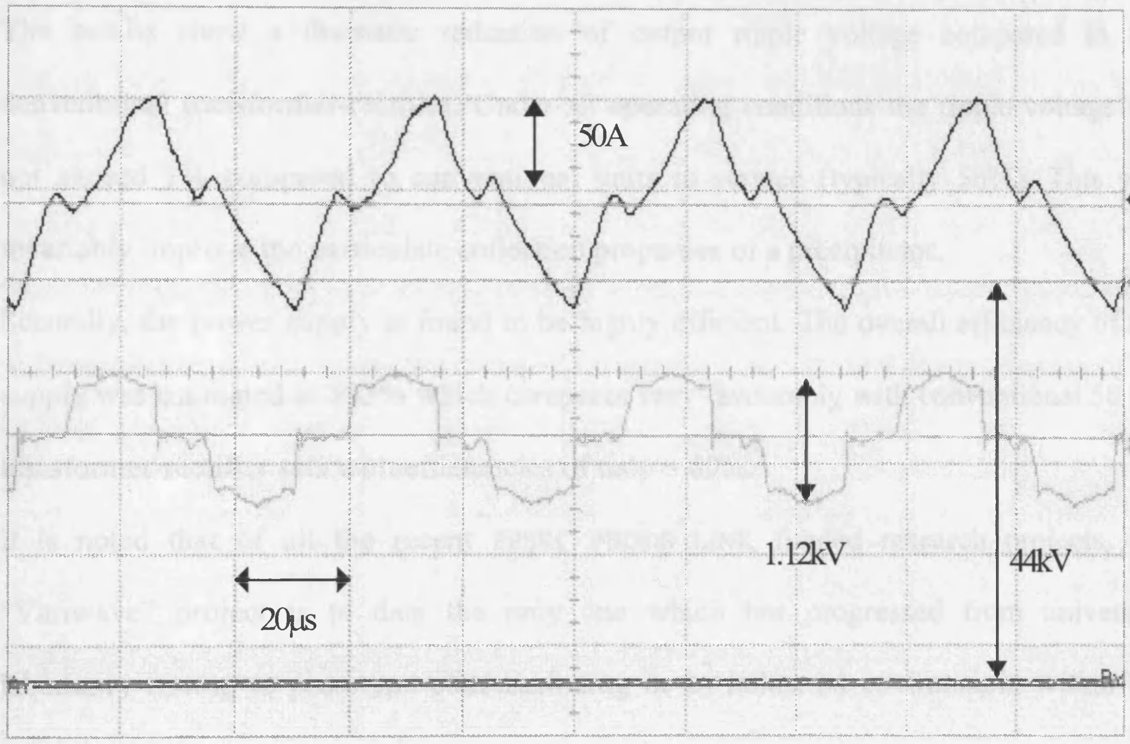

Figure 8-8 Voltage and current waveforms for an output voltage of 44kV. *Top*: transformer primary current. *Centre*: transformer primary voltage. *Bottom*: output voltage.

8.3 Summary

The prototype precipitator was temporarily installed in National Power's 2035MW coal-fired Didcot "A" Power Station, UK under a short-term test programme to evaluate the power supplies effectiveness at energising a precipitator field within the station.

The results show a dramatic reduction of output ripple voltage compared to the conventional transformer-rectifier. Under all operating conditions the ripple voltage did not exceed 1% compared to conventional units in service (typically 50%). This will invariably improve the particulate collection properties of a precipitator.

Secondly, the power supply is found to be highly efficient. The overall efficiency of the supply was estimated at >95% which compares very favourably with conventional 50 Hz transformer-rectifier sets with efficiencies of only ~ 60%.

It is noted that of all the recent EPSRC PEDDS LINK funded research projects, the "Variwave" project is to date the only one which has progressed from university laboratory testing to prototype commissioning in an industrial environment within the timescale of the project.

8.4 References

1. **Parker** KR, "Applied Electrostatic Precipitation", 1997 Chapman and Hall, ISBN 0 7514 0266 4

9. CONCLUSIONS AND RECOMMENDATIONS FOR FURTHER WORK

9.1 Technological advances

The aim of this research was to address the limitations of conventional precipitator power supplies by utilising modern semiconductor device technology, modern magnetic materials and novel methods of high voltage insulation.

These technological advances were applied to develop a prototype precipitator power supply with significant operational improvements over conventional power supplies.

- **The combination of high voltage, high frequency and high power operation**

A technological advance of the power supply is its combination of high frequency (20kHz), high power (25kVA) and high voltage (50kV) operation.

High frequency operation is possible due to the ferrite core transformer design. This leads to a more compact design for such a high power rating in comparison with conventional low frequency power supplies.

- **Compact and novel transformer design**

The high voltage transformer represents a significant technological advantage. The application of pressurised sulphur hexafluoride as the encapsulation medium overcomes the problems associated with conventional oil insulated transformers.

The use of machinable nylon 6,6 for both the bobbins and the framework gives excellent flexibility to design and manufacture and permits a bobbin design which minimises leakage inductance and parasitic capacitance whilst not compromising electrical insulation requirements.

The electrical stress relief rings used to obviate the electric stress in the bobbins is a technical advance on the conventional 'winding spacing' technique employed by many high voltage manufacturers.

The use of high frequency ferrite material for the core minimises the size and weight of the transformer –rectifier structure in comparison with conventional units.

- **Internationally competitive precipitator power supply**

The prototype power supply clearly displays operational advances over the conventional unit. The electrical efficiency of the prototype is greatly improved from around 60% conventional supply) to an estimated >95%.

The power supply dramatically reduces the output voltage ripple magnitude from around 50% (conventional units) to lower than 1% which can have considerable benefits to the precipitator particulate collection process.

The three-phase boost rectifier is also an operational advancement. Although a boosted DC link was not required in the final prototype due to the 560V primary voltage design of the transformer, application of the rectifier in future units will improve the quality of power drawn by the supply and also aid further transformer size reductions.

Furthermore, The compact 'all in one cubicle' design of the supply is an advancement since installation costs to the customer will be significantly lower.

A major European precipitator manufacturer, FLS Miljφ have recently developed a switched mode supply [1]; this technology is clearly perceived by precipitator users as the way forward. The supply developed under this research has several significant features not found on the FLS Miljφ unit. These include the novel and compact transformer design, the use of gas insulation rather than oil and the optional controllable boosted dc link.

The technical advances of the prototype power supply would certainly make a production model commercially competitive in the worldwide precipitator marketplace.

9.2 Recommendations for further work

Recommendations for future work to improve upon the design, construction and operation of the prototype unit are detailed:

9.2.1 Improvement of transformer design

Construction of the transformer did bring with it a number of complications, which if addressed in future work would be beneficial to the manufacturer.

- **Ferrite material**

It had been hoped that specific cores shapes of the required size could be manufactured by a UK manufacturer. However, despite an intensive search this proved impossible within the time constraints of the project. Instead, easily available I sections where used as the 'building bricks' of the core. Each I section had to be machined to overcome the appreciable size tolerances of ferrite and then cemented together.

This took a considerable time; in future work a further more upto date search of worldwide ferrite manufacturers who are capable of engineering a complete half core would be highly beneficial. A complete core would also add structural strength to the transformer and aid assembly / disassembly.

- **Redesign of pressure vessel gasket and minimisation of gas pressure**

The mechanical design of the transformer pressure vessel is based upon a conventional container-lid structure where the two are sealed together by a rubber gasket under high bolt compression. Gas loss over time due to the gradual gasket thinning and expansion was found to be a complication. Future work may examine a re-design of the gasket (possibly using an 'O' ring) to alleviate this problem.

Minimisation of gas pressure would be advantageous in that it would lower the required wall/lid thickness of the container. If the pressure was minimised to atmospheric, then gas leakage, particularly with a dense gas such as sulphur hexafluoride would be minimal.

However, lowering of the gas pressure would also lower the electrical insulation strength of sulphur hexafluoride. This would require a redesign of the secondary nylon bobbins and the nylon frame structure within the container.

- **Use of a more environmentally friendly gas**

Future work may examine the move away from sulphur hexafluoride (SF_6) in favour of an alternative gas which is less harmful to the environment.

Although SF_6 is none toxic, it can contribute to the greenhouse effect when released into the atmosphere.

SF6 is also relatively expensive in comparison with similar gases with electrical insulation properties such as nitrogen, but it does, however, have superior electrical insulation strength in comparison with these gases.

9.2.2 Development of digital based control electronics with computer interfacing

The control and instrumentation circuitry within the prototype power supply had to be robust and of minimal complexity to allow rapid modifications to be made if required before undergoing field trials. The circuits were based upon analogue designs and constructed on separate plug in boards to aid modifications and possible fault finding.

Future work could be the development of a commercial digital based control board with the ability to communicate within a computer network.

It is envisaged that in future commercial power supplies, real-time control and monitoring of all the units within a precipitator installation will be performed by a dedicated computer system [2].

9.2.3 Development of a pulsing unit.

Pulsing units which superimpose high voltage pulses (typically 60kV, 100μs) with a repetition frequency of 20 to 300Hz on the DC output of transformer-rectifier units may improve the particulate collection efficiency of a precipitator [3].

Future work could be the development of a pulsing unit capable of being retro-fitted as an extra module to the new power supply

9.2.4 Development of matrix converter technology to control power to the high voltage transformer-rectifier

Current research into high frequency inverters has generally centred upon indirect converters utilising IGBT technology, namely voltage or current fed inverters.

Series, parallel or series-parallel resonant tank inverters have been used where the leakage reactance and parasitic capacitance of the transformer are utilised to form part or all of the resonant element of the inverter [4-7].

In general, indirect converters have an intrinsic need for an initial rectification stage and an intermediate storage stage. They are, therefore, bound to use large reactive elements. Furthermore, the intermediate storage destroys all information about input voltage waveforms and phasing.

A recommendation for future research is the investigation of a direct AC-AC high frequency matrix converter to control power to the high voltage transformer-rectifier.

The matrix converter is an "all silicon" topology omitting the need for costly passive components and minimising topology size.

9.2.4.1 A proposed high frequency matrix converter

Figure 9-1 shows the configuration of a proposed high frequency matrix converter. It consists of six bilateral switches, each switch containing two IGBT'S and two blocking diodes.

The general features of this proposed converter are summarised :

- The converter delivers directly from a 3 phase mains supply, a high frequency, single phase, voltage fed quasi-square wave (QSW) to the primary winding of the high voltage transformer.
- A high frequency, single phase, quasi-square wave output is synthesised by six distinct IGBT modulation functions shown in table 9-1. Each function contains the necessary high frequency switching algorithm to achieve a high frequency QSW output.
- Crossover from modulation function one through to six occurs at the six points in the mains period where two line voltages converge. Thus, the high frequency QSW output resides within a six-pulse envelope of the three-phase mains supply.
- The high frequency modulation functions ensure that switch overlap is embedded within the switching patterns. This maintains a bi-directional current path at any transition time.

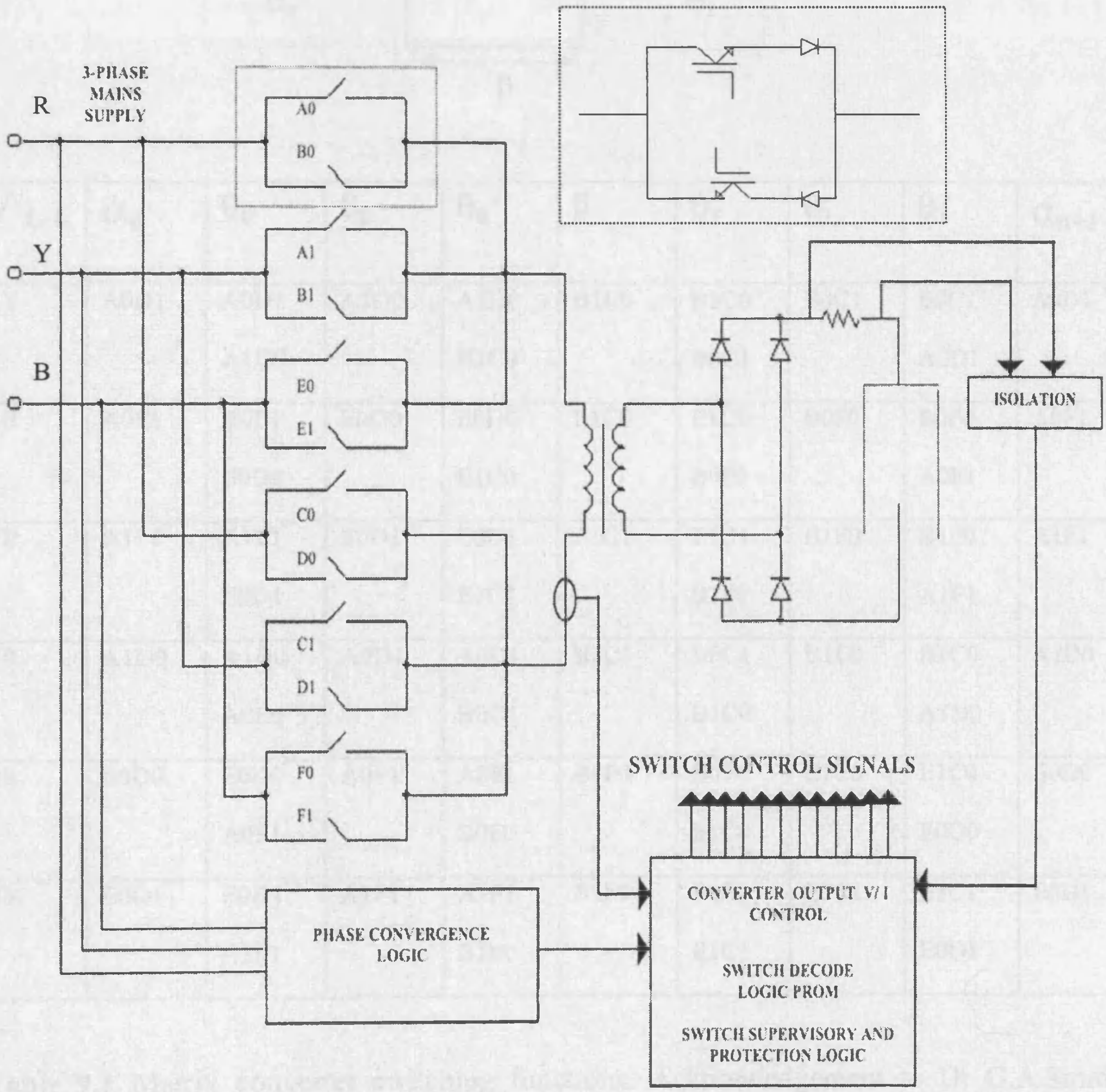

Figure 9-1 Proposed matrix converter

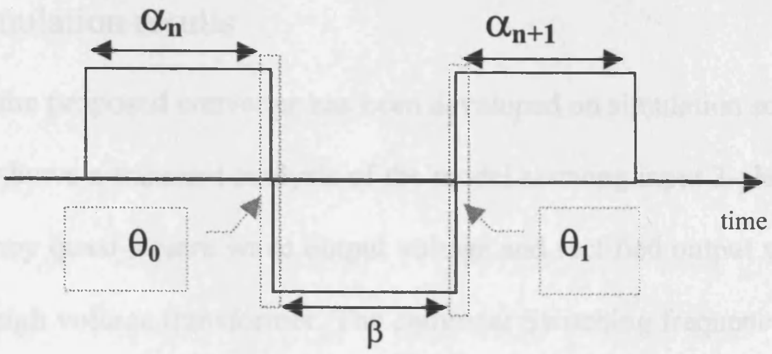

V_{L-L}	α_n	θ_0	θ_0	θ_0	β	θ_1	θ_1	θ_1	α_{n+1}
RY 1	A0D1	A0D1 A1D0	A1D0	A1D0 B1C0	B1C0	B1C0 B0C1	B0C1	B0C1 A0D1	A0D1
RB 2	A0F1	A0F1 E0D0	E0D0	E0D0 E1C0	E1C0	E1C0 B0F0	B0F0	B0F0 A0F1	A0F1
YB 3	A1F1	A1F1 E0D1	E0D1	E0D1 E1C1	E1C1	E1C1 B1F0	B1F0	B1F0 A1F1	A1F1
YR 4	A1D0	A1D0 A0D1	A0D1	A0D1 B0C1	B0C1	B0C1 B1C0	B1C0	B1C0 A1D0	A1D0
BR 5	E0D0	E0D0 A0F1	A0F1	A0F1 B0F0	B0F0	B0F0 E1C0	E1C0	E1C0 E0D0	E0D0
BY 6	E0D1	E0D1 A1F1	A1F1	A1F1 B1F0	B1F0	B1F0 E1C1	E1C1	E1C1 E0D1	E0D1

Table 9.1 Matrix converter switching functions. Acknowledgement to Dr G.A.Smith (Loughborough University) for his assistance in development of the switching functions.

9.2.4.2 Simulation results

A model of the proposed converter has been developed on simulation software. Figure 9-2. shows a transient analysis of the model showing input 3-phase mains voltage, high frequency quasi-square wave output voltage and rectified output voltage of the high frequency, high voltage transformer. The converter Switching frequency in this particular simulation has been decreased to facilitate viewing.

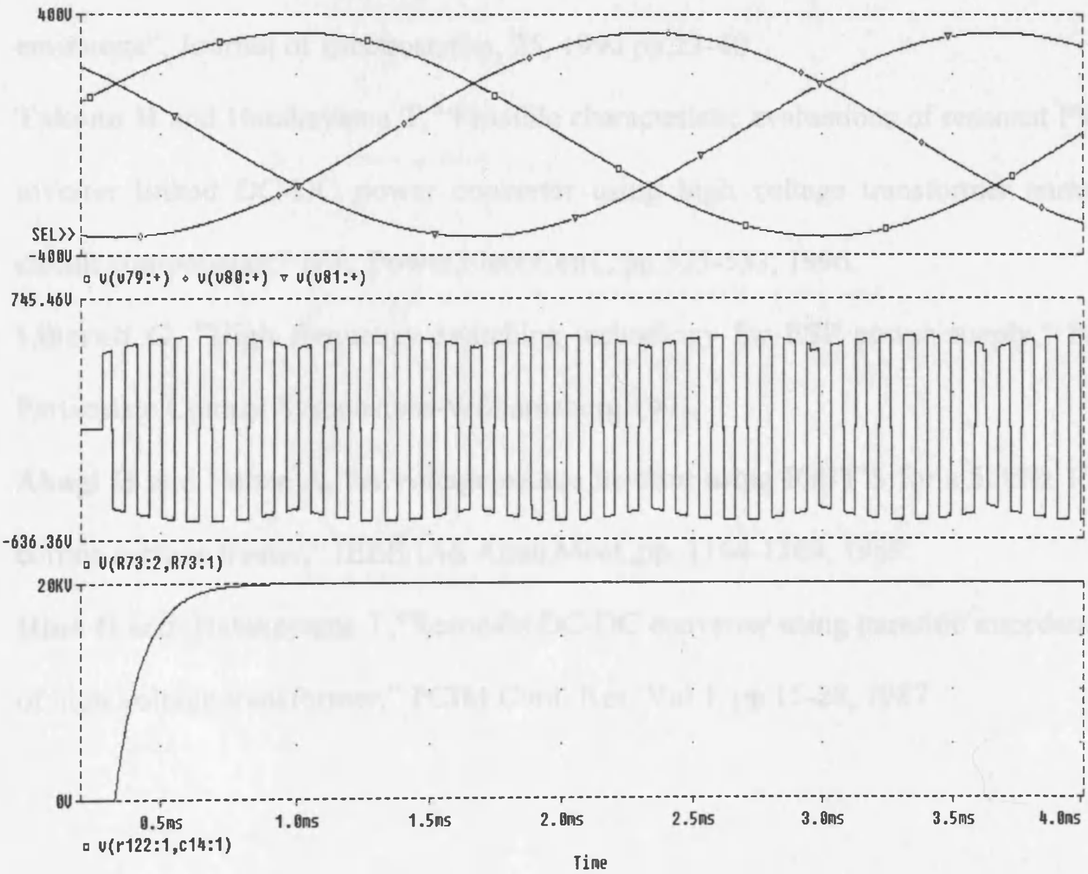

Figure 9-2 Pspice simulation results of matrix converter

9.3 References

1. **Reyes** V, "A novel and versatile switched mode power supply for ESP'S", Proceedings, ICESP, Sep. 20-25, 1998, Korea
2. **Reyes** V, and Lausen P, "Utilization of computer systems for control and operation of electrostatic precipitators", 5Th International Conference on Electrostatic Precipitation, session C4, EPRITR 103048 Vol. 2, Cal, USA, 1993
3. **Dinelli** G, "Pulse power electrostatic technologies for the control of flue gas emissions", Journal of Electrostatics, 25, 1990 pp.23-40
4. **Takano H** and Hatakeyama T, "Feasible characteristic evaluations of resonant PWM inverter linked DC-DC power converter using high voltage transformer parasitic circuit components," IEE, Power.Elect.Conf., pp.525-533, 1996.
5. **Liberati G,** "High frequency switching technology for ESP power supply," Proc. Particulate Control Symposium-Williamsburg 1991.
6. **Akagi H** and Nabae A, "A voltage source inverter using IGBT'S for a 50kHz 10kV corona surface treater," IEEE/IAS Annu.Meet.,pp. 1164-1169, 1989.
7. **Hino** H and .Hatakeyama T,"Resonant DC-DC converter using parasitic impedance's of high voltage transformer," PCIM Conf. Rec, Vol 1, pp 15-28, 1987

10 APPENDICES

APPENDIX A MAGNETIC AND THERMAL DESIGN USING THE McLYMAN DESIGN METHOD

Magnetic and Thermal design using McLyman Design Method

("K" values are coefficients defined by McLyman)

$V_p := 587$ V - primary square wave voltage

$V_o := 50000$ V - secondary voltage

$P_o := 25000$ VA - output power

$f := 20000$ Hz - operating frequnecy

$\eta := 0.98$ efficiency - specified efficiency

$\Delta T := 50$ deg. C - allowable temperature rise

$B_m := 0.25$ Tesla - maximum core flux density

1. Calculation of power handling capability, P_t

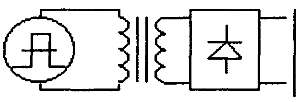

$P_{in} := P_o$ VA - approximate power input

$P_t := 2 \cdot P_{in}$ $P_t = 5 \cdot 10^4$ VA - apparent power handling capability

2. Calculation of area product, A_p

$k := 4$ coefficient indicating square wave input

$K_u := 0.01$ (window utilisation factor) $K_j := 323$ (current density coefficient)

$$A_p := \left(\frac{P_t \cdot 10^4}{k \cdot B_m \cdot f \cdot K_u \cdot K_j} \right)^{1.16} \qquad A_p = 3.243 \cdot 10^4 \quad \text{cm}^4$$

3. Evaluation of core geometry

3.1 V olume of transformer core

$K_v := 17.9$ (volume coefficient for C-core)

$volume := K_v \cdot A_p^{0.75}$ $volume = 4.326 \cdot 10^4$ cm^3

3.2 Transformer core surface area, A_t

$K_s := 39.2$ (surface area coefficient for C-core)

$A_t := K_s \cdot A_p^{0.5}$ $A_t = 7.059 \cdot 10^3$ cm^2

3.3 Transformer current density, J

$K_j := 468$ Current density coefficient for C-core at temperature rise of 50 deg. C

$J := K_j \cdot A_p^{-0.125}$ $J = 127.755$ A/cm^2

4. Total estimated transformer losses, P_Σ

$$P_\Sigma := \frac{P_o}{\eta} - P_o \qquad P_\Sigma = 510.204 \quad \text{W}$$

5. Maximum efficiency when P_e (core loss) = P_{cu} (copper loss)

Best case efficiency when $P_e = P_{cu}$

$$P_{cu} := \frac{P_\Sigma}{2} \qquad P_{cu} = 255.102 \qquad P_e := P_{cu} \qquad P_e = 255.102 \quad \text{W}$$

6. Calculation of core loss

For Fernk type I100/57/44 (mmg-neosid) at 0.25T and 20kHz:

$P_{Fe25} := 0.2$ W/cm^3 at 25 deg. C $\qquad P_{Fe100} := 0.3$ W/cm^3 at 100 deg. C

So at T=ambient + 50 deg. C, i.e. T=75 deg. C

$$P_{Fe} := P_{Fe25} + \frac{75-25}{100-25}\cdot\left(P_{Fe100} - P_{Fe25}\right) \qquad P_{Fe} = 0.267 \quad \text{W/cm}^3$$

We need an <u>effective</u>volume of core of greater than: $\dfrac{P_e}{P_{Fe}} = 956.633$ cm^3

The worst case efficiency is for $P_e >> P_{cu}$ so we need an effective volume of core:

$$\frac{P_\Sigma}{P_{Fe}} = 1.913 \cdot 10^3 \quad \text{cm}^3$$

7. Calculation of primary turns, n_p

Cross sectional area of mmg I100/57/44 core $\qquad A_c := 4\cdot 2.464\cdot 2.4646 \qquad A_c = 24.291$ cm^2

$$n_p := \frac{V_p \cdot 10^4}{4\cdot B_m \cdot A_c \cdot f} \qquad n_p = 12.083$$

To ensure flux density is not exceeded use $n_p := 13$ turns

8. Transformer current density

$J = 127.755$ A/cm^2

9. Primary current, I_p

$$I_o := \frac{P_o}{V_o} \qquad I_o = 0.5 \qquad I_p := \frac{V_o \cdot I_o}{V_p} \qquad I_p = 42.589 \quad \text{A}$$

10. Calculate base wire size for primary, A_w

$A_w := \frac{I_p}{J}$ $A_w = 0.333$ cm²

11. American Wire Gauge

Since there are 2 parallel primary windings area of each= $A := \frac{A_w}{2}$ $A = 0.167$ cm²

This is approximately AWG5. It is possible to use AWG7 (area of 0.105 cm ^{2})
if primary losses can be neglected. For 2 in parallel, area = 0.21 cm ^{2}

12. Calculation of primary resistance

mean length per turn: $MLT_p := 19.2$ cm

Resistivity of copper: $\rho := 1.71881 \cdot 10^{-6}$ Ω.cm

resistance per cm $R_p := \frac{\rho}{0.21}$ $R_p = 8.185 \cdot 10^{-6}$ Ω/cm

temperature coefficient of resistance at 75 deg. C: $\xi := 1.24$

$R_p := MLT_p \cdot n_p \cdot R_p \cdot \xi$ $R_p = 2.533 \cdot 10^{-3}$ $R_p \cdot 1000 = 2.533$ mW

13. Primary copper loss

$I_p^2 \cdot R_p = 4.595$ W

14. Calculation of secondary turns

$n_s := \frac{n_p}{V_p} \cdot V_o$ $n_s = 1.107 \cdot 10^3$

To allow use of a nominal 80% duty cycle on the primary $n_s := \frac{n_s}{0.8}$ $n_s = 1.384 \cdot 10^3$

And so $n_s := 1400$ was chosen

15. Calculate base wire size for secondary

$A_w := \frac{I_o}{J}$ $A_w = 3.914 \cdot 10^{-3}$ cm²

therefore use AWG21

16. Calculation of secondary resistance

mean length per turn: $MLT_s := 2 \cdot \pi \cdot 15.5$ cm

resistance per cm (interpolating by 1.26513): $R_s := 418.9 \cdot 10^{-6}$ Ω/cm from AWG table

$R_s := MLT_s \cdot n_s \cdot R_s \cdot \xi$ $R_s = 70.823$ W

17. Calculation of temperature rise

Assume that $P_{\Sigma}=P_{cu}+P_{Fe}$
Assume that thermal energy is distributed throughout the core and winding assembly

Heat transfer by thermal radiation:

$k_r := 5.7 \cdot 10^{-12}$ Stefan-Boltzman constant, W.cm $^{-2}$.K^{-4}

$\varepsilon := 0.95$ emissivity

$T_2 := 75 + 273$ hot body temperature, K

$T_1 := 25 + 273$ cold body temperature

$W_r := k_r \cdot \varepsilon \cdot \left(T_2^{\,4} - T_1^{\,4}\right)$ $W_r = 0.0367$ W/cm^2 of surface area

Heat transfer by convection:

$k_c := 1.4 \cdot 10^{-3}$

$F := 3.5$ air friction factor: 1 for vertical surface, 1.25 for horz. flat surface
SF_6 is at least 3.5 times better than air at low flow rates

$\theta := 50$ deg. C temperature rise

$\zeta := 1.25$ depends on surface shape, varies from 1 to 1.25

$P := 2$ relative barometric pressure

$W_c := k_c \cdot F \cdot \theta^{\zeta} \cdot \sqrt{P}$ $W_c = 0.9213$ W/cm^2 of surface area

Total heat transfer:

$W := W_r + W_c$ $W = 0.9581$ W/cm^2

Assuming worst case efficiency, η, (i.e. $P_{cu} = \Sigma P$)
the minimum surface area required is:

$A_{smin} := \dfrac{P_{\Sigma}}{W}$ $A_{smin} = 532.538$ cm^2

(Actual area is approximately 1500 cm ^{2}
Approximately 50% of this area is exposed - so well within spec.)

APPENDIX B PUBLICATIONS

The following publications are associated with this work. Those marked Δ are bound with this thesis.

Devine PJ, "The requirements of a high voltage power supply for electrostatic precipitators", Leicester University Department of Engineering, Internal Report no. 96-24, 1996

Δ Devine, PJ and Lefley, PW, "A high power unity power factor three-phase rectifier for high voltage applications", Proceeding of The Universities Power Engineering Conference, Crete, 1996, pp. 417-420

Δ Devine, PJ, Lefley PW & Fothergill JC, "A high power high frequency transformer for high voltage application", Proceedings of The Universities Power Engineering Conference, UK, 1998, pp.511-515

Δ Devine PJ and Lefley PW, "A method for supplying a high frequency, high voltage transformer based upon a forced commutation cycloconverter (matrix converter) topology", Proceedings of the Universities Power Engineering Conference, UK,1999, pp. 436-440

Δ Fothergill JC, Devine PJ & Lefley PW, "A novel design for a transformer for high voltage, high frequency, high power use", accepted paper, IEEE transactions on Power Delivery, 1999

A HIGH POWER UNITY POWER FACTOR THREE-PHASE RECTIFIER FOR HIGH VOLTAGE APPLICATIONS.

P.J. Devine and P.W.Lefley.

University of Leicester, United Kingdom

ABSTRACT

Conversion of AC mains supply voltages to a DC level has traditionally been achieved with diode or phase rectification. The unfavourable characteristics of the input current drawn can lead to a number of problems including:

- Low input power factor.
- High supply peak currents leading to mains voltage distortion.
- High reactive component sizes.

To overcome these problems power factor correction methods are becoming increasingly popular. This paper presents a three-phase unity power factor rectifier for particular use in high voltage, high power applications. The converter draws sinusoidal input current waveforms with a power factor approaching unity.

The output variable boost characteristic of the rectifier is taken advantage of, in that a high voltage DC bus (in the order of 800VDC) may be utilised. This is of particular interest in the field of high voltage, high frequency, inverter fed DC power supplies (>10kV) and can significantly reduce the magnitude of primary winding current. As a result there may be a substantial decrease in size and weight of the output transformer.

An initial circuit model has been investigated on the PsPICE circuit simulation package to determine suitable circuit parameters from which a prototype was built. A discussion on the performance and analysis of the prototype will be given.

1. INTRODUCTION.

Conversion of AC line voltages to a DC level has traditionally been achieved with diode or phase rectification. The low power factor and large harmonic line currents which occur due to the use of these rectifiers are well known problems.

Several techniques have been put forward to keep power supply quality at acceptable levels in accordance with IEC standards (IEC 555-2) and IEEE recommendations (IEEE-519).

These techniques can be classified into two main categories.

- Passive and active filter techniques.
- Unity power factor AC-DC converters.

The first category deals with well known rectification systems where both power factor and harmonic distortion are corrected to a certain extent. The use of passive filtering has been the most commonly used method being both simple to implement and operate. However, passive filtering requires magnetic components operating at low frequencies and tends to be bulky and expensive.

Active filtering techniques (harmonic injection techniques for example) tend to require a large number of passive components, semiconductor switching devices and complex control algorithms and are therefore very costly.

The second category indicates an intent to minimise the harmonics created by a rectification system and operate it at improved power factor. In these systems active switching methods are used to control the DC output voltage whilst maintaining nearly sinusoidal input line currents at near unity power factor. These topologies have been the object of increasing interest since 1980.

In (1), which constituted a major breakthrough in the development of three phase rectifier systems an unidirectional three phase boost rectifier is introduced.

This has the following characteristics:

- Approximately sinusoidal input currents.
- Operation at power factors approaching unity.
- Resistive fundamental mains behaviour.
- Controllability of the DC output voltage which is higher than the peak AC line voltage.
- Simplicity of the power circuit structure and control systems.

This converter is of special interest in the field of process technology power supplies, e.g., the application of this converter for supplying the DC link voltage of a PWM inverter makes possible the following:

- The control of the DC link voltage to a constant value independent of the mains voltage.
- The maximum utilisation of the rated power of the PWM inverter.

Another key area of technology for which this converter can be applied is the initial AC to DC conversion stage within a high voltage DC power supply (>5kV).

Such power supplies can be found in many industrial and medical processes that require the generation of high DC voltage levels at high power ratings, e.g., x-ray generation equipment in medical and physics research facilities and electrostatic precipitators used as pollution control systems in many industrial processes.

The output voltage variable boost characteristic of this converter is taken advantage of, in that a high voltage DC bus in the order of 800V or more may be utilised. This can significantly reduce the magnitude of the primary winding current in the subsequent inverter section of the supply. As a result there may be a significant decrease in the size and weight of the output transformer.

This paper addresses the analysis and design of a three phase AC-DC converter drawing high quality input current waveforms from the mains for such an application.

2. DESCRIPTION OF THE PROPOSED SYSTEM CONFIGURATION.

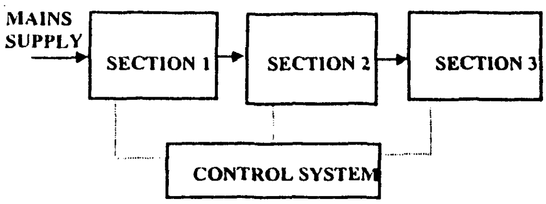

Section 1: Three phase AC-DC converter.
Section 2: High frequency inverter.
Section 3: High voltage, high frequency transformer and high voltage side rectification.

Fig. 1. System layout of the proposed high voltage DC power supply.

Fig. 1 shows the system layout of the proposed high voltage DC power supply. Of particular interest to this paper is the three phase AC-DC converter of section 1.

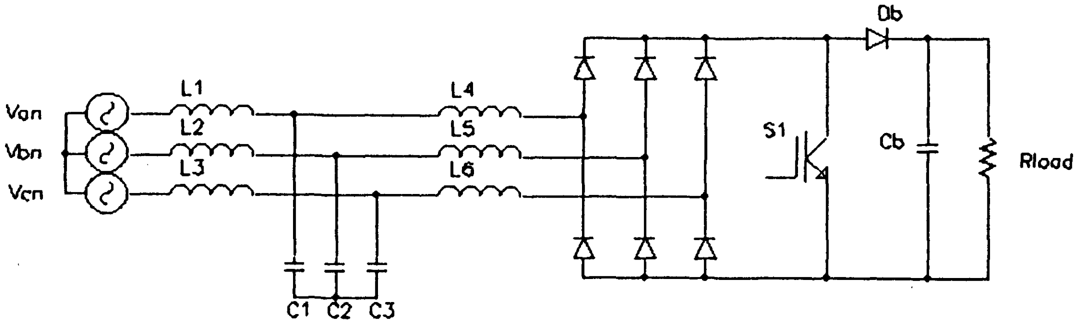

Fig. 2 Structure of the power circuit of the three phase unity power factor AC-DC converter. High frequency spectral components filter (L1,L2,L3 C1,C2,C3). Boost inductors (L4,L5,L6). Three phase diode bridge (Dr). Active switching device (S1) shown as an IGBT in this model. Boost/blocking diode (Db). Boost capacitor (Cb). Output modelled as a resistive load (Rload) in this model.

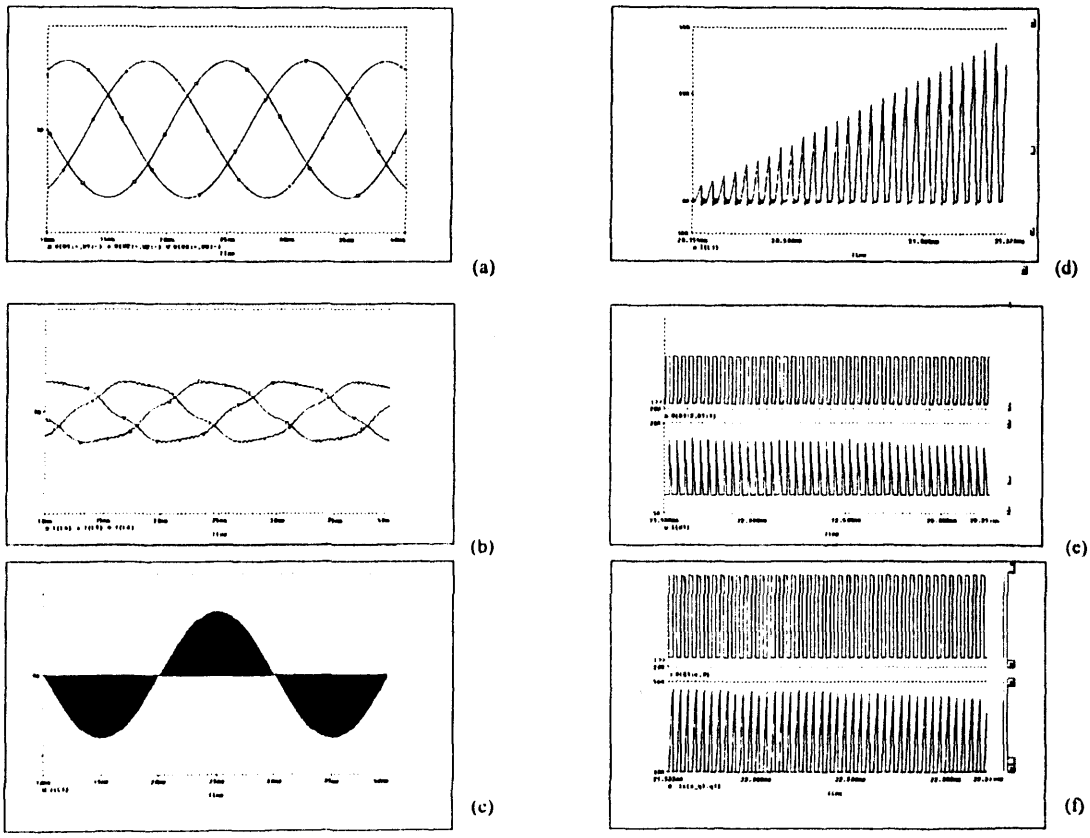

Fig. 3 PsPICE simulation of the three phase AC-DC converter being operated with a constant switching frequency.
(a) Mains phase voltages Van,Vbn,Vcn. (b) Input phase currents after filtering. (c) Boost inductor (L4) current.
(d) Boost inductor (L4) current viewed over a shorter timebase. (e) Boost diode blocking voltage (top) and current (bottom).
(f) Switching device (S1) voltage (top) and current (bottom).

2.1 PRINCIPLE OF OPERATION.

A circuit diagram of the three phase unity power factor AC-DC converter is shown in Fig.2. This shows the three phase supply (Van,Vbn,Vcn), the high frequency spectral components filter, the unity power factor rectifier stage consisting of the three 'boost' inductors (L4-6), a three phases diode rectifier (Dr), an active switch (S1), a 'boost' diode (Db) and an output filter capacitor (Cb). Consideration of the circuit operation will initially be given without inclusion of the high frequency spectral components filter network (L1-3, C1-3).

During the 'On' time of the active switch (S1) all three input phases are short circuited through the three 'boost' inductors, the three phase diode rectifier and the switch.
As a result of this the three input currents begin simultaneously to increases at a rate proportional to the instantaneous values of their respective phase voltages (Fig. 3(d)). The circuit is operated at a constant switching frequency. The duty cycle of the switch however is modulated for variations in load and is such that the input currents are always discontinuous.
The specific peak current magnitudes during each 'On' interval are proportional to the average value of their respective input phase voltages during each 'On' time. Assuming that each of the input phase voltages varies sinusoidally then the input current peaks will also vary sinusoidally (Fig. 3(c)). Assuming discontinuous input current mode the average value of these peaks also varies sinusoidally.
Consequently all three input AC currents consist of a fundamental component at mains supply frequency and a band of high frequency components centred around the switching frequency (25kHz in this simulation)

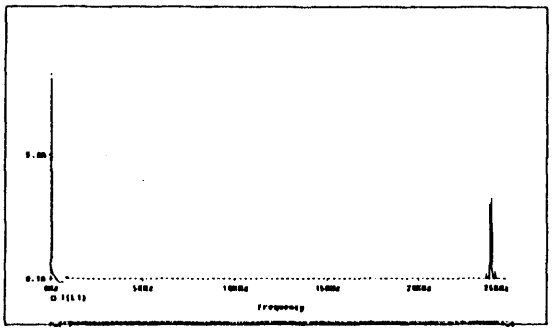

Fig. 4. Harmonic spectrum of input current without filter.

The fundamental component and high frequency switching component of the input current can be seen in Fig. 4.
During the 'Off' time of the switch the energy stored in the three boost inductors is discharged through the converter (Fig. 3(e)). The time required to discharge the boost inductors is dependant on the phase input voltage and the voltage across the three phases bridge rectifier during the 'Off' time. The average values of the input currents during this time are therefore not proportional to the phase voltage.
Generally,the 'Off' time of the switch is kept much shorter then the 'On' time to ensure that the average input currents during each switching cycle are proportional to the average phase input voltages during the same switching cycle.

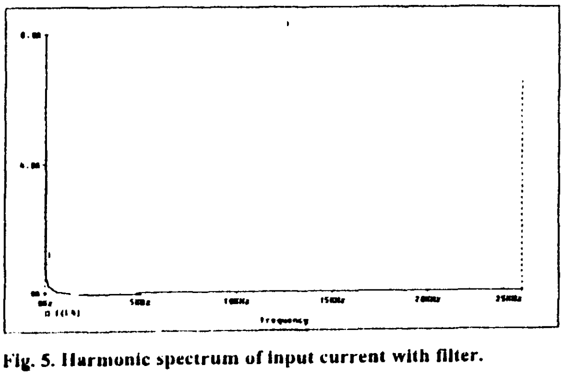

Fig. 5. Harmonic spectrum of input current with filter.

The unwanted spectral components of the input current waveform are centred around the switching frequency of the circuit as shown in Fig. 4. Since the switching frequency will be very high compared to that of the mains. A high frequency spectral components filter will successfully reduce the harmonic contents of the input current waveform. This can be seen in Fig. 5 which shows the harmonic spectrum of the input current with the filter in operation.

The converter draws nearly sinusoidal input currents from the three phase supply with a power factor approaching unity (Fig. 3(b).

2.3 APPLICATION OF THE CONVERTER TO HIGH VOLTAGE DC POWER SUPPLIES.

The voltage boost characteristic of the converter is well known from conventional converter theory as being:

$$\frac{V_a}{V_b}=\frac{1}{1-\alpha}$$

Where V_a= DC output voltage.
V_b= DC input voltage.
α = duty ratio of the active switch.

For the three phase boost converter of Fig. 2 the DC input voltage V_b is replaced by the three phase rectifier output voltage.

$$\frac{V_a}{V_r}=\frac{\sqrt{3}}{1-\alpha}$$

Where V_a = DC output voltage.
V_r = Three phase rectifier output voltage.
α = duty ratio of the active switch.

Pforr (5) showed that for the three phase unity power factor converter input power factor improves as the voltage boost ratio (Va/Vr) increases. This can be seen in Fig. 6.

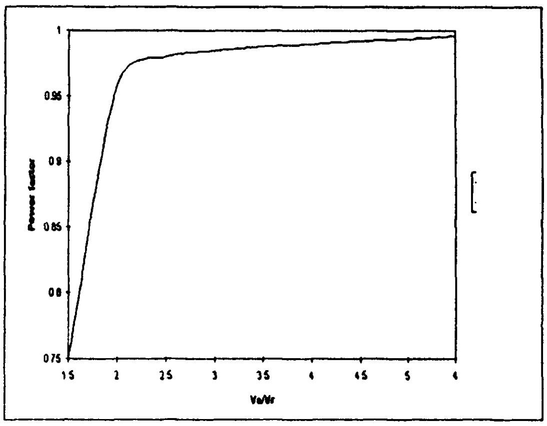

Fig. 6. Relationship between voltage boost ratio and input power factor.

For high voltage applications the implementation of this converter topology as the initial AC to DC conversion stage of a high voltage DC power supply has two desirable features.

1: The DC output voltage of the converter can be boosted to a level well above the conventional 575VDC obtained from a three phase diode rectifier. This allows a reduction in magnitude of currents in the inverter section of the supply and consequently a reduction in size and weight of the high voltage, high frequency inverter fed transformer.

2: By the very nature of this topology input power factor improves as the boost ratio of the converter increases.

3.0: EXPERIMENTAL RESULTS.

A hardware prototype of the three phase unity power factor converter has been constructed and tested using a power MOSFET as the active switch. The prototype has the following parameters:

- 1.5kVA output power.
- Output DC voltage = 650V.
- Input rms phase voltage = 160V.
- MOSFET switch frequency = 25Khz

Experimental waveforms obtained from the prototype are shown in Fig. 7.

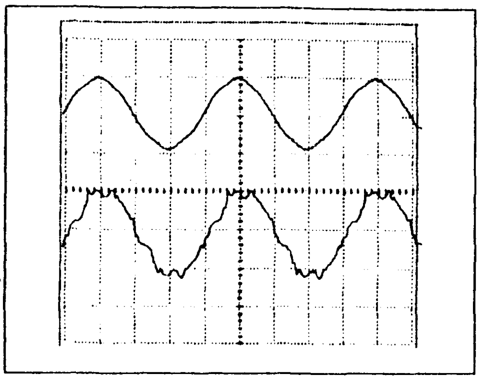

(a)

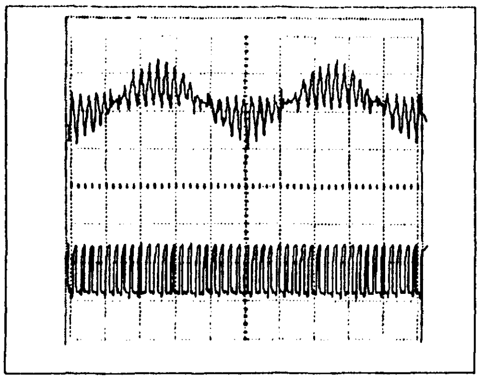

(b)

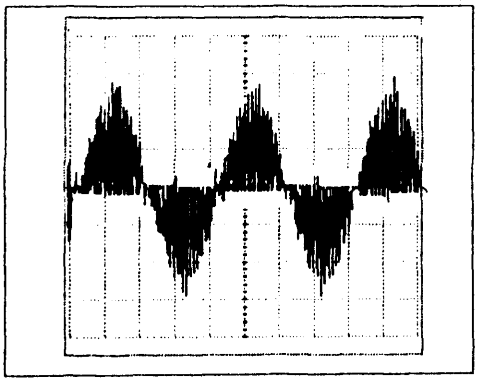

(c)

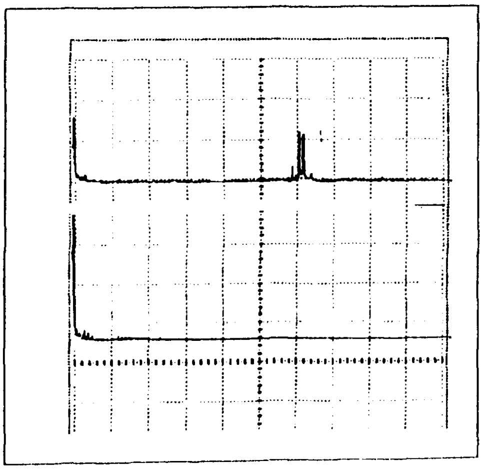

(d)

Fig.7. Experimental waveforms obtained from the prototype converter. (a) Mains supply voltage Van (top) and current (bottom) with the high frequency spectral components filter in operation.
(b) Boost inductor current(top) with the converter operating at a low switching frequency to show the effect of MOSFET switching (bottom).
(c) Converter input current without the high frequency spectral components filter.
(d) Harmonic spectrum of converter input current without filter (top) and with filter (bottom).

4.0 CONCLUSIONS.

A three phase unity power factor converter has been implemented as the initial AC-DC conversion stage of a high voltage DC power supply. The advantages of this rectifier over the traditional three phase diode bridge are the following:

- Current is drawn from the mains supply with near unity power factor and minimal harmonic distortion.
- The converter provides a boosted DC output voltage level capable of driving a subsequent high voltage inverter fed high frequency transformer.

A prototype of the converter has been designed and constructed. Experimental results verify the simulated results achieved with the PsPICE simulation software.

4.1 FUTURE WORK.

A higher power and higher DC output voltage rated converter will be designed and constructed. This will be tested in conjunction with the inverter stage of the DC power supply.

ACKNOWLEDGEMENT.

The authors acknowledge the technical support of the Engineering Department at Leicester University.

REFERENCES.

(1) Prasad, A.R, "An Active Power Factor Correction Technique for Three Phase Diode Rectifiers". IEEE Trans on Power Electronics, Vol 6, No. 1, Jan 1991.

(2) Kolar, J.W, " A comprehensive design approach for a three phase high frequency single switch discontinuous mode boost power factor corrector based on analytically derived converter component ratings". IEEE Trans on Industry Applications. Vol 31, No. 3, May/June 1995.

(3) Tou, M, " Analysis and design of a single controlled switch three phase rectifier with unity power factor and sinusoidal input currents". IEEE 1995, 0-7803-2482-X/95.

(4) Koczara, W, " Unity power factor three phase rectifier" . Power Quality Conf., Munich, Germany, Oct 1992, pp 79-88.

(5) Pforr, J, " Single ended resonant pre-converters for high frequency induction heaters". Ph.D. theses, University of Teesside, 1992.

(6) Devine, P.J, " The requirements of a high voltage DC power supply" . Internal publication, Leicester University, 1995.

ADDRESS OF AUTHORS.

Leicester University Engineering Departement,
University of Leicester,
University Road,
Leicester, LE1 7RH
UK.
e-mail: PJD3@le.ac.uk & PWL3@le.ac.uk.
FAX : +44 116 2522619.

A HIGH POWER HIGH FREQUENCY TRANSFORMER FOR HIGH VOLTAGE APPLICATIONS.

P.J. Devine, P.W.Lefley, J.C.Fothergill.

University of Leicester, United Kingdom.

ABSTRACT.

The paper considers the design of a high voltage (17kV) step-up 17kVA transformer designed for use with a high frequency (30kHz) switched mode power supply (SMPS). A comparison of single phase rectifier circuits with SMPS is made highlighting the advantages of moving towards high frequency inverter technology in applications such as electrostatic precipitator power supplies. High frequency operation will allow much more precise control over the operating parameters of the power supply such as voltage step levels and response to variations in load demand.
The design considerations for a high voltage transformer are presented and, in particular, the issues of insulation requirements, parasitic elements, core loss, heat dissipation and corona effects are considered in detail.
The transformer uses a ferrite core design to allow operation at high frequencies which results in significant saving in size and weight.

1. INTRODUCTION.

Conversion of AC mains voltages to a high voltage (>10kV), high power (>10kVA) DC level is a key area of technology which is a requirement in many industrial and medical imaging processes, e.g., electrostatic precipitators used as dust control systems and x-ray generation equipment in medical and physics research facilities.
In the majority of cases this high voltage DC requirement is achieved with a single phase AC regulator (figure 1). The regulator controls the supply to the high voltage transformer. A bridge rectification network is implemented on the secondary of the transformer to produce a high voltage DC level.

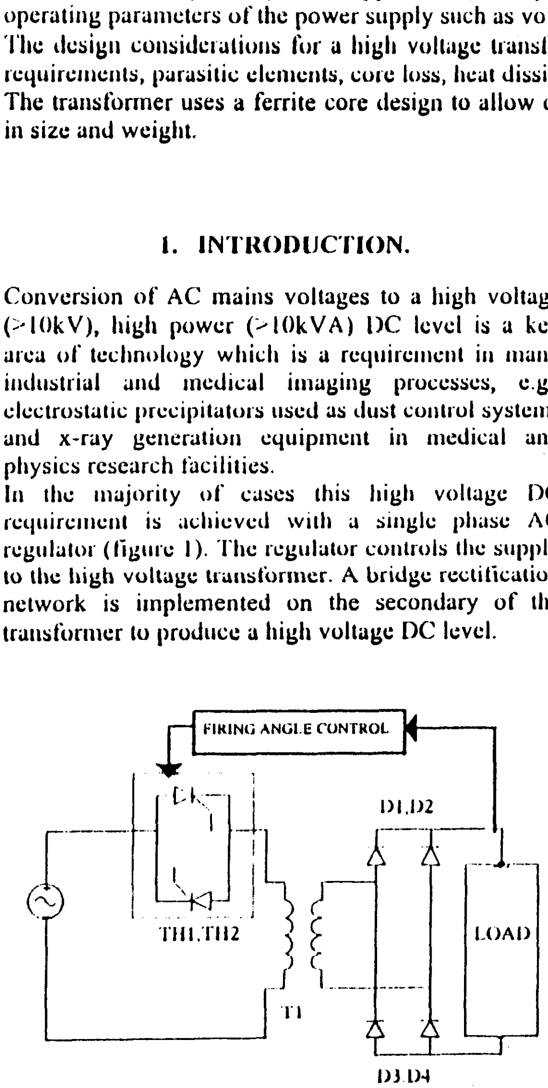

Fig. 1. Conventional high voltage DC power supply.

TH1,TH2: Thyristor set.
T1: High voltage, low frequency transformer.
D1,D2,D3,D4: High voltage bridge rectifier.

Power and voltage control is accomplished by variation of the firing angle of the thyristor set.
There has been little progress from this topology over the years due, in part to the lack of availability of high frequency, high voltage transformers on the market. This has made conventional 50/60Hz design the more attractive solution. This topology whilst robust and simple has severe drawbacks as far as operation is concerned :

- Low quality input currents and low power factor.
- Sluggish operating characteristics.
- Low power supply efficiency.
- Size, weight and civil engineering costs associated with the oil insulated transformer.
- EMC problems.

A high frequency switched mode based power supply is being developed. The improvements expected from the adoption of high frequency switched mode operation are three fold :
1: High frequency switching operation will allow much more precise control over the operating parameters such as output voltage level, current level, voltage rise times and response to variations in load demand.
2: The high frequency switching will allow a significant reduction in the size and weight of the high voltage transformer. This reduction in size and weight leads to a compact design which minimises the installation and maintenance costs.
3: Ability to modulate the output voltage.
In some applications the ability to pulse the DC output voltage of the converter from one level to another at a specific and programmable magnitude, time duration and period has substantial benefits, e.g., in electrostatic precipitators this method may improve dust/gas particle charging and collection.

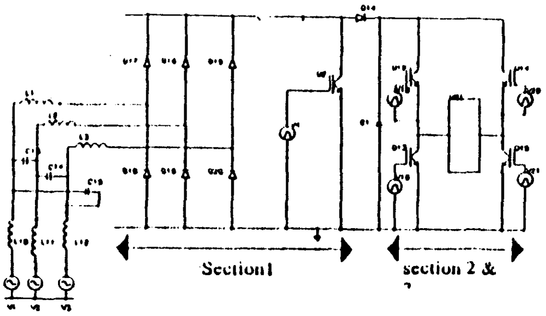

Section 1: Three phase unity power factor rectifier.
Section 2: High frequency inverter.
Section 3: High voltage, high frequency transformer and high voltage side rectification.

Fig. 2. System layout of the proposed high voltage DC power supply.

The design and construction of section 1 of the system is addressed in [1]. Of particular interest to this paper is the design and construction of the high voltage, high frequency transformer.

2. TRANSFORMER DESIGN.

The design of a high frequency, high voltage transformer differs widely from the standard transformer design methodologies used for mains voltage applications [2]. One must analyse several related issues:

1: Insulation requirements.
2: Parasitic elements.
3: Core loss and heat dissipation.
4: Corona effects.

High voltage transformers generally have a large turns ratio, typically 600:1 to 900:1.

Sufficient insulation thickness between the primary and secondary windings is required to avoid electrical breakdown. Therefore, the electromagnetic coupling of the primary and secondary winding will not be as tight as in conventional low voltage transformers [3]. This results in a parasitic leakage inductance referred to the primary side which can effect the maximum power throughput of the transformer. Hence, there is a trade off between insulation distance and leakage inductance.

Furthermore, the high number of turns required for the secondary winding causes a high distributed capacitance. When referred to the primary this capacitance value is multiplied by the square of the turns ratio and therefore is not negligible [4,5]. This parasitic capacitance induces an ineffective current through the secondary winding which results in a loss of transformer efficiency.

Corona discharge can seriously effect the operation and life expectancy of a high voltage transformer. Any sharp corner or protrusions may lead to an enhanced electric field and corona in this vicinity. A corona will create highly reactive molecules which will, in time degrade the insulation leading to electrical breakdown.

Bearing these factors in mind a high voltage, high frequency transformer is designed with the following electrical specification:

Vprimary = 750V (quasi-square wave).
Vsecondary = 17kV.
Power rating = 17kVA.
Switching frequency = 30kHz.
Maximum flux density = 0.2T.
Insulation requirement = 100kV.
Maximum electric field = 3kV/mm.

2.1. Magnetic core design.

The design procedure adopted for the design of the core required for this transformer is based upon previous designs for high frequency, high power transformers in aerospace and astronautical applications where size, weight and power rating are extremely important factors [6,7].

Because the power rating of the transformer is high (17kVA) there are no suitable "U" or "C" ferrite cores on the market. To overcome this problem a number of "I" cores have been machined to the required size and shape and bonded, under the ferrite manufacturers assistance, to provide the required core cross sectional area and geometric size.

The ferrite used is a high saturation manganese-zinc designed for high power, high frequency applications. The power loss density of the material at the working frequency and flux level is low (< 0.1 W/cm^3) as shown in figure 3.

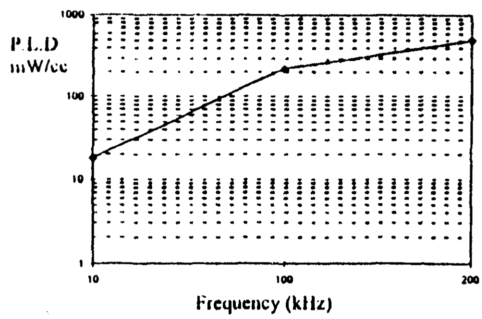

Fig. 3. Power Loss Density vs. Frequency.

Figure 4. shows that these losses are further minimised at elevated operating temperatures since the power loss density of this material reduces as the operating temperature rises. This is another beneficial characteristic of this ferrite.

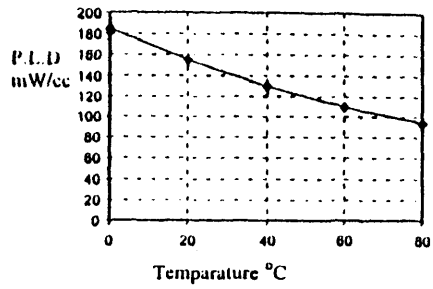

Fig. 4. Power Loss Density vs. Temperature.

2.2. Minimisation of parasitic elements.

An equivalent circuit model of a high voltage transformer is shown in figure 5. This shows the parasitic leakage inductance L_p, magnetising inductance L_m, and parasitic capacitance C_p referred to the primary.

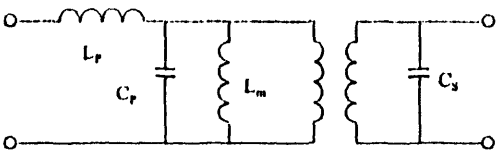

$$C_p = \left(\frac{n_2}{n_1}\right)^2 C_s \qquad (1)$$

Fig. 5. Equivalent circuit model of a high voltage transformer.

The leakage inductance L_p arises due to the imperfect coupling of the primary and secondary windings and according to [5] is calculated as follows:

$$L_p = \frac{\pi n_p^2 (t_p + t_s)}{h}\left(\frac{m_1 + m_2}{3} + m_3\right) \times 10^{-7} \qquad (2)$$

where L_p is the leakage inductance referred to the primary winding (H) ; n_p is the number of primary turns ; t_p and t_s are the average one turn lengths of the primary and secondary windings (m) ; h is the effective height of the two windings (m) and m_1, m_2 and m_3 are the geometric sizes of the transformer shown in figure 6.

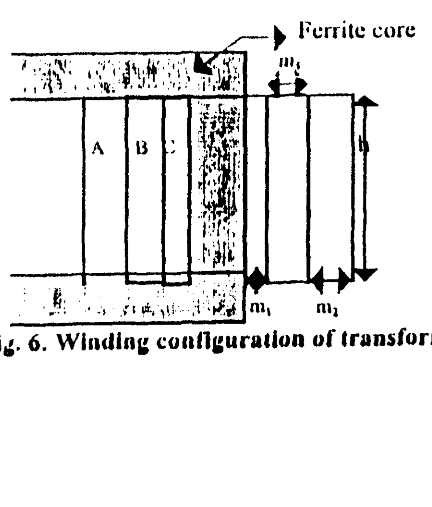

Fig. 6. Winding configuration of transformer.

Referring to figure 6, A is the secondary winding ; B is the insulation between primary and secondary winding ; C is the primary winding ; m_1 is the primary winding thickness (m) ; m_2 is the secondary winding thickness(m) and m_3 is the insulation thickness(m).
According to (2) the leakage inductance is a function of both the geometric size of the transformer and more importantly, the square of the number of primary turns. L_p can therefore be reduced greatly by lowering the number of primary turns.
However, according to (3) lowering the primary turns will result in an increase of operational flux density.

$$n_p = \frac{V_p \times 10^4}{4BA_c f} \qquad (3)$$

Where Vp is the applied primary voltage (V) ; B is the operational flux density (T) ; A_c is the ferrite core cross sectional area (cm^2) and f is the operating frequency (Hz).
Thus, the number of turns must be determined as a result of judicious compromise between these conflicting factors.
Parasitic capacitance C_p arises due to the significant secondary capacitance owing to a high number of secondary turns [5].

$$C_p = \frac{8\pi\varepsilon_r\varepsilon_0 \, r h_2 n^2}{3d(m_L - 1)m_s^2} \qquad (4)$$

Where C_p is the primary referred capacitance (F) ; ε_0 is the dielectric constant of a vacuum (F/m) ; ε_r is the relative dielectric constant of the insulating medium used ; r is the average radius of the secondary winding (metres) ; h_2 is the effective height of the secondary windings (metres) ; n is the turns ratio ; d is the distance between layers of the secondary winding (metres) ; m_L is the number of layers of secondary windings and m_s is the number of secondary windings.
According to (1) and (4) this capacitance value when referred to the primary is hugely influenced by the turns ratio (n) of the transformer.
Generally, the turns ratios of high voltage transformers are between 600:1 and 900:1 depending on the desired output voltage. If a voltage requirement results in a turns ratio higher than this then the power supply is usually sectionalised or voltage multiplier circuits are added after the high voltage rectification stage which can adversely effect the dynamic performance of the power supply.
Turns ratio and therefore parasitic capacitance can be significantly reduced in the transformer by driving the primary winding at a high voltage level ($\geq$ 750V quasi square wave). This requires the DC link section of the supply to be energised to this voltage level which implies a voltage boost element. This section of the supply is analysed in [1].

2.3. Insulation and electric stress management within the transformer.

One of the incentives for adopting high frequency switched mode technology in this application is to

minimise the size of the transformer. A factor influencing this size is the maximum electric stress which can be tolerated by the insulating media within the transformer. Oil insulated transformers are heavy and prone to leaking. The oil needs to be regularly cleaned or impurities build up at high stress points which can lead to electrical breakdown.
Inert gases generally have a dielectric strength 2 to 3 times higher than that of air. A method of reducing the required insulation gap between primary and secondary windings is to encapsulate the transformer in a sealed unit containing such a gas at a pressure slightly above atmospheric. Another advantage of adopting this technique is that such gases can have heat transfer coefficients up to 3 times that of air which assists heat dissipation from the core and windings.
Solid insulation may be used but presents difficulties during transformer development (if breakdown occurs then it may be necessary to start again) and it may prevent sufficient heat loss. Some solid insulation is required for mechanical support of the secondary windings.
Stress rings are employed to prevent high divergent fields at conductor corners which would otherwise discharge and lead to rapid degradation of the insulation. Such a structure is shown in figure 7.

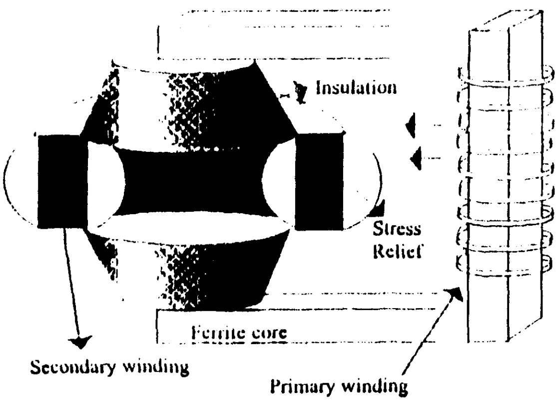

Fig. 7. Structural diagram of the transformer.

3.0 CONCLUSIONS.

A high voltage, high frequency transformer based upon the design considerations outlined in this paper has been designed and constructed. Its electrical characteristics are currently being analysed and will be presented to the conference.
By adoption of techniques outlined in this paper it has been possible to minimise the undesirable effects of leakage inductance and parasitic capacitance.
It has also been possible to control the electric field stresses within the transformer structure and so prolong the life expectancy of the high voltage transformer.

ACKNOWLEDGEMENTS.

The project is an EPSRC / DTI PEDDS link project with Deakin Davenset Rectifiers Ltd whose support is gratefully acknowledged.

REFERENCES.

(1) Devine , P.J, Lefley ,P.W, "A high power unity power factor three phase rectifier for high voltage applications.". UPEC, Sept 1996, pp 417-420.

(2) Devine, P.J, " The requirements of a high voltage DC power supply" . Internal publication, Leicester University, 1995.

(3) Liberati, G. "High voltage, high power switched mode power supply for Ion production". ENEL C.R.T.N.

(4) Perez, M.A, "A new topology for high voltage, high frequency transformers.". IEEE 1995, 0-7803-2482-X/95.

(5) Takano, H, "Feasible characteristic evaluations of resonant inverter linked DC-DC power converter using high voltage transformer parasitic components". Power electronics and variable speed drives, Sept 23-25 1996, IEE No 429, pp 525-533.

(6) Petkov, R. "Optimum design of a high power, high frequency transformer". IEE Transaction on power electronics, Vol 11, No 1, 1996, pp 33-41.

(7) Mcylman, T. " Transformer design handbook". Jet Propulsion Laboratory, California Institute of Technology.

ADDRESS OF AUTHORS.

Leicester University Engineering Department,
University of Leicester,
Leicester, LE1 7RH
UK.
E.mail:PJD3@le.ac.uk,PWL3@le.ac.uk,
ICF@le.ac.uk.
FAX : +44 116 2522619.

A METHOD FOR SUPPLYING A HIGH FREQUENCY, HIGH VOLTAGE TRANSFORMER, BASED UPON A FORCED COMMUTATION CYCLOCONVERTER (MATRIX CONVERTER) TOPOLOGY.

P.J.Devine, P.W.Lefley
University of Leicester, United Kingdom

ABSTRACT

Conversion of AC mains voltages to a high voltage (> 20kV), high power DC level is a key area of technology which is a requirement in many industrial processes, for example particulate emission control by electrostatic precipitation. In the majority of present installations the high voltage requirement is achieved with a single phase thyristor based AC regulator. This topology, whilst robust and simple, has severe drawbacks notably sluggish operating characteristics [1], low supply efficiency due to the high reactance of the mains frequency transformer and the associated costs due to the size and weight of the 50/60 Hz transformer. A direct AC-AC high frequency matrix converter is proposed. The converter delivers, directly from a 3 phase mains supply, a high frequency (20kHz), single phase, voltage fed quasi-square wave (QSW) to the primary winding of a high frequency, high voltage, ferrite core based transformer developed as part of a high voltage power supply. The advantages to be gained from this include a reduction in size of the magnetic structure, the eradication of costly DC link components and the allowance of much faster and precise control over operational parameters than has previously been achieved with a thyristor based AC regulator.

Introduction.

Conversion of AC mains voltages to a high voltage, high power DC level is a key area of technology which is a requirement in many industrial processes, for example electrostatic precipitators used in flue gas or dust emission control. In the majority of present installations the high voltage requirement (10-80 kV) is achieved with the single phase thyristor based AC regulator shown in Fig. 1.

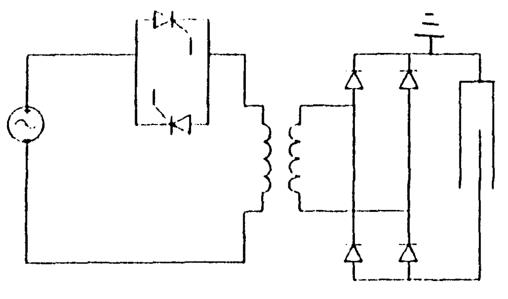

Fig. 1. Conventional high voltage DC power supply.

Power and voltage control is achieved by variation of the firing angle of the thyristor set. This topology, whilst robust and simple, has severe drawbacks notably sluggish operating characteristics [1], low supply efficiency due to the high reactance of the mains frequency transformer and the associated civil engineering costs due to the size and weight of the oil insulated transformer. Present research in this area is involved with transferring from a mains frequency operation to a high frequency switched mode operation. The advantages of this would be a significant reduction in the magnetic structure dimensions and the allowance of more precise control over operational parameters such as output voltage ripple, voltage rise times and response to variations in load demand. The research has generally centred upon indirect converters utilising IGBT technology, namely voltage/current fed inverters and series, parallel or series-parallel resonant tank inverters used in situations where the leakage reactance and parasitic capacitance of the transformer are not negligible and are utilised to form part or all of the resonant element of the inverter [2-5]. In general, indirect converters have an intrinsic need for an initial rectification stage and an intermediate storage stage. They are, therefore, bound to use large reactive elements. Furthermore, the intermediate storage destroys all information about input voltage waveforms and phasing. A direct AC-AC high frequency matrix converter is proposed. The converter delivers, directly from a 3 phase mains supply, a high frequency, single phase, voltage fed quasi-square wave (QSW) to the primary winding of a high frequency, high voltage transformer developed as part of an electrostatic precipitator power supply. One of the notable properties of this converter is its dynamic range of operation. The converter is capable of supplying a QSW output of 0 to 20 kHz with a duty ratio controllable from 0 to 100%.

The generalised matrix converter is shown in Fig. 2. The general features of which are summarised below:

1. The converter consists of nine bilateral switches, implemented as either nine pairs of anti-parallel thyristors or nine bridge rectifier embedded IGBT'S as shown in Fig. 3.

2. The general application of this converter to date has been to AC variable speed induction motor drives [6].

3. High frequency modulation of the switches results in a sinusoidal output voltage waveform of zero to 95% of the input [7]

4 Output frequency can be controlled from 0 (DC) to typically 200 Hz. The reason for this frequency ceiling is to achieve a large separation between the fundamental sinusoidal output frequency and the switch modulation frequency [8,9]

Proposed Matrix Converter.

Fig. 4. shows the configuration of the proposed high frequency matrix converter. It consists of six bilateral switches, each switch containing two IGBT'S and two blocking diodes.

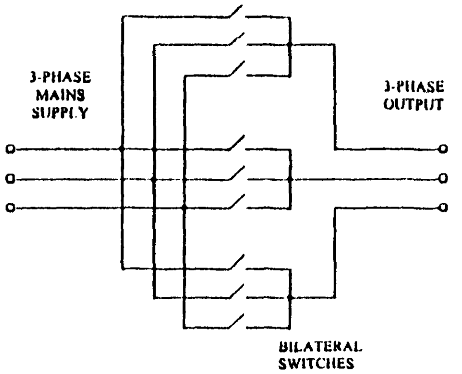

Fig. 2. Generalised matrix converter

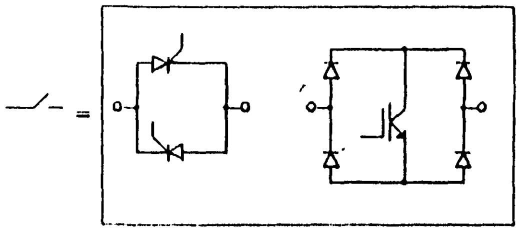

Fig. 3. Bilateral switch configurations

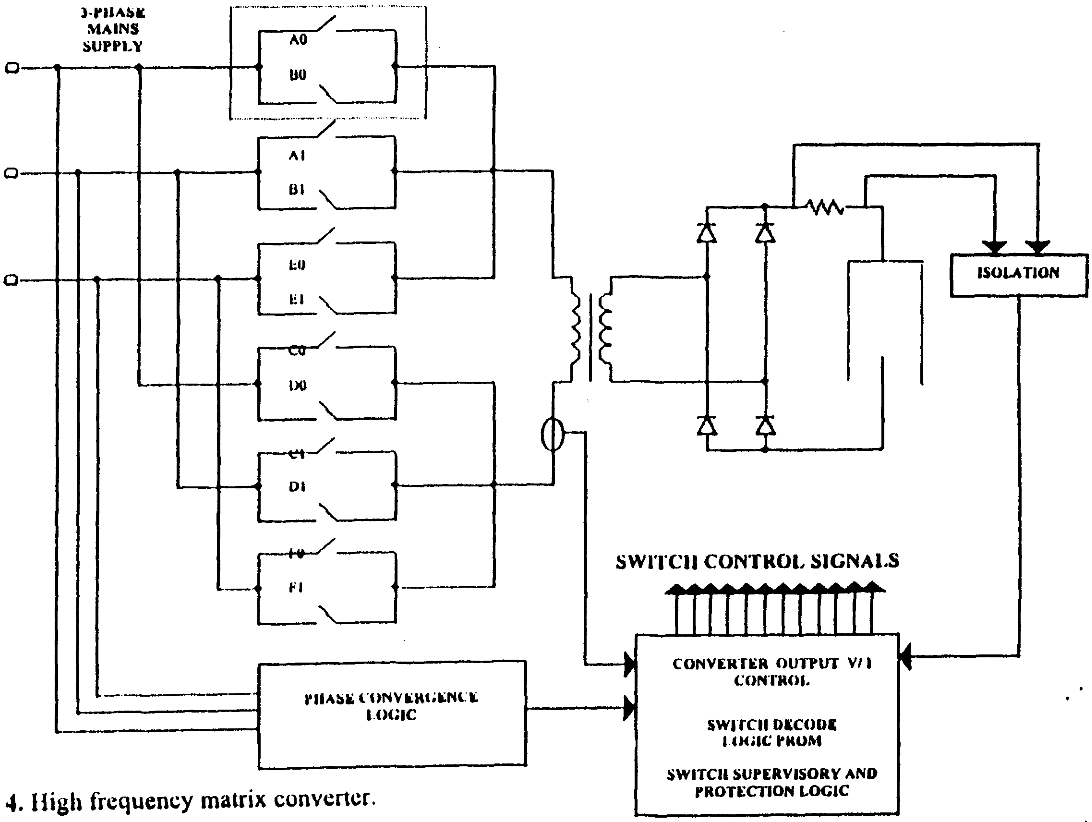

Fig. 4. High frequency matrix converter.

The general features of the high frequency matrix converter:

1. A high frequency, single phase, QSW output is synthesised by six distinct IGBT modulation functions. Each function contains the necessary high frequency switching algorithm to achieve a high frequency QSW output.
2. Crossover from modulation function one through to six occurs at the six points in the mains period where two line voltages converge. Thus, the high frequency QSW output resides within a six pulse envelope of the 3-phase mains supply.
3. A notable feature of both the converter topology and high frequency switching algorithm is that switch overlap is embedded within the switching patterns. This maintains a bi-directional current path at any transition time.
4. Output frequency, voltage and current are controlled by PWM control circuitry.

Experimental Results.

A full model of the proposed converter has been developed on simulation software.
Fig. 5. shows a transient analysis of the model showing input 3-phase mains voltage, high frequency QSW output and rectified output voltage of the high frequency, high voltage transformer. Switching frequency in this particular simulation has been decreased to facilitate viewing.

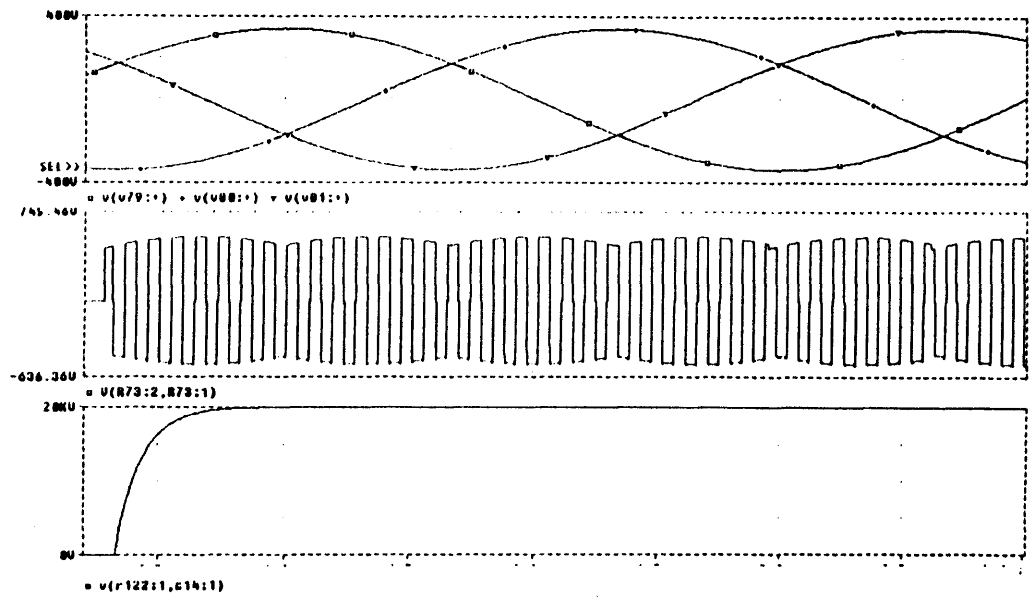

Fig. 5. Simulation results.

Conclusions.

A novel high frequency AC-AC converter has been described. The converter is capable of producing a high frequency, single phase, QSW output directly from a three-phase mains supply. The advantages to be gained from this include a reduction in size of the magnetic structure, the eradication of costly DC link components and the allowance of much faster and precise control over operational parameters than has previously been achieved with a thyristor based AC regulator.

References.

[1] M.Pihl, "New power supply unit improves control response of electrostatic precipitators," ABB review 2/1998, ABB Flackt Industri AB.

[2] H.Takano and T.Hatakeyama, "Feasible characteristic evaluations of resonant PWM inverter linked DC-DC power converter using high voltage transformer parasitic circuit components," IEE, Power.Elect.Conf., pp.525-533, 1996.

[3] G.Liberati, "High frequency switching technology for ESP power supply," Proc. Particulate Control Symposium-Williamsburg 1991.

[4] H.Akagi and A.Nabae, "A voltage source inverter using IGBT'S for a 50kHz 10kV corona surface treater," IEEE/IAS Annu.Meet.,pp. 1164-1169, 1989.

[5] H.Hino, T.Hatakeyama, "Resonant DC-DC converter using parasitic impedance's of high voltage transformer," PCIM Conf. Rec, Vol 1, pp 15-28, 1987

[6] C.L.Neft and C.D.Schauder, "Theory and design of a 30-Hp Matrix Converter," IEEE/IAS Ann. Meet. Conf. Rec., pp. 934-939, 1988.

[7] M.Venturini, "The generalised transformer: A bi-directional sinusoidal waveform frequency

[8] M.Venturini, "A new sine wave in, sine wave out conversion technique eliminates reactive elements," Powercon 7, Vol 3, pp.1-15, 1980

[9] B.K.Bose, "Modern power electronics," IEEE Press, PC0276-6, 1992.

Address of authors.

Leicester University Engineering Department,
University of Leicester,
Leicester, LE1 7RH
UK.
E.mail:PJD3@le.ac.uk
FAX : +44 116 2522619.
Power Research Group
University of Leicester,
Leicester, LE1 7RH

A Novel Prototype Design for a Transformer for High Voltage, High Frequency, High Power use

Dr. John C. Fothergill SMIEEE, Philip W. Devine and Dr. Paul W. Lefley
Electrical Power Engineering Research Group, Department of Engineering,
University of Leicester, Leicester LE1 7RH, UK

ABSTRACT

A prototype transformer has been designed and built which is novel in its combination of high voltage (50 kV), high frequency (20 kHz) and high power (25 kVA) specifications. The design technique utilized a spreadsheet approach which facilitated an iterative design procedure. The transformer used a ferrite core, nylon insulated secondary bobbins and pressurized sulfur hexafluoride encapsulation. It was designed as part of a high-voltage switched-mode power supply for driving electrostatic precipitators. The transformer was field tested at a large coal-fired power station and was found to have an efficiency of better than 98%.

Keywords: EHV transformers, gas insulated transformers, HF transformers, power transformers, AC-DC power conversion, dielectric materials/devices, ferrite materials/devices, HVDC insulation

I. INTRODUCTION

Conversion of AC mains voltages to a high voltage (>10kV), high power (>10kW) DC level is a key area of technology which is a requirement in many industrial processes; for example in particulate emission control using electrostatic precipitators.

In the majority of cases this high voltage DC requirement is achieved with a single phase AC regulator (Fig. 1). The regulator controls the supply to the high voltage transformer. A bridge rectification network is implemented on the secondary of the transformer to produce a high voltage DC level.

Power and voltage control is accomplished by variation of the firing angle of the thyristor set. There has been little progress from this topology over the years due, in part, to the lack of availability of high frequency, high voltage transformers of sufficient power ratings. This has made conventional 50/60Hz design the more attractive solution. This topology whilst robust and simple has severe drawbacks as far as operation is concerned:

- Low quality input currents and low power factor.
- Sluggish operating characteristics.
- Low power supply efficiency.
- Large size, weight and civil engineering costs associated with the oil-insulated transformer.

A high frequency switched mode based power supply has been developed with an output voltage of 50 kV at 0.5 A continuous rating for electrostatic precipitation. There are several improvements that may be expected from the adoption of high frequency switched mode operation:

1. High frequency switching operation will allow much more precise control over the operating parameters such as output voltage level, current level, voltage rise times and response to variations in load demand.

2. High frequency switching will allow a significant reduction in the size and weight of the high voltage transformer. This reduction in size and weight leads to a compact design, which minimizes the installation and maintenance costs.

3. High frequency switching will allow the reactance of the transformer core to be much lower and hence the efficiency of the power supply can be improved.

4. The ability to modulate the output voltage. In some applications the ability to pulse the DC output voltage of the converter from one level to another at a specific and programmable magnitude, time duration and period has substantial benefits, e.g., in electrostatic precipitators this method may improve dust/gas particle charging and collection.

The transformer must be designed to be driven from a voltage sourced H-bridge inverter, Fig. 2. There is sufficient flexibility with this type of inverter for using a range of voltage control strategies e.g. pulse width or phase shift control. Furthermore, the load may be made resonant if required. This flexibility in inverter control and operation is important to avoid undesirable affects such as ringing. Such effects may occur because of the nature of the transformer, exhibiting parasitic capacitance and inductance, which affects the voltage and current waveforms in the inverter.

A thorough and careful design of a high voltage high frequency transformer is required to ensure that the electrical and magnetic loadings are optimized, that the electrostatic and thermal stresses are acceptable for the voltage and power requirements, and that the parasitic parameters are minimized.

The design of a high frequency, high voltage transformer for electrostatic precipitator power supplies differs widely from the standard transformer design methodologies [1]. Several related issues must be analyzed:

1. Insulation requirements.

2. Parasitic elements.

3. Core loss and heat dissipation.

4. Corona effects.

5. Rectification

High voltage transformers generally have a large turns ratio, typically 600:1 to 900:1.

Sufficient insulation thickness between the primary and secondary windings is required to avoid electrical breakdown. Therefore, the electromagnetic coupling of the primary and secondary winding will not be as tight as in conventional low voltage transformers [2]. This results in a parasitic leakage inductance referred to the primary side that can effect the maximum power throughput of the transformer. Hence, there is a trade off between insulation distance and leakage inductance.

Furthermore, the high number of turns that is required for the secondary winding causes a high distributed capacitance. When referred to the primary this capacitance value is multiplied by the square of the turns ratio and therefore is not negligible [3, 4]. This parasitic capacitance induces an ineffective current through the secondary winding which results in a loss of transformer efficiency.

Corona discharge can seriously effect the operation and life expectancy of a high voltage transformer. Any sharp corner or protrusions may lead to an enhanced electric field and corona in this vicinity. A corona will create highly reactive molecules, which may degrade the insulation and lead to electrical breakdown.

The transformer was designed to drive a full-wave rectifier and to have a modular design so that different maximum voltages could be specified. The transformer was therefore designed with two secondary bobbins each driving a separate diode bridge as shown in Fig. 3. In order to ensure equal voltage sharing, a capacitive divider was also used.

Bearing these factors in mind a high voltage, high frequency transformer for an electrostatic precipitator power supply was designed with the following electrical specification:

- $V_{primary}$ = 587 V (quasi-square wave).
- $V_{secondary}$ = 50 kV.
- Power rating = 25 kVA.
- Switching frequency = 20 kHz.

The transformer was field tested as part of a HF HV supply for electrostatic precipitators in a large coal-fired power station.

II. TRANSFORMER DESIGN

The transformer design required consideration of the insulation materials, the magnetic material and the management of electrical, magnetic and thermal stresses.

A. Magnetic Design

Because of the high frequency requirement, it was decided to use a ferrite core. In order to accommodate two bobbins (one for the low voltage and one for the high voltage winding) a rectangular core was used with a 50 mm × 50 mm (2" × 2") cross-section. This was made from 100 mm × 25 mm × 25 mm (4" × 1" × 1") sections, since they were the largest available; these were ground to give good fits between the sections. To ensure low lossees the flux density was limited to 0.25 T.

A method described by McLyman [5] was used for the magnetic calculations. This method was implemented using MathCAD; the output of which is in Appendix A. This implementation was very useful as it facilitated an iterative design process in which the consequences of a parameter change were immediately reflected on the computer screen.

The important parameters are

- Two primary windings in series, each containing 13 turns of AWG7 wire giving a primary copper loss of 4.6 W.

- Two secondary windings in parallel, each containing 700 windings of AWG21 wire.

- Total losses (copper and "iron") of 510W.

B. Insulation Materials

In addition to the solid insulation required for the bobbins, the insulating encapsulation needed to be defined.

It is clear that the secondary bobbin needed to be large enough to prevent surface tracking from the high voltage winding to the transformer core or the primary winding. The thickness of the bobbin also had to be great enough to prevent breakdown through the insulation. Tracking always occurs when the surface electric field exceeds that of either the solid or the encapsulation surrounding it. It may occur at lower fields because of physical and chemical inhomogeneities on the surface and because of geometric field enhancements. Although reliable figures appear to be hard to find, a distance of at least 1 kV/mm is commonly allowed for well-controlled surface conditions. (For example Rowland and Nichols [6] found voltages of at least 15 kV were required to sustain dry band arcing over a 10 mm gap on an "arc resistant thermoplastic compound".)

The voltage waveform to be experienced by the high voltage bobbin was rather unusual in this application since it was of high frequency (20 kHz) and had a negative DC offset of half the peak-to-peak AC voltage. The negative DC offset may give rise to space charge injection [7] and consequent field distortion within the insulation. The maximum ("Poissonian") field within the material may therefore be greater than the average ("Laplacian") applied field. The high frequencies may also lead to accelerated aging processes due, for example, to partial discharges. A polymeric insulation was to be used for ease of machining. Because of the large bobbin size, it was decided not to use a very expensive material such as PTFE. Nylon 6,6 was chosen as a compromise between ease of manufacture, cost and insulation properties. The breakdown strength of such materials under these conditions is not readily available but work by Dissado, Montanari, Crine, Lewis and others (e.g. [8, 9, 10]) suggests that they should be able to withstand such conditions indefinitely at fields up to approximately 10 kV/mm. Because of the unknowns, especially to do with space charge effects, it was decided to limit the electric field in the bobbin to 5kV/mm. Nevertheless, this is still high; typically 0.5 kV/mm AC or 1.0 kV/mm DC are the maximum used in high voltage supplies for safety critical applications [11].

Given these considerations for the high voltage bobbin, it was necessary to consider the choice of materials for the transformer encapsulation. A solid encapsulation is likely to have many drawbacks, especially during the design phase of a prototype. It is likely to be inferior in transporting heat from the transformer, it would be impossible to make modifications to the transformer once the encapsulation was in place and, if the encapsulation suffered electrical breakdown, it may be necessary to completely re-build the transformer. A fluid encapsulation such as transformer oil or an insulating gas was therefore considered. Transformer oil is a good medium for heat transport. Under ideal natural convection conditions it has heat transfer coefficient of approximately 95 $W.m^{-2}K^{-1}$; this is equivalent to forced air cooling with a flow velocity of approximately 25 m/s [12]. For prototyping oil causes severe disassembly problems, as the oil needs to be removed from the surfaces of all components. Impurities in oil tend to accumulate at points of high field divergence, i.e. at the most critical points, due to dielectrophoresis [13] leading to localized discharging. It is therefore usual to continuously pump and filter the oil; this is inconvenient for a small transformer.

For these reasons, it was therefore decided to use a gaseous encapsulation. Although it may be possible to use air at normal atmospheric pressure (this is the case in many high voltage laboratory supplies), this would make the transformer rather large as the breakdown strength of air is only 2 – 3 $kV.mm^{-1}$ even under ideal parallel plate conditions. The air would also need to be clean and dry and therefore maintained in a sealed container. Sulfur hexafluoride, SF_6, has a much better dielectric strength, Fig.4. It can be seen that, even at a pressure of 1 bar, the breakdown strength of SF_6 exceeds the maximum design strength for the bobbin (5 $kV.mm^{-1}$). At 2 bar, the breakdown strength is comparable with nylon 6,6 and so tracking resistance is unlikely to be improved above this pressure. It was therefore decided to use SF_6 at a minimum of 2 bar as the encapsulation material for the transformer.

C. Thermal Analysis

The McLyman technique was also used for checking the thermal design of the transformer. The MathCAD output, shown in Appendix A, shows such thermal calculations. A maximum temperature rise of 50°C was specified. The method indicates a minimum required area of 533 cm^2, which is considerably less than the area of approximately 1500 cm^2 that was actually used (although only about 50% of this area was exposed). A temperature rise of less than 50°C was therefore to be expected.

D. Design of High Voltage Bobbin and Electrostatic Analysis

Fig. 5 shows a drawing of the high-voltage bobbin on which the high-voltage secondary winding was wound, Fig. 6 shows a photograph of the bobbin. The bobbin contains two unusual features.

Firstly, in order to obviate the divergent electric stress that would otherwise occur at the ends of the windings, stress relief rings are used. These rings, which are split to prevent shorted turns around the transformer core, are connected to the ends of the windings; indeed they form the connections. The usual way to relieve stress is to alter the winding spacing at the ends but this can be very wasteful of space. The stress relief rings decrease the divergent field ($\approx V/r$) due to the high voltage, V, by increasing the effective radius of the wire, r. In this way the maximum field, on the inside of the stress relief ring, is limited to 5 kV.mm^{-1}.

The other unusual feature is a slotted bobbin that allows layered windings. In this way it was possible to increase the number of turns considerably without placing large demands on the insulation of the winding wire; indeed this was only rated at 600 V. Furthermore the parasitic capacitance between the ends of the windings is reduced. A single cylindrical winding along the surface of the bobbin, which only had 300 turns, was found to have a parasitic capacitance of 130 nF at 1 kHz. However the arrangement shown here, which had more windings (700 turns), had a reduced capacitance of 64 nF. Such an arrangement does give rise to locally high divergent fields at the corners at the bottom of the slots and an electrostatic analysis was made to ensure that a field of 5 $kV.mm^{-1}$ was not exceeded. The results of this analysis are shown in fig 7.

III. TEST RESULTS

The transformer was tested as part of the high frequency, high voltage power supply described earlier. It was installed in National Power's 2035 MW coal-fired "Didcot A" power station at Didcot (near Oxford) UK where it replaced a conventional 50 Hz transformer rectifier and supplied an electrostatic precipitator field. Precipitators are difficult loads since they are prone to arcs and sparks, during which time they act as virtual short circuits, and the current they draw is very unsteady due to the corona discharge and continuously changing coal dust burden. The power electronics contained protection circuits to ensure that the supply voltage was rapidly reduced during arcing and sparking. The load was therefore a useful test to ensure that the unit was sufficiently powerful and robust but it was difficult to obtain accurate results because of the unsteady current drawn.

Fig. 8 shows the measured current-voltage characteristics of the electrostatic precipitator load; the line is an exponential curve drawn to assist the eye. The current increased rapidly above a corona inception voltage of approximately 30 kV. The circled groups of measurements at approximately 0.2 A (~38 kV) and 0.4 A (~43 kV) were almost certainly made as the supply was recovering from a spark in the precipitator. The voltage is increasing at this point but little corona current is being produced. By extrapolation of the exponential, it may be estimated that the transient arcing current was several amps at the higher voltages. The dotted exponential curve shows the average "steady-state" characteristics of the precipitator.

Conventional transformer-rectifier sets have ripples that are typically 50% of the mean voltage [14]. Arcing occurs if the peak of the voltage ripple exceeds a critical value and so for much of the cycle, when the voltage is much less than this critical value, little corona current is produced. Typically the mean current is much less than half that produced at the peak. Furthermore the ripple produces a considerable capacitive displacement current which increases the size of the secondary transformer windings. In this high frequency supply, very little ripple was observed. At 30 kV the ripple was 85±10V, at 44 kV it was 230±20V; i.e. it was much less than 1% under all conditions. It is therefore possible for the supply to produce more than twice as much current without arcing occurring.

Fig. 9 shows the primary current and voltage waveforms for an output of 38 kV. As the primary voltage is provided by a phase-controlled H-bridge, there is a dead time between both positive and negative cycles when the duty cycle is less than 100%. By considering the voltage waveform in Fig. 9 it can be seen that the period is approximately 50 μs corresponding to a switching frequency of 20 kHz. The duty cycle was set to 40% with the dead times equal to 10 μs and the positive and negative on times being 15 μs. The primary voltage was ±500 V. During the positive (negative) on times the current increased (decreased) reasonably linearly, due to the magnetizing inductance, to a value of approximately + (-) 64 A. During the dead times all four H-bridge transistors are off but there is a current path through their flywheel protection diodes. The current during this period is otherwise uncontrolled and the small current oscillation during the dead time probably corresponds to a resonance of the magnetizing inductance with the parasitic capacitance.

It was difficult to estimate the efficiency of the transformer accurately because of the measurement uncertainty in the continuously fluctuating secondary current and unfortunately the experimental arrangement precluded measurement of the instantaneous secondary current. All our estimates lead us to believe that the efficiency of the transformer with rectifier was better than 97%. The total rectifier voltage drop was 200 V which, at 0.4 A, would give an 80 W power loss and contribute ~0.5% to the overall power lost. The best indication of power loss was the temperature rise of the transformer core, which was measured using a thermistor. The temperature rose from 16±2°C to 33°C, a rise of 17±2°C, when the output was 45 kV, 0.4 A, a power of 18 kW. The design calculations, Appendix A, suggest that with a loss of 510 W, a temperature rise of 50°C would be found for a core surface area of 533 cm². The actual exposed surface area was approximately 800 cm². An estimate of the actual power lost is therefore $\frac{17°\mathrm{C}}{50°\mathrm{C}} \times \frac{800\ \mathrm{cm}^2}{533\ \mathrm{cm}^2} \times 510\ \mathrm{W} = 260\ \mathrm{W}$. For an output power of 18 kW this corresponds to an efficiency of 98.5%. The overall efficiency of the power supply was estimated to be >95% which compares very favorably with conventional 50 Hz transformer - rectifier sets with efficiencies of only ~60%.

IV. CONCLUSIONS

A highly efficient high-voltage high-frequency transformer has been designed, built and field tested. The transformer formed part of a switched-mode power supply for electrostatic precipitators. The design, which is still at a prototype stage, was found to be much more efficient and smaller than conventional 50/60 Hz transformer rectifier sets. The unit will now be developed for manufacture.

V. ACKNOWLEDGEMENTS

The project was funded by the UK Engineering and Physical Sciences Research Council (EPSRC) and the Department of Trade and Industry (DTI) through their LINK PEDDS scheme. The project was in collaboration with National Power (NP) and KH Deakin (ES) Ltd (later Elequip Project Ltd). Their financial and technical support is gratefully acknowledged. The authors would like to thank Mr. R.I. Deakin, Mr. M. Selby (NP), Mr. D.A. Rose (DTI), Mr K.R. Parker and Mr. D.F. Warne for their considerable technical assistance and support throughout the project. They would also like to thank Mr. A. Smith and Mr. A. Joseph for their cooperation and assistance with the field trial at Didcot A power station.

List of references for *Fothergill et al*

1. P.J. Devine, "The requirements of a high voltage DC power supply", Leicester University Engineering Department, 1995
2. G. Liberati, "High voltage, high power switched mode power supply for ion production", ENEL, CRTN
3. M.A. Perez, " A new topology for high voltage, high frequency transformers", IEEE 1995, 0-7803-2482-X/95
4. H. Takano, "Feasible characteristic evaluations of resonant inverter linked DC-Dc power converter using high voltage transformer parasitic components", Power electronics and variable speed drives, Sept 23-25, 1996, IEE no. 429, pp 525-533
5. Wm. T. McLyman, Transformer and inductor design handbook, New York : Dekker, 1978
6. S.M. Rowland, and I.V. Nichols, "Effects of dry-band arc current on ageing of self-supporting dielectric cables in high fields" IEE Proc., Science, Measurement and Technology, vol. 143, no. 1, Jan 1996, pp. 10-14
7. J.C. Fothergill and L.A. Dissado (eds), Space Charge in Solid Dielectrics, The Dielectrics Society, 1998, ISBN 0 9533538 0 X, 259-272
8. L.A., Dissado, G. Mazzanti, and G.C. Montanari, "The role of trapped space charges in the electrical aging of insulating materials", IEEE Trans. DEIS, vol. 4, no. 5, Oct. 1997, pp. 496-506
9. J-P. Crine, "A molecular model to evaluate the impact of aging on Space Charges in Polymer Dielectrics", IEEE Trans. DEIS, vol. 4, no. 5, Oct. 1997, pp. 487-495
10. P. Connor, J.P. Jones, J.P. Llewellyn, T.J. Lewis, "Mechanical origin for electrical ageing and breakdown in polymeric insulation," Proceedings of the 1998 IEEE 6th International Conference on Conduction and Breakdown in Solid Dielectrics, Conf. code 49244, pp. 434-438
11. J.W. Williams, "Navy/Industry "NAVMAT" High Voltage Guidelines – An Overview", 1995 High Voltage Workshop, University of Utah, USA
12. Conti-Elektro-Berichte, July/September 1966, p. 189
13. Pohl, H.A. Dielectrophoresis, Cambridge University Press, Cambridge, 1978
14. K.R. Parker (ed.) Applied Electrostatic Precipitation, Chapman and Hall 1997

Biographies for Fothergill *et al*

John Fothergill was born in Malta in 1953. He graduated from the University College of North Wales, Bangor where he also completed an M.Sc. and then a Ph.D. in 1979. Following this he worked at STL (Harlow), the research laboratories for the Standard Telecommunication Company, on power cable insulation. He is now a senior lecturer in the Department of Engineering at the University of Leicester, UK. His main area of interest is in high voltage dielectrics on which he has co-authored a book. He is a Fellow of the IEE and a Senior Member of the IEEE. He presented the invited opening lecture at the High Voltage Workshop in Daytona Beach in 1998.

Philip Devine was born in 1971. He graduated from the University of Leicester in 1994 and is currently studying for a Ph.D. by part-time study. Prior to his degree he worked for Heenan Drives Ltd. He was employed as a Research Assistance on the project described in this paper and is now a Teaching Company Associate. His main area of interest is in high voltage power electronics.

Paul Lefley was born in Ipswich, UK in 1964. He graduated from the University of Nottingham in 1985, and was awarded a Ph.D. from the same institution in 1989. He worked for Mobicom Ltd. from 1988-89. In 18989 he returned to Nottingham Univeristy where he was awarded a three year Post-Doctoral Fellowship. In 1992 he moved to the University of Leicester where he took up the post of lecturer. His main area of interest is power electronics and machines. Whilst at Leicester he has been chairman and treasurer of the IEE East Midlands Power Division, and chairman of the 34th University Power Engineering Conference.

Figure Captions for *Fothergill et al*

Fig. 1: Conventional high voltage DC power supply. TH1, TH2: Thyristor set. T1: High voltage, low frequency transformer. D1, D2, D3, D4: High voltage bridge rectifier

Fig. 2: Voltage fed H-bridge output stage of the proposed high voltage DC power supply

Fig. 3: Transformer with two secondary bobbins driving separate diode bridges

Fig. 4: 50Hz breakdown strength in a homogeneous field for a 20mm inter-electrode gap as a function of absolute gas pressure

Fig. 5: Side-view of high-voltage bobbin showing stress-relief rings and slots for layered windings

Fig. 6: Photograph of the high voltage bobbin

Fig. 7: Electrostatic electric field analysis around slots in the high voltage bobbin. The hashed regions corresponding to the windings which are assumed to be equipotential regions. The highest fields of 5 $kV.mm^{-1}$ can be seen to occur on the corners of the slots.

Fig. 8: Measured current-voltage characteristic under electrostatic precipitator load

Fig. 9: Primary voltage (lower trace) and current (upper trace) for 38 kV output

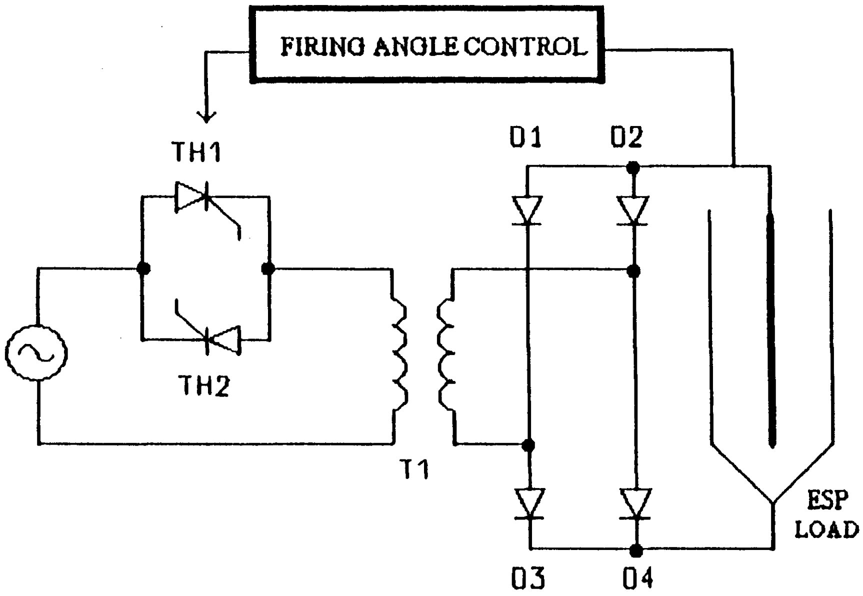

Fothergill et al: Fig. 1 (Fig1.tif)

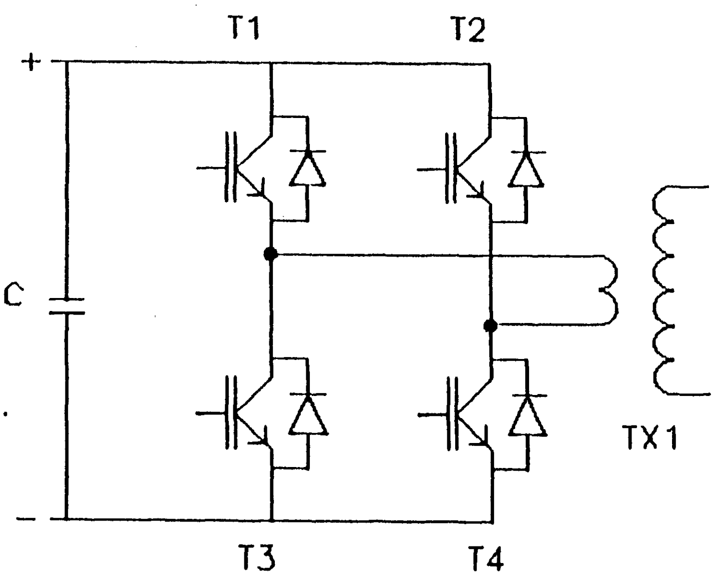

Fothergill et al: Fig. 2 (Fig2.tif)

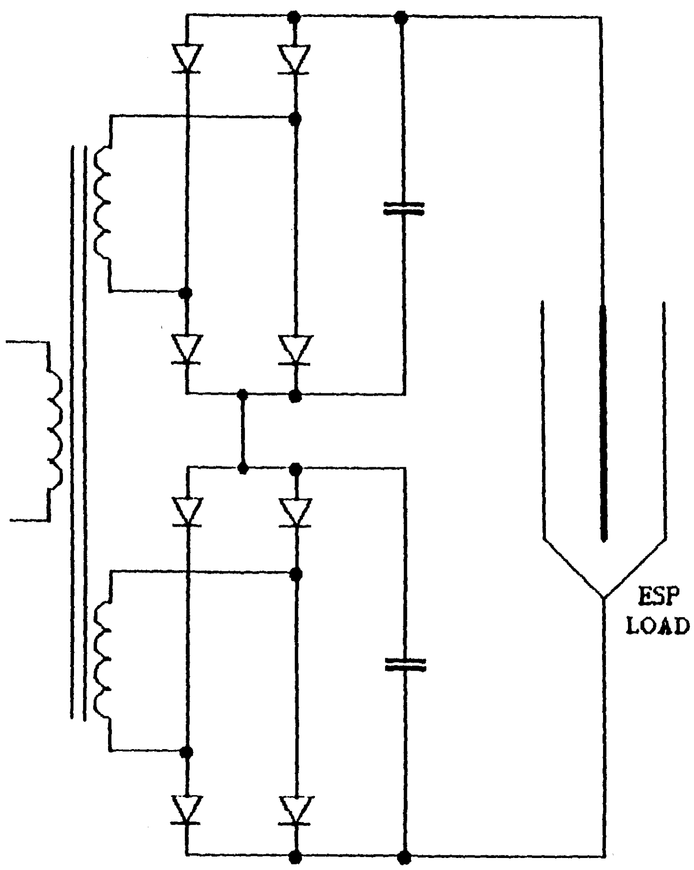

Fothergill et al: Fig. 3 (fig3.tif)

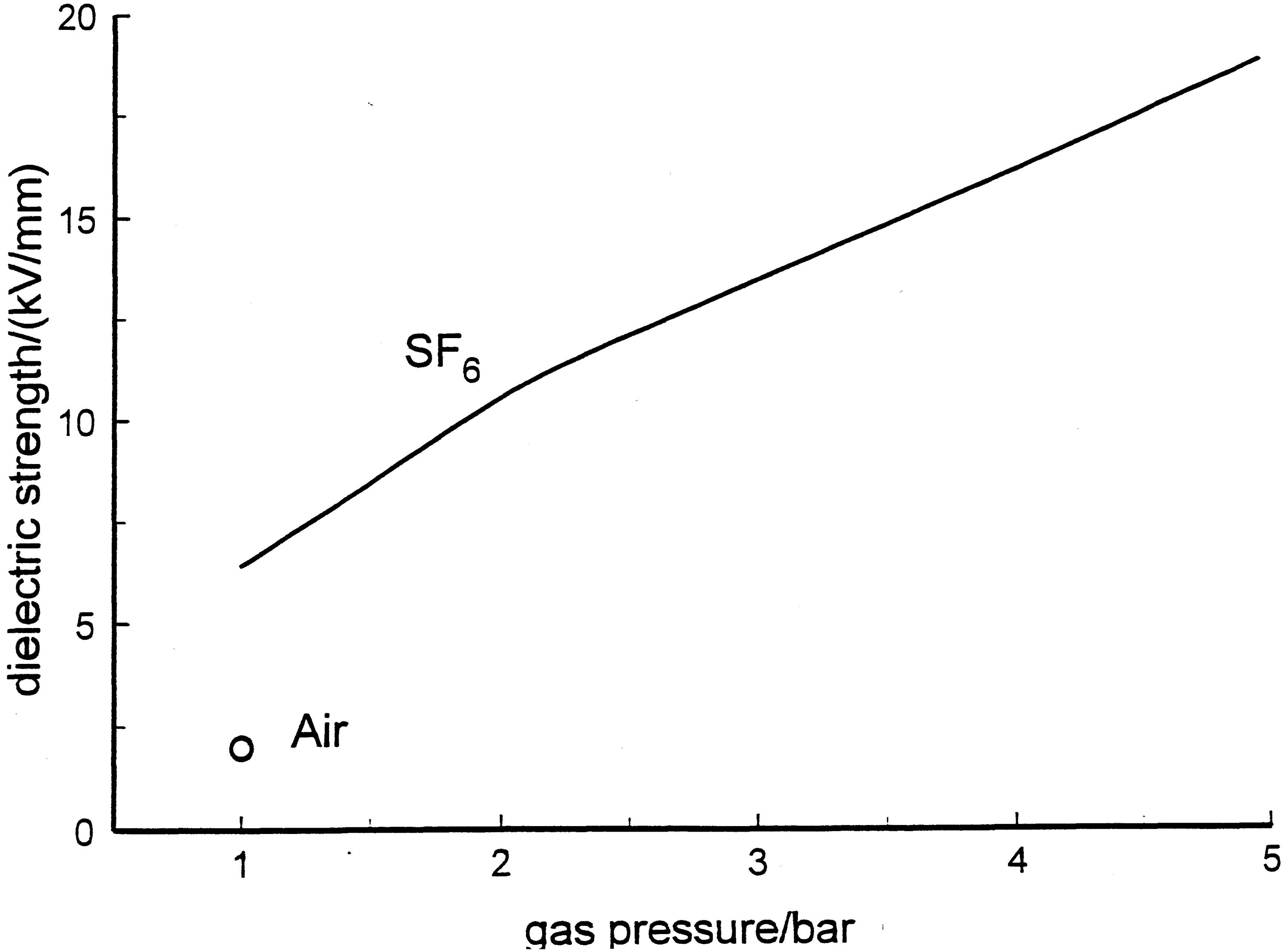

20
15
10
5
0
dielectric strength/(kV/mm)
SF6
Air
1
2
3
4
5
gas pressure/bar

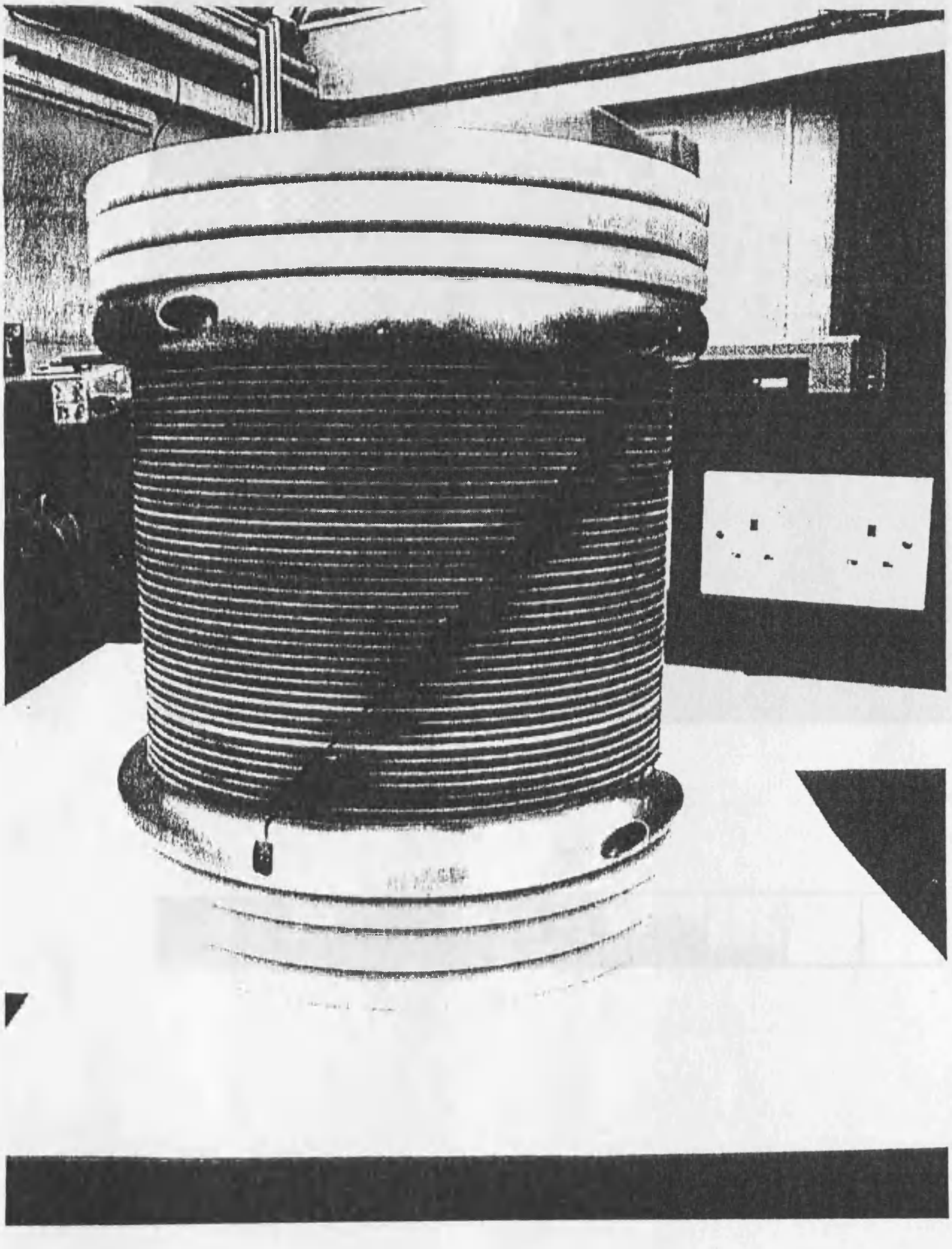

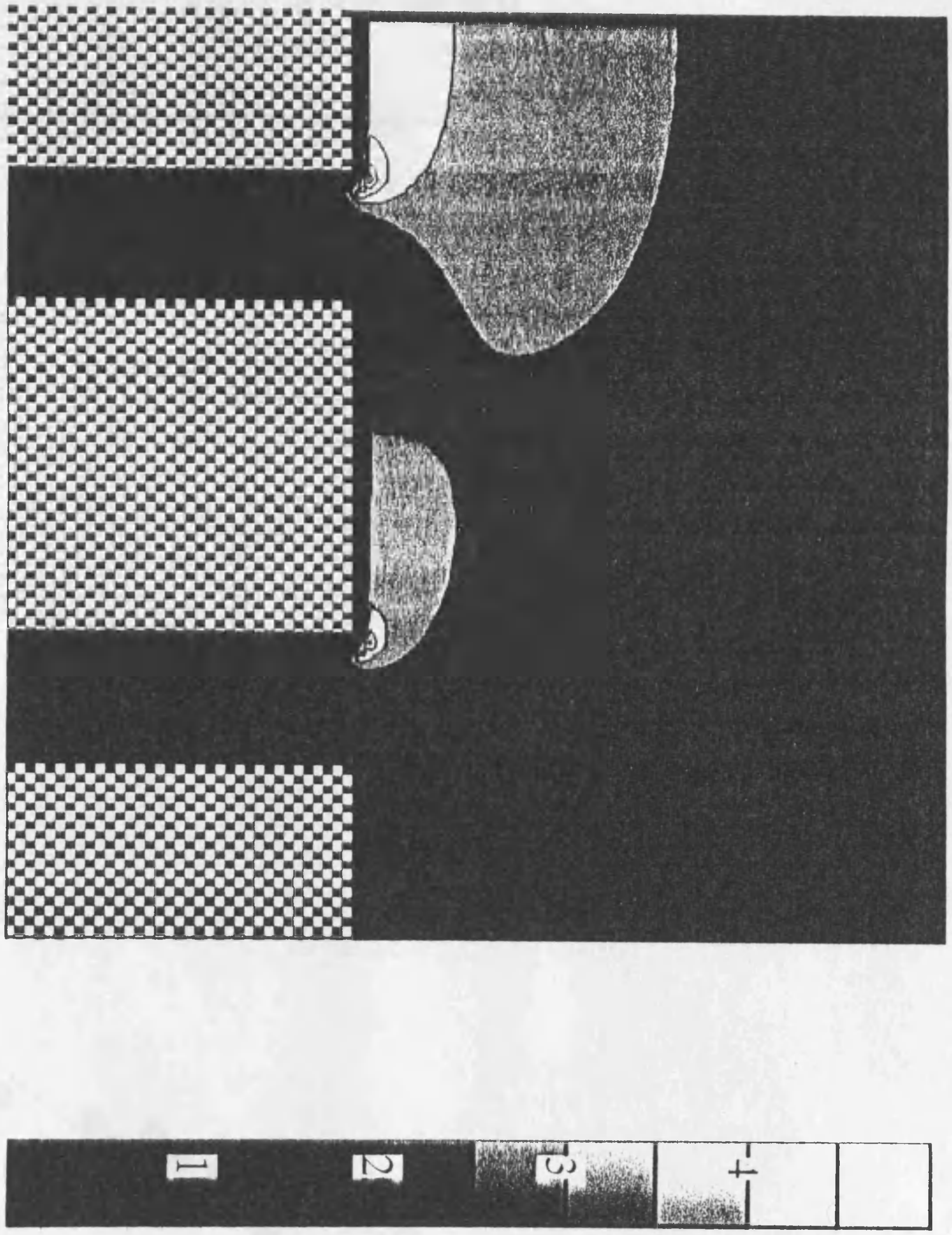
1
2
3
4

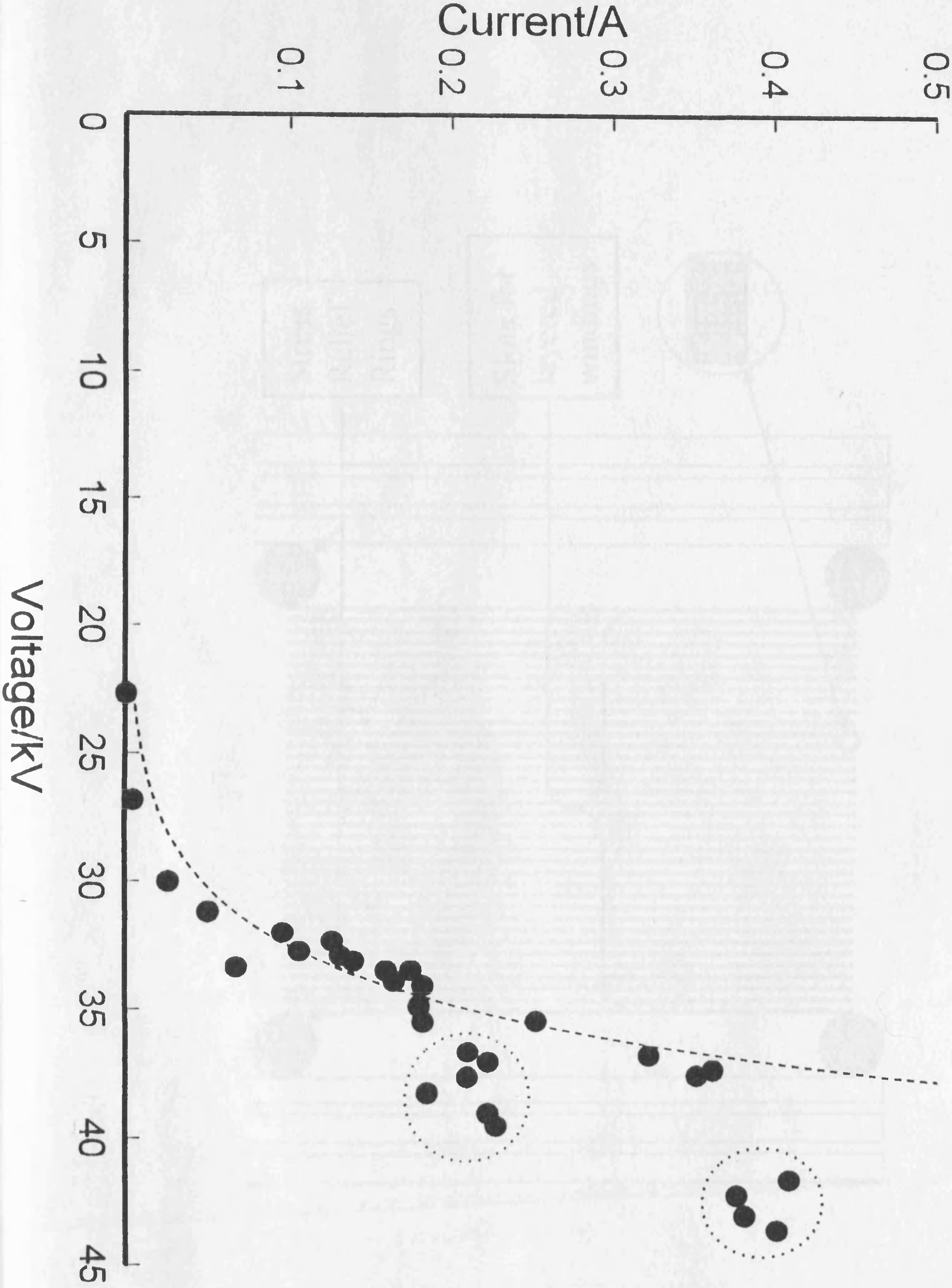
Current/A
0.1
0.2
0.3
0.4
0.5
Voltage/kV
0
5
10
15
20
25
30
35
40
45

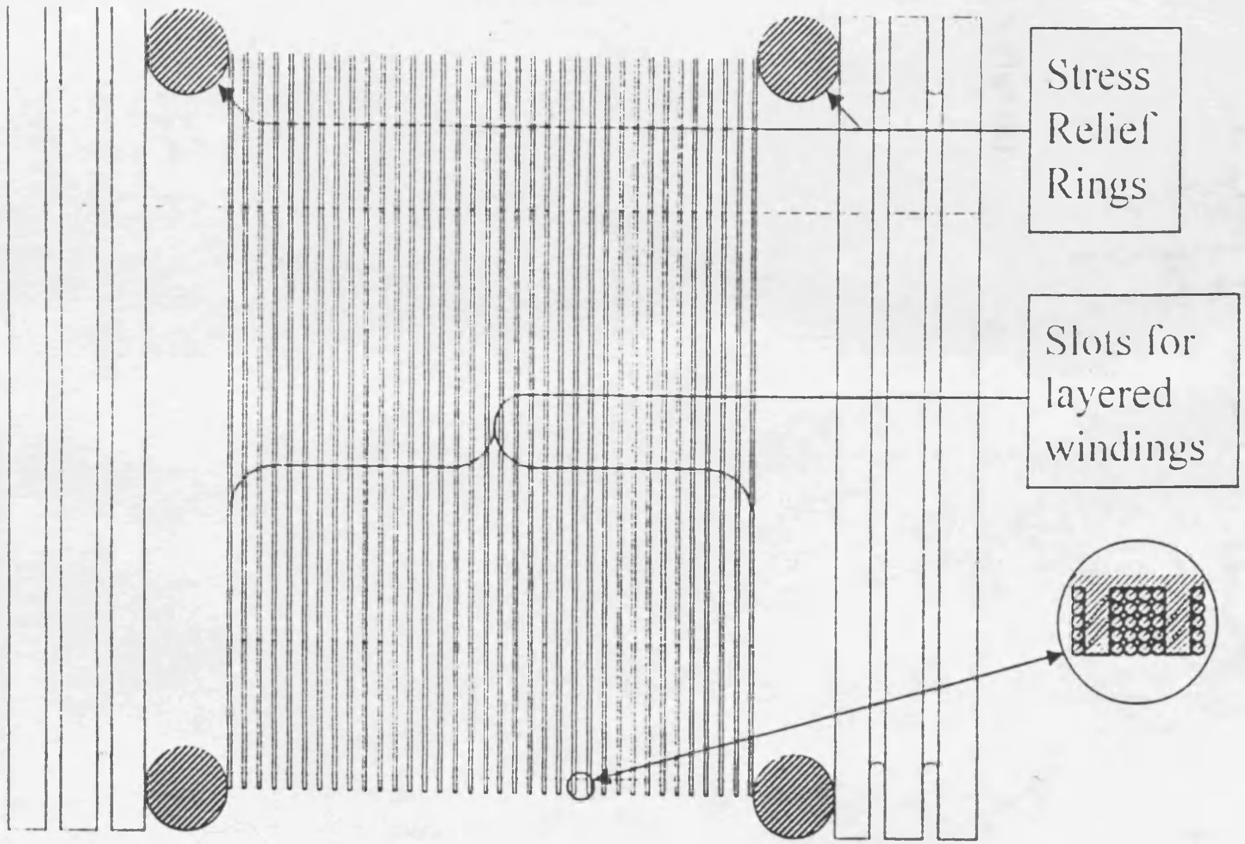
Stress Relief Rings
Slots for layered windings

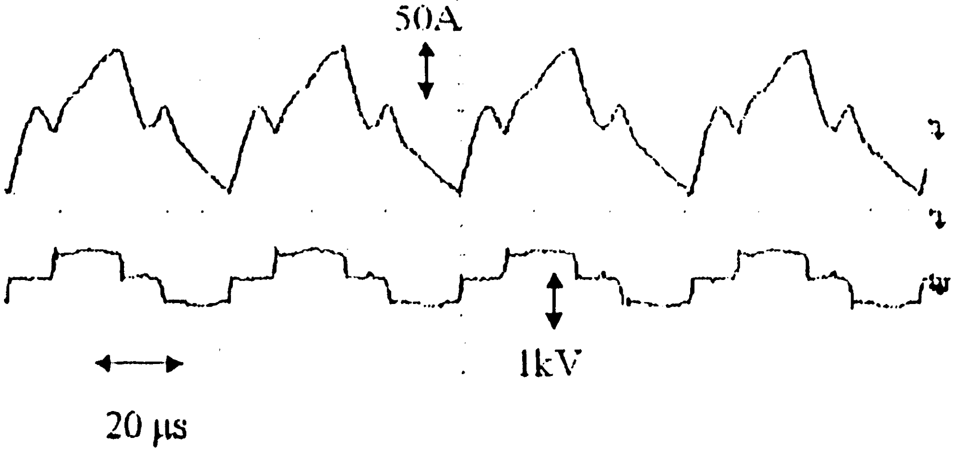

Fothergill et al: Fig. 9 (fig9.tif)